UNIVERSITE D'ABOMEY - CALAVI (UAC)

Registered under N°: 005-22/UAC/VR-AA/SA

A DISSERTATION

Submitted

In partial fulfillment of the requirements for the degree of

Doctor of Philosophy (Ph.D.) of the University of Abomey-Calavi (Benin Republic)

In the framework of the

Graduate Research Program on Climate Change and Water Resources (GRP-CCWR)

By

Mrs. Adama GASSAMA-JALLOW

Public defense on: 17/03/2021

======

ASSESSMENT OF THE IMPACT OF CLIMATE CHANGE ON GROUNDWATER RESOURCES OF THE GREATER BANJUL AREAS IN THE GAMBIA

======

SUPERVISORS:

Major Supervisor: Prof. Serigne FAYE, Full Professor, Cheikh Anta Diop University, Dakar – Senegal
Co-Supervisor: Prof Daouda MAMA, Full Professor, University of Abomey-Calavi, Benin Republic

======

Reviewers:

BOUKARI Moussa, Full Professor, University of Abomey Calavi, UAC, Benin,
GNAZOU D.-T. Masamaéya, Associate Professor, Université de Lomé, Togo,
NGOUNOU NGATCHA Benjamin, Full Professor, Université de Ngaoundéré Cameroun

======

JURY

CHABI OROU Jean	Prof., University of Abomey Calavi, UAC, Benin	President
BOUKARI Moussa	Prof., University of Abomey Calavi, UAC, Benin	Reviewer
GNAZOU D.-T. Masamaéya	Prof., Université de Lomé, Togo	Reviewer
NGOUNOU NGATCHA Benjamin	Prof., Université de Ngaoundéré Cameroun	Reviewer
YALO Nicaise	Prof., University of Abomey-Calavi, UAC, Benin	Examiner
Serigne FAYE	Prof., Université Check Anta Diop, Dakar, Senegal	Supervisor
MAMA Daouda	Prof., University of Abomey Calavi, UAC, Benin	Co-Supervisor

Dedication

I dedicate this work to Allah (SWA) and my beautiful caring mother Ajaratou Fatou Ceesay, my husband, Mr. Cherno Baba Jallow, my children, Ms. Lala Gaye, Musa Sabally, and Khadijatou Sabally for their continuous support, care, prayers, and love that they have given me. Love you all deeply and dearly.

Acknowledgment

This Ph.D. work is realized in the framework of the West African Science Service Center on Climate Change and Adapted Land Use (WASCAL) and funded by the German Ministry of Education and Research (BMBF) in collaboration with the Benin Ministry of Higher Education and Scientific Research (MESRS). I also thank the management of the WASCAL Doctoral Graduate School of Université d'Abomey Calavi and all my colleagues of WASCAL Graduate School for their support. I also appreciate the support of my supervisor Prof. Mama Daouda of Universite d'Abomey Calavi.

I am highly indebted and grateful to Prof. Serigne Faye, Djim Mouhamadou Lamine Dioungue, Moustapha Diaw, Hugguett Emvoutou, Maguette Dieng, Amadou Konateh, Mr. Sowe, Terrence, and the entire department of Geology, Cheikh Anta Diop University for their tireless and continuous support throughout this study. Furthermore, I would like to give my special thanks to Prof Serigne Faye for allowing me to take hydrogeology courses for a whole semester to upgrade my knowledge in the field and gain modeling experience. I cannot express with words how you have impacted my life and your tremendous scientific support throughout the study.

My sincere appreciation and thanks also go to the Government of The Gambia for allowing me to go for studies while still keeping my job. I would also like to acknowledge and thank the Department of Water Resources, the Water Division at NAWEC, and Alhagie Kawsu Conta for all the data and documents provided to facilitate this work.

Lastly and most importantly, my heartfelt gratitude goes to my mother, Ajaratou Fatou Ceesay, my husband, Mr. Cherno Baba Jallow, my children, Ms. Lala Gaye, Musa Sabally, and Khadijatou Sabally for their support, prayers, and encouragement always. They always stood by me and gave me all the support and care that I needed. Special Thanks to my mother for giving me the best education that I deserve. To my wonderful caring and supportive husband for allowing me to go away for studies for many years without getting me a replacement. Finally, to my lovely, understanding, and supportive daughter, Ms. Lala Gaye for taking care of all my transactions and supporting me always. To my beautiful grandchildren, Musa and Khadijatou Sabally, for their company and always putting a smile on my face especially when I am stressed with too much work.

Abstract

Groundwater is an important natural water resource, and it serves as an alternative source of water supply for surface water in the Greater Banjul Areas (GBA), which is saline. These resources regardless of their importance have been increasingly threatened by pollution due to saline intrusion and infiltration of chemicals from agricultural activities, urbanization, industrial development, seasonal climate variability, and climate change. Subsurface storage and groundwater recharge are affected by climate variability and change through changes in precipitation pattern and intensity. In coastal areas of the GBA, the aquifers are affected by marine water intrusion dur to sea level rise. In the past decades, reduced precipitation has been persistent in the country which contributes to a drop in water table level and hence shortage in water supply in many areas. This research aims to assess the impact of climate change on groundwater quality and quantity of the GBA, Southwest of The Gambia.

The hydrodynamics and hydrochemistry of the GBA basin were assessed for 118 wells and 52 boreholes respectively. The Piper diagram was used to assess the groundwater type of the study area. The analysis of the Piper diagram identified eight major water-types based on the major ion chemistry of groundwater and which is grouped into three: i) bicarbonate (m-HCO_3, Ca-HCO_3, and Na-HCO_3) facies, ii) chloride (Na-Cl and m-Cl) facies, iii) and iv) mixed (m-m and Na-m) facies. The order of dominance of the anions in groundwater samples is HOC^{3-} > NO_3 > Cl^-> SO^{4-}>Br, and the cations Na^+> Ca^{2+} > Mg_{2+} >K^+. Mean and median values show that most groundwater samples do not exceed the WHO standard. 23% of samples have NO_3 content above the WHO guideline (50mg/L) with a maximum of 545 mg/L located in the urbanized areas. The high nitrate concentration suggests organic pollution through agricultural chemicals, one-site sanitation and domestic wastewater.

The Thornthwaite model was used to estimate groundwater recharge trends for RCP4.5 and RCP8.5 scenarios. The output of the Thornthwaite model (recharge) was used as input into the three-dimensional finite difference groundwater flow model MODFLOW to simulate groundwater dynamics and the impacts of present and future climate change on groundwater heads after calibration. Three different scenarios (Abstraction scenario: A1=2500m^3/day; A2=4000m^3/day, Climate change scenario and Abstraction and climate change scenario) were used to evaluate the groundwater head trend over the 2006-2050 period. The results obtained show a decreasing groundwater recharge trend for both the RCP4.5 and RCP8.5 scenarios and hence a decrease in groundwater head. In RCP4.5, the annual groundwater recharge decreases by 5% (-5%) during the period 2006-2020 and by 8% (-8%) during the period 2030-2060 while it increases between these two periods (2006-2020 and 2030-2060) by 5.5% (+5.5%). Generally, groundwater head for the two scenarios is decreasing and this is more significant in RCP8.5 than in RCP4.5. The decreasing head over time with RCP8.5 has a growth rate estimated at -14%. Climate change adaptation policies and a sustainable management strategy for the basin should be in place, including legislation to regulate the indiscriminate drilling of boreholes and dumping of solid and liquid waste, and regulate the abstraction of groundwater in an unsustainable manner.

***Keywords*:** Greater Banjul Area, Climate Change, Recharge, Hydrochemistry, MODFLOW, RCPs, APN

Synthèse de la Thèse

Résumé

L'eau souterraine est une ressource naturelle en eau très importante et elle est une source alternative de l'approvisionnement en eau pour les eaux de surface qui sont salines dans la région de Grand Banjul (GB). Ainsi, cette ressource vu son importance a été très souvent traitée de la pollution issue de l'intrusion saline et de celle de l'infiltration des substances chimiques venant des activités agricoles, de l'urbanisation, du développement industriel, de la variabilité saisonnière et du changement climatique. La recharge du stockage des eaux de subsurface et des eaux souterraines sont affectées par les variabilités climatiques et des changements d'intensité des précipitations. Dans la région de Grand Banjul, les aquifères sont affectés par l'intrusion saline et l'augmentation du niveau de la mer. Depuis ces dernières décennies, la diminution des précipitations a persisté dans le pays. Ce qui contribue à la diminution du niveau de l'eau et, par conséquent, réduit considérablement les quantités servant à l'alimentation en eau dans plusieurs localités. L'objectif de cette étude est d'évaluer l'impact des changements climatiques sur les eaux souterraines du point de vue quantité et qualité dans la région de Grand Banjul, au Sud-Ouest de la Gambie.

Les points d'eau dont 114 puits et 52 forages ont été soumis à une étude hydrodynamique et hydrochimique. Le diagramme de Piper utilisé, basé sur les ions majeurs, a identifié huit (08) faciès prédominants répartis en trois (03) groupes à savoir: i) le faciès bicarbonaté (m-HCO_3, Ca-HCO_3 and Na-HCO_3), ii) le faciès chloruré (Na-Cl and m-Cl) et iii) le faciès mixte (m-m and Na-m). L'ordre de grandeur des anions de ces eaux souterraines est de HOC_3^- > NO_3^- > Cl^- > SO_4^{2-} > Br^- et de Na^+ > Ca^{2+} > Mg^{2+} > K^+ pour les cations. Les valeurs moyennes et celles médianes (en mg/l) montrent que la plupart des échantillons ne dépassent pas les normes de l'Organisation Mondiale de la Santé (OMS). 23% de ces échantillons localisés en zone fortement urbanisée, présentent des concentrations en NO3 au-dessus des normes OMS (50 mg/l) avec une valeur maximale de 545 mg/l. Ces valeurs excessives suggèrent une pollution organique provenant des stations d'assainissement et des eaux domestiques usées. Le modèle de Thornthwaite a été utilisé pour estimer la tendance de la recharge au travers des scénarios RCP4.5 et RCP8.5. Les résultats de ce modèle ont été utilisés comme données d'entrée pour le modèle d'écoulement tridimensionnel de différence finie. MODFLOW a ainsi permis de simuler la dynamique des eaux souterraines et les impacts présents et futurs face à la variabilité des changements climatiques sur la recharge et la variations de niveaux d'eau souterraine. Trois (03) scénarios (scenario d'abstraction: A1=2500m^3/jr; A2=4000m^3/jr; scénario changement climatique et abstraction; et scénario recharge climatique) sont utilisés pour évaluer la tendance de la recharge pour la période 2006-2050. Les résultats obtenus à partir du modèle de Thornthwaite montrent une diminution de la recharge pour les scénarios RCP4.5 et RCP8.5. Pour RCP4.5, la tendance de la recharge annuelle est à la baisse de 5% (-5%) pendant la période 2006-2020 et de 8% (-8%) pendant la période 2006-2060; tandis que qu'elle augmente entre les deux périodes (2006-2020 and 2030-2060) de 5.5% (+5.5%). Généralement, la recharge des eaux souterraines pour les deux (02) scénarios est décroissante et est

plus significative pour RCP8.5 que pour RCP4.5. La diminution de la recharge au cours du temps avec RCP8.5 a une augmentation du taux d'estimation de -14%. Les mesures d'adaptation aux changements climatiques et à la stratégie de gestion durable de ce bassin intègrent une législation qui permettra d'une part de réguler la prolifération anarchique des forages, et le pompage des déchets liquides et solides; et d'autre part de réguler l'usage des eaux souterraines façon incontrôlée.

Mots-clés: hydrodynamique, hydrochemie, modèle d'écoulement souterrain, GB, Gambie, MODFLOW, RCP, APN

1. Introduction

Les eaux souterraines constituent une importante ressource naturelle d'eau douce dans la plupart des régions du monde et qui est la seule source d'eau potable. Comme pour la plupart des régions arides et semi-arides où l'approvisionnement en eau douce est rare, la région de Grand Banjul (GB) dépend entièrement des ressources souterraines pour satisfaire ses besoins en eau. La croissance économique de la GBA dépend entre autres de la disponibilité, de la qualité et de l'accessibilité de l'eau douce. Dans la zone étudiée, les eaux de surface sont rarement utilisées à des fins domestiques et d'irrigation. La zone d'étude est située en aval du fleuve Gambie, où le fleuve et ses affluents sont constamment salins en raison de l'influence permanente de l'eau de mer sur les marées. Par conséquent, l'utilisation des eaux de surface à des fins domestiques, d'irrigation agricole et industrielles dans la GBA est presque impossible à moins d'appliquer une technologie de désalinisation de l'eau. En outre, l'extension du front salin dans le fleuve a également diminué la qualité des eaux souterraines dans les aquifères côtiers, les terres agricoles arables, la productivité des poissons et les mangroves dans la zone d'étude. Certains forages et puits peu profonds situés à proximité de la zone côtière deviennent déjà salins. Ce qui pourrait être dû à la forte concentration de certains ions tels que le chlorure dans le sol, à la salinité élevée du sol, à la surexploitation des eaux souterraines et au changement climatique qui provoquent l'intrusion d'eau de mer; d'autant plus que le taux de recharge des eaux souterraines diminue avec la baisse des précipitations annuelles et l'augmentation de l'évapotranspiration ces dernières années. Par conséquent, la demande d'eau douce de qualité pour les habitants des zones côtières augmente.

Il est important de comprendre les composantes en amont (précipitations) des eaux souterraines, ensuite la recharge des eaux souterraines; ceci pour gérer durablement les réserves d'eau souterraine (Tillman et al., 2016) dans une région pour le présent et l'avenir. Etant donné que les eaux souterraines sont la seule source d'eau douce à usage domestique, agricole et industriel dans la région du Grand Banjul, l'estimation de la recharge des eaux souterraines et l'évaluation de l'hydrodynamique et de l'hydrochimie des eaux souterraines favorisent une gestion efficace des eaux souterraines dans le bassin de la GBA pour l'avenir. L'objectif de cette étude est donc d'évaluer l'impact du changement climatique et des prélèvements élevés sur la quantité et la qualité des ressources en eau souterraine, en estimant le taux de la recharge ou la hauteur de charge hydraulique et l'hydrochimie de l'aquifère peu profond de la GBA.

2. Zone d'Étude

La zone d'étude, appelée Grand Banjul (GB), est située dans la partie Sud-Ouest de la Gambie entre la latitude 130 00″ - 130 30″ N et la longitude 160 50″ et 160 20″ W. Elle couvre deux municipalités : Le Conseil municipal de Banjul (CMB) et le Conseil municipal de Kanifing (CMK), et quatre districts administratifs de Kombo Nord, Kombo Ouest, Kombo Centre et Kombo Est. Elle est limitée au Nord par le fleuve Gambie, à l'Est par Bullock Bolong, au Sud par la Casamance et au Sud-

Ouest par l'océan Atlantique. Elle couvre une superficie de 1001,7 km^2, soit environ 9 % de la superficie totale du pays. La zone étudiée est densément peuplée avec 926 120 habitants. Ce qui représente environ 49 % de la population totale du pays (recensement national, 2013).

La zone d'étude a un climat soudano-sahélien, qui est caractérisé par deux saisons distinctes: une courte saison des pluies de Juin à Octobre (environ 1200 mm/an) et une longue saison sèche s'étendant de Novembre à Mai. Les températures annuelles moyennes dans la zone d'étude sont d'environ 27°C. Pendant la saison sèche, les températures moyennes diurnes peuvent atteindre 36 °C (entre Mars et Juin). La moyenne mensuelle de l'humidité relative culmine pendant la raison humide avec des valeurs pouvant atteindre 90 %. L'évapotranspiration est la plus faible pendant la saison des pluies (Août-Septembre) et atteint son maximum pendant la saison sèche lorsque les températures sont élevées. L'évapotranspiration est estimée à 1412 mm par an, avec un maximum d'environ 190 mm en mai.

3. Matériaux et méthodes

Les données historiques relatives au bilan hydrique (précipitations, évapotranspiration), à la géologie et à la géométrie (SRTM, épaisseur de l'aquifère, conductivité et transmissivité hydrauliques) et aux prélèvements d'eau obtenues auprès du Département des ressources en eau, des sociétés de forage et de la Division de l'eau (NAWEC) ont été compilées en plus des données de terrain de 2018 avant et après la mousson obtenues au cours de cette étude. Les données hydrochimiques ont été obtenues à partir d'analyses chimiques effectuées pour 52 eaux souterraines et 6 échantillons d'eau de surface ont été collectés dans toute la zone d'étude. En outre, des échantillons d'eau ont été collectés en Novembre pour analyser les ions majeurs et les éléments mineurs tels que le Br. Cette analyse a été effectuée au laboratoire d'hydrochimie du Département de géologie de la Faculté des Sciences et Technologies de l'Université Cheikh Anta Diop, à Dakar, au Sénégal, en utilisant des méthodes standardes. Les analyses ont été effectuées selon la méthode de chromatographie ionique à l'aide de l'équipement AQUION-DIONEX. Les processus d'échanges ont été réalisés au moyen de colonnes AS14 A - AERS 500 pour les anions, et CS12 À - CERS 500 pour les cations. Un multiparamètre WTW MULTI 3430 SET G a été utilisé pour déterminer le pH, la température et la conductivité électrique au laboratoire. L'objectif était d'évaluer : (1) la qualité des eaux souterraines sur la base de différents indices pour les usages de boisson et d'irrigation, et (2) les faciès et processus hydro-géochimiques à l'origine de la minéralisation des eaux souterraines. Le diagramme de Piper (1994) a été utilisé pour caractériser les types d'eaux souterraines de l'aquifère peu profond de la GB et comprendre les sources des constituants dissous dans l'eau.

Le modèle de bilan hydrique mensuel Thornthwaite a été utilisé pour simuler la variation temporelle de la recharge en eau souterraine (GWR) au cours des trois dernières décennies (1984-2016) sont déduites par les stations de Banjul et Yundum. Les valeurs de recharge obtenues à partir du modèle de Thornthwaite ont été utilisées comme paramètre d'entrée dans MODFLOW pour simuler la

dynamique de la tête des eaux souterraines pour l'avenir (2019-2050) en utilisant les RCP4.5 et RCP8.5 des projections climatiques de la phase 5 du projet d'intercomparaison des modèles couplés. On s'attend généralement à ce que la recharge et la hauteur de la nappe phréatique simulées pour l'avenir soient inférieures à la moyenne historique des dernières décennies. Les effets potentiels de la variabilité naturelle du climat sur les ressources en eau constituent une question de gestion de l'eau de plus en plus urgente à l'échelle locale et mondiale (Velasco et al., 2017)

4. Résultats et discussion

L'analyse statistique des paramètres physico-chimiques (profondeur de l'eau, pH, T°C, CE) de 52 points d'échantillonnage de l'aquifère peu profond (puits et forages) pendant la pré-mousson (Mai) et la post-mousson (Novembre) de 2018 est présentée dans le tableau 1. Les résultats montrent une grande variation dans la CE de 24,8 à 1958 µS/cm avec une moyenne de 201,69 µS/cm, en Mai et de 30 à 1530 µS/cm avec une moyenne de 222 µS/cm en Novembre 2018, et montrant ainsi une minéralisation faible à élevée de l'eau souterraine qui reflète les différentes sources, la géochimie et le processus de dilution. Les valeurs de pH allant de 3,9 à 7,8 reflètent le caractère acide à neutre de l'eau souterraine. Les valeurs de température moyenne de 29°C révèlent le caractère peu profond de l'aquifère où les échanges de chaleur sont facilement réalisés grâce à la température ambiante.

Tableau 1: Statistiques descriptives des paramètres physicochimiques

Parameter	**pH**		**Electric Conductivity**		**Temperature**	
Units	-		µs/cm		°C	
Sampling date	Pre-monsoon	Post-monsoon	Pre-monsoon	Post-monsoon	Pre-monsoon	Post-monsoon
N total	52	52	52	52	52	52
Mean	5.9	5.6	225.0	247.6	28.6	29.9
Stan Dev	0.8	0.9	336.7	310.8	1.6	1.4
Variance	0.7	0.8	113390.7	96587.1	2.7	1.8
Minimum	5.1	3.9	24.8	30.0	24.5	26.7
Median	5.7	5.3	104.8	125.0	28.7	29.7
Maximum	8.6	7.8	1985.0	1530.0	32.2	33.0

Les résultats de l'analyse montrent que l'ordre de dominance des anions dans les échantillons d'eaux souterraines est HCO_3^- > NO_3^- > Cl^- > SO_4^{2-} > Br^-, et les cations Na^+ > Ca^{2+} > Mg^{2+} > K^+. Les valeurs moyennes et médianes montrent que la plupart des échantillons d'eaux souterraines ne dépassent pas la norme de l'Organisation Mondiale de la Santé (OMS). Cependant, 23 % des échantillons ont une teneur en NO_3 supérieure à la recommandation de l'OMS (50 mg/L), avec un maximum de 545 mg/L situé en zone urbaine. La forte concentration de nitrates dans ce contexte suggère une pollution organique par l'assainissement et les eaux usées domestiques à certains endroits. Selon le diagramme de Piper (Figure 1), il y a trois types faciès, à savoir m-HCO_3 (40%) et Ca-HCO_3

(16%) situés dans la zone centrale, et Na-Cl (26%) qui sont les eaux de surface et de la zone urbanisée. La prédominance du type d'eau m-HCO_3 et Ca-HCO_3 au centre de la GB correspondant à une monticule à +19 m indique les zones de recharge préférentielle comme le suggère la carte piézométrique. Ce type d'eau pourrait résulter de la dissolution de la calcite lors de l'infiltration. Ce qui corrobore avec la corrélation positive entre Ca+Mg et HCO_3 proche de la ligne d'équilibre [1:1]. En plus de ce processus, la dissolution des évaporites (Halite et Gypse) ainsi que les échanges de base seraient impliqués comme le montrent les tracés binaires des ions majeurs et le calcul de l'indice de saturation. Les résultats de l'étude révèlent que la plupart des eaux souterraines de la GB sont jugées potables

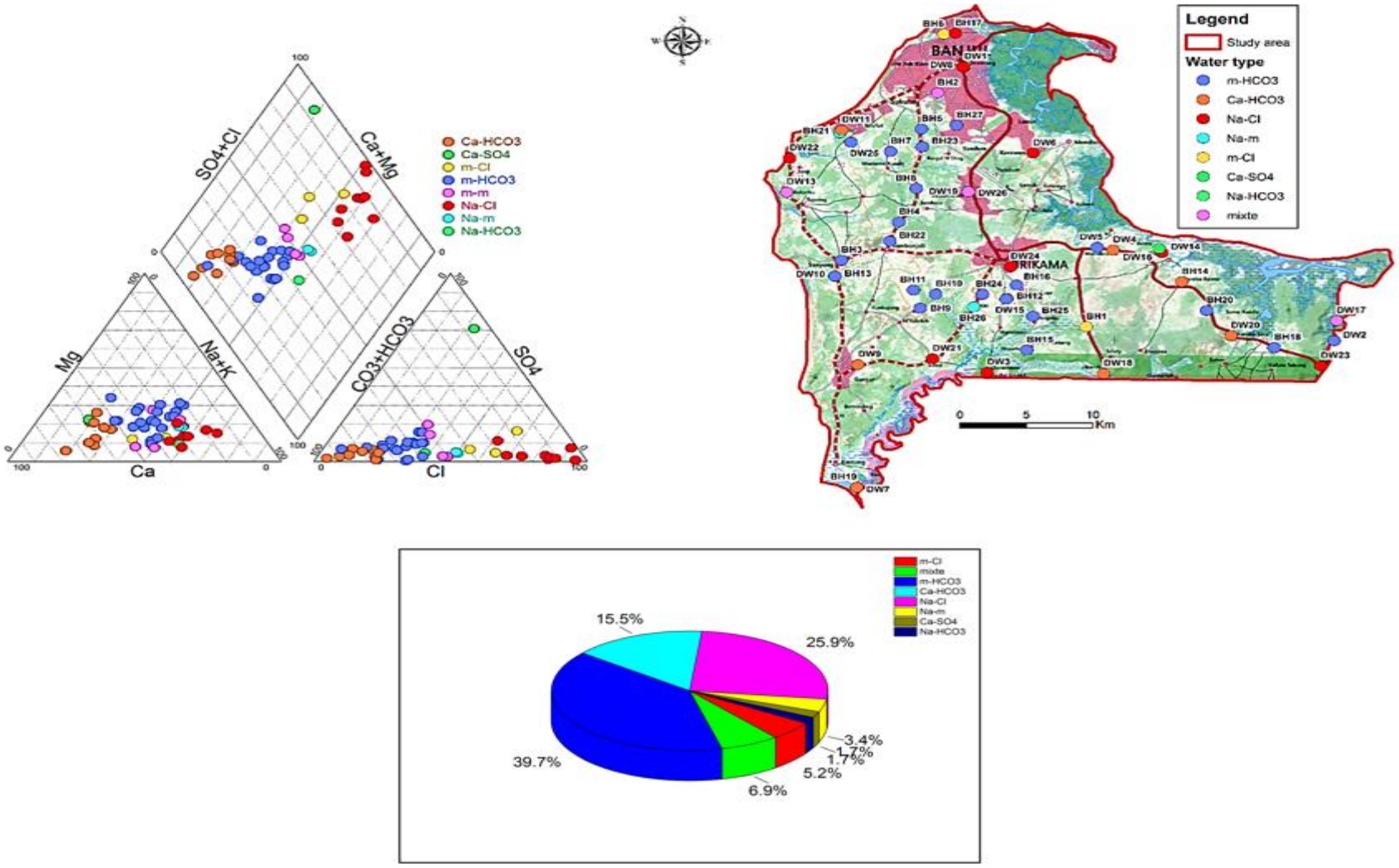

FIGURE 1: DIAGRAMME TRILINEAIRE PIPER MONTRANT LE REGIME HYDROCHIMIQUE DES EAUX SOUTERRAINES ET LA DISTRIBUTION DES TYPES D'EAUX SOUTERRAINES DANS LA ZONE D'ETUDE. M=MELANGE, CL-CHLORURE, MG=MAGNESIUM, CA-CALCIUM, NA-SODIUM. K=POTASSIUM, SO4-SULFATE, CO3-CARBONATE ET HCO3-BICARBONATE

[x]

Les résultats montrent la variation temporelle des précipitations, de la recharge des eaux souterraines et de l'évaporation réelle actuelle des stations de Banjul et de Yundum, générée par le modèle de bilan de masse de Thornthwaite. On peut observer que la GWR dépend principalement des précipitations puisque les valeurs réelles d'évapotranspiration sont plus ou moins les mêmes dans les deux stations. Il se produit surtout pendant le pic de la saison des pluies (Août) où les précipitations dépassent l'évapotranspiration réelle et le stockage de l'humidité.

Cependant, il existe une variation régionale du GWR, la valeur de recharge la plus élevée étant observée à Yundum, la partie centrale de la GBA, et la valeur la plus faible à Banjul, la partie Nord de la zone d'étude. Ainsi, les valeurs de recharge augmentent du Nord au Sud en fonction du régime des précipitations. La valeur annuelle moyenne de la recharge est estimée à 172 mm à Yundum et à 97 mm à Banjul au cours de la période 1984-2016 (Tableau 2).

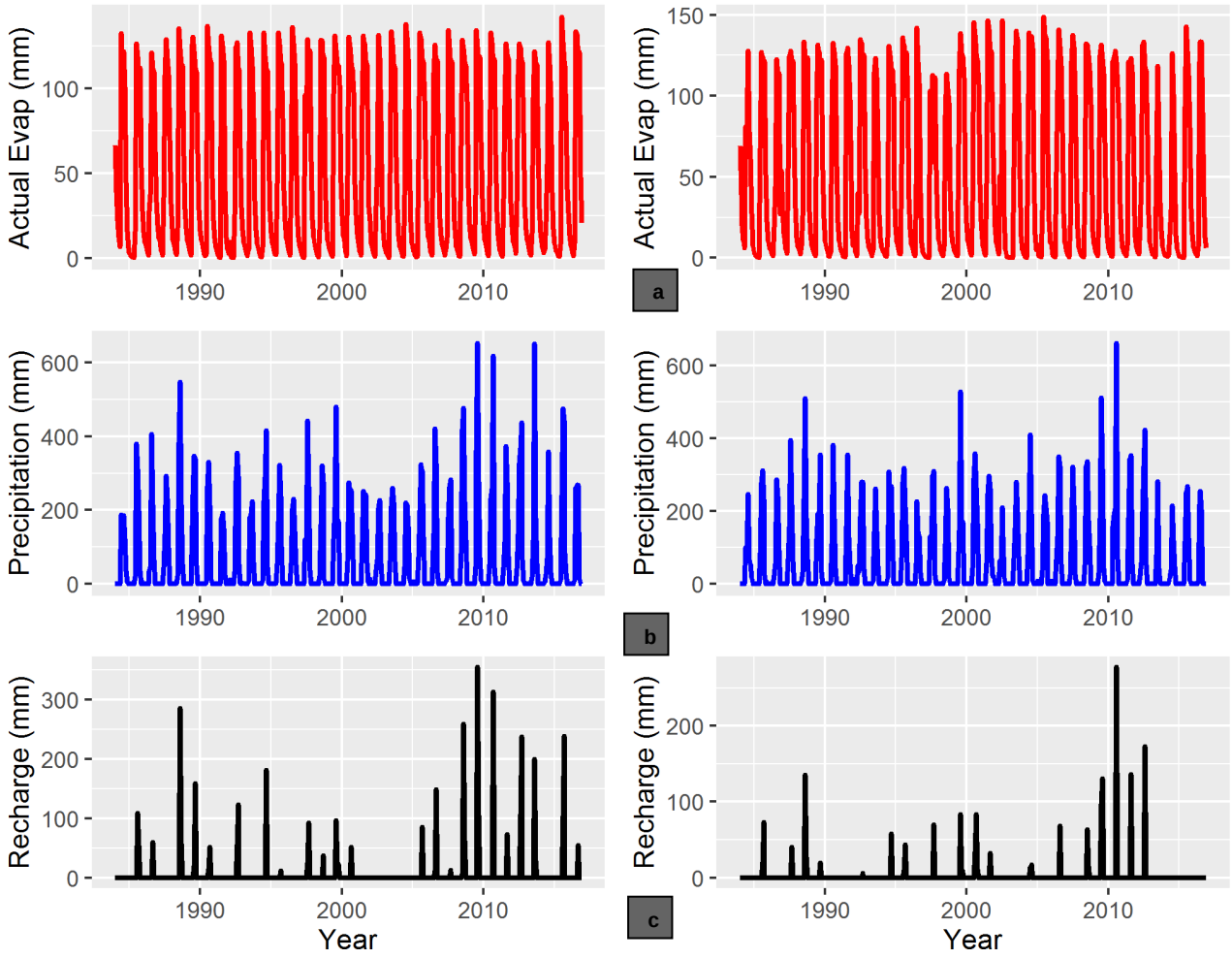

FIGURE 2: (A) VARIATION TEMPORELLE DE L'EVAPORATION REELLE; (B) PRECIPITATIONS; ET (C) RECHARGE DES EAUX SOUTERRAINES, A PARTIR DES STATIONS DE BANJUL ET DE YUNDUM, GENEREE PAR LE MODELE THORNTHWAITE DE 1984 A 2016 .

Tableau 2 : Valeur annuelle moyenne (mm) des paramètres de sortie du modèle de Thornthwaite, PET : Évapotranspiration potentielle (mm) ; P : Précipitations ; AET : Évapotranspiration réelle (mm) ; RO : Ruissellement ; R : Recharge de 1984 à 2016

Stations	PET	P	AET	RO	R
Yundum	1343	930	628	186	172
Banjul	1356	830	616	166	97

5. Estimation de la recharge en eau souterraine projetée

Le modèle de bilan hydrique mensuel par étapes de Thornthwaite a été utilisé pour simuler la tendance future de la recharge des eaux souterraines de la GBA. Les données climatiques brutes des séries chronologiques du portail en ligne CLIMAP du projet ANACIM-IRD ont été utilisées dans cette étude (http://retd1.teledetection.fr/climap/, consulté en Novembre 2019). Une méthode de correction des biais a été appliquée aux données climatiques simulées pour corriger les données d'entrée climatiques fournies par les modèles de circulation générale (AOGCM) ou les modèles climatiques régionaux (RCM) de CORDEX afin de permettre la comparaison des impacts observés et simulés pendant la période de référence historique, et pour une transition en douceur vers l'avenir. L'ensemble des données climatiques met les biais sur une grille globale de 0,5 °C x 0,5 °C et à des pas de temps quotidiens. Les données de précipitations et de températures projetées des scénarios RCP4.5 et RCP8.5 ont été utilisées comme données d'entrée dans le modèle pour estimer la tendance de la recharge sur l'horizon 2006-2020.

Les résultats de la figure 3 montrent la prévision de la recharge des scénarios RCP4.5 et RCP8.5 à partir du modèle Thornthwaite. Dans le scénario RCP4.5, la tendance annuelle de la recharge diminue de 5 % (-5 %) au cours de la période 2006-2020 et de 8 % (-8 %) au cours de la période 2030-2060. Tandis qu'elle augmente de 5,5 % (+5,5 %) entre ces deux périodes (2006-2020 et 2030-2060).

De manière générale, la recharge des eaux souterraines pour les deux scénarios est en baisse; ce qui est plus important dans la RCP8.5 que dans la RCP4.5. La tendance à la baisse dans le temps avec la RCP8.5 a un taux de croissance estimé à -14%. Les valeurs de CE taux de croissance seront appliquées au modèle calibré afin d'évaluer l'impact du changement climatique sur la hauteur des eaux souterraines à l'horizon 2050. Cela peut donc s'expliquer par le fait que les précipitations annuelles moyennes pour la RCP8.5 sont inférieures à celles de la RCP4.5. De même, la recharge diminue dans les deux scénarios mais dans le RCP4.5, elle se stabilise au milieu du siècle grâce à la mesure d'atténuation mise en place pour réduire les émissions. Contrairement au RCP8.5, un scénario d'émissions de Gaz à effet de serre (GES) à long terme (c'est-à-dire un scénario de statu quo), sans aucune mesure d'atténuation, la tendance des précipitations et de la recharge continue à diminuer jusqu'à la fin du 21e siècle.

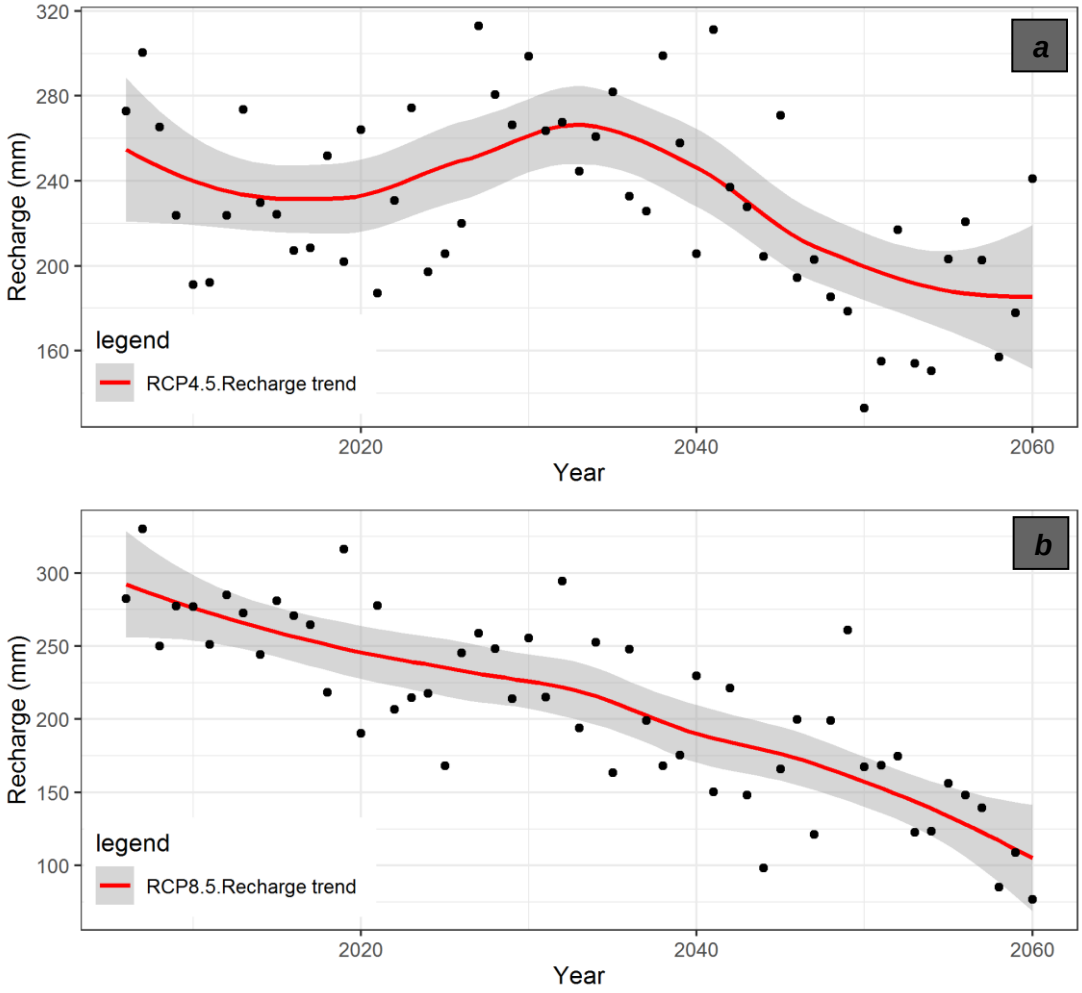

FIGURE 3: TENDANCE DE LA RECHARGE ANNUELLE MOYENNE SELON LES SCENARIOS RCP4.5 ET RCP8.5 AU COURS DE LA PERIODE 2006-2050

6. Conclusion

Une évaluation de la qualité des eaux souterraines de l'aquifère peu profond de la GB a été réalisée à partir d'échantillons prélevés dans 52 ouvrages et 6 eaux de surface. Les résultats des analyses de l'eau ont été utilisés pour identifier les processus et mécanismes affectant la chimie des eaux souterraines de la GB. Les valeurs moyennes et médianes du pH reflètent le caractère acide à neutre de l'eau souterraine peu profonde. La conductivité électrique (CE) va de 24 à 1985 µs/cm avec des valeurs de la moyenne et d'écart-type élevées suggérant des sources de variables, des processus géochimiques et de dilution selon les zones.

Le diagramme de Piper montre que l'ordre d'abondance des anions dans les échantillons d'eau souterraine est HCO_3^- > NO_3^- > Cl^- > SO_4^{2-} > Br^-, et les cations Na^+ > Ca^{2+} > Mg^{2+} > K^+. Les valeurs moyennes et médianes montrent que la plupart des échantillons d'eaux souterraines ne dépassent pas la norme de l'OMS. La forte concentration de nitrates dans les eaux souterraines de la GBA par endroits

suggère une pollution organique due à l'assainissement et aux eaux usées domestiques. Le diagramme de Piper a révélé que la plupart des eaux souterraines de la GBA sont caractérisées par les faciès bicarbonatés (m-HCO_3, Ca-HCO_3 et Na-HCO_3) qui sont dominants (56,9 %) dans les contextes hydrogéologiques et géologiques couvrant l'aquifère peu profond. Le deuxième faciès dominant est celui chloruré (Na-Cl et m-Cl) avec 31,1 %. Le type mixte (m-m et Na-m) est le moins représenté avec 12 %. La dominance des faciès hydrochimiques m-HCO_3 et Ca-HCO_3 au centre de la GB correspondant à une monticule, indique les zones de recharge préférentielle comme le suggère la carte piézométrique. Ce type d'eau pourrait résulter de la dissolution de la calcite lors de l'infiltration; CE qui est justifié par la corrélation positive entre Ca+Mg et HCO3 proche de la ligne d'équilibre [1:1]. En plus de CE processus, il est impliqué la dissolution des évaporites (Halite et Gypse) ainsi que les échanges de base comme le montrent les tracés binaires des ions majeurs et le calcul de l'indice de saturation. Les résultats ont révélé que la plupart des eaux souterraines de l'aquifère peu profond de la zone d'étude sont jugées potables.

Le modèle de différences finies (MODFLOW) a été appliqué pour évaluer l'impact du changement climatique sur les ressources en eau souterraine du bassin de la région du Grand Banjul. Les résultats globaux montrent que le niveau des eaux souterraines diminue principalement en raison des prélèvements d'eau élevés et de l'effet du changement climatique. Avant de simuler la dynamique des eaux souterraines du bassin de la GB, la recharge des eaux souterraines a été estimée à l'aide du modèle Thornthwaite pour deux scénarios de changement climatique (RCP 4.5 et RCP8.5). Les résultats ont révélé qu'il y a une diminution continue dans les deux scénarios RCP4.5 et RCP8.5 jusqu'à la fin de 2050. Cette diminution du taux de recharge est plus importante dans le scénario RCP8.5.

Cette étude conclut donc que les ressources en eaux souterraines sont affectées par le changement climatique. Ainsi, des stratégies d'utilisation et de gestion durables devraient être mises en place pour assurer la sécurité et la disponibilité de l'approvisionnement en eau pour l'avenir. Les décideurs devraient être informés de ces résultats, bien que l'étude ait été réalisée avec certaines incertitudes du modèle ainsi que des données d'observation. Dans l'ensemble, le modèle a donné une bonne simulation des conditions climatiques réelles de la zone d'étude.

TABLE OF CONTENTS

Dedication i

Acknowledgment ii

Abstract iii

Synthèse de la Thèse iv

Résumé iv

List of Acronyms xx

LIST OF FIGURES xxii

LIST OF TABLES xxv

CHAPTER 1: GENERAL INTRODUCTION 1

1.1 General Context – Problem Statement – Justification 1

1.2 Literature Review 3

1.2.1 Hydrodynamic of Groundwater 3

1.2.2 Hydrochemistry of Groundwater 4

1.2.2 Climate change impact on groundwater resources 5

1.3 Research Questions 6

1. 4 Thesis Objectives 7

1.4.1 Main Objective 7

1.4.2 Specific Objective 7

1.5 Hypothesis 7

1.6 Novelty 7

1.7 Scope of the Thesis 8

1.8 Expected Results 8

1.9 Thesis Structure 8

CHAPTER 2: STUDY AREA 10

2.1 Location and socio-economic situation 10

2.2 Climate context 14

2.2.1 Rainfall in the Study Area 14

2.2.2 Temperature 19

2.2.3 Relative Humidity 20

2.2.4 Insolation 20

2.2.5 Wind Speed 21

2.2.6 Evaporation and Evapotranspiration 22

2.3 Geomorphology and Hydrography 23

2.3.1 Geomorphological Context 23

2.3.2. Hydrography 28

2.4. Soil 32

2.4.1 Description of Soil Types 32
2.4.2 Soils of The Gambia 33
2.4.3 Soils of the Study Area 34
2.5 Land Use and Land Cover 36
2.6 Geological Context 38
2.6.1 Regional Geological Settings – S-M Basin 38
2.6.2 Geological Settings of the Gambia 40
2.6.3 Geological Settings of the Study Area 42
2.7 Hydrogeology Context 46
2.7.1 Regional Hydrogeology 46
2.7.2 Local Hydrogeology 48
2.7.3 Aquifer Thickness 51
2.8 Hydrology 56
CHAPTER 3: DATA, MATERIALS AND METHODS 60
3.1 Data 60
3.1.1 Climate data 60
3.1.2 Topographic data 60
3.1.3 Pumping test data 61
3.1.4 Geological data 61
3.1.5 Hydrochemical data 61
3.1.6 Population data 62
3.2 Materials 62
3.3 Methods 63
3.3.1 Geomorphology and Hydrography 63
3.3.2 Source of Data and SRTM Processing method 63
3.3.3 Treatment 64
3.3.4 Soil 64
3.3.5 Hydrodynamic Methodology 65
3.3.5.1 Methodology 65
3.4 Hydrochemistry 69
3.4.1 Laboratory Analysis 69
3.5 Methods of Estimating Groundwater Recharge 69
3.5.1 Methods of Estimating Recharge in the Unsaturated Zone 69
3.5.2 Methods based on the study of the saturated zone 72
3.5.3 Method of Estimating ETo and Recharge by Water Balance Method 73
3.6 choice and justification of methods used in this study 78
3.7 Potential Recharge Zone Mapping 78

3.7.1 Methodology 78
3.8 Groundwater Modelling 83
3.8.1 Conceptual Model 83
3.8.2 Numerical Model 86
3.9 Discretization and Boundary Conditions 87
3.10 Calibration 89
3.11 Steady-State Calibration 89
3.12 Global Climate Models 90
3.13 Representative Concentration Pathways 91
3.14 CLIMATE CHANGE IMPACTS ON GROUNDWATER RESOURCES 91
I. Scenarios Development 91
3.15 Conclusion 93
CHAPTER 4: HYDRODYNAMIC ASSESSMENT 94
4.1 Introduction 94
4.2 Water Depth 94
4.3 Piezometric Level and Groundwater Fluctuation 97
4.4 Groundwater Table Fluctuation 101
4.5 Aquifer Thickness 102
4.6 Hydrodynamic Parameters 104
4. 7 Conclusion 104
CHAPTER 5: GROUNDWATER RECHARGE ESTIMATION TECHNIQUES 105
5.1 Introduction 105
5.2 Application of the Thornthwaite Method to Calculate Infiltration 106
5.3 Application Penman Method to Infiltration Calculation 111
5.4 Application of Turc Method to Potential Evapotranspiration Calculation 114
5.5 Comparison and Critical Analysis of the Results Obtained 116
5.6 Potential Recharge Zone Mapping 118
5.6.1 Introduction 118
5.6.2 Geology 119
5.6.3 Land Use/Land Cover 121
5.6.4 Slope of the Land 123
5.6.5 Drainage 125
5.6.6 Groundwater Fluctuation 127
5.6.7 Transmissivity 129
5.6.8 Soil 131
5.6.9 Delineation of Groundwater Recharge Zone 133
5.6.10 Conclusion 135

CHAPTER 6: HYDROCHEMISTRY OF GROUNDWATER 136
6.1 Introduction 136
6.2 Statistical Analysis of Hydrochemical Data 137
6.3 Physicochemical Characterization 139
6.3.1. Spatial Distribution of Electrical Conductivity 140
6.3.2. Spatial Distribution of pH 144
6.3.3 Temperature 146
6.4 Piper Diagram 146
6.5 Geochemistry of Groundwater 149
6.6 Multivariate Statiscal Analysis 152
6.6.1 Principal Component Analysis 153
6.6.1 Correlation Analysis of Chemical Parameters 158
6.6.2 Hierarchy Cluster Analysis 161
6.7 Saturation Indices (Si) 166
6.8 Conclusion 168
CHAPTER 7: GROUNDWATER MODELLING AND CLIMATE CHANGE IMPACTS ON GROUNDWATER RESOURCES 171
7.1 Groundwater Modelling 171
7.1.1 Introduction 171
7.1.2 Results 172
7.1.3 Conclusion 179
7.2 CLIMATE CHANGE IMPACTS ON GROUNDWATER RESOURCES OF THE GBA 179
7.2.1 Introduction 179
7.2.2 Groundwater Recharge Estimation with Thornthwaite Model 180
7.2.3 Projected Groundwater Recharge 182
7.2.4 Groundwater Dynamics under High Abstraction and Climate Change 184
7.2.5 Results and Interpretations 185
7.2.4 Conclusion 196
CHAPTER 8: GENERAL CONCLUSION AND PERSPECTIVES 197
8.1 Introduction 197
8.2 Recharge Estimation 197
8.2 .1 Thornthwaite Method 197
8.2 .2 Penman method 198
8.2 .3 Turc Method 198
8.2 .4 Groundwater Potential Recharge Zone 198
8.3 Geochemistry 199
8.4 Recharge Projection with Thornthwaite Model 199

8.5 Climate Change Impact on Groundwater 200
8.6 General Conclusion 200
8.7 Perspectives 201
REFERENCES 203
APPENDICES 210

List of Acronyms

AET	Actual Evapotranspiration
AHP	Analytical hierarchy process
CORDEX	Coordinated Regional Downscaling Experiment
CT	Continental Terminal
DEM	Digital Elevation Model
DFA	Digital Field Analysis
DSA	Deep Sandstone Aquifer
DTMs	Digital Terrain Models
DWR	Department of Water Resources
EC	Electrical Conductivity
ESRI	Environmental Sciences Research Institution
ETo	Reference/Initial Evapo-Transpiration
ETP	Potential Evapo-Transpiration
ETR	Real Evapo-Transpiration
FAO	Food and Agriculture Program
GBA	Greater Banjul Areas
GIS	Geographic Information System
GPS	Global Positioning System
GCMs	Global Circulation Models
HWSD	Harmonized World Soil Database
IAP	Ion Activity Product
IIASA	International Institute for Applied Systems Analysis
IPCC	Intergovernmental Panel on Climate Change
ISRIC	International Soil Reference Information Centre
ITCZ	Intertropical Convergence Zone
JRC	Joint Research Centre
MCE	Multiple Criteria Evaluation
NAWEC	National Water and Electricity Cooperation
PET	Potential Evapotranspiration
RCP	Representative Concentration Pathway
RH	Relative Humidity
SI	Saturation index
SMB	Senegal-Mauritania Basin

SOTER	SOil and TERrain Digital Database
SPI	Standardized Precipitation Index
SRTM	Shuttle Radar Topography Mission
SSA	Shallow Sand Aquifer
SWC	Soil Water Capacity
UNESCO	United Nations Educational, Scientific and Cultural Organization
WRB	World Reference Base

LIST OF FIGURES

Figure 1: diagramme trilinéaire piper montrant le régime hydrochimique des eaux souterraines et la distribution des types d'eaux souterraines dans la zone d'étude. m=mélangé, cl-chlorure, mg=magnésium, ca-calcium, na-sodium. k=potassium, so4-sulfate, co3-carbonate et hco3-bicarbonate x
Figure 2: (a) variation temporelle de l'évaporation réelle; (b) précipitations; et (c) recharge des eaux souterraines, à partir des stations de banjul et de yundum, générée par le modèle thornthwaite de 1984 à 2016 xi
Figure 3: tendance de la recharge annuelle moyenne selon les scenarios rcp4.5 et rcp8.5 au cours de la periode 2006-2050 xiii
Figure 4: Interannual variation of rainfall at Banjul and Yundum from 1960 to 2016 15
Figure 5: Monthly variation of rainfall at Banjul and Yundum from 1984 to 2016 15
Figure 6: Values of the Standardized Precipitation index calculated for Banjul and Yundum stations, 1946-2016 17
Figure 7: Monthly mean rainfall for (A) Banjul and (b) Yundum, 1943-1976 and 1977-2009 19
Figure 8: Monthly average temperature from 1984 to 2016 measured at Banjul and Yundum stations 19
Figure 9: Monthly average RH from 1984 to 2016 measured at Banjul and Yundum stations 20
Figure 10: Monthly average insolation from 1984 to 2016 measured at Banjul and Yundum stations 21
Figure 11: Monthly average wind speed from 1984 to 2016 measured at Banjul and Yundum stations 21
Figure 12: Correlation between temperature, evaporation and rainfall at Yundum statiion, 1984-2016 22
Figure 13: Correlation between temperature, evaporation and rainfall at Banjul station, 1984-2016 23
Figure 14: Correlation between annual ETP and Rainfall at Banjul station, 1946-2016 23
Figure 15: Degital Elevation Model of the study area 25
Figure 16: Slope map (with +/-4m accuracy) of the study obtained from DEM 27
Figure 17: Hydrographic network of the GBA Basin (Source: https://usgs.gov, Access on 05/04/2018) 29
Figure 18: Morphometric description of the drainage network and their corresponding watershed in the GBA extracted from the MNT 30
Figure 19: (a) Soil map of the study area; (b) Spatial distribution of Soil Texture in the GBA: Clay (Cl), Sandy-Clay (SaCl), Clay-Loam (ClLo), Sandy-Clay-Loam (SaClLo) and Sandy-Loam (SaLo). 35
Figure 20: Land cover map of the GBA 37
Figure 21: The Geology map of the Senegal-Mauritania Sedimentary Basin (Diene et al., 2014, modified) 39
Figure 22: A schematic East-West cross-section of the Tertiary and Quatenary Sequences of The Gambia (Geology and Mineral Resources of The Gambia, 1988, modified) 41
Figure 23: Geology map of the GBA showing the different formation in the Continental Terminal (Extracted from the geology map of The Gambia, 1988, modified) 45
Figure 24: The hydrogeological map of the Senegal-Mauritania Sedimentary Basin (Diene et al., 2014, modified) 47
Figure 25: Hydrogeological correlation of boreholes across The Gambia (Adopted from P. O. Jarju, 2014, cited in Njie& Corr, 2006) 50
Figure 26: Aquifer thickness of the CT of the study area. 52
Figure 27: West-East hydrogeological correlation of boreholes across the study area 54
Figure 28: North-South hydrogeological correlation of boreholes across the study area 55
Figure 29: Zonation of the River Gambia Estuary and salinity profile (Adopted from P. O. Jarju, 2009, cited in Njie & Corr, 2006 58
Figure 30: Interannual variation of saline front of the River Gambia from 1973 to 1997 59

Figure 31: Organization chart of the methodological approach for the realization of the digital terrain model using SRTM image and the extraction of slope, drainage network and watersheds 63
FIGURE 32: (A) WATER SAMPLE COLLECTION AND SWL MEASUREMENT IN THE FIELD 65
Figure 33: (b) Map of the location of water sampling points 66
Figure 34: Location of static water level (SWL) measurement points 68
Figure 35: Flow chart showing groundwater potential recharge mapping methodology 80
Figure 36: (a) Conceptual model; (b) the bottom and top surface of the shallow aquifer 85
Figure 37: Model boundary conditions with locations of boreholes/wells 88
Figure 38: Water depth map of the shallow aquifer of the study area: (a) pre-monsoon (May) and (b) post-monsoon (November), 2018 field campaigns. 96
Figure 39: Piezometric map of the shallow aquifer of the study area: (a) pre-monsoon and 98
Figure 40: Piezometric map of the shallow aquifer of the study area: (b) post-monsoon, 2018; 99
Figure 41: Piezometric map of the shallow aquifer of the study area: (c) Groundwater Fluctuation Map 100
Figure 42: Seasonal Fluctuation of groundwater water Level at OB2 piezometer 102
Figure 43: Aquifer thickness of the CT of the study area. 103
figure 44: relationship between eff. rainfall, and monthly average values of infiltration, etp, etr, and stock of 125 mm for banjul station (1984-2016) calculated with the thornthwaite 110
figure 45: relationship between eff. rainfall, and monthly average values of infiltration, etp, etr, and stock of 125 mm for yundum station (1984-2016) calculated with the thornthwaite 110
Figure 46: Relationship between Eff. Rainfall, and monthly average values of infiltration, ETP, ETR, and stock of 125 mm for Banjul station (1984-2016) calculated with the Penman 113
Figure 47: Relationship between Eff. Rainfall, and monthly average values of infiltration, ETP, ETR, and stock of 125 mm for Yundum station (1984-2016) calculated with the Penman 113
Figure 48: Relationship between Eff. Rainfall, and monthly average values of infiltration, ETP, ETR, and stock of 125 mm for Banjul station (1984-2016) calculated with the Turc 115
Figure 49: Relationship between Eff. Rainfall, and monthly average values of infiltration, ETP, ETR, and stock of 125 mm for Yundum station (1984-2016) calculated with the Turc 115
Figure 50: Monthly evolution of mean potential evapotranspiration using ETPp. ETPth and ETPturc methods compared to Effective Rain (Eff. Rain) from 1984-2016 at Banjul and Yundum stations. 118
Figure 51: Geology: (a) Thematic layer; (b) Fuzzy Normalization 120
Figure 52: LULC: (a) Thematic layer; (b) Fuzzy Normalization 122
Figure 53: Slope: (a) thematic layer; (b) Fuzzy Normalization 124
Figure 54: Drainage density: (a) Thematic layer; (b) Fuzzy normalization 126
Figure 55: Groundwater fluctuation: (a) Thematic layer; (b) Fuzzy normalization 128
Figure 56: Aquifer transmissivity: (a) Thematic layer; (b) Fuzzy Normalization 130
Figure 57: Soil: (a) Thematic layer; (b) Fuzzy normalization 132
Figure 58: Groundwater potential recharge zone map 134
Figure 59: Box plot of the groundwater concentration of major ions in the GBA shallow aquifer 139
FIGURE 60: SPATIAL DISTRIBUTION OF EC (µS/CM) MEASURED IN THE FIELD: (A) PRE-MONSOON, (B) POST-MONSOON 2018; 142
Figure 61: Spatial distribution of EC (µS/cm) measured in the field: EC Contour: (c) pre-monsoon and (d) post-monsoon 2018 143
Figure 62: Distribution of pH measured in the field: (a) pre-monsoon and (b) post-monsoon, 2018. 145
Figure 63: Piper trilinear diagram showing hydrochemical regime of groundwater and distribution of groundwater types in the study area. m=mixed, Cl-Chloride, Mg=Magnesium, Ca-Calcium, Na-Sodium. K=Potassium, SO4-Sulphate, CO3-Carbonate, and HCO3-Bicarbonate 148

Figure 64: Geochemical processes of groundwater in the study area. Major Ions/Chloride ratios Vs. Chloride: (a) Na/Cl Vs. Cl, (b) Mg/Cl Vs. Cl, (c) K/Cl Vs. Cl, (d) Ca/Cl Vs. Cl, (e) SO4/Cl Vs. Cl, (f) NO3/Cl Vs. Cl and (g) HCO3/Cl Vs. Cl (circles: fresh groundwater; triangles: surface water) 150
Figure 65: Bivariate plots showing the relationship between: (a) Ca + Mg versus HCO3 + SO4. (b) (Ca + Mg) – (SO4 + HCO3) versus Na + K - Cl; (c) Na + K versus HCO3; and (d) Ca + Mg versus HCO3 + SO4.....152
Figure 66: (a) Cattel Scree plot of principal components with Eigenvalue >1; (b) Plot of PC1 and PC2 loading scores for the dataset of water samples; (c) Plot of PC1 and PC3 loading scores for the dataset of water samples; (d) Plot of PC2 and PC3 loading scores for the dataset of water samples; 156
Figure 67: Correlation Matrix of the 11 physicochemical parameters measured during post-monsoon of 2018.....160
Figure 68: Dendrogram for clustering of 52 groundwater sampling sites using the Euclidean distance metric (Ward's method).....163
Figure 69: (a) Mean value of the physicochemical parameters with the 3 clusters. 164
Figure 70: (b) Mean value of the physicochemical parameters with the 3 clusters. 165
Figure 71: (c) Mean value of the physicochemical parameters with the 3 clusters. 166
Figure 72: Saturation Indices (SI): (a) Calcite Vs. Ca + CO3; (b) Dolomite Vs. Ca + Mg + HCO3; (c) Gypsum Vs. Ca + SO4; (d) Halite Vs. Na + Cl.....168
Figure 73: Flow chart showing that mathematical models are based on the conceptual understanding of the aquifer system as expressed by mathematical equations (modified from Mercer and Faust, 1981) 172
Figure 74: Model calibration in Steady-State Flow (A) Hydraulic conductivity distribution; (B) Recharge estimation.....174
Figure 75: Comparison between observed and model simulated hydraulic heads (mbsl) in the steady-state condition in the GBA Basin 176
Figure 76: Hydraulic Head distribution under Steady-State simulation.....177
Figure 77: Mass balance during Steady-state calibration.....178
Figure 78 : (A) TEMPORAL VARIATION OF ACTUAL EVAPORATION; (B) PRECIPITATION; AND (C) GROUNDWATER RECHARGE, FROM BANJUL AND YUNDUM STATION GENERATED BY THE THORNTHWAITE MODEL FROM 1984-2016.....181
Figure 79: MEAN ANNUAL RECHARGE TREND THROUGH RCP4.5 AND RCP8.5 SCENARIOS DURING 2006-2050 183
Figure 80 : RELATIONSHIP BETWEEN PRECIPITATION AND RECHARGE: (A) RCP4.5; (B) RCP8.5.....184
Figure 81: SIMULATED HEAD OF 2019-2050 HORIZON BASED ON (A) REFERENCE; (B) AL; AND (C) A2 SCENARIOS.....186
Figure 82: HEAD TIME SERIES BASED ON REFERENCE, A1, AND A2 SCENARIOS DURING 2019-2050.....187
Figure 83: SIMULATED HEAD FOR 2050 HORIZON BASED ON: (A) REFERENCE; (B) RCP4.5; AND (C) RCP8.5 SCENARIOS.....189
Figure 84: TIME SERIES HEAD BASED ON REFERENCE, RCP4.5 AND RCP8.5 SCENARIOS DURING 2019-2050.....190
Figure 85: SIMULATED HEAD OF 2050 HORIZON BASED ON (A) REFERENCE; (B) A1-RCP4.5; AND (C) A1-RCP8.5 SCENARIOS 192
Figure 86: TIME SERIES HEAD BASED ON REFERENCE, A1-RCP4.5 AND A1-RCP8.5 SCENARIOS DURING 2019-2050 TIME SLICE.....193
Figure 87: COMPARISON OF CLIMATE CHANGE SCENARIOS (RCP4.5 AND RCP8.5) AND HIGH ABSTRACTION (A1=2500 M3/DAY) ON THE GROUNDWATER DYNAMICS OF THE FOUR OBSERVATION BOREHOLES (OBS1-OBS4) IN THE SHALLOW AQUIFER OF THE GBA.....195

LIST OF TABLES

Table 1: Population distribution in the study area 14
Table 2: Mean annual rainfall (mm) at Yundum and Banjul Stations 18
Table 3: Stream Hierarchy of GBA Drainage Basin 31
Table 4: Chronostratigraphic Classification of the Meso-Cenozoic Strata in the Gambia (Adopted from the Mineral Resources of The Gambia, 1995, Modified) 42
Table 5: Saaty's scale of preferences in the pair-wise comparison process (Saaty, 1980) 82
Table 6: Results of calculation of the balance according to Thornthwaite method for the period 1984-2016 at Banjul station 108
Table 7: Results of calculation of the balance according to Thornthwaite method for the period 1984-2016 at Yundum station 108
Table 8: Results of the annual average of the Thornthwaite calculation for the period 1984-2016 at Banjul and Yundum stations 109
Table 9: Result of calculation of the balance according to the Penman method for the period 1984-2016 at Banjul station 111
Table 10: Result of calculation of the balance according to the Penman method for the period 1984-2016 at Yundum station 112
Table 11: Results of the annual average of the Penman calculation for the period 1984-2016 at Banjul and Yundum stations 112
Table 12: Results of calculation of the balance according to Turc method for the period 1984-2016 at Banjul station 114
Table 13: Results of calculation of the balance according to Turc method for the period 1984-2016 at Yundum station 114
Table 14: Results of the annual average of the Turc calculation for the period 1984-2016 at Banjul and Yundum stations 115
Table 15: Comparison of results obtained by the Thornthwaite, Penman, and Turc methods for the period 1984-2016 at Banjul and Yundum stations 117
Table 16: Statistical analysis of annual averages of potential evapotranspiration from Thornthwaite (ETPth), Penman (ETPp), and (ETPturc) for Banjul and Yundum. 118
Table 17: Pairwise comparison matrix for criterion weightage by AHP 133
Table 18: Descriptive Statistics of Hydrochemical Parameters 138
Table 19: Descriptive Statistic of the Physicochemical Parameters 140
Table 20: (a) Eigenvalue, variability and cumulative % of each of the extracted components; (b) Correlation of physicochemical variables in each PCs 155
Table 21: Total variance explained by each PC and the loading matrix of PCs 158
Table 22: Pearson's Correlation Matrix of the 11 physicochemical parameters 159
Table 23: Mean parameter values of the three Cluster water groups (determined from HCA). 164
Table 24: Summary of steady-state calibration statistics 175
Table 25: Mean annual water budget for groundwater in GBA Basin 178
Table 26: Mean annual value (mm) of output parameters from Thornthwaite model, PET: Potential Evapotranspiration (mm); P: Precipitation; AET: Actual Evapotranspiration (mm); RO: Runoff; R: Recharge from 1984-2016 182
Table 27: Mean annual value (mm) of output parameters from Thornthwaite model. PET: Potential Evapotranspiration (mm); P: Precipitation; AET: Actual Evapotranspiration (mm); RO: Runoff; R: Recharge from 183

CHAPTER 1: GENERAL INTRODUCTION

This chapter presents the general context, problem statement, justification, objectives of the study, and literature review. Recharge estimation using three different numerical methods, hydrodynamic and hydrochemical chemical analysis of groundwater, various studies on climate model applications, aquifer water balance modeling/assessment, and the impacts of climate change on groundwater water resources of the study area are studied.

1.1 General Context – Problem Statement – Justification

Water resources are indispensable in every living system. They played a key role in economic and social activities such as water supply and sanitation, agriculture, industry, urbanization, transportation, hydropower electricity, fishing, etc. Although access to freshwater is considered a universal human right, over 40 percent of all people without improved drinking water live in sub-Saharan Africa. According to the United Nations, about 1.8 Billion people globally use contaminated sources of drinking water.

Groundwater is an important natural freshwater resource in most parts of the world which serves as the only source of potable water. Groundwater is a very crucial resource in semi-arid areas, including The Gambia, where freshwater supply is scarce. The Gambia is among the least water stressed countries in the world as total water withdrawal is less than 1.5 % of the total renewable water resources potential of 6.5km3 per year (Gambia Government, 2019). However, uneven distribution of fresh sources and constraints in water resources development and management of safe drinking water make access difficult for many segments of the population, especially those in the rural areas who often rely on unsafe water sources (Gambia Government, 2019). The GBA like many regions in the world relies on groundwater resources to meet its water needs. The economic growth of the GBA depends among other things on the availability, quality, and accessibility of freshwater. Surface water is not used for domestic and irrigation purposes in the GBA. The GBA is located downstream of the River Gambia where the river and its tributaries are constantly saline because of the permanent tidal influence of seawater. During the dry season, the saline-freshwater interface moved upstream of the River Gambia (P. O. Jarju, 2009) to about 250 km and retrieved back to 100 km towards the west in the rainy season. Hence using surface water for domestic, agricultural irrigation and industrial purposes in the GBA is almost impossible unless a desalinization technology is applied to the water. Furthermore, the extension of the saline

front in the river has also decreased the quality of groundwater in coastal aquifers, arable agricultural lands, fish productivity, and mangroves in the study area. Some boreholes and shallow wells close to the coastal zone already become saline and this could be due to high concentration of some irons such as chloride in the ground, highly saline soil, over-extraction of groundwater, and climate change causing seawater intrusion especially as the rate of groundwater recharge decreases with the declining annual rainfall and increasing evapotranspiration in recent years. Consequently, the demand for quality freshwater has increased for coastal dwellers.

Other factors increasing the demand for groundwater supplies and thus the overexploitation of these resources in the GBA over the past decade are mainly due to rapid population growth, industrial development, urbanization, agricultural expansion, and climate change. Besides, groundwater in big cities/towns close to the municipal waste and sewage dump sites (for example, the Bakoteh dumpsite, and Kotu wastewater pond) are vulnerable to pollution. The improper disposal and management of both solid waste and sewage can lead to the contamination of groundwater within the study area. Furthermore, water pollution is a significant problem due to lack of adequate sanitation facilities and awareness. In addition to water contamination, Moreover, these problems are expected to be exacerbated by climate variability and change and the absence of compensatory and adaptive management strategies (Gambia Government, 2019), particularly in coastal areas due to sea-level rise (Jaiteh Malanding, 2010a; Penny Urquhart, 2016).

Climate change is undeniably happening and poses additional risks to water resources. According to the latest report by the Intergovernmental Panel on Climate Change (IPCC), global average surface air and ocean temperatures are increasing at rates unequivocal to any other period on record (IPCC, 2007). In West Africa, the impacts of climate change with the anticipated reduction in precipitation and an increase in potential evaporation rates are expected to affect the rates of groundwater recharge. In the past decades, most countries in sub-Saharan Africa including the Gambia have experienced high variability and intensity rainfall and increasing drought incidents lead to flooding and reduction in groundwater levels respectively. These extreme conditions constitute significant threats to water resource, agriculture and public health management (Parry *et al.*, 2007). The Gambia experienced a decrease in annual rainfall amounts of about 30% from 1950 to 2000 which is as a result of reduction in the duration of the rainy period and the amount of rainfall (P. O. Jarju, 2009) which has negatively affected groundwater recharge rates and thus influenced water availability. Land cover is one of the most important factors controlling recharge to the

groundwater table (Graham, 2015). The Gambia's climate and human-induced environmental problems include deforestation and desertification. Deforestation is primarily caused by the expansion of agriculture while land degradation is a combination of unsustainable cultivation practices and changing climatic conditions. It has the potential to affect both the quantity and quality of groundwater and surface water due to increase runoff and pollution of water resources.

Despite the importance of groundwater, little research has been done on the potential impact of climate change on these resources and how this will affect the relationship between groundwater and surface water that are hydraulically connected (Alley, 2001). In the Gambia, no such research has been conducted before. For efficient and sustainable use of these resources, research as to how a changing climate will affect groundwater needs to be conducted under future climate. The need for a consistent policy of rational management of groundwater resources of the study area has become evident. However, a rational water management, should be based on a thorough understanding of water availability, quality and movement. Hence the need for this study which aims to investigate climate change impact on groundwater resources focusing on evaluation of water quantity and quality for present and predict how this resource will evolve in the future (Mid-Century, 2006–2050) and as well identify the potential recharge zones and flows direction of groundwater in the GBA. This research hypothesizes that changing climate in the future will negatively affect the groundwater resources of the study area. The fundamental research question, therefore, is what are the impacts of climate change on the groundwater resources of the GBA?

1.2 Literature Review

1.2.1 Hydrodynamic of Groundwater

Water is a fundamental requirement for life. Although 90% of the earth's surface is covered with water, only 2% of this resource is freshwater. Water on earth is found on the surface (surface water), sub-surface (groundwater) and glaciers (Sridharan, 2017). In many parts of the world, groundwater is the main source of freshwater that is used for domestic, industrial and agricultural purposes. In 2015, it was projected that 663 million people worldwide still do not have access to improved drinking water sources (WHO/ UNICEF, 2015), which are mostly supplied by unprotected wells and surface water. Since water is regarded as the fundamental pillar of life, safeguarding its quality and quantity is very paramount for effective and sustainable water resource management. Groundwater is

generally defined as water that is found in the zone of saturation below the ground (Ochungo et al., 2019). It is the only source of water for domestic and irrigation purposes in the Greater Banjul Areas (GBA) like most semi-arid regions of the world. The demand for groundwater has increased due to population growth in the GBA. Surface water is not used for domestic and irrigation practices in the study area due to the salinization of the river and its tributaries. Thus, it is indispensable to assess the quality and quantity of groundwater resources of the GBA as a source of drinking water and irrigation. The major ions of groundwater have to be analyzed to determine its suitability for domestic and irrigation purposes (Brindha & Elango, 2011).

1.2.2 Hydrochemistry of Groundwater

Hydrogeochemistry is used by many researchers to assess groundwater resources of an area (Blanchette et al., 2010). To have a comprehensive understanding of the nature of groundwater, through hydrogeochemical study of groundwater of an area has to be carried out. The chemical parameters of groundwater play a crucial role in classifying and assessing water quality (Sadashivaiah et al., 2008). Seher Dirican, 2015 stated that the purpose of using the physicochemical parameter is to test the quality of water before it is used for domestic, agriculture or industrial purposes.

The main aim of assessing the hydrochemistry of groundwater is to determine the physicochemical characterization of groundwater in order to have a better understanding of the hydrochemical functioning of the hydro-system of the study area and consequently determine the quality of the water for domestic and agricultural uses. Hydrochemical analyses of groundwater also help to understand the nature of groundwater, its spatial and temporal variation and as well to determine the groundwater types in the study area. In this study, physicochemical parameters (water depth, pH, T°C, EC) were measured from 52 sampling points of the shallow aquifer (borehole and wells) and 6 surface water during 2018 pre-monsoon (May) and post-monsoon (November). In addition, water samples were collected in November to analyze major ions and minor elements such as Br. The specific objectives are to evaluate: (1) the groundwater quality based on different indices for drinking and irrigation uses, and (2) hydro-geochemical facies and processes driving groundwater mineralization.

The Piper plots of major ions concentration of dissolved anion (SO_4, Cl, Br, and NO_3), and alkalinity (HCO_3) and cations (Na, Mg, Ca and Ka) were used to identify the water types

of groundwater in the GBA. Similarly, a statistical description of these ions is given in Table 13.

1.2.2 Climate change impact on groundwater resources

The Gambia is among the least developing countries that are most vulnerable to climate change and variability due its low-lying topography, coupled with high dependence on subsistence rain-fed agriculture and inadequate drainage and storm water management system in the context of rapidly expanding un-regulated urban expansion to the (Jaiteh Malanding, 2010b). Climate change poses major development challenges in productive sectors such as agriculture, forestry, wildlife and tourism would be adversely affected by rises in sea level (Camara, 2013). Global climate change is predictable to have negative impacts on water resources due to increased variability in extreme events such as droughts and floods (Kevin Hiscock, 2006).

Groundwater is an essential water resource in the Gambia, particularly in the Greater Banjul Area (GBA), where groundwater is the only source of water for domestic, agricultural and industrial purposes. Surface water (the river and its tributaries) in the study area are saline throughout the year because of permanent tidal influence of seawater. Hence using surface water for domestic, agricultural irrigation and industrial purposes in the GBA is almost impossible unless a desalinization technology is applied on the water.

The quality of groundwater in coastal aquifers is deteriorating due to marine water intrusion caused by sea level rise and in other parts of GBA due to pollution from infiltration of agricultural chemicals. Recharge in the shallow aquifer of the study area is mainly from infiltration of rainwater through the unsaturated zone. Climate change and variability will likely have variable long-term effects on groundwater recharge rates and mechanisms through reduced rainfall. However, the effects of climate change on recharge may not necessarily be negative in all aquifers during all periods of time (Jakeman et al., 2016). In the face of climate change and other factors affecting the quantity and quality of groundwater, urgent actions need to be taken to assess its availability and quality in order to make sustainable management and planning of the resources.

Climate change impacts have been felt in the Gambia in the mid-20th century. Long-term rainfall recorded from Banjul station for the last half of the 20th century (i.e. 1950 to 2000) indicates a decrease in annual rainfall amounts of about 30%. This has been evident in the reduction in the quantity of rainfall amounts recorded in the month of August and also the

length of the rainy season, particularly during the period 1968 to 1985, and in 2002 (P. A. O. Jarju, 2009). This erratic rainfall pattern has led to lowering of groundwater level due to less amount of infiltrated rainwater to the water table and also marine water intrusion into coastal aquifers.

Many initiatives have been undertaken by the Government of the Gambia and partners with the aim of addressing climate change effects on different sectors. For instance a national climate change policy was development which identified priority areas of implementation, adaptation and mitigation measures. Climate Change and Development in the Gambia is a study that examines the threats associated with anthropogenic climate change; vulnerable ecosystems and ecosystem services; and evaluates how to integrate responses to climate change and adaptation measures into strategies for poverty reduction, to ensure sustainable development.

The National Climate Change Policy of The Gambia, 2016 has been developed with the focus to enhance institutional arrangements for coordination and mainstreaming, outlines a new integrated approach to resource mobilization, and develops a clear policy direction for human resource development. It also focuses attention on policy priorities in four key thematic clusters, and emphasizes the links between climate change adaptation and disaster risk reduction. Lastly, it outlines the approach to be followed to develop the implementation framework for the Policy, through the subsequent National Climate Change Response Strategy and Action Plan. Water resources vulnerability and impacts to climate change: Since the 1960s, large areas of freshwater swamps and the river in western Gambia have been replaced by salt pans or salt water marshes, as a result of reduced freshwater inflow from storm runoff. An increase in sea level would enable saltwater to penetrate farther inland and upstream beyond the estuary area and into freshwater wetlands, and to infiltrate groundwater aquifers. Increased salinity would be harmful to some aquatic plants and animals, and would threaten human use of water.

1.3 Research Questions

- Which recharge approach is the most appropriate for groundwater recharge estimation for the GBA?
- What is the rate and direction of groundwater flow in the GBA Shallow (Continental Terminal) Aquifer?
- What ions determines the groundwater quality of the shallow aquifer of the GBA?

- ❑ To what extent will the impact of climate change and high abstraction affect groundwater availability and quality in the GBA?

1. 4 Thesis Objectives

1.4.1 Main Objective

The aim of this study is to analyse how climate change will impact groundwater resources of the Greater Banjul Area (GBA) by modelling the groundwater dynamics for sustainable management of the resources.

1.4.2 Specific Objective

The specific objectives of the thesis are to:

- understand the hydrodynamics of the shallow (Continental Terminal) aquifer of the GBA;
- evaluate the groundwater quality of the Continental Terminal (CT) of the GBA;
- model groundwater regime of the GBA under steady state condition;
- Simulate the response of the groundwater system to high abstraction and climate change under RCP 4.5 and RCP 8.5 scenarios.

1.5 Hypothesis

The hypothesis below is formulated and tested in this study:

- ❑ The best recharge estimation method will be the Turc
- ❑ The groundwater flow direction is expected to originate from the mould moving towards water bodies (River and tributaries)
- ❑ Groundwater quality is expected to be within the WHO acceptance guidelines for drinking water
- ❑ Groundwater head in the GBA aquifer will decline due to high abstraction and climate change impacts.

1.6 Novelty

There was no such study conducted in the GBA that addressed the impact of climate change and high abstraction on groundwater resources as well as delineated the potential

recharge zones. Thus, the results obtained in this study can be a guide for future researchers. For example, the three groundwater recharge estimation methods used in this study and the identification of potential recharge zone using remote sensing, GIS and MCE could be used as a reference or benchmark for future studies. The hydrochemical, potential recharge zone and projected climate change results from this study will be a guide for policy makers and groundwater managers in water resources management.

1.7 Scope of the Thesis

This study focuses on the impact of climate change on groundwater resources of the shallow aquifer of the Greater Banjul Area (GBA). The work is based on analysis of the water balance components by calculating the groundwater recharge due to rainfall and groundwater abstractions. Numerical methods for recharge estimation were done for Thornthwaite, Turc and Penman methods but water table fluctuation and Isotopic methods were not within the scope of this study due to data constraint and access to well equipped laboratory. Groundwater quality and dynamics were analyzed. Future groundwater availability was considered in this study by evaluating changes in groundwater head over 2019-2050 horizon under the influence of climate change and high abstraction.

1.8 Expected Results

At the end of this research we expect:

- Recharge estimation in the GBA shallow aquifer using the best recharge estimation methods;
- Delineation of the potential recharge zone of the study area;
- The assessment of groundwater quality in the GBA shallow (CT) aquifer;
- The assessment of the impact of climate change on groundwater resources of the GBA by 2050.

1.9 Thesis Structure

This thesis is structured into 7 chapters. Chapter 1 provides the general introduction which gives a general context of the problem statement, justification including literature review, hypothesis, novelty, objectives, and researcher questions that this research seeks to

answer and the expected results. Chapter 2 describes the geographic and climatology of the study area highlighting the location and socio-economic situation, climatic condition, soil, geomorphology, and hydrography, the geology and hydrogeology of the study area is described in this chapter. Descriptions of the various data collected, the tools and methods used in analyzing the data are detailed in chapter 3. It also describes the MODFLOW model and input data used, the model setup, and calibration of the model. Chapter 4 deals with the results and discussion on the hydrodynamics and hydrochemical analysis of groundwater quality. Chapter 5 discusses the results of the different groundwater recharge methods used such as the water balance (Thornthwaite, Penman, and Turc), and makes a comparison between the methods. This chapter further highlighted the results of the potential recharge zones of the study area. Chapter 6 concentrates on concepts of Visual MODFLOW and the adaptation of this model to the study area. This involves the calibration and predictive analysis of the model. It also discussed results obtained from the assessment of the water balance components from the MODFLOW model are also discussed in this chapter. This chapter further seeks to assess climate change impacts on groundwater recharge of the study area. Chapter 7 highlights the general conclusions, perspectives, and recommendations.

CHAPTER 2: STUDY AREA

This chapter describes the location and socio-economic activities of the study area (i.e. The GBA) in detail by considering several characteristics of the study area such as location, topography, climate, geomorphology, geology, hydrogeology, hydrology soil, and land use/cover.

2.1 Location and socio-economic situation

The Gambia is situated on the West coast of Africa between latitude 13^0 3″ and 13^0 49″ N and longitude 16^0 48″ and 13^0 47″ W. The country is bordered on the West by the Atlantic Ocean and on the remaining three sides by the Republic of Senegal. The Gambia has a total land area of 11,295 km², 20% of which is considered a wetland.

The River Gambia flows from east to west dividing the country into the north and south banks. The Gambia lies within the tropical sub-humid eco-climatic zone, with a rainfall range between 800 and 1400 mm annually. The country has a Sahelian climate, characterized by a long dry season (November to May the following year) and a short wet season (June to October) (Gambia, 2012b). According to the 2013 National Population Census, the total population of the Gambia is about 1.9 million people with a population growth rate of 2.8% (GBoS, 2013). Compared to the 2003 population figure of about 1.5 million with a population density of 129 persons per square kilometer, the country noticed an increased population of nearly 400,000 people.

The agriculture sector accounts for about 30% of the country's GDP and provides employment for over 44% of the population (Gambia, 2012a) and 70% of the domestic exports (Courtney et al., 2016). Most agricultural production is centered on subsistence crops and cash crops such as cashews, peanuts, groundnuts, and cotton. In addition to agriculture, the tourism and service sector is the major economic driver for the Gambia, accounting for 60% of the GDP (Courtney et al., 2016).

The study area is the Greater Banjul Areas (GBA) located at the Southwestern part of the Gambia between latitude 13^0 00″ - 13^0 30″ N and longitude 16^0 50″ and 16^0 20″ W (Figure 1). It is limited to the north by the River Gambia, to the East by Bullock Bolong, to the south by Cassamance, and south-west by the Atlantic Ocean. It covers an area of 1001.7 km^2, which is about 9% of the total land area of the country. The study area covers two municipalities: Banjul City Council (BCC) and Kanifing Municipal Council, and four

administrative districts of Kombo North, Kombo West, Kombo Central, and Kombo East. The study area has a Sudano-Sahelian climate, which is characterized by 2 distinct seasons: a short rainy season from June to October and a long dry season extending from November to May with temperatures as low as 15°C.

It is densely populated with 926,120 inhabitants which accounts for about 49% of the country's total population (GBoS, 2013). A greater number of the economically active population in the study area particularly the eastern part is involved in agricultural activities, which include cultivation of cash crops (groundnuts, mangoes, and cashew nuts); food crops (cassava, potatoes, and rice) and horticulture (vegetable gardening). Outside the rainy season, all agricultural and domestic water needs are mainly supplied from the Shallow Sand/Continental Terminal (CT) aquifer exploited through local wells and boreholes. Other major economic activities in which communities along the coastal line and tributaries of the study area are engaged in fishing and oysters harvesting. However, most of the arable agricultural lands are converted to settlements due to the increasing population and this is partly because of immigration from rural areas to the GBA for finding jobs.

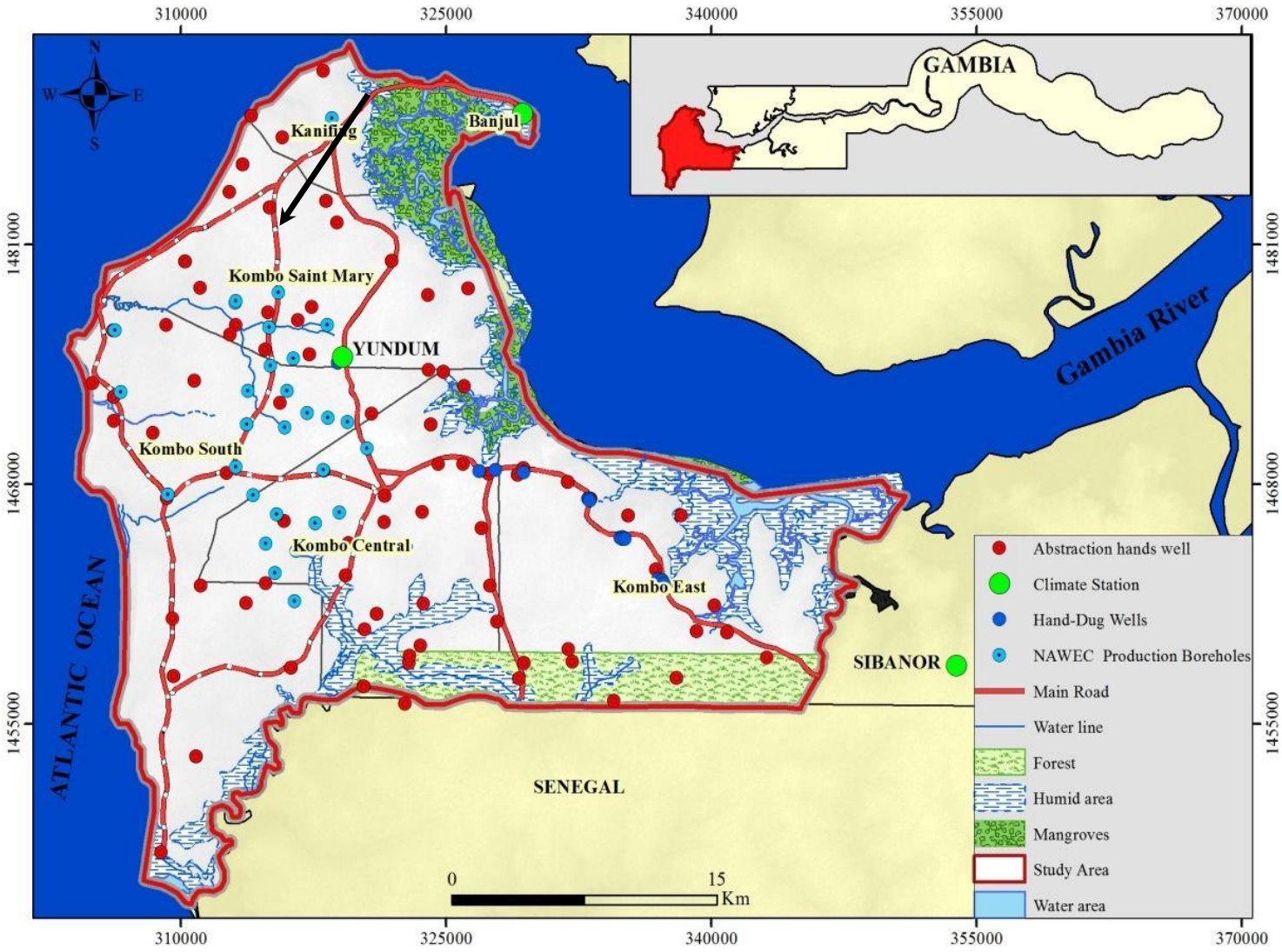

FIGURE 1: LOCATION OF STUDY AREA SHOWING THE DISTRIBUTION OF SAMPLING POINTS

[12]

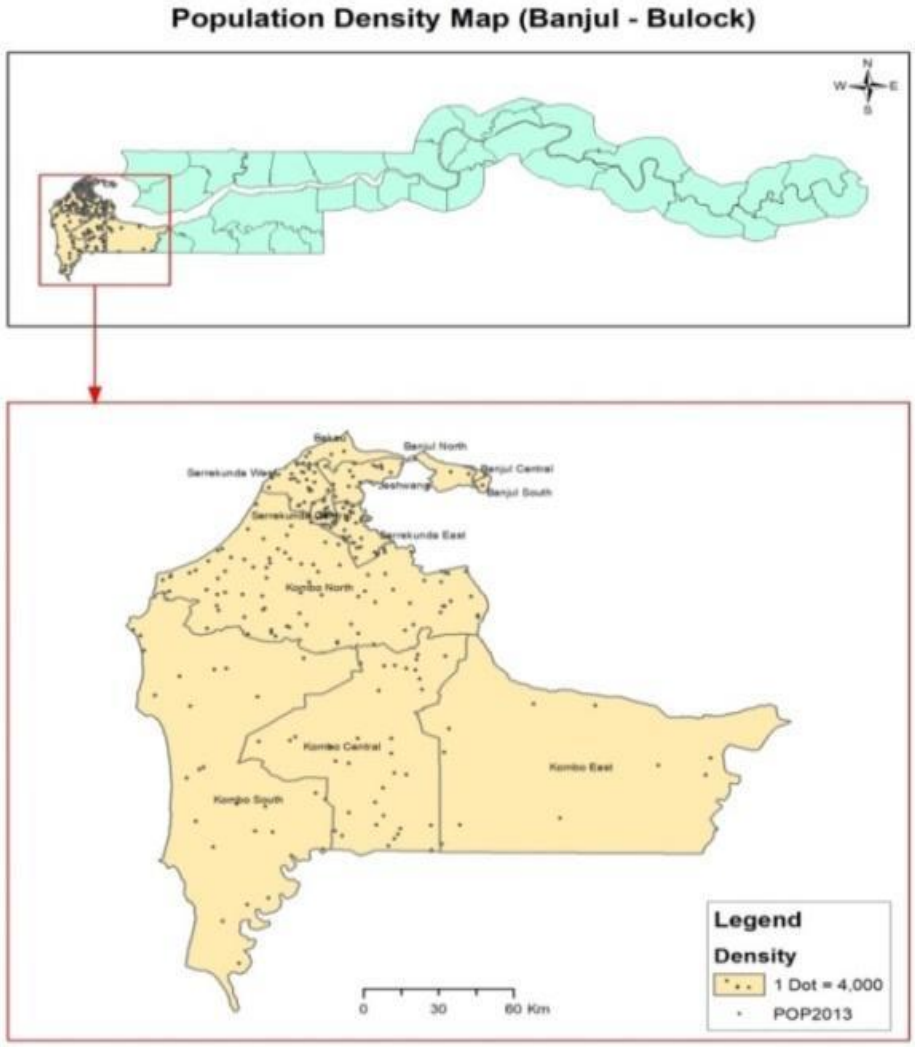

FIGURE 2: POPULATION DENSITY MAP SHOWING THE CONCENTRATION OF POPULATION IN THE STUDY AREA (GBOS, 2013)

TABLE 1: POPULATION DISTRIBUTION IN THE STUDY AREA

LGA	DISTRICT	AREA (km^2)	POP 2013
Banjul	Banjul Central	0.776201	11562
Banjul	Banjul North	7.39638	11285
Banjul	Banjul South	1.194809	8207
Kanifing	Bakau	9.752759	28554
Kanifing	Jeshwang	13.531605	66604
Kanifing	Serekunda Central	3.96262	75304
Kanifing	Serekunda West	13.071201	96559
Brikama	Kombo North	184.408194	339377
Brikama	Kombo South	278.041092	106780
Brikama	Kombo Central	168.920235	140029
Brikama	Kombo East	298.162373	41859
Total		**979.217526**	**926,120**

2.2 Climate context

2.2.1 Rainfall in the Study Area

The study area has a tropical sub-humid climate, which is characterized by two distinct seasons (wet and dry). The rainy season in the GBA lasts for 5 months (June-October) with hot humid weather. Rainfall in the GBA is under influence of the north-south migration of the Inter-Tropical Convergence Zone (ITCZ) as is the case for the whole of the country.

The highest rainfall is recorded in August (Figure 7) for all the two stations having a monthly mean of about 357 mm and 374 mm for Banjul and Yundum respectively. More than 70% of the annual rainfall is experienced from July to September. There is high spatial and temporal variability of average annual rainfall in the country. A large South-East gradient exists with the highest rainfall in the Southern part (about 1200 mm/year) and lowest rainfall towards the East (less than 800 mm/year) of the Country. The study area found in the Southwest part of the country has the highest rainfall record than other regions of the country. The annual mean rainfall for the GBA is about 900 mm/yr. The spatial distribution of annual average rainfall in the GBA is highly variable (Figure 6).

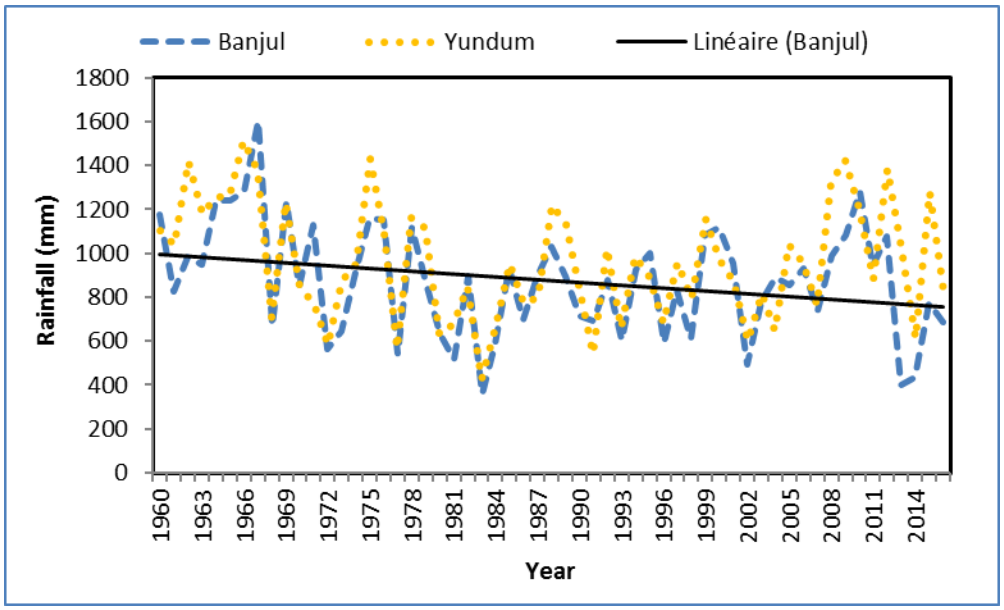

FIGURE 4: INTERANNUAL VARIATION OF RAINFALL AT BANJUL AND YUNDUM FROM 1960 TO 2016

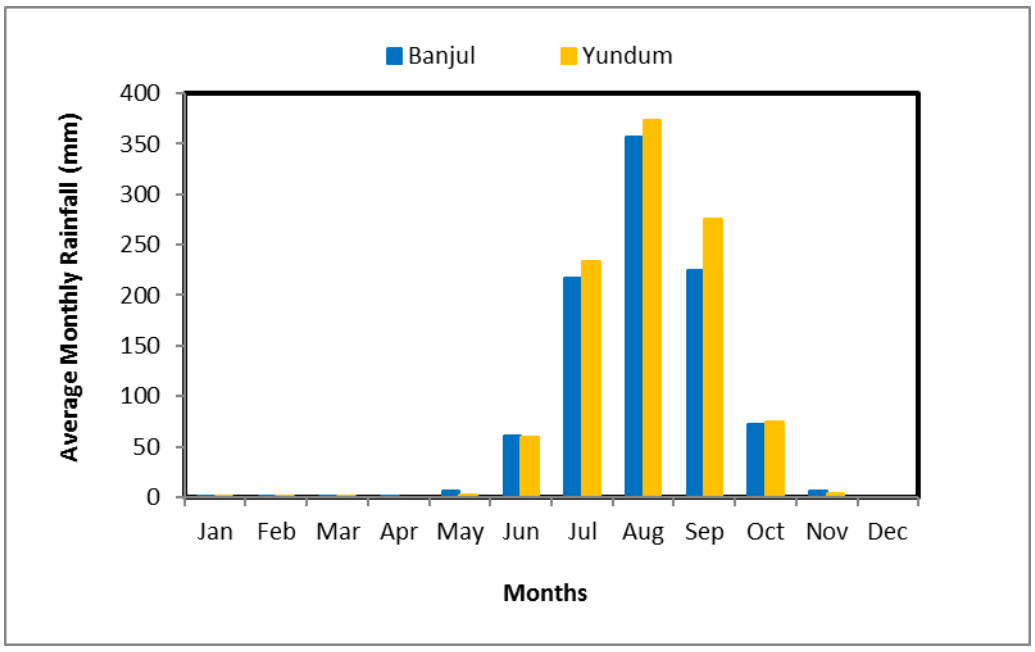

FIGURE 5: MONTHLY VARIATION OF RAINFALL AT BANJUL AND YUNDUM FROM 1984 TO 2016

The high variability in annual mean rainfall can be studied by calculating the Standardized Rainfall Index (SPI). McKee et al. (1993) developed the Standardized Precipitation Index (SPI) to define and monitor wet and dry periods based on rainfall variables. SPI is the difference between precipitation and the long-term mean for a particular period divided by the standard deviation a (normalized index) representing the probability of

occurrence of an observed rainfall amount when compared with the rainfall climatology at a certain geographical location over a long-term reference period (Hidayat et al, 2018; Pramudya et al., 2017; Mckee et al., 1993). According to McKee et al. (1993), he classified the SPI value for extremely wet (>= 2.0), very wet (1.5 to 1.99), moderately wet (1.0 to 1.49), near normal (-0.99 to 0.99), moderately dry (-1.49 to -1.0), severely dry (-1.99 to -1.5) and extremely dry (>= -2.0). The negative SPI values represent rainfall deficit, whereas positive SPI values indicate rainfall surplus. The intensity of drought events can be classified according to the magnitude of negative SPI values such that the larger the negative SPI values are, the more serious the event would be (Dieng et al., 2017). However, these annual averages hide disparities related to the variations. The SPI formula proposed by McKee et al. (1993) enables us to analyze the temporal variability of rainfall and thus identify the dry, medium, and wet years compared to an average of one given period. It is calculated as follows (McKee et al., 1983):

$$SPI_R^i = \frac{P_{R-}^i P_R}{\sigma_R} \quad (1)$$

Where, SPI_R^i is Standardized Precipitation Index;

P_R^i is the mean annual precipitation of the station R;

P_R is the mean inter-annual rainfall; and

σ_R is the standard deviation of the inter-annual rainfall at station R

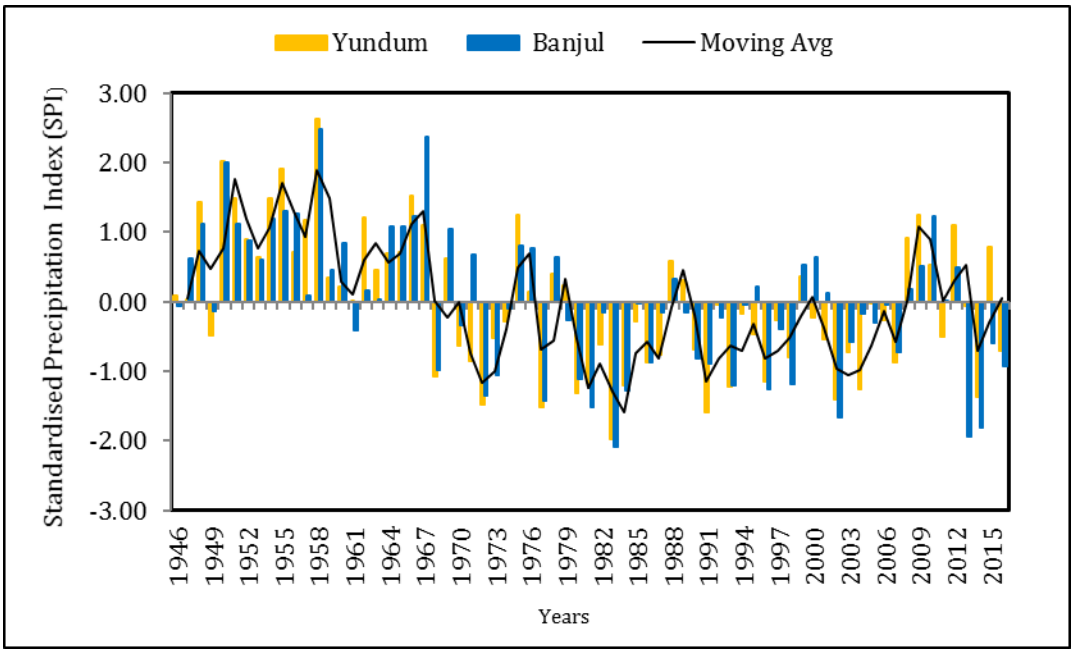

FIGURE 6: VALUES OF THE STANDARDIZED PRECIPITATION INDEX CALCULATED FOR BANJUL AND YUNDUM STATIONS, 1946-2016

When the value of SPI for a certain period is less than zero (SPI < 0), it is considered dry or deficit; when SPI value is greater than zero (SPI > 0), it's referred to as wet or surplus and average when the SPI = 0.

The SPI was calculated from the rainfall data recorded for Banjul and Yundum stations between 1946 and 2016. From Figure 5 above we see that both stations depict the same trend. There was a surplus of rainfall from 1946 to 1970 (pre-industrial revolution) which is referred to as the wet period having a mean annual rainfall of 1145 mm/year and 1258 mm/year for Banjul and Yundum respectively. A trend of rainfall deficit has been observed around 1970 to 2000 and this is considered the dry period. This pattern reflects the dry period of the Sahel rainfall index. Mean annual rainfall in Banjul and Yundum is 828 mm/year and 931 mm/year respectively. There has been a lot of rainfall variation from early 2000 to date. Considering 1961-1990 (reference period by the IPCC) as the reference period for this study with averages of 977 mm/year for Yundum and 904 mm/year for Banjul as compared to the averages in 1946-1970, there is a deficit of rainfall heights of more 240 mm for both stations.

TABLE 2: MEAN ANNUAL RAINFALL (MM) AT YUNDUM AND BANJUL STATIONS

Year	Yundum	Banjul
1946-1970	1258	1145
1961-1990	977	904
1990-2016	931	828

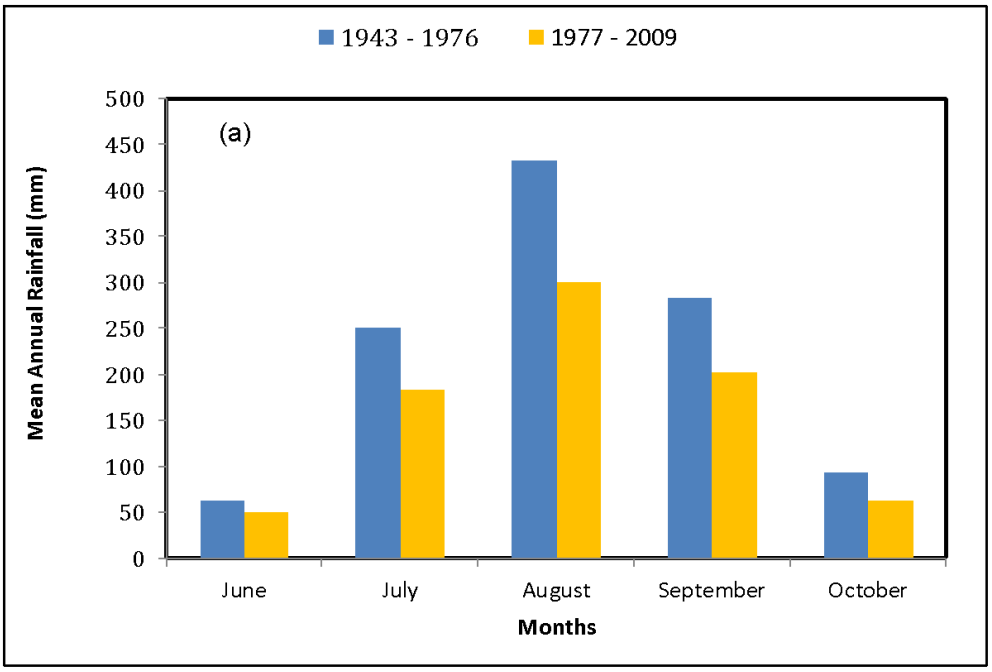

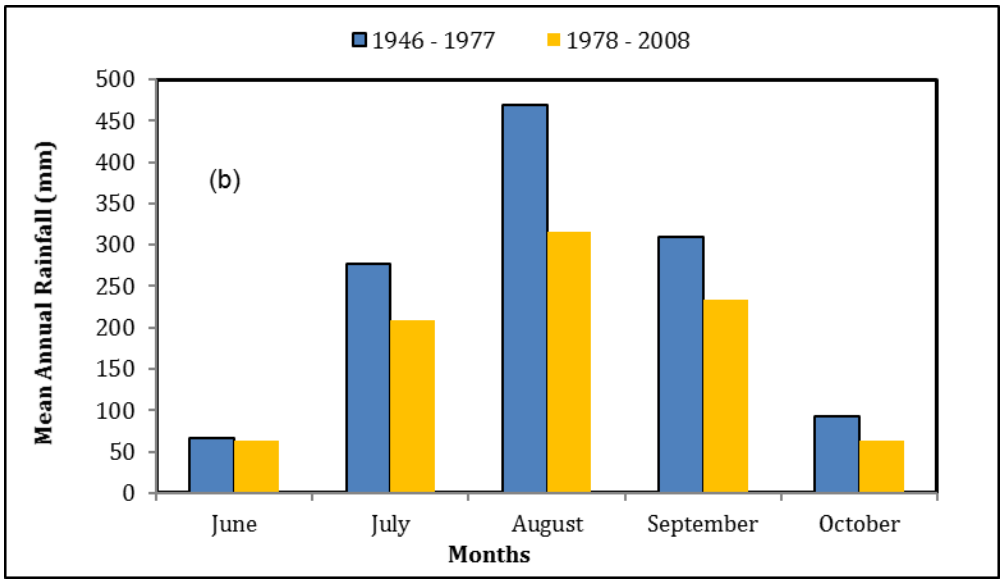

FIGURE 7: MONTHLY MEAN RAINFALL FOR (A) BANJUL AND (B) YUNDUM, 1943-1976 AND 1977-2009

2.2.2 Temperature

The average monthly temperatures in the study area range between 24°C up to 29°C (Figure 7). In the dry season, mean daytime temperatures could rise as high as 36°C between March and June. The mean annual temperature for the GBA is around 27^0C. Generally, monthly average temperatures in the study area are high with the highest peaks in October. The hottest months of the year are June to July and October. Low temperatures are experienced in the Harmattan from November-February.

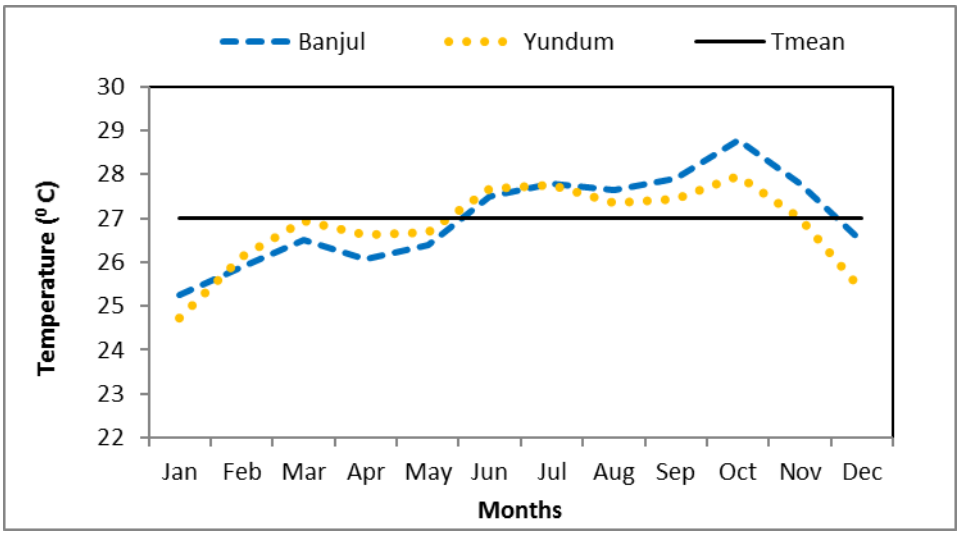

FIGURE 8: MONTHLY AVERAGE TEMPERATURE FROM 1984 TO 2016 MEASURED AT BANJUL AND YUNDUM STATIONS

2.2.3 Relative Humidity

The monthly change in relative humidity (RH) coincides with the two seasons of the year. The monthly mean relative humidity peaks during the wet season with values as high as 86% (Figure 8) for Yundum and around 79% for Banjul. This is the period in which there is a lot of moisture in the atmosphere and it is an indication of high rainfall in this area. The RH starts to go down in November up to April and it starts to rise again in April. The mean monthly minimum relative humidity during the dry season could be as low as 47%. Yundum is more humid during the rainy seasons which contributes to high rainfalls recorded in this area and any of the other regions in the country.

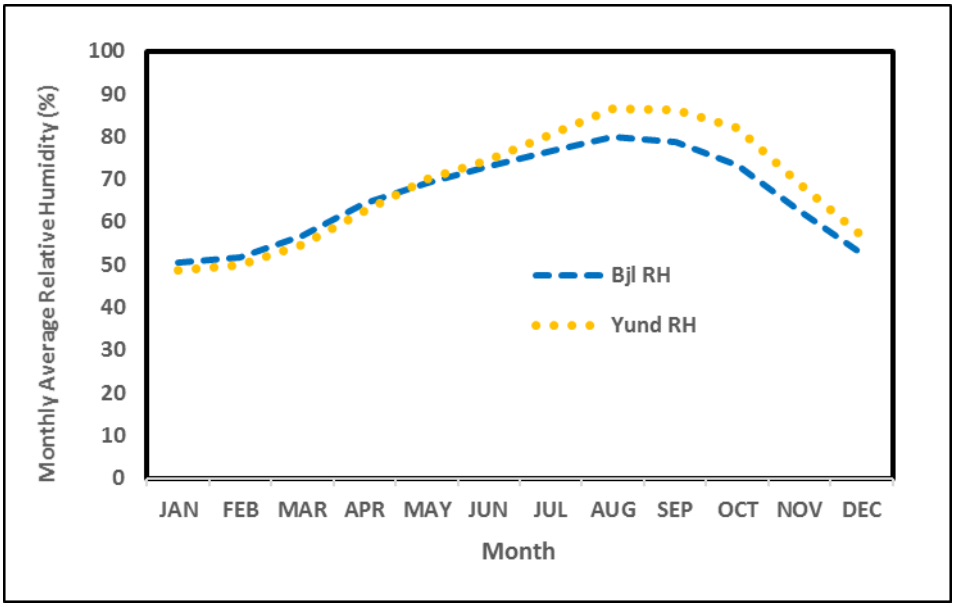

FIGURE 9: MONTHLY AVERAGE RH FROM 1984 TO 2016 MEASURED AT BANJUL AND YUNDUM STATIONS

2.2.4 Insolation

Average solar insolation in the study area 8.3 hours (Figure 9) and its maximum value is about 9 hours during April. On the other hand, minimum insolation of 6.3 hours occurs during the rainy season while relative humidity is at its peak. Yundum has the highest mean insolation during the dry season and the lowest in the wet reason than the other two stations in the study area.

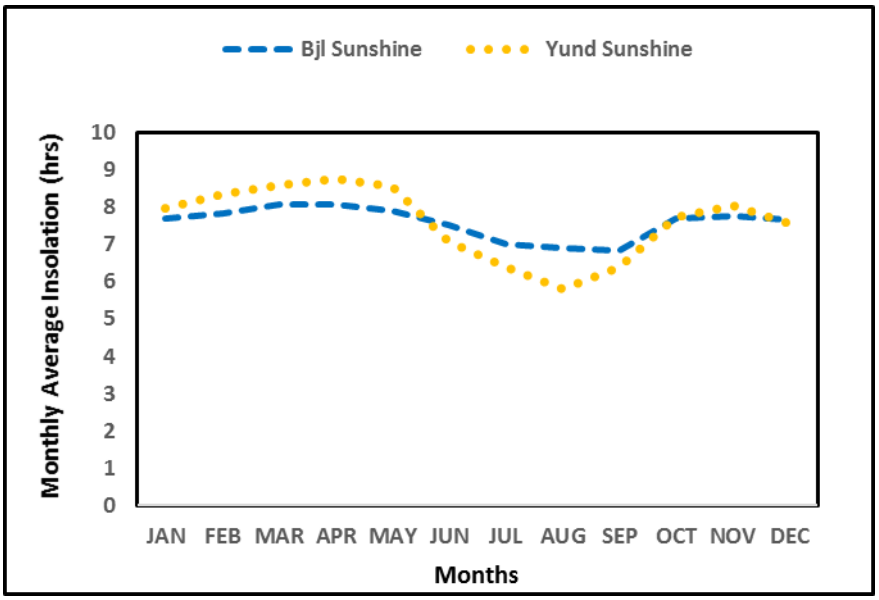

FIGURE 10: MONTHLY AVERAGE INSOLATION FROM 1984 TO 2016 MEASURED AT BANJUL AND YUNDUM STATIONS

2.2.5 Wind Speed

Two major winds determine the climate of the Gambia. In the dry season, the North-East Trade Winds or Harmattan, originating from the Sahara Desert and blows from North to North-East from November to May dominates the climate. This wind is very dry and hot with little or no moisture in it. On the other hand, the South-West Monsoon Winds originating from the Atlantic Ocean dominates the climate during the rainy (wet) season from June to October. These winds carry a lot of moisture responsible for rainfall in our region.

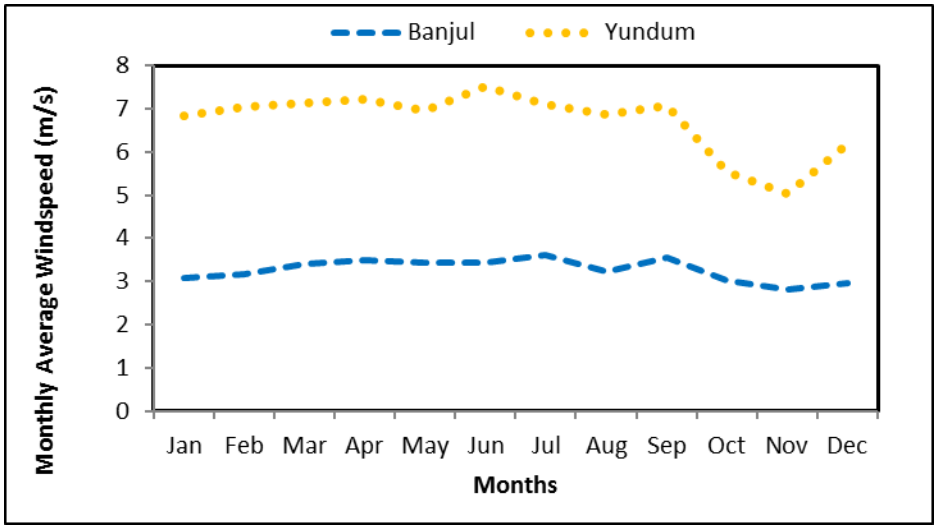

FIGURE 11: MONTHLY AVERAGE WIND SPEED FROM 1984 TO 2016 MEASURED AT BANJUL AND YUNDUM STATIONS

2.2.6 Evaporation and Evapotranspiration

Evaporation is the main process of water transfer in the hydrological cycle. It is measured using a Piche evaporimeter. It is more pronounced in the dry season than in the rainy season. Evapotranspiration (ET) is defined as the movement of water from the earth's and water body surfaces (direct evaporation) and transpiration from a vegetation surface to the atmosphere. Evapotranspiration with unlimited water supply is called potential evapotranspiration (PET). It is the maximum value that evapotranspiration can have when the soil reaches its maximum retention capacity. The maximum value of the actual evapotranspiration (AET) is equal to the PET when the soil has unlimited water. AET is very difficult or even impossible to determine directly due to the complexity of the biological behavior of plants and soil diversity. In the study area, evaporation is lowest during the rainy season (August-September) and reaches its minimum value in August when temperatures are low and rainfall achieves its maximum in the same month. In May, when the temperature is very high, evaporation is at its peak. This shows the correlation between temperature and evaporation maximum in May during the dry season (Figure 11) when temperatures are high.

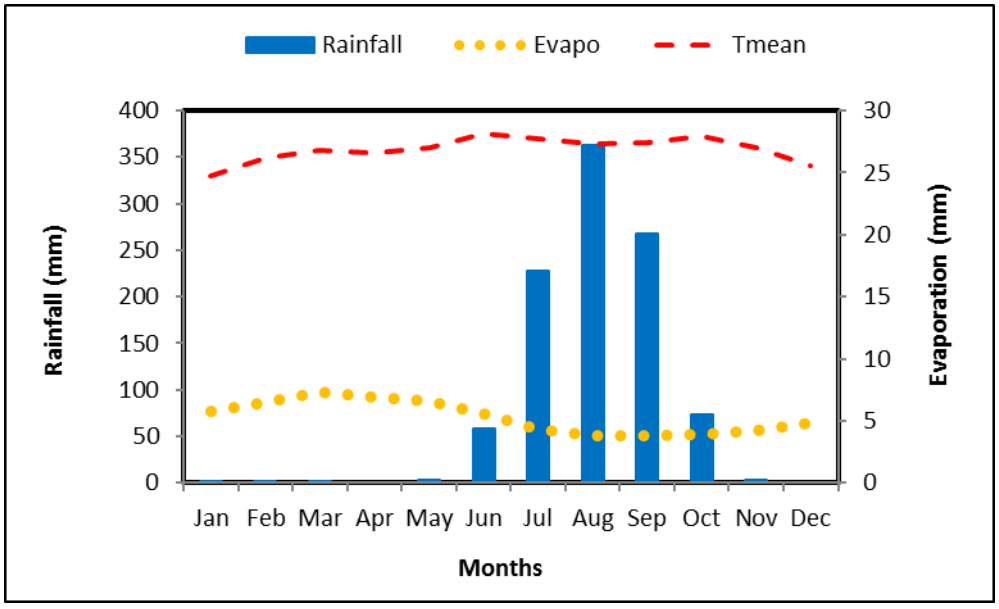

FIGURE 12: CORRELATION BETWEEN TEMPERATURE, EVAPORATION AND RAINFALL AT YUNDUM STATIION, 1984-2016

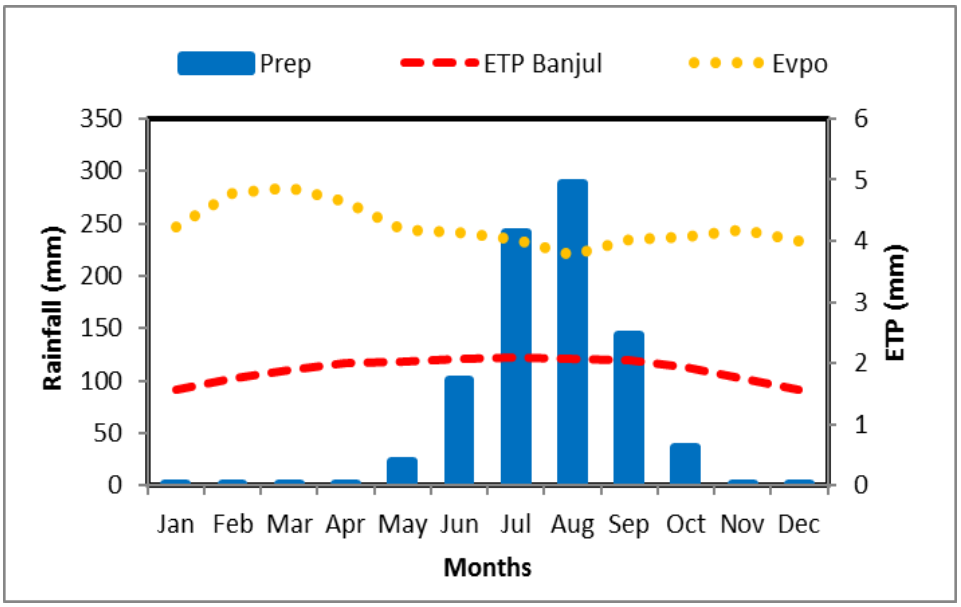

FIGURE 13: CORRELATION BETWEEN TEMPERATURE, EVAPORATION AND RAINFALL AT BANJUL STATION, 1984-2016

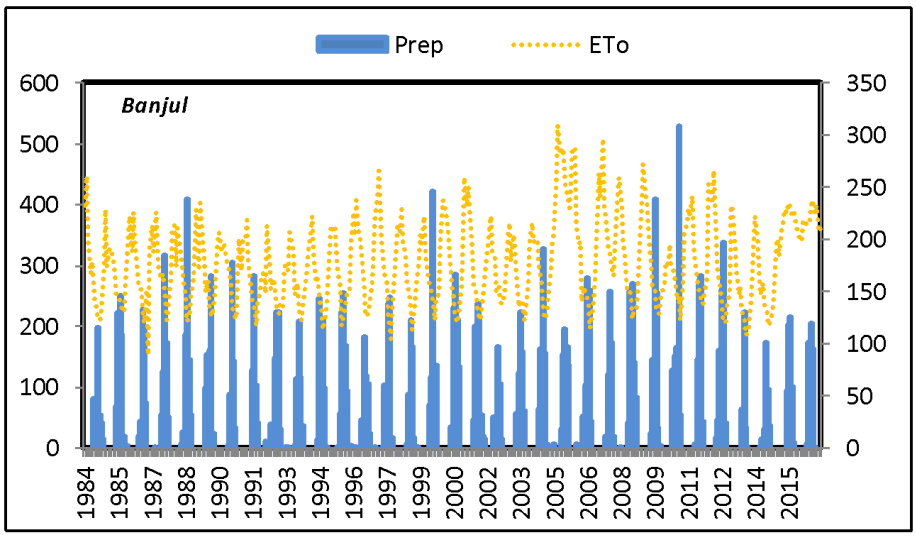

FIGURE 14: CORRELATION BETWEEN ANNUAL ETP AND RAINFALL AT BANJUL STATION, 1946-2016

2.3 Geomorphology and Hydrography

2.3.1 Geomorphological Context

Geomorphology, which is concerned with landform, materials and their related processes, is relevant in all aspects of environmental management involving physical phenomenon. Geomorphic process is the outcome of multifaceted interaction between agents of geology, climate, hydrology, topography, soils and organisms.

2.3.1.1 Regional Geomorphology Context

The geomorphology of The Gambia is dominated by the River Gambia and its floodplains, river banks and wetlands (Jaiteh Malanding, 2010b). The river water in western part of the Gambia is saline, which is responsible for the highly saline soils (clay and alluvium) along its floodplains and mangrove areas. The topography of the country is low-lying and its elevation is not more than 50 m. More than 50% of the landmass of the Gambia is below 20 (masl), less than 40% is 10m high or below and 4% is above 50 (masl). The eastern part of the country is characterized by a dissected plateau with sand hills. The coastal areas on the western part of the country on the other hand is dominated by the soils are generally unconsolidated marine and aeolian sand. The ferruginous sandstones, which underlie the unconsolidated soils, form cliffs of about 20 meters high.

2.3.1.2 Local Geomorphological Context

The topography of The Gambia is low-lying with elevation less than 60m above sea level. The valley floor is the area immediately along the River Gambia and its tributaries is characterized by poorly drained alluvial sediment formations which are subjected to regular seasonal flooding. The valley makes up nearly 4,048 km^2, 39% of the land area of the country (The Gambia, 2015). In the study area, the valley broadens and seasonally inundated swamps appear on either side of the river. These swamps can extend for more than 2km away from the river. It has poorly drained soil along the valleys of the River Gambia and its tributaries. Therefore, the geomorphology of the study area is dominated by the River Gambia which divides the country into two strips of land.

A Digital Elevation Model

The DEM of the study area obtained shows altitudes ranging from -10 to 47 m. The general pattern of the area is characterized by low plateaus (hills) 20-40 m in altitude located in the northwest and east of the zone (Figure 14). A network of narrow low-sloping valleys draining the waters towards the River Gambia and Atlantic Ocean during the rainy season. However, the elevation of the study area decreases towards the entire riverbanks and mangrove areas in the north and the Atlantic Ocean on the west with altitude ranging from -10 to 8m. This constitutes 20% of the land of the study area. Highly elevated areas of less 50m are found in the north-western, central and south-eastern part of the study area

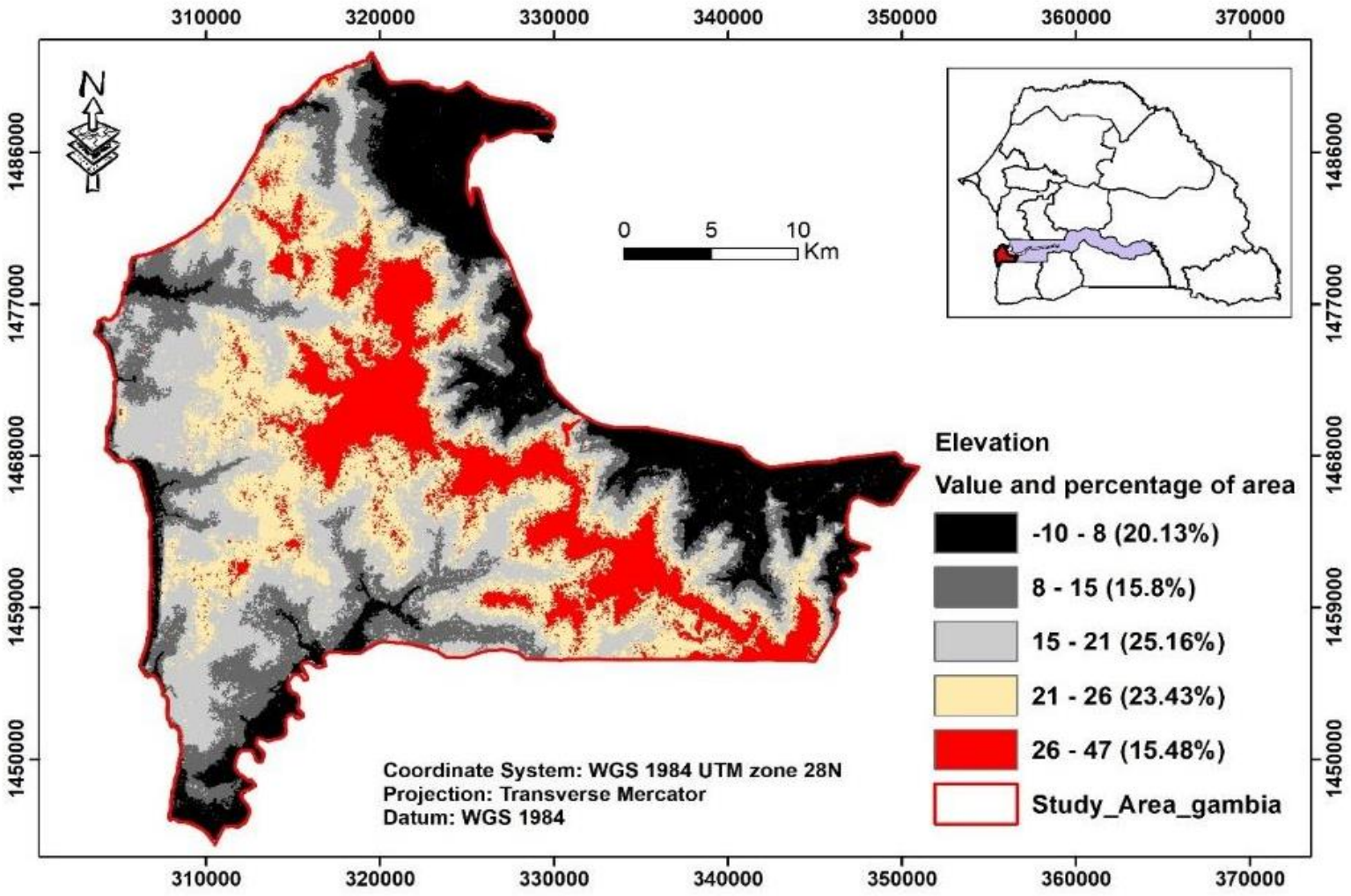

FIGURE 15: DEGITAL ELEVATION MODEL OF THE STUDY AREA

B. Slope

The slope map of the topography was extracted from the DTM; it shows values ranging from 0 and 22^0. The highest slopes (greater than 22^0 are encountered at around the boundaries of the river and the tributaries in the study area (Figure 15). Slope determination is useful in the assessment of runoff and hence the calculation of groundwater recharge in the study area.

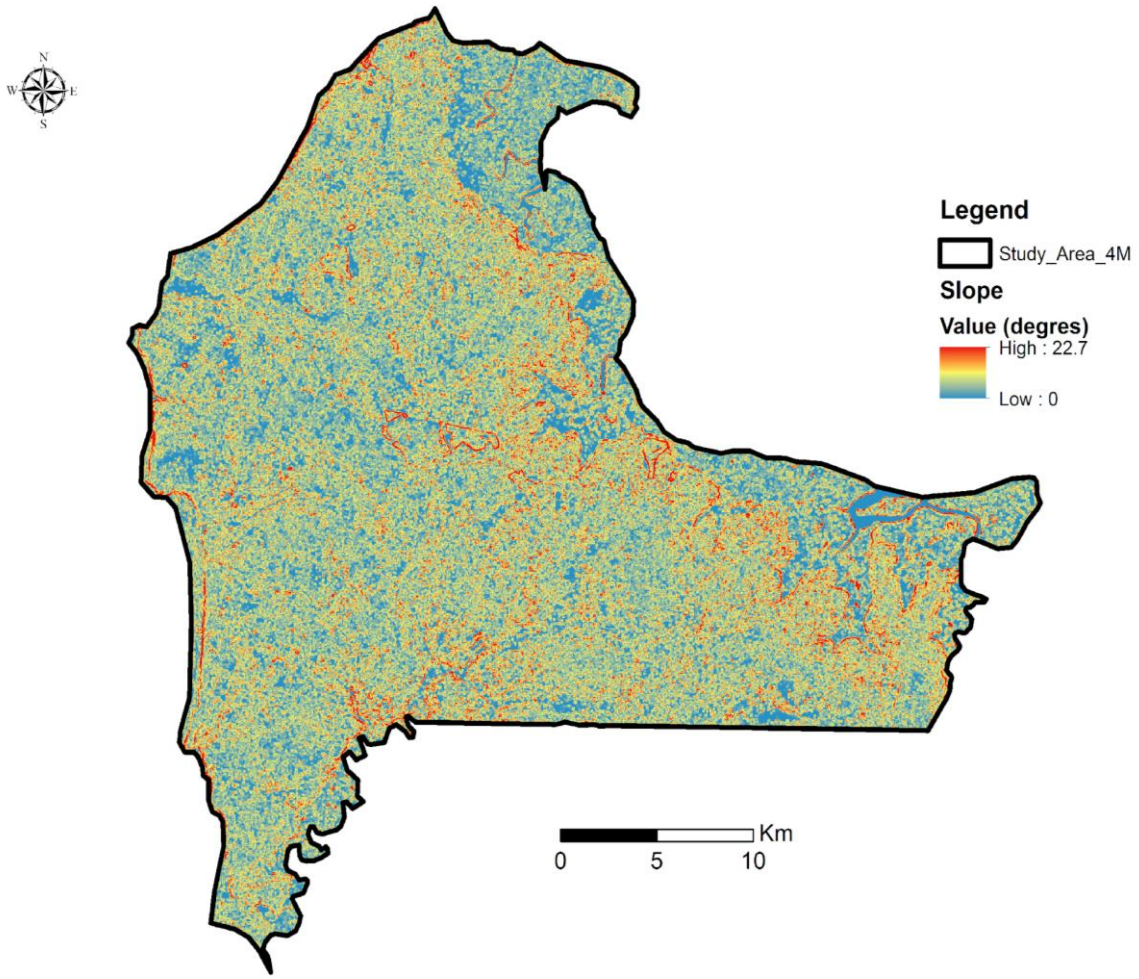

FIGURE 16: SLOPE MAP (WITH +/-4M ACCURACY) OF THE STUDY OBTAINED FROM DEM

2.3.2. Hydrography

A hydrographic network map (Figure 16) is very useful which enables the delineation of watersheds identification and the drainage networks. The ArcToolbox tool was used for the extraction of the hydrographic network of the study area from the DTM, which is equivalent to the geomorphology previously obtained. The spatial analysis tools were used to apply a filter on the DTM and generate the flow directions and flow accumulation zones. These images were then reclassified into a raster extension and converted to polylines under shape file extension. This treatment made it possible to extract the hydrograph of the study area, determine its hydrographic characteristics and enhance the identification of five watersheds of different sizes and shapes that are named according to the district in which they are located. However, the morphometric map (Figure 17) remains to be validated because a comparative map is not available, the different morphometric characteristics of the sub-basins of the study area have been distinguished (Table 3):

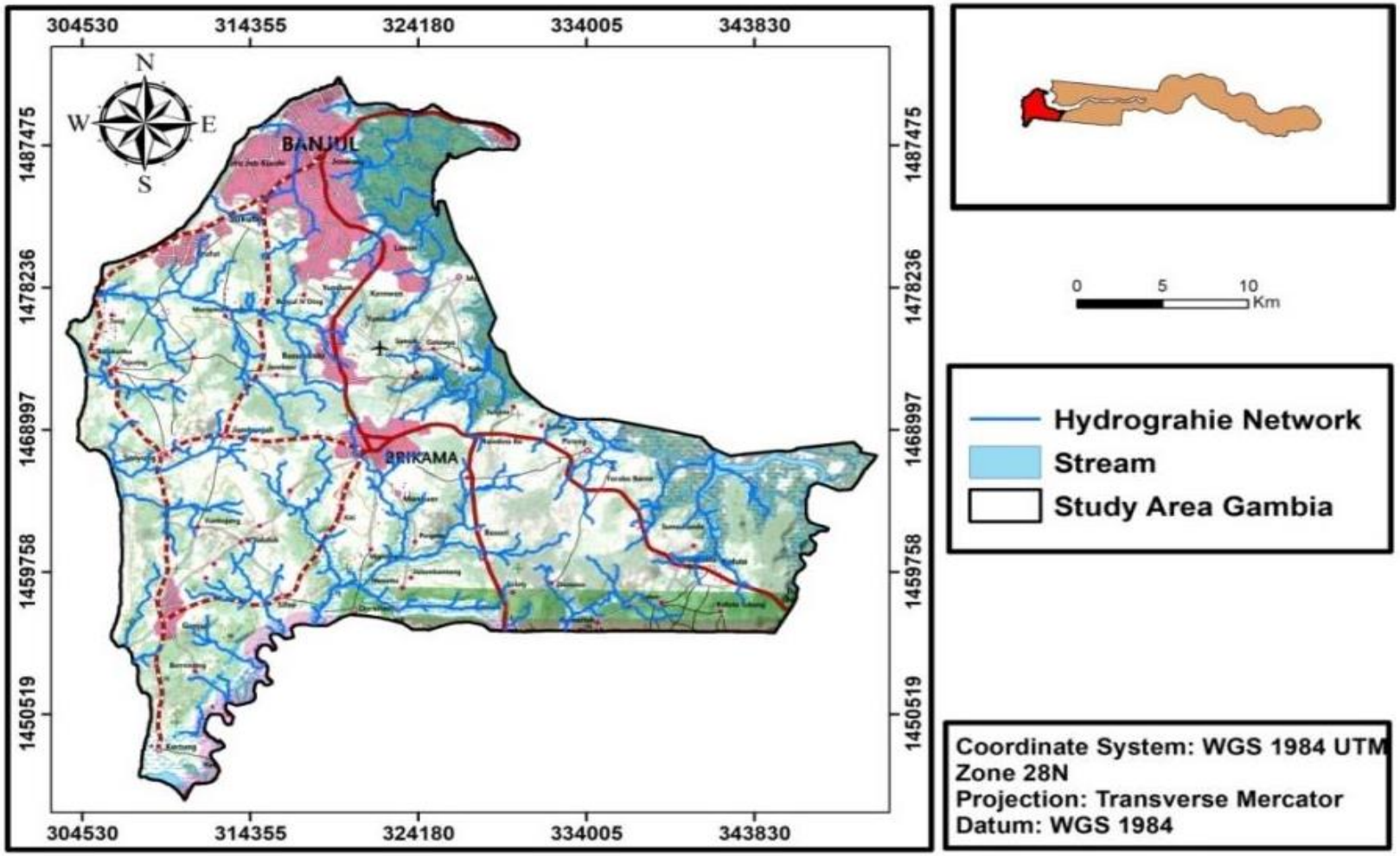

FIGURE 17: HYDROGRAPHIC NETWORK OF THE GBA BASIN (SOURCE: HTTPS://USGS.GOV, ACCESS ON 05/04/2018)

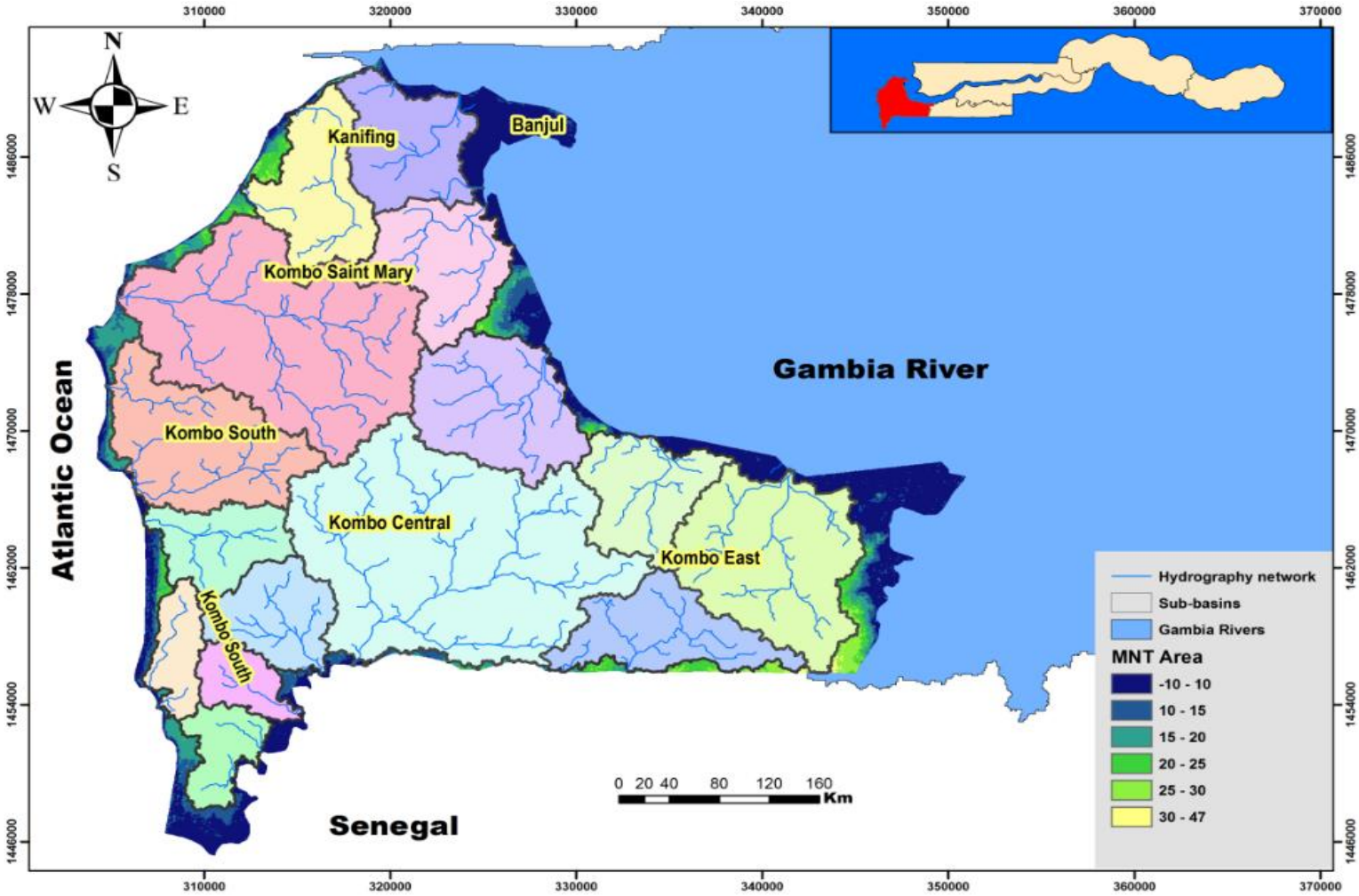

FIGURE 18: MORPHOMETRIC DESCRIPTION OF THE DRAINAGE NETWORK AND THEIR CORRESPONDING WATERSHED IN THE GBA EXTRACTED FROM THE MNT

TABLE 3: STREAM HIERARCHY OF GBA DRAINAGE BASIN

Watersheds	Area (km²)	Perimete (km)	Length (km)	Width (km)	Verificatic Surface	Height Differenc	Slope (m)	Ig (m/km)	Specific Slope (m)	Ip Roche
Kanifing	42.52	38.00	1.63	16.41	2.59	42.52	10.00	0.61	3.97	0.87
	44.52	42.00	1.76	18.61	2.39	44.52	10.00	0.54	3.59	0.82
	45.58	40.00	1.66	17.38	2.62	45.58	10.00	0.58	3.89	0.85
Kombo South	67.61	53.00	1.80	23.64	2.86	67.61	10.00	0.42	3.48	0.73
Kombo Saint Mary	138.76	73.00	1.74	32.19	4.31	138.76	10.00	0.31	3.66	0.62
	39.49	38.00	1.69	16.62	2.38	39.49	10.00	0.60	3.78	0.87
	59.00	42.00	1.53	17.66	3.34	59.00	10.00	0.57	4.35	0.84
	29.59	33.00	1.70	14.45	2.05	29.59	10.00	0.69	3.76	0.93
Kombo Central	182.20	87.00	1.80	38.80	4.70	182.20	10.00	0.26	3.48	0.57
	43.29	49.00	2.09	22.58	1.92	43.29	10.00	0.44	2.91	0.74
Kombo East	81.50	51.00	1.58	21.75	3.75	81.50	10.00	0.46	4.15	0.76
	33.00	32.00	1.56	13.57	2.43	33.00	10.00	0.74	4.23	0.96
	17.73	26.00	1.73	11.45	1.55	17.73	10.00	0.87	3.68	1.04
	16.44	24.00	1.66	10.42	1.58	16.44	10.00	0.96	3.89	1.10
	18.68	28.00	1.81	12.51	1.49	18.68	10.00	0.80	3.46	1.00

The Kombo Central watershed is the largest watershed in the study area having a catchment area of 182.2 km^2 and a perimeter of 87m. This watershed drains itself into the Casamance in the south. The Allahein River is found in the Kombo Central watershed which drains into the Atlantic Ocean. Kombo Saint Mary Watershed is the second largest with a catchment area of 138.76 km^2. It has slopes that decrease from 10m to 3.48m with an average altitude of 30 m; The Kotu Stream is located in this basin and it has a catchment of 65 km^2. Kombo South Basin has an area of 67.61 km^2. The Tanji and Tujereng rivers are found in this basin. The Kombo East basin consists of a stream that runs through Bullock, Faraba and Pirang. It covers an area of 81.5 km^2. Kanifing Basin has a catchment area of and the Oyster and Cape creeks are found in this sub-basin. This basin has an altitude less than 10m.

All the sub-basins in the north have their source from the River Gambia and flows (drains) back to the river. The sub-basins in the west drain into the Atlantic Ocean and the ones on the south drain into the Cassamance. Other than the major tributaries (Mandinari, Bullock, etc.) of the River Gambia, all other tributaries (e.g. Kotu Stream) have a short lifespan, which flows only during the rainy season. The tributaries found in these sub-basins are saline due to the tidal influence of marine water. The economic activities that go on in these sub-basins are fishing, tourism etc.

2.4. Soil

2.4.1 Description of Soil Types

Haplic: have no applicable other than a qualifier.

Cambisols are moderately developed soils that lack discrete horizons. They are extensive throughout Africa and can have varied characteristics depending on the nature of the parent material, climate and terrain (Jones, et al., 2013).

Fluvisols are a mineral soil found usually on flat landscape that is occasionally flooded by rising groundwater or surface waters such as coastal lowlands, river floodplains, tidal marshes and mangroves throughout Africa. The material forming this soil is transported and deposited by flowing river water. Their characteristics and fertility depend on the nature and sequence of the sediments and length of periods of soil formation after or between flood events (Jones, et al., 2013).

Gleysols: Like Fluvisols, Gleysols are also mineral soils developed in waterlogged (wetlands) or low-lying areas caused by rising groundwater levels and the soil is saturated with water for a long period. They originate from a wide range of unconsolidated materials, mainly of fluvial, marine and lacustrine sediments of Pleistocene of Holocene age, with basic to acidic mineralogy (Jones, et al., 2013).

Lixisols are slightly acid soils and its clay content increases with depth. The clay is predominantly kaolinite with low nutrient-holding capacity, occurring mainly in the dry savannah region with low biomass production. Lixisols do not hold much organic matter and lack a well-developed soil structure. The soil structure is damaged by high-intensity rainfall making it prone to erosion. If the soil is not protected, a crust may develop which prevents infiltration of rainwater into the soil (Jones, et al., 2013).

Luvisols are mineral soils in which soil formation is determined by climate/vegetation of wet tropical and subtropical regions. They have high activity clay. Upland area Luvisols are mostly associated with Cambisols while the lowland Luvisols are associated with Solonetz or Gleysols (Jones et al., 2013). Luvisols have a well-developed soil structure, which makes it have a good water-holding capacity.

Acrisols are mineral soils in which soil formation is determined by climate/vegetation of wet tropical and subtropical regions. Acrisols are acidic soils dominated by kaolinite and display a clay accumulation horizon in the subsoil (Jones et al., 2013). They have low nutrient-holding capacity. These soils are quite common in Africa.

Arenosols develop as a result of the weathering of quartz-rich parent material (Jones et al., 2013; USDA, 1967) or in recently deposited sands (e.g. dunes in deserts and beaches). Their soil structure is normally absent or very weakly developed which makes it an easily erodible sandy soil without vegetation cover. They have low water- and nutrient-holding capacity and are the dominant soil in Africa (Jones, et al. 2013). Arenosols are very permeable and have rapid infiltration, high hydraulic conductivity and low water holding capacity.

Ferralsols are strongly weathered soils with low nutrient-holding capacity that are found mostly in high rainfall areas and Tertiary land surfaces. These weatherable minerals are lost over time and consequently stable materials like aluminum oxides, iron oxides, and kaolinite which give Ferralsols their strong red and yellow colors become dominant (Jones et al,. 2013).

Solonchaks are mineral soils that are characterized by high amounts of soluble salts concentrating within 30 cm of the top soil surface. They are formed from their saline parent materials with high evaporative conditions. Solonchaks are mostly found in arid and semi-arid regions and its formation is conditioned by climate/vegetation (Jones et al., 2013).

Vertisols are dark-coloured clay mineral soils. They have more than 30% clay with a variable texture. These soil swell when wet and cracks when dry. There is a high evaporative rate during the dry season due to their cracking. They have a high water-holding capacity. Vertisols have high crop yield potential if well managed. They have a very low infiltration rate when their surface soil is sealed (Jones et al., 2013).

2.4.2 Soils of The Gambia

The soils of the Gambia are mainly continental terminal Fluvisols, Lixisols, Regosols and alluvial soils. The continental terminal soils mostly sands or loamy sands that can be classified as ferruginous or ferralitic soils. The alluvial soils (Fluvisols) are depositions of the River Gambia and its tributaries. They are mostly hydromorphic and fine textured, containing more than 80% silt plus clay. The alluvial soils are deeper than continental terminal soils. Their water table is high which hindered the penetration of roots on these soils. According to the Harmonized World Soil Database (HWSD) for Africa, the main soil types of the Gambia are Acrisols, Fluvisols, Lixisols and Regosols (Atlas, 1979).

2.4.3 Soils of the Study Area

The study area is characterized by flat terrain. The main types of soil of the study area are Acrisols, Fluvisols, Lixisols, Gleysols and Luvisols (Figure 18a). Other soils types are the Arenosols, Solonchaks and Vertisols. **Arenosols** are sand dunes that cover some parts of the river and coastal plains. **Solonchaks and Vertisols** are not common in the study area**.** Solonchaks are only encountered around the tributaries (Mandinari and Bullock Bolong) or floodplain of the river. These soils are saline in nature, which is mainly due to the evaporation of tributaries. **Fluvisols** are the most encountered soil that covers more than half of the study area (upland, Mangroves, river floodplains and tributaries). **Fluvisols** indicate soils that are formed on alluvial sediments. Infiltration rates in Fluvisols are low in the backswamps because of their clayey nature. However, on the natural levee hydraulic conductivity is high due to more silty or loamy nature. Salinization is a major challenge for Fluvisols found in the river floodplains, coastal lowlands, and mangroves areas. Nonetheless, rice and vegetables are the main crops grown in some of these areas. **Lixisols** are mostly found in the northern part around Kanifing and Bakau areas. They are well-developed soil structure infiltration of rainwater into the soil. **Gleysols** are mostly found and distributed in the north central and southeastern part of the country. Groundwater levels in this type of soil are high and close to the surface. They are soils that are saturated with water. They are very important for agriculture. **Luvisols** are commonly found in the central part of the northwest and eastern of the study area. They have a well-developed soil structure.

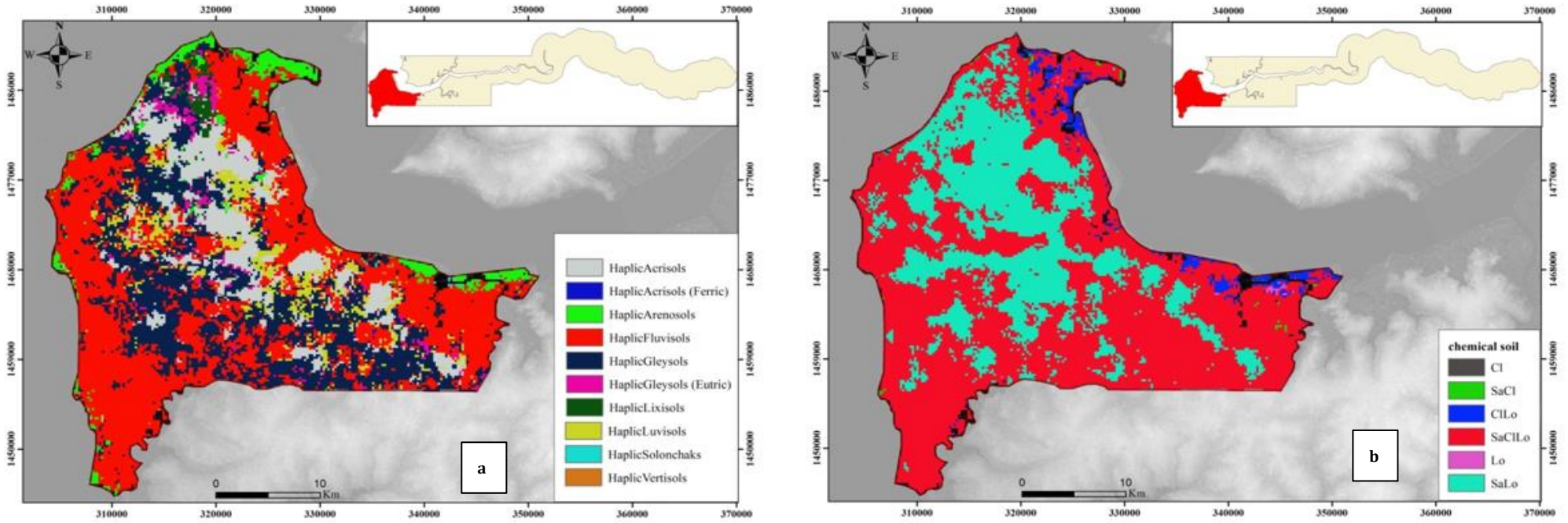

FIGURE 19: (A) SOIL MAP OF THE STUDY AREA; (B) SPATIAL DISTRIBUTION OF SOIL TEXTURE IN THE GBA: CLAY (CL), SANDY-CLAY (SACL), CLAY-LOAM (CLLO), SANDY-CLAY-LOAM (SACLLO) AND SANDY-LOAM (SALO)

Figure 18b shows the spatial distribution of soil texture in the GBA. The study area has three main soil types; sandy soil, loam soil and clay soil. The most dominant soil type is sandy-clay-loam which spread throughout the study area except the central part which is dominantly sandy-loam. Clay-loam and poorly drained clay soils dominate along the river floodplains and the tributaries.

2.5 Land Use and Land Cover

The Gambia lies along the boundary of two vegetation types, the Southern Guinea and Sudan Savanna forest (The Gambia Government, 2014). The GBA is located on the Southern Guinea Savanna. Its natural vegetation cover is characterized by woodland, cropland, grassland, settlements and the wetlands (Figure 19). The wetlands consist of mangroves, barren flats and saline water swamps (Gambia Government, 2020). Over a century ago, the land cover of the country including the study area has experienced significant transformation of the land cover due to anthropogenic and natural factors. The fast rate of population growth has increased the need for more land use for settlement, farming and industrial purposes. These led to the depletion of the country's forest resources. Natural factors include persistent droughts and saltwater intrusion upstream of the River Gambia. The woodland cover of the whole country has experienced a significant decrease of 57% in 1968 and 41% in 1993.

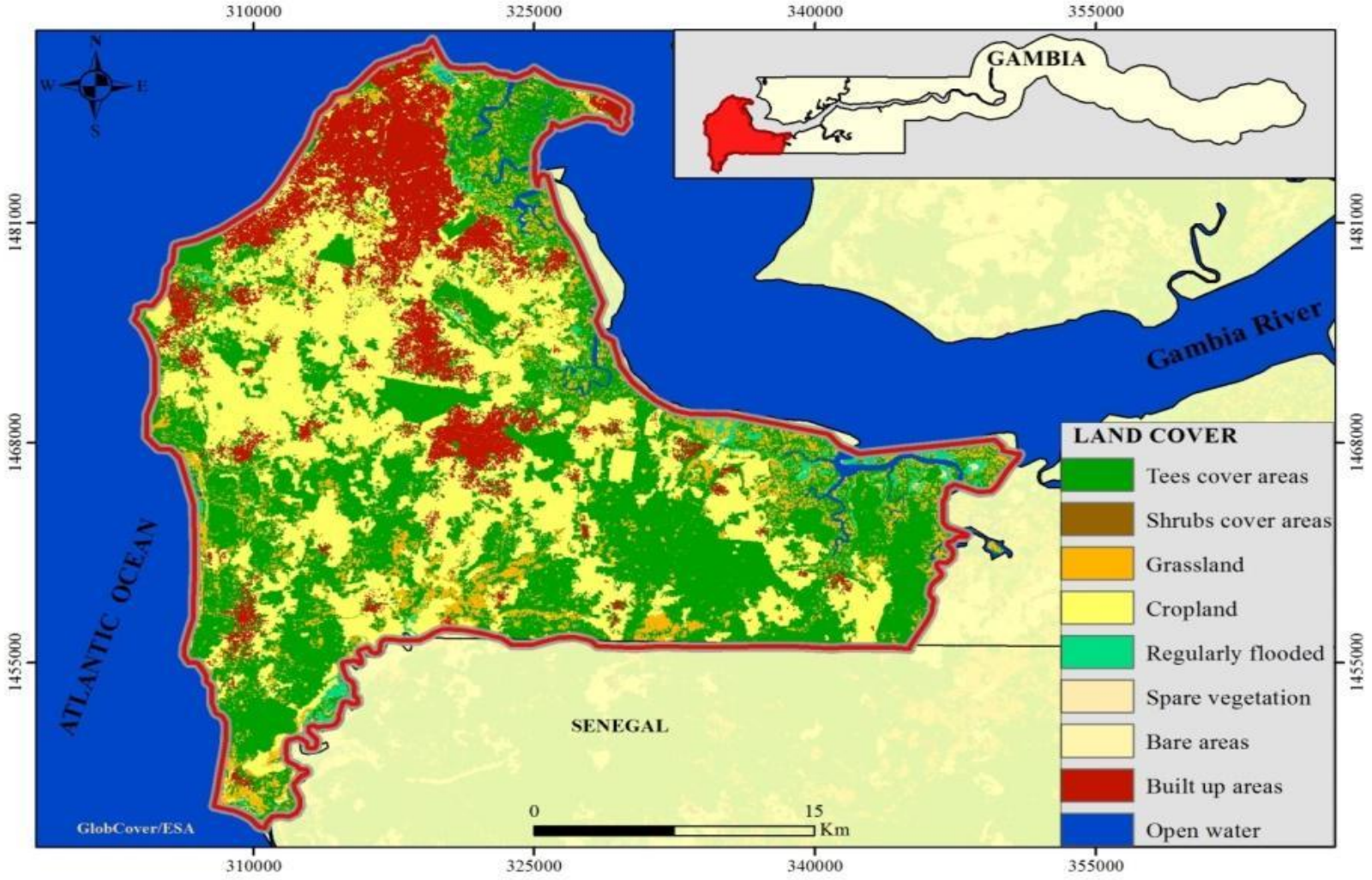

FIGURE 20: LAND COVER MAP OF THE GBA

2.6 Geological Context

2.6.1 Regional Geological Settings – S-M Basin

The Meso-Cenozoic regional coastal sedimentary basins of Africa known as the Senegal-Mauritania Sedimentary (S-M) Basin (TRAVI et al., 2017)(Figure 20) extends from Northern Mauritania to South Guinea Conakry (Kane, 2015; RITZ M., 1988) passing through Senegal and Gambia. The M-S Basin covered an area of about 350 000 km^2 and it is the largest of the Meso-Cenozoic northwest African basins (Ndiaye et al., 2016; Gorin et al., 2016; IAEA, 2017). The basin was formed during the late Palaeozoic and early Mesozoic era and comprises the Triassic, middle to upper Jurassic, Cretaceous, Tertiary and Quaternary formations (Diène et al., 2014).

Diéne et al., (2014) gave a brief description of the different formations of the Senegalese-Mauritanian Sedimentary Basin as in the figure below:

I. **The Upper Cretaceous** formation is composed of Maastrichtian rocks that are in sandy facies with frequent interbedded sandstones and clays in the eastern part of the basin.
II. **The Lower Tertiary** formation is comprised of Paleocene that is made up of limestone, and occasional calcareous marl, that is karstified in the western part of the basin; and Eocene composed of clayey and marly facies, or, limestone with phosphate, especially in the West.
III. **The Upper Tertiary** formation consists of Oligocene consisting of sand and clay in the center of the basin; and Continental Terminal, composed of detritic formations consisting of sandy and clayey series from Miocene and sand and clayey sandstone from Pliocene.
IV. **The Quaternary** formation comprises Aeolian sands, river alluvium and marine deposits on the deltas and along the rivers; and calcareous deposits.

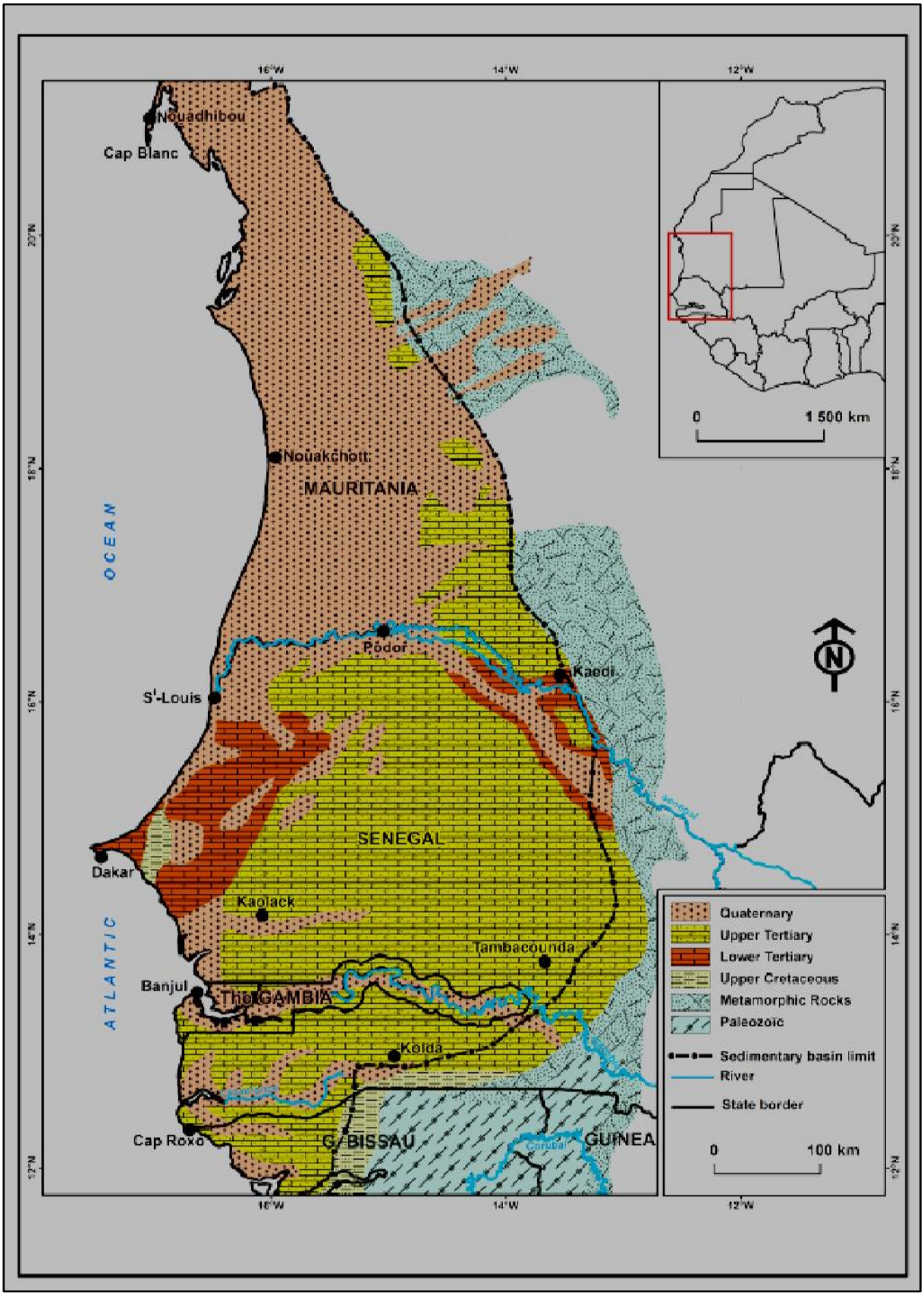

FIGURE 21: THE GEOLOGY MAP OF THE SENEGAL-MAURITANIA SEDIMENTARY BASIN (DIENE ET AL., 2014, MODIFIED)

2.6.2 Geological Settings of the Gambia

The Gambia is situated at the centre of the Meso-Cenozoic regional coastal sedimentary basin, where the exposed strata are all composed of Late Tertiary and unconsolidated deposits of Quaternary sediments. The stratigraphic classification of the Meso-Cenozoic strata in the Gambia is given in Table 4.

The Quaternary sediments occur across the whole country. The Quaternary strata have been classified into the Holocene and Pleistocene formations. The Holocene formation is composed of deposits of marine and coastal sands, aeolian sands/silts, alluvial clays and salts, sometimes with organic intercalations. The Holocene deposits are found along the Gambia River including its tributaries and close to the sea. The Holocene formation is underlain by Pleistocene sandy clays and Pliocene fine-medium grained sands. The Pleistocene ironstone crust consisting of iron oxides, gravels, sands, silts and clay matrices predominates in the east of the country. The Pleistocene alluvium, which is made up of undivided sands, silts and clays. The Pliocene formations contain varying amounts of silts, clay and laterites. The Eocene series comprises clayey and marly facies, or limestone with phosphate, especially in the West.

The oldest strata of the country, which is confined to the valley of the Gambia River, are Tertiary rocks (Dunsmore et al., 1976). The Upper Tertiary Sequence consists of Oligocene, Miocene or Pliocene formations known as the Continental Terminal (CT) series (Figure 21). The CT is composed of sands, sandstones, silts, clays and kaolinitic claystones. The stratigraphic thickness of the Continental Terminal Series ranges between 50 and 150 m. The CT mostly occurs in the west and centre of the country.

The Lower Tertiary Sequence consisting of Paleocene and Eocene formations, underlain the Upper Tertiary sequence. The Paleocene sediments are mainly marine shales and carbonates. The Eocene sediments are entirely covered by the Upper Tertiary (continental terminal). The sediments of the Eocene consist mainly of shales and marly limestones (carbonates). Paleocene, mainly consist of limestone, and sometimes calcareous marl, that is Karstified in the western part of the basin.

The Maastrichtian sequence is overlain by the lower Tertiary sequence. The Maastrichtian formation consists of poorly consolidated sediments. This formation is composed of fine to coarse grained sands and sandstones with subordinate grey-black shales,

phosphatic nodules and lignite bands. The sands of the Maastrichtian originate from the continental shelf having fluviatile characteristics.

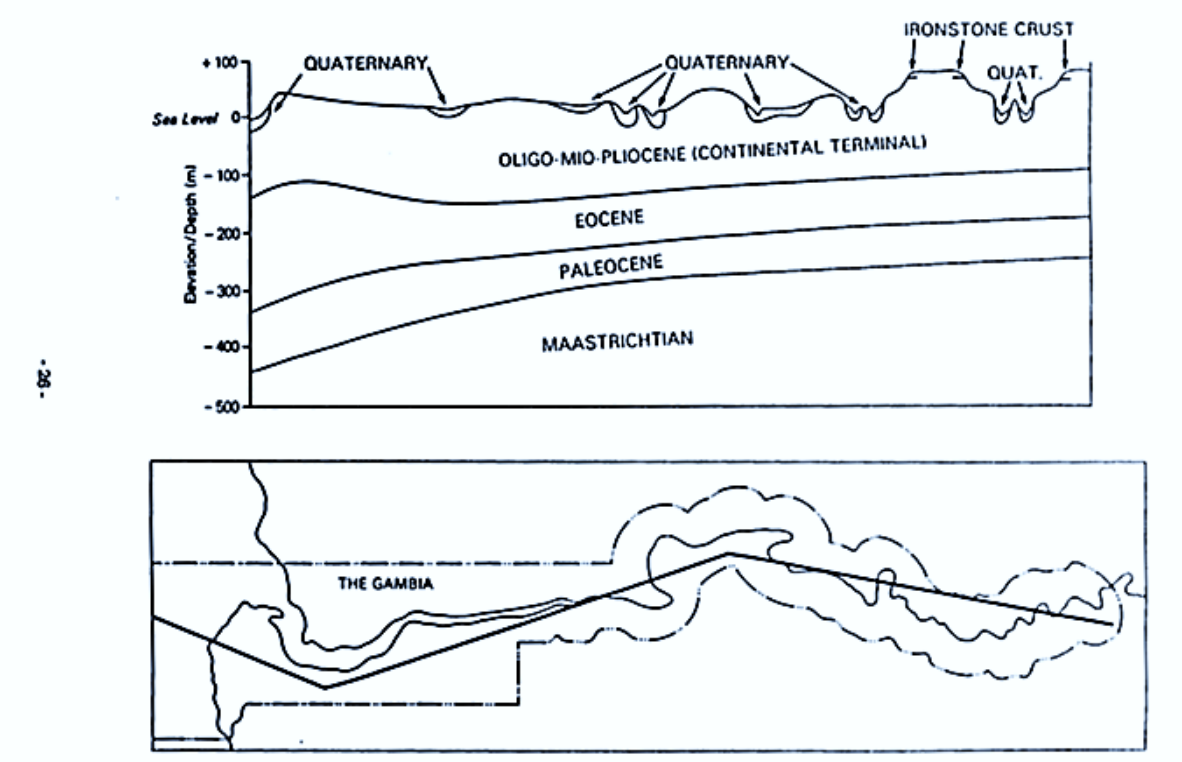

FIGURE 22: A SCHEMATIC EAST-WEST CROSS-SECTION OF THE TERTIARY AND QUATENARY SEQUENCES OF THE GAMBIA (GEOLOGY AND MINERAL RESOURCES OF THE GAMBIA, 1988, MODIFIED)

TABLE 4: CHRONOSTRATIGRAPHIC CLASSIFICATION OF THE MESO-CENOZOIC STRATA IN THE GAMBIA (ADOPTED FROM THE MINERAL RESOURCES OF THE GAMBIA, 1995, MODIFIED)

Syst.	Series	Stage	Major lithologies	Exposed depth (m)
Quaternary	Holocene		Grey clay, sand & quartz sand	0–20
	Pleistocene		Earth–yellow and red sandy clay & mild clay, with gravel bed at the bottom	20–50
Tertiary	Pliocene–Miocene		Upper: ferruginous quartz sandstone & sand–bearing mudstone; Lower: kaolinitic quartz graywacke	50–90
	Oligocene		Greyish green claystone and fine sandstone	90–146
	Upper Eocene		Greyish green limestone, marl & limestone gravel	146–182
	Middle Eocene		Greenish grey marly rocks & grey limy rocks	182–293
	Lower Eocene		Greyish green, chert–bearing, marly rocks	293–330
	Paleocene		Chalky limestone with finely crystalline limestone	330–450
Cretaceous	Upper	Maastrichtian	Glauconite–bearing sandstone intercalated with greyish black silicic ceramic clay and lignite	450–908
		Campanian–L.Senonian	Argillaceous rock with limestone, lignite and glauconite	908–1416
		Turonian	Claystone with limestone & shale	1416–1525
		Cenomanian	Upper: clayey shale & claystone; Lower: greyish brown & green claystones with dolomite, marl & sandstone	1525–2382
	Lower	Albian	Carbonate & clastic rock	2382–3500
		Aptian	Sandstone, shale & carbonate	3500–3709

2.6.3 Geological Settings of the Study Area

The study area is covered by the Quaternary (Holocene and Pleistocene) sequence and Tertiary sequence of Miocene - Pliocene formations (Figure 22) known as the Continental Terminal is made of sands, sandstones, silts, clays and kaolinitic claystones. Continental terminal is overlain by the Quaternary sequence. The coastal lowlands and river floodplains are made of the Pleistocene and Holocene formations. These comprise the Pleistocene alluvium of undivided sand, silt and clay, while the Holocene marine fluvial deposits are found on the estuary of the River Gambia and its tributaries.

2.6.3.1 The Quaternary Strata

The Quaternary strata have been classified into the Holocene and Pleistocene series distributed in the study area. This formation comprises ferruginous quartz sandstone and ferruginous rocks containing sand and argillaceous matter.

A. Holocene

This series composed of the following formations (Fm):

- The Essau Fm (QE) comprises of white medium-fine quartz sand, locally ilmenite-bearing quartz sand; 5-20 m thick; marine facies; distributed on beaches in western Gambia;
- Farafenni Fm (QF) is made up of Grey symmict sand, silt, clay and salt, containing cockle shells. It is 1-5 m thick in depth. The sedimentary are of alternately fluvial and marine facies which is distributed in River Gambia and its tributaries;
- River Gambia Fm (QG) is composed of grey clayey silt and clayey symmict sand. It is 1-5 m thick in depth. The sedimentary are of modern fluvial-alluvial facies distributed in River Gambia and its tributaries;
- Darsilami Fm (QD) comprises white medium-fine quartz sand, with grey quartz sand at the top. Its depth is about 1-8 m thick. The sedimentary of this formation are Marine which is distributed in the River Gambia and its tributaries.

B. Pleistocene

The middle Pleistocene consists mainly of ferruginous quartz-sandstone gravel beds or ferruginous conglomerates. The upper Pleistocene has more ferruginous material which forms ferruginous conglomerate. This series composed of the following formations (Fm):

- Basse Fm (QB) comprises earth-yellow clayey, fine-grained sandy clay in the upper part; greyish-white silts mild clay in the lower. This formation is composed of fluvial which are distributed on terraces of the two sides of the River Gambia and its tributaries. It is about 2-10 m thick;
- Yundum Fm (QY), Red sub-sandy, sandy mild clay and gravelly mild clay. It is about 1-5 m thick. This formation comprises fluvial, pluvial and alluvial distributed throughout the study.

2.6.3.2 The Tertiary Strata

The Tertiary strata have been classified into the Upper and Lower Tertiary Series. Only the upper tertiary is distributed in the study area and not the lower tertiary. The Upper Tertiary is composed of the Pliocene to Miocene (Continental Terminal) Series. The lower tertiary comprises upper-middle-lower Eocene and the Paleocene. The sequence of the

Paleocene to Eocene is dominated by limy and marly rocks, and that of the Oligocene to Pliocene, by clayey rocks and sandstone.

A. Miocene to Pliocene Series

The formation of this sequence is the Sapu Fm (NS) and Kuntaur Fm (NK). The Sapu Formation belongs to the Upper Tertiary which is mostly found in the Eastern and Central part of The Gambia and they are composed of low hilly platforms and cliffs along the banks of the River Gambia. It has a depth of about 3 - 12 m. It is composed of brown Ferruginous quartz sandstone & sand-bearing ferruginous rock with ferruginous kaolinitic quartz greywacke. The Kuntaur Formation is the oldest sequence exposed on the surface of The Gambia and other strata can be seen only downward in deep boreholes. This formation is in conformable contact with its overlying Sapu Formation representing the result of a continuous deposition. The Kuntaur formation does not occur in the study area.

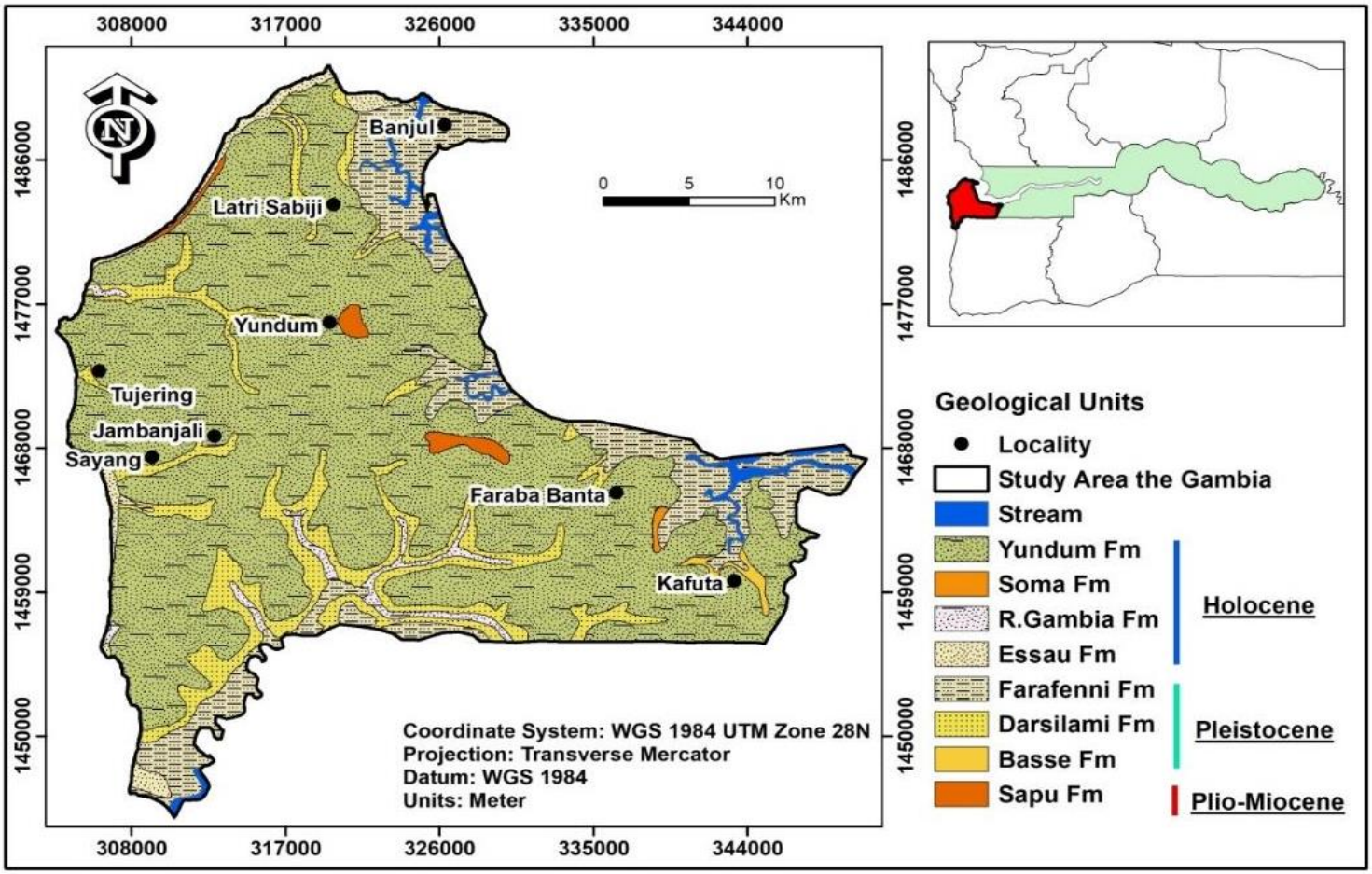

FIGURE 23: GEOLOGY MAP OF THE GBA SHOWING THE DIFFERENT FORMATION IN THE CONTINENTAL TERMINAL (EXTRACTED FROM THE GEOLOGY MAP OF THE GAMBIA, 1988, MODIFIED)

2.7 Hydrogeology Context

2.7.1 Regional Hydrogeology

The hydrogeological Transboundary Aquifer of the Senegal-Mauritania Basin (SMB) is the largest basin in the Atlantic margin of North-West Africa characterized by the existence of several aquifer units of different countries (Kane et al., 2015). The basin contains a variety of aquifers that are the main sources of drinking water supply for over 80% of the population (Diène et al., 2015, Kane et al., 2015). This resource is shared by four aquifer countries, The Gambia, Guinea Bissau, Mauritania and Senegal. There are three main aquifer systems providing exploited groundwater resources in the SMB referred to as (Mauritanian, 2017):

1. the superficial aquifer system covering the whole SMB and often discontinuously;
2. the intermediate aquifer system including Eocene and Paleocene carbonate Formations; and
3. The deeper aquifer system covers the whole sedimentary basin.

Groundwater in the Continental Terminal occurs in the Oligocene and Miocene detritic sediments with variable depth ranging between 10-150 m and it covers the entire sedimentary basin. In the Eocene limestone aquifer, groundwater is extracted by production boreholes up to 90 m thick.

The alluvial aquifer of the shallow aquifer is encountered along the River Gambia and its tributaries. This aquifer consists mainly of clays and fine sands, or coarse or gravelly alluvium interbedded with clayey sand.

The sedimentary basin laid on the ante-Mesozoic basement composed of metamorphic and plutonic rocks and consists of the Triassic, middle to upper Jurassic, Cretaceous, Tertiary and Quaternary formations. The Maastrichtian and Quaternary are the most important aquifers in the basin (Diène et al., 2015). The deep Maastrichtian aquifer is shared by four countries: Gambia, Guinea Bissau, Mauritania and Senegal. It occurs at a depth of up to 250 – 450 m. This aquifer extends in the entire sedimentary basin of the Gambia. It comprises mainly of coarse sands and sandstone interbedded with some clay units. The deep confined Maastrichtian aquifer contains considerable groundwater resources. It stretches over nearly 200,000 km^2, from the northern part of Mauritania to the South of Guinea Bissau. In Gambia, the presence of 2 to 5 mg/l of total dissolved solids including fluoride in the Maastrichtian aquifer make the water unsuitable for drinking (P. O. Jarju, 2009). In addition no proper studies has been conduct on the Maastichtian aquifer of the Gambia.

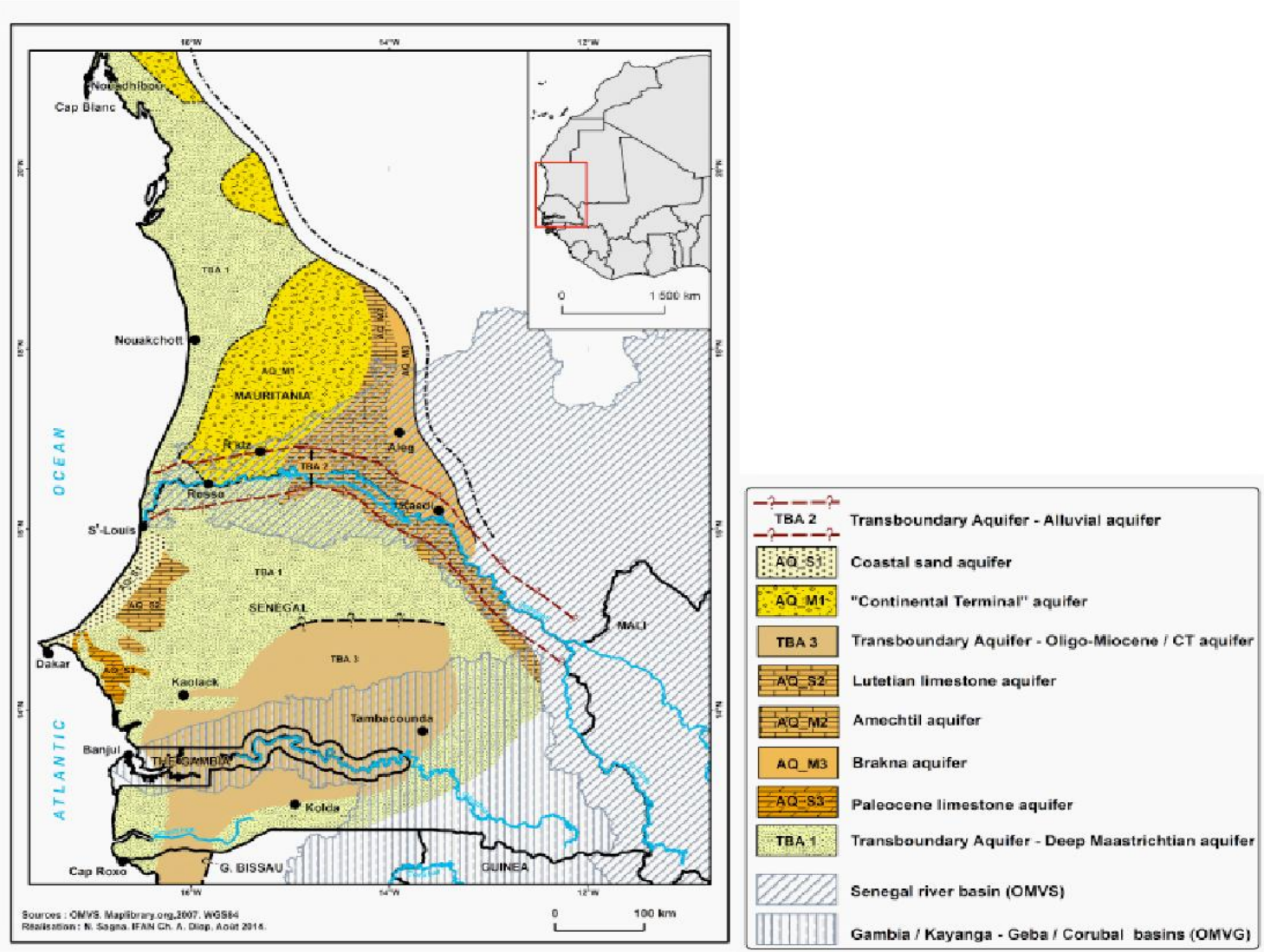

FIGURE 24: THE HYDROGEOLOGICAL MAP OF THE SENEGAL-MAURITANIA SEDIMENTARY BASIN (DIENE ET AL., 2014, MODIFIED)

2.7.2 Local Hydrogeology

Like all arid and semi-arid regions, groundwater is an important resource of The Gambia. Groundwater is the major source of potable water supply in GBA. More than 90% of the country's population and the entire population of the GBA rely on this resource. The GBA aquifer belongs to the Senegal-Mauritania Aquifer System. It is underlained by Mesozoic and Cenozoic sedimentary sequences. There are two main aquifers in the Gambia (Gambia Government, 1992):

I. *Shallow Sand Aquifer*

The Shallow Sand Aquifer (Quaternary and CT) occurs in the succession underlying the whole sedimentary basin of the study area. The Shallow Sand Aquifer (SSA) is dominantly made of sand and sandy clay. The SSA aquifer is intergranular and the best groundwater potential occurs in the sand layers. This aquifer generates a yield of 1-30 l/s and can be greater than 30 l/s in the most productive areas. The Portable water supplies are obtained from this aquifer (i.e Quaternary and CT) through extraction by boreholes or wells. It is normally discovered at 10 m to 120 m depth. The Shallow Sand Aquifer system comprises two units, known as the phreatic and semi-confined aquifers. The two aquifers are separated by a clay-silt aquitard of 15m to 30m thick that allows limited hydraulic connection between the two aquifers (Gambia Government, 2014). The phreatic aquifer occurs at depths ranging from 4 to 30 mbgl. This aquifer is mainly tapped by dug wells and some shallow boreholes while extraction from the Semi-confined aquifer is mainly done by production boreholes which are found at depth ranging from 30 to more than 100 mbgl. Transmissivity values in the phreatic aquifer range from 50 to 300 m^2/day, whilst estimated hydraulic conductivity ranges from 5 to 30 m/day (Department of Water Resources).

The Semi-confined aquifer has transmissivities ranging from 20 m^2/d to almost 4 000 m^2/d and permeability on the other hand range between 10 and 40 m/d (Gambia Government, 1992). The SSA is close to the surface and is recharged by direct infiltration from rainwater and it is also exposed to pollution due to anthropogenic activities (e.g. infiltration of agricultural chemicals during irrigation) leading to degradation of groundwater quality.

II. Deep Sandstone Aquifer

The deep sandstone aquifer (DSA) occurs in the succession of the Upper Cretaceous age comprises mainly Maastrichtian to Paleocene sandstone (Gambia Government, 2000).

This aquifer occurs at 250 m to 450 m depth and comprises mainly unconsolidated sands and loosely cemented calcareous sandstone, interbedded with marl, silt, clay and thin limestone bands. The bottom of the aquifer forms the sediments of Maastrichtian to Palaeocene sandstone (Gambia Government, 1992). The confined DSA has very old fossil water between 4000 to 40000 years old. Transmissivities values are around 500 m^2/day, and hydraulic conductivity range between 30 and 100m/day. The potential yield has been estimated at 40 l/s (Gambia Government, 2014). The storage in this aquifer has been estimated at 650,000 m^3 of which only 80,000 m^3 is thought to be portable (Department of Water Resources).

In the study area, groundwater in the DSA is highly mineralized, with total dissolved solids in the range of 1000 to 2000 mg/l, and fluoride concentrations are between 2 and 5 mg/l (Gambia Government, 2014). Exploitation of the DSA would require deep boreholes of up to 380m. Thus the focus of this study is groundwater found on the surface formations of the Quaternary Sands and the Continental Terminal (Shallow Sand Aquifer) of the study area.

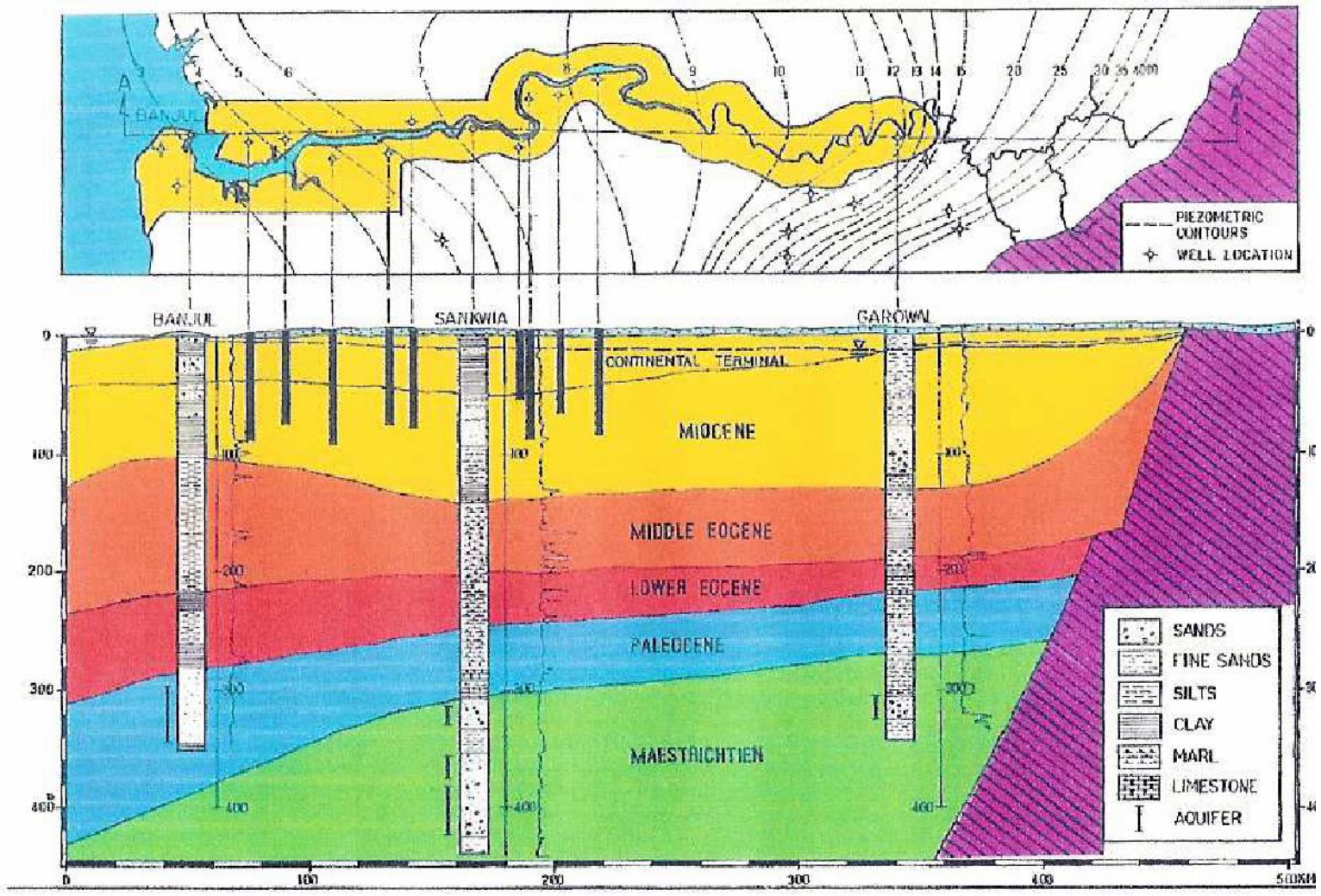

FIGURE 25: HYDROGEOLOGICAL CORRELATION OF BOREHOLES ACROSS THE GAMBIA (ADOPTED FROM P. O. JARJU, 2014, CITED IN NJIE& CORR, 2006)

2.7.3 Aquifer Thickness

The top of the aquifer defined through a 20m Digital Elevation Model (DEM) highlight a plateau in the center and south-eastern part of GBA which rise from +32 to +20 mbsl. Toward the coastland in the North, West and East, the topography is at around +4 mbsl. The substratum layer was identified through borehole logs drilled throughout GBA. It consists of clay formations which separates CT and the intermediate aquifer (Oligo-Miocene). The corresponding layer thickness ranges from 20m in the north up to 100m in the south-eastern GBA (Figure 25).

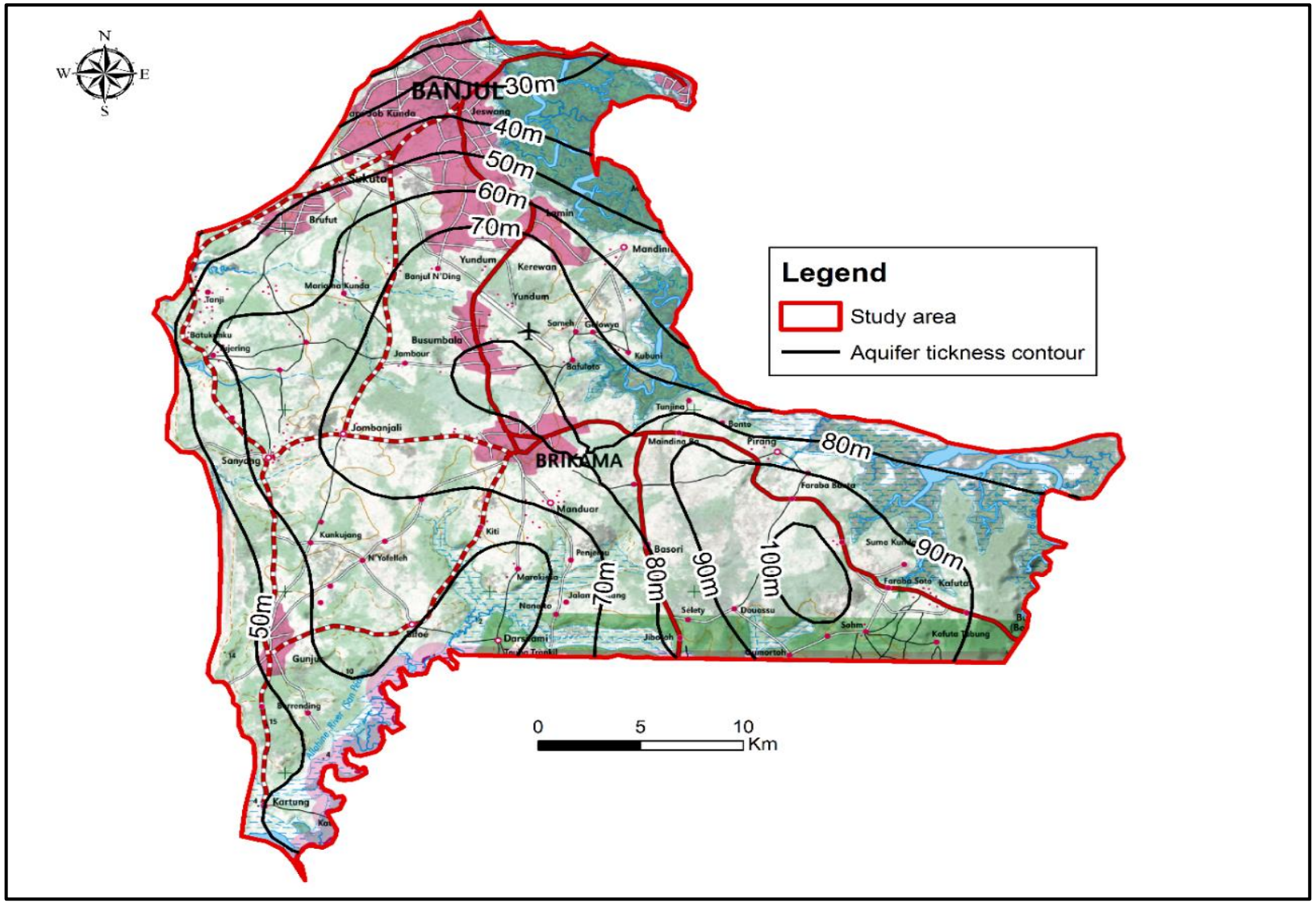

FIGURE 26: AQUIFER THICKNESS OF THE CT OF THE STUDY AREA.

Geological cross sections West-East and North-South were compiled from the lithological log data of drill holes located in the study area. Existing ground elevation data from drill holes were collected. The lithological correlations were made based mainly on the lithological logs and the bottom of the aquifer was inferred by interpolation. From the cross section in Figure 26, it can be seen that all the boreholes are within the shallow aquifer which comprises the stratigraphic boundaries Quaternary and Mio-Pliocene. The aquifer is overlain by sand with some silt and sandy-clayey soil. Small laterite was encountered at the borehole E9 location in Brikama. A strip of sand-laterite spread from Brikama to Kuroto. A layer of clay was also encountered in borehole A27 in Brikama. A similar hydrogeological setting has been seen in the cross section in Figure 27.

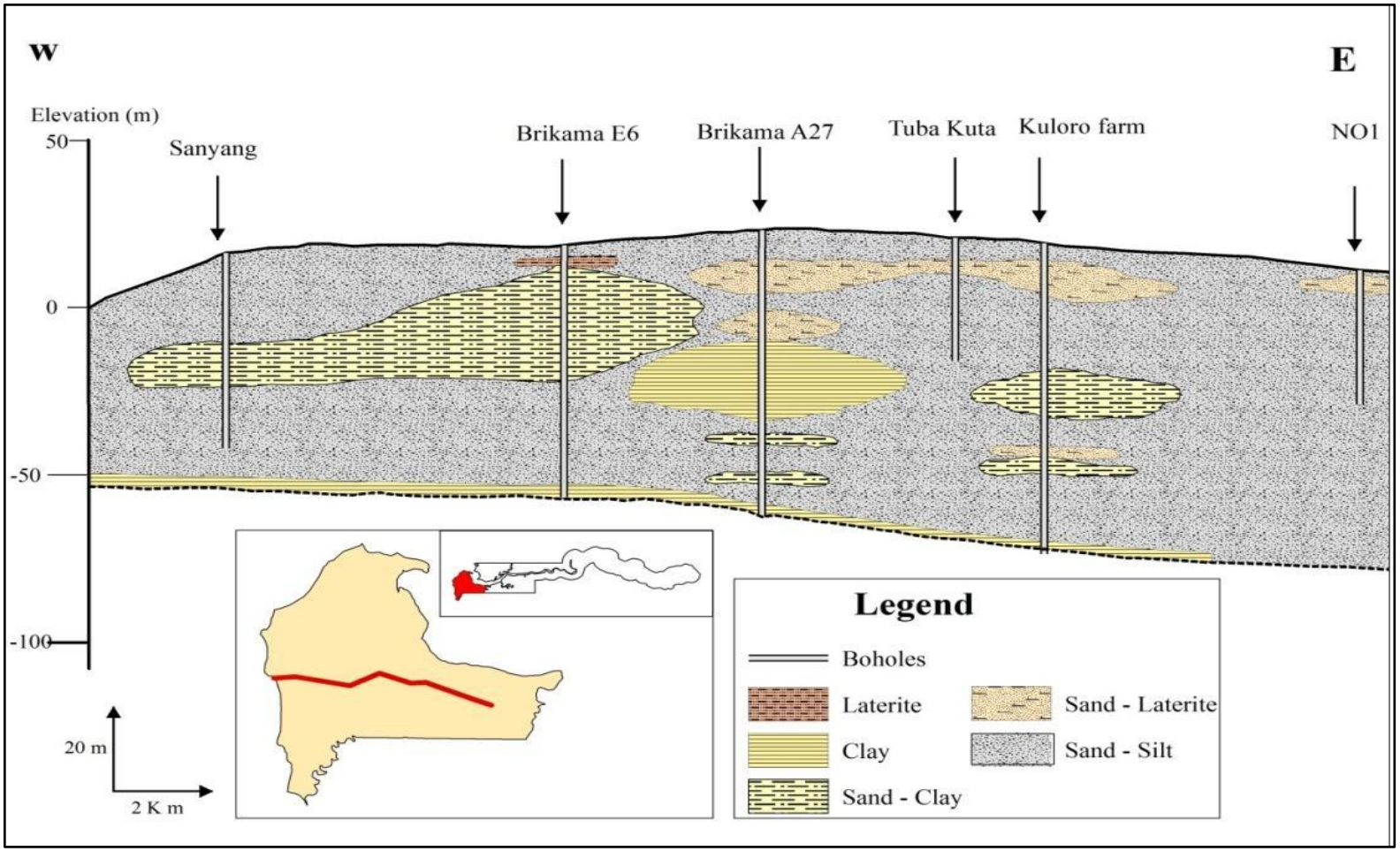

FIGURE 27: WEST-EAST HYDROGEOLOGICAL CORRELATION OF BOREHOLES ACROSS THE STUDY AREA

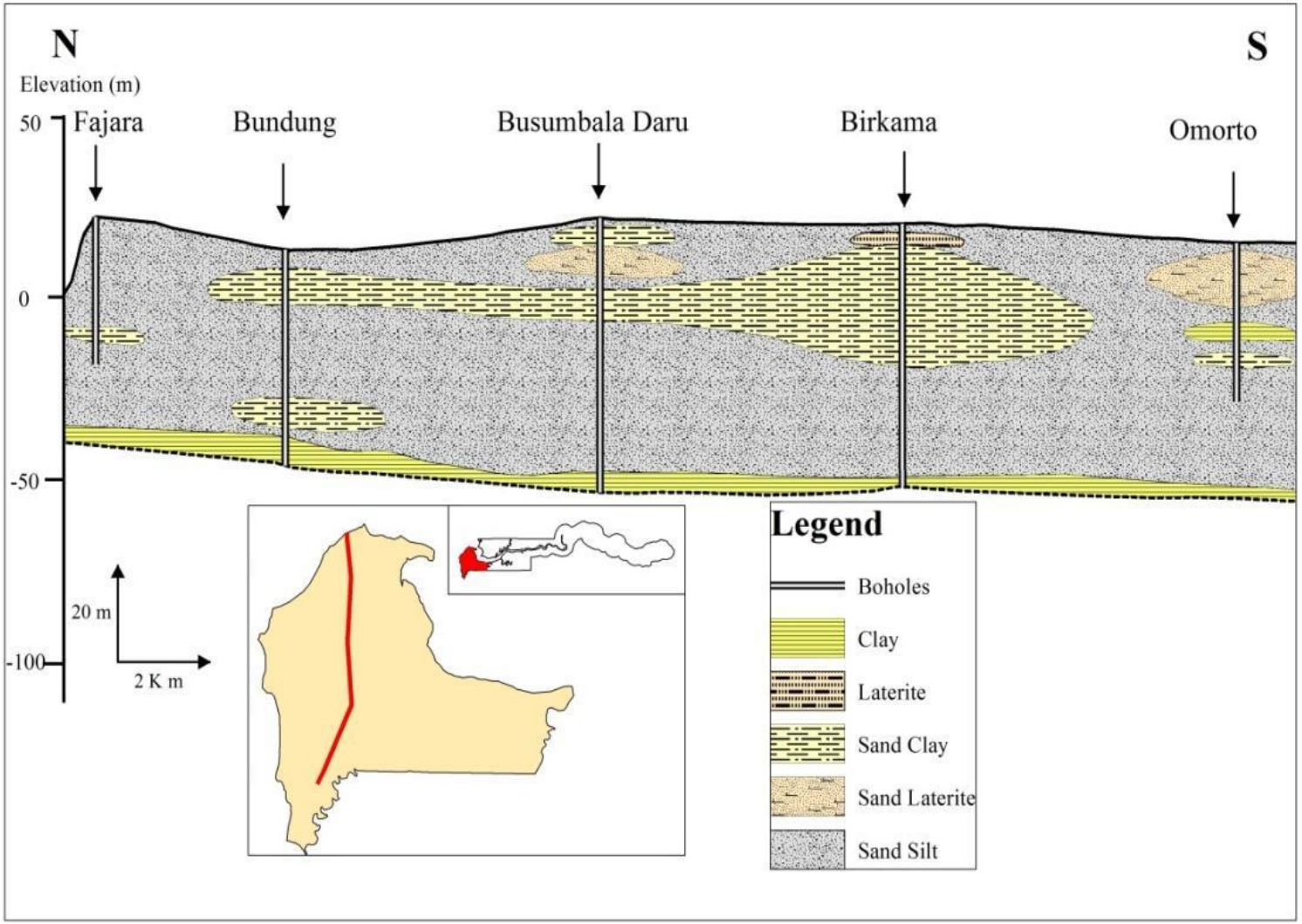

FIGURE 28: NORTH-SOUTH HYDROGEOLOGICAL CORRELATION OF BOREHOLES ACROSS THE STUDY AREA

2.8 Hydrology

The Gambia River Basin is situated in the West African Atlantic region between latitudes 11^0 22' N and 14^0 40'N, and between longitudes 11^0 13' W and 16^0 42' W. It has a length of 1150 km and land area of 77,054 km^2 with a drainage area of 10,556 km^2 (Diène et al., 2015; UNEP, 2008). The river flows from to Fouta Djallon Mountains Highlands in the Guinea through Senegal, runs the whole length of the Gambia, and empties itself at the estuary of the Atlantic Ocean. The water resources of the Basin are shared between The Gambia, Senegal, Guinea and Guinea Bissau. The percentage of share of drainage of the Basin is: Gambia 13.7%, 15.4 % in Guinea, 0.021 % in Guinea Bissau, and 70.9 % in Senegal (UNEP, 2008). The population within the Basin area is 19.9 million people with a population density of 49 persons per square kilometer (UNEP, 2008). The inhabitants around the Basin are engaged in agricultural, fishing, mining activities and the water used for domestic purposes in some areas.

The basin's hydrological system is an evolution of tropical type. The highest tides occur from July to October reaching its maximum the month of September. The flow measured at Kedougou station was 76.9m^2/s during the period of 1970 to 2004. The River encountered a seasonal variation of flow ranging between 0.308m^3/s in May and 328m^3/s in September (UNEP, 2008) when it attained the highest water level. The downstream of the River Gambia is affected by saltwater intrusion from 100 km during the rainy season to 250 km in the dry period. The study area located on this part of the River Gambia made it impossible for utilization of surface water for domestic, agriculture and industrial use and thus groundwater is the only freshwater available for use.

The study area is part of the Tertiary Continental Terminal Series dissected by the River Gambia and its tributaries (Dunsmore et al., 1976). The River Gambia and its tributaries make up the hydrologic system of The Gambia. The River Gambia is divided into 3 zones according to the limit of the saline front (Figure 28):

- The Upstream (Upper Valley) is the zone where the river water fresh throughout the year and flooding happens occasionally;
- The Mid-stream (Central Valley) of the river is where tidal influence happens; the river water is fresh only during the rainy season. And
- The Downstream (Lower Valley) is the zone at which permanent tidal influence occurs and the river water is constantly saline.

The freshwater flow in the river is seasonal. Since the early 1970s, the salinity front has been increasing. This is noticed during the dry season (November-June) when the freshwater-saline front of the River Gambia extends up to 250 km upstream. In the rainy season, the salinity front retrieves back to about 100 km downstream (P. A. O. Jarju, 2009).

The study area is located along perennially saline zone of the River Gambia, which leaves the option of obtaining portable water for the GBA entirely from groundwater (i.e. Boreholes and dug wells). Salinity of the downstream part of the river and its tributaries (bolongs) makes it almost impossible to use for irrigation purposes. Therefore, agriculture in the study area is most rain-fed and farming irrigation (horticultural) is done at small scale using groundwater. Boreholes and/or dug wells, the only source of potable water, in some coastal areas (Bakau, Kartong, Sanyang, Tanji, etc.), are already saline which could be caused by the interaction between the saline surface water and groundwater. These conditions are expected to be exacerbated by climate change induced sea level rise. Hence, the demand for portable water in coastal zones of the study area will increase.

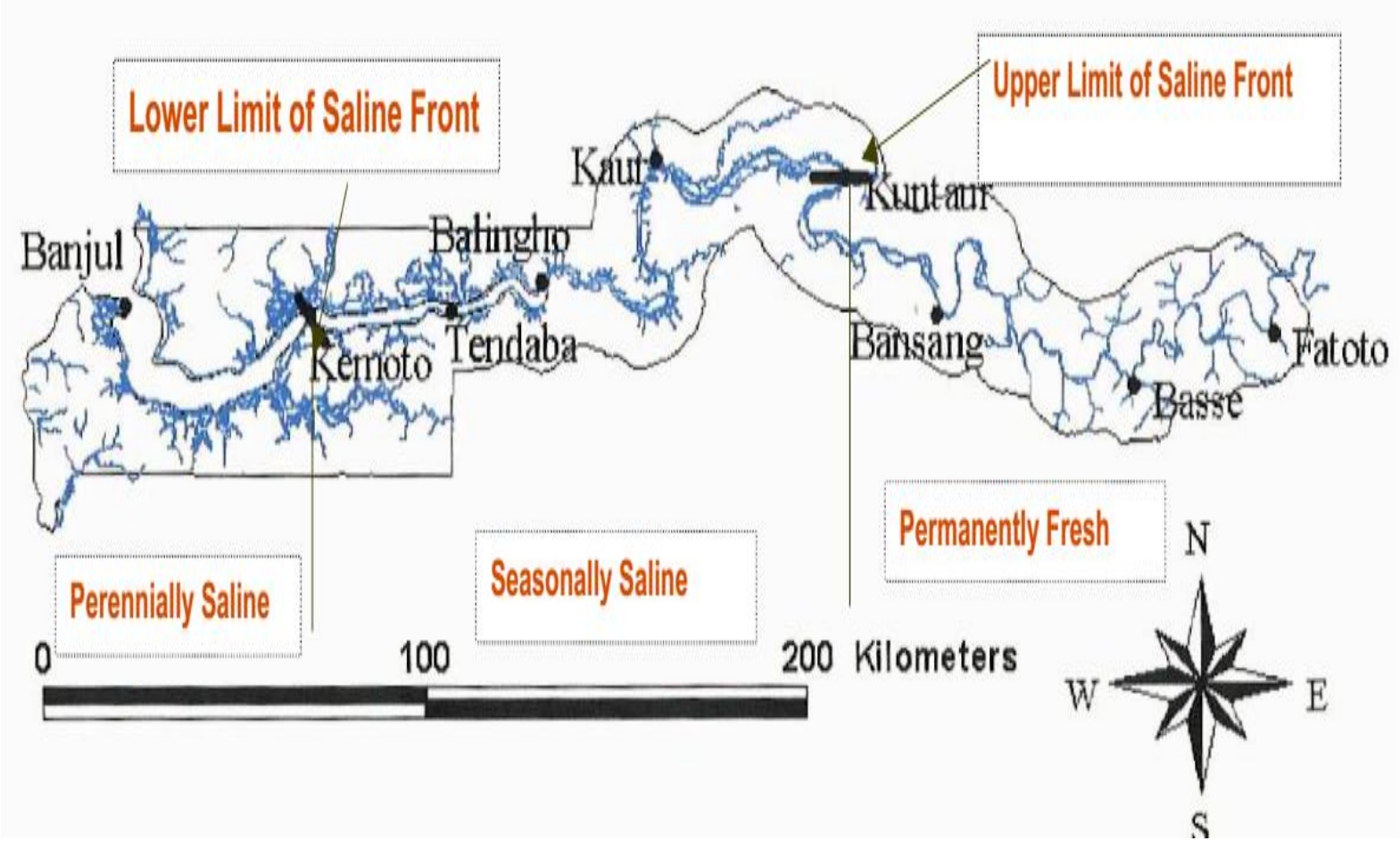

FIGURE 29: ZONATION OF THE RIVER GAMBIA ESTUARY AND SALINITY PROFILE (ADOPTED FROM P. O. JARJU, 2009, CITED IN NJIE & CORR, 2006

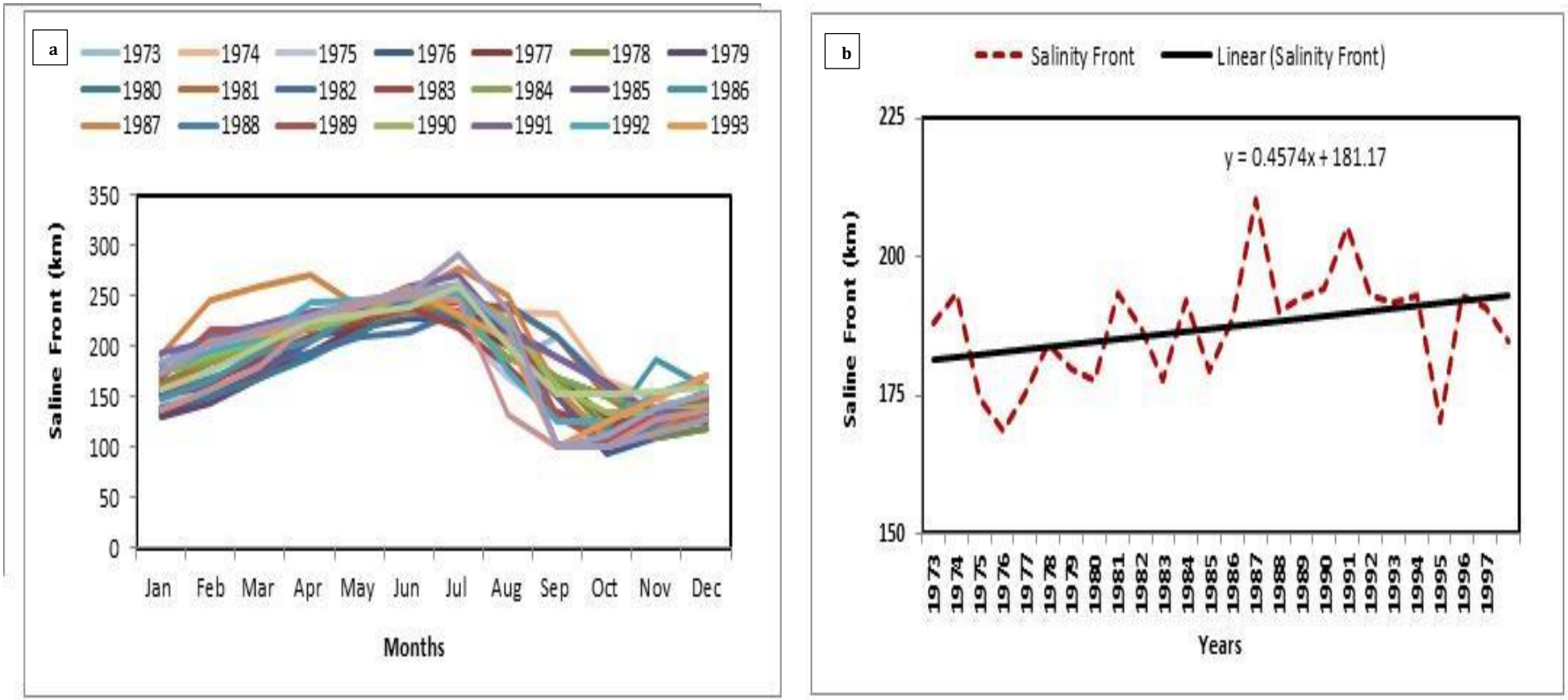

FIGURE 30: INTERANNUAL VARIATION OF SALINE FRONT OF THE RIVER GAMBIA FROM 1973 TO 1997

CHAPTER 3: DATA, MATERIALS AND METHODS

In this chapter, description of the different data collected, the material used and the tool and methodology applied on the data and the statistical analysis used. The chapter is divided into four sections. The first section deals with data source and description of the geomorphology and hydrograph of the study area. The results of the geomorphology can be found in chapter 2. The second section deals with the sources and classification of the soil types and chemical soil of the study area. The second section deals with the data collection of the geology, hydrogeology and hydrology of the study area. The third section deals with the data collection and analysis of the hydrodynamics and hydrochemistry of groundwater in the shallow aquifer of the GBA. The fourth section is about the description of the different recharge methods used and the potential recharge zone of the study area. The last section deals with the modelling of the present and future water balance components using Thornthwaite's model. The same section described the groundwater dynamics of the study area using the MODFLOW model. RCMs data were collected from CORDEX Africa for RCP4.5 and RCP8.5 scenarios for the period 2006-2050 horizon. The data was Bias-corrected both rainfall and temperature data.

3.1 Data

3.1.1 Climate data

The daily temperature (1946-2016), precipitation (1946-2016), relative humidity (1984-2016), sunshine duration (1984-2016), and wind speed (1984-2016), measured by the synoptic station, and was obtained from Department of Water Resources (DWR), The Gambia. These data were used in recharge estimation methods by Thornthwaite, Turc and Penman method and as well for the simulation of future groundwater dynamics of the study area. Projected climate scenario data (RCP4.5 and RCP8.5) in CORDEX were used to assess the impact of climate change on groundwater resources. The daily potential evapotranspiration data was deduced from the daily temperature using ESPERE software.

3.1.2 Topographic data

The topographic map was collected from the Ministry of Lands and Survey of The Gambia. Information on the topography of the study area was deduced from the Digital Elevation

Model (DEM) provided by HydroSHEDS. The HydroSHEDS (Hydrology of data and map based on SHuttle Elevation Derivatives at multiple Scales) data, which is derived from elevation data of Shuttle Radar Topographic Mission (SRTM), was used in this study to extract surface elevation data. The HydroSHED has a resolution of five-degree by five-degree tiles (or 90 m x 90 m approximately). Prior to using it in this current study, it was reconverted to 500 m x 500 m, which is the model cell size. DEM was used in the topography of the study area and to facilitate groundwater modeling.

3.1.3 Pumping test data

The pumping test data were collected were a drilling company and the Water Division NAWEC, which were used to calculate the transmissivity data and then hydraulic conductivity data (T = K*e). These data were used for groundwater modeling. The drilling boreholes log data (static water level) were collected from a drilling company and the Water Division NAWEC and used to estimate the historical groundwater level and as well used as the starting hydraulic head in steady-state simulation. These data were also used to infer the aquifer layers during the modeling. During the field campaign, 118 boreholes water level data were collected in pre-monsoon and post-monsoon of 2018. These data were used to simulate groundwater level in steady-state calibration.

3.1.4 Geological data

The geological map and reports were collected from the Department of Geology, under the Ministry of Petroleum and Energy, Gambia. The map was used to characterize the aquifer features of the study area.

3.1.5 Hydrochemical data

The hydrochemical data for groundwater quality assessment were collected from 58 sampling points (52 groundwater and 6 surface water) during the field campaign in pre-monsoon and post-monsoon of 2018. These water samples data were analyzed in the Hydrochemistry Laboratory of the Department of Geology, Faculty of Science and Technology, Cheikh Anta Diop University, Dakar, Senegal using standard methods. These data were used to assess the water quality of the continental shallow aquifer of the GBA based on the concentration of the different ions in groundwater.

3.1.6 Population data

The population of the GBA was obtained for The Gambia Bureau of Statistics. This population data was used to determine the population of the study area.

3.2 Materials

The materials used in this study are:

- **ArcGIS 10.3 software** used to create piezometric maps and the physicochemical graphs and also used to map most of the figures used in this study and interpolated some data using Kriging method.
- **Statistica version 10** and **MS Excel 2013** application used to store and analyze field data and generate different graphs and tables.
- **Camera** used to take some photos over the period of fieldwork.
- **Laptop** used to run all the models used in this study;
- **0.5 l of polythene bottles for a water sample** were used to collect surface water and groundwater samples from the field area to the laboratory for analysis;
- **Thornthwaite model**, this model was used to simulate groundwater recharge;
- **GPS** used to measure the geographical position of the data point;
- **Visual MODFLOW** used to simulate groundwater dynamics in steady conditions and future groundwater heads for four piezometers (Obs1, Obs2, Obs3 and Obs4);
- **AQUION-DIONEX Equipment** used for hydrochemical data analyses which were carried out using the ionic chromatography method;
- The exchange processes were realized through **AS14 A – AERS 500** columns for anions, and **CS12 A – CERS 500** for cations.
- A **WTW MULTI 3430 SET G Multiparameter** was used to determine pH, temperature and electrical conductivity at the laboratory.
- The **Hydrolab Quanta multiparameter probe** is a device designed to measure physicochemical parameters in the field. It was used to measure field parameters (pH, temperature and electrical conductivity) during the rainy seasons of 2018.

3.3 Methods

3.3.1 Geomorphology and Hydrography

The SRTM image processing methodology for the study area is summarized in Figure 30. This treatment led to the extraction of the DTMs of the study area, which thus constitute their geomorphological and hydrographic maps.

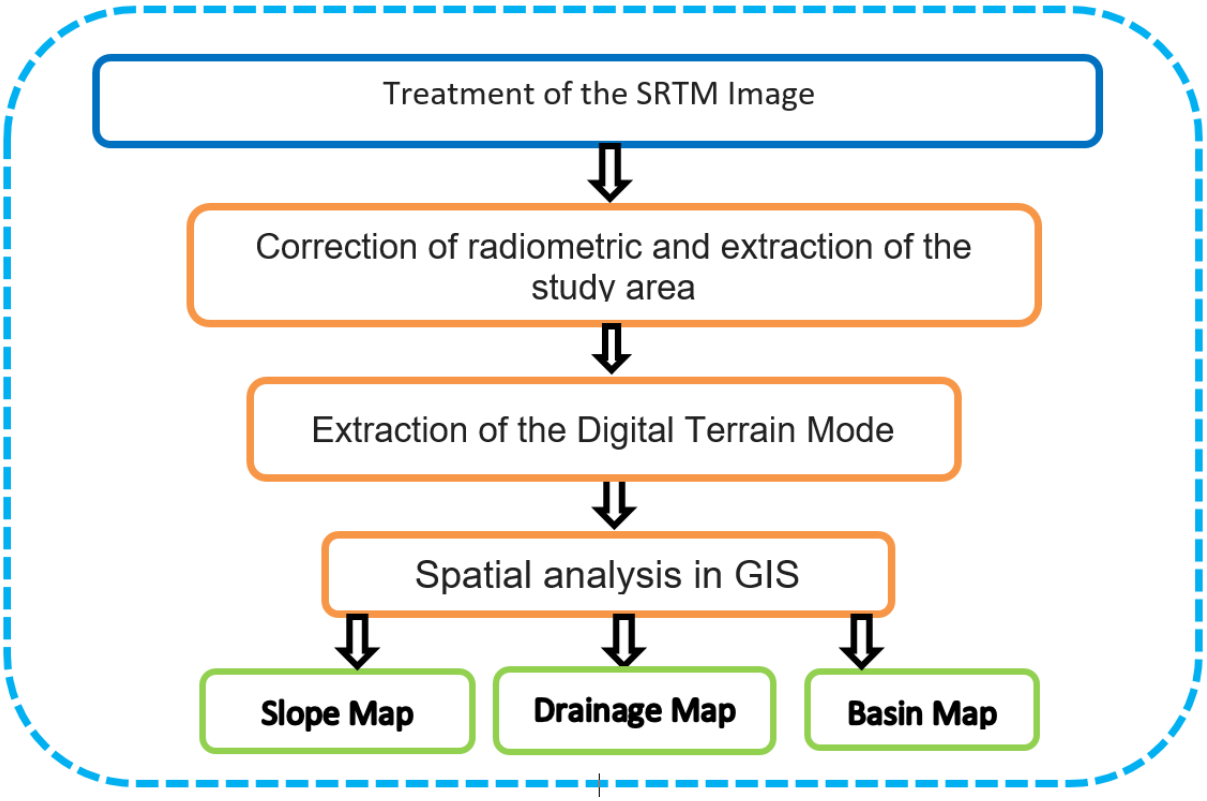

FIGURE 31: ORGANIZATION CHART OF THE METHODOLOGICAL APPROACH FOR THE REALIZATION OF THE DIGITAL TERRAIN MODEL USING SRTM IMAGE AND THE EXTRACTION OF SLOPE, DRAINAGE NETWORK AND WATERSHEDS

3.3.2 Source of Data and SRTM Processing method

3.3.2.1 Source of Data

The satellite imagery of the Shuttle Radar Topography Mission (SRTM), with 30m resolution was obtained from https://usgs.gov. The SRTM images are subjected to some corrections related to the functions, purposes and objectives of the study to be conducted.

3.3.2. 2 SRTM Processing Method

There are several tools for processing satellite data. The ArcGIS 10.3 software from ESRI 1999-2014 allowed the processing of this SRTM image.

3.3.3 Treatment

In order to generate the map of the study area, the ArcMap tool was used. Our study area was extracted from the SRTM image of the Gambia. Interpolations technique was used through the Spatial Analyst Tools, to obtain a DTM that reflects the reality of the terrain of the study area. Geomorphological analysis is the analysis of the topographic surface referred to as the Digital Field Analysis (DFA), which is applied to a series of formalized algorithms to the Digital Terrain Model (DEM) to derive altitudes or different topographic variables (Moore et al., 1993). DTMs are therefore digital representations of terrain in terms of altitude and are called DEMs. These maps illustrate a digital elevation distribution that is a digital representation of the surface of the earth. To eliminate any information previously overlaid on the study area, the UTM coordinate system was applied on it to attain reliable geographical information. The image was then geo-referenced to improve and restore the likelihood of Digital Elevation Models (DEM) and hence reduced the background noise locally and enhanced the signal. The final image obtained therefore constitutes a DTM and a corrected DEM that will serve as a basis to generate other maps (slope, drainage, geomorphology and hydrography) relevant to our study.

3.3.4 Soil

3.3.4.1 Choice and source of images

3.3.4.1.1 Choice

The choice of the images of a thematic cartography rests on the technical characteristics namely the stereoscopy and the spectral, spatial, temporal radiometric resolutions.

3.3.4.1.2 Source of Images

The soil map used in this study was primarily derived from the Harmonized World Soil Database (HWSD) that has been developed for Africa under the Land Use Change and Agriculture Program of the FAO and IIASA (Austria) in partnership with ISRIC – World Soil Information and the European Commission Joint Research Centre (JRC)/ European Soil Bureau Network (Jones, et al., 2013). The original HWSD data for Africa is combination of existing regional and national sources of soil information such as SOTER and SOTWIS with the FAO-UNESCO Soil Map of the World [FAO/UNESCO 1971-1981] at a scale of

1:5000000 for the Sahara, West Africa and most of central Africa. The soil names were obtained by harmonizing the Digital Soil Map of the World (FAO-74), SOTER (FAO-90) and the JRC Soil Atlas which were converted to the World Reference Base (WRB) system. The GIS software was used to process the soil data and generate the final map. The digital cartographic data (map) have been colored using a legend based on codes indicating the WRB Reference Group (Jones, et al., 2013). The legend of the soil map shows the different soil type preceded by a WRB qualifier "Haplic". The description of the qualifier and the different soil types are given chapter 2.

3.3.5 Hydrodynamic Methodology

3.3.5.1 Methodology

3.3.5.1.1 In-Situ Measurements and Sampling

Two field campaigns were carried out in May and November of 2018. The groundwater samples and field parameters (pH, temperature and electrical conductivity) were collected and measured at the field using the Hydrolab Quanta multiparameter probe during the rainy seasons of 2018. Hydrolab Quanta multiparameter probe is a device designed to measure physicochemical parameters in the field. In the field, the geographical coordinates of all water points of the selected sites were also taken with the help of a GPS device. 58 water samples for physicochemical (pH, temperature (T) and electrical conductivity (EC)) analyses were collected from 24 boreholes (BH), 6 streams (S) and 28 dug wells (DW) by using prewashed polyethylene bottles distributed in the study area (Figure 31). Two samples were taken per water point, one non-acidified sample for anion analyses and another sample acidified with HNO_3 acid for cations analyses. Water levels of 118 water points (101dug wells, 1 borehole, and 16 piezometers) were also measured with the help of a sound probe (deep meter) throughout the study area. These measurements help us to produce the piezometric map.

FIGURE 32: (WATER SAMPLE COLLECTION AND SWL MEASUREMENT IN THE FIELD

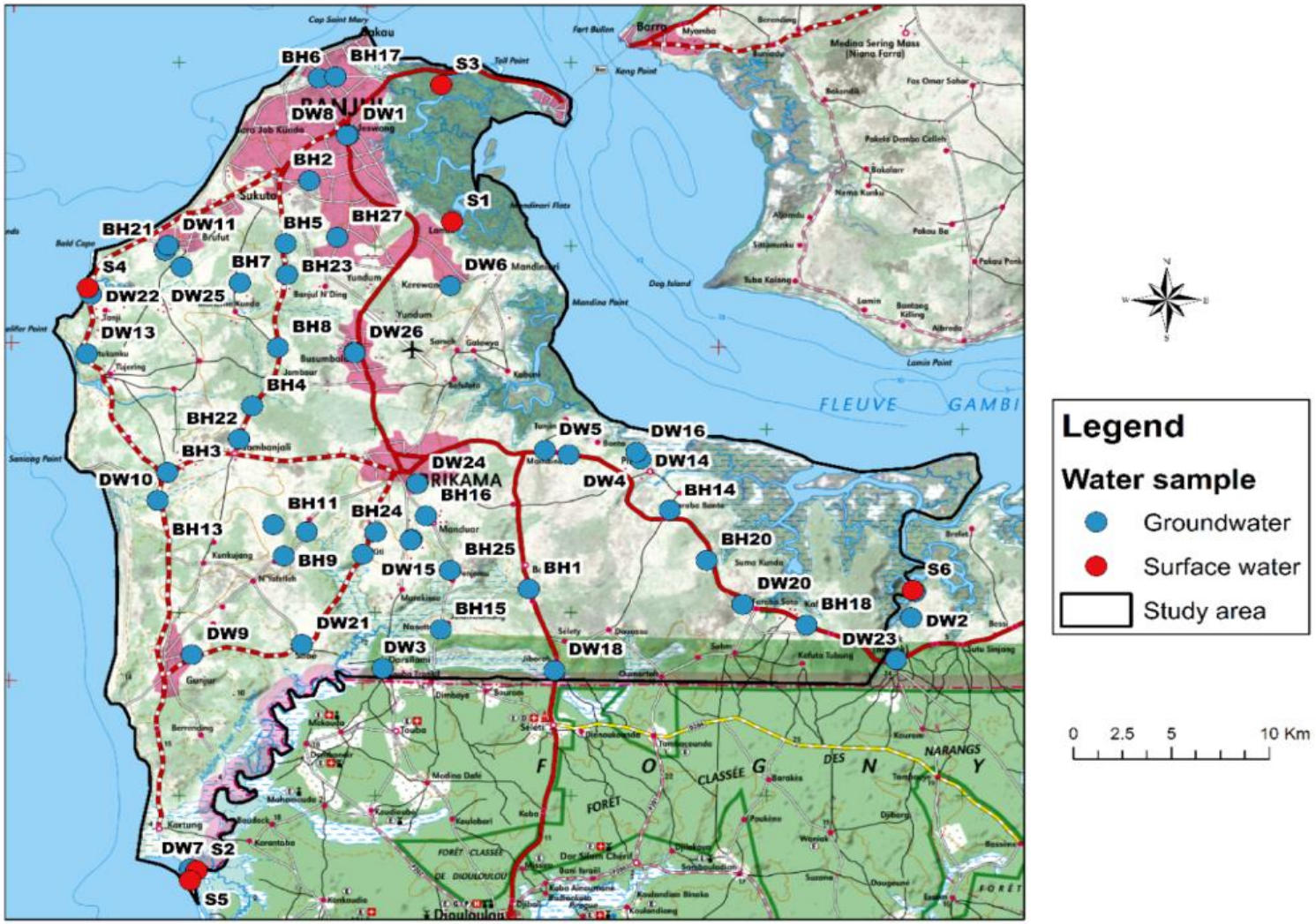

FIGURE 33: MAP OF THE LOCATION OF WATER SAMPLING POINTS

3.3.5.1.2 Data Processing

The measured hydrogeological data processing was carried out using computer software such as Statistica version 10 and MS Excel 2010 application used to store and analyze field data and generate different graphs and tables. ArcGIS 10.3 software was also used to create piezometric maps and the physicochemical graphs.

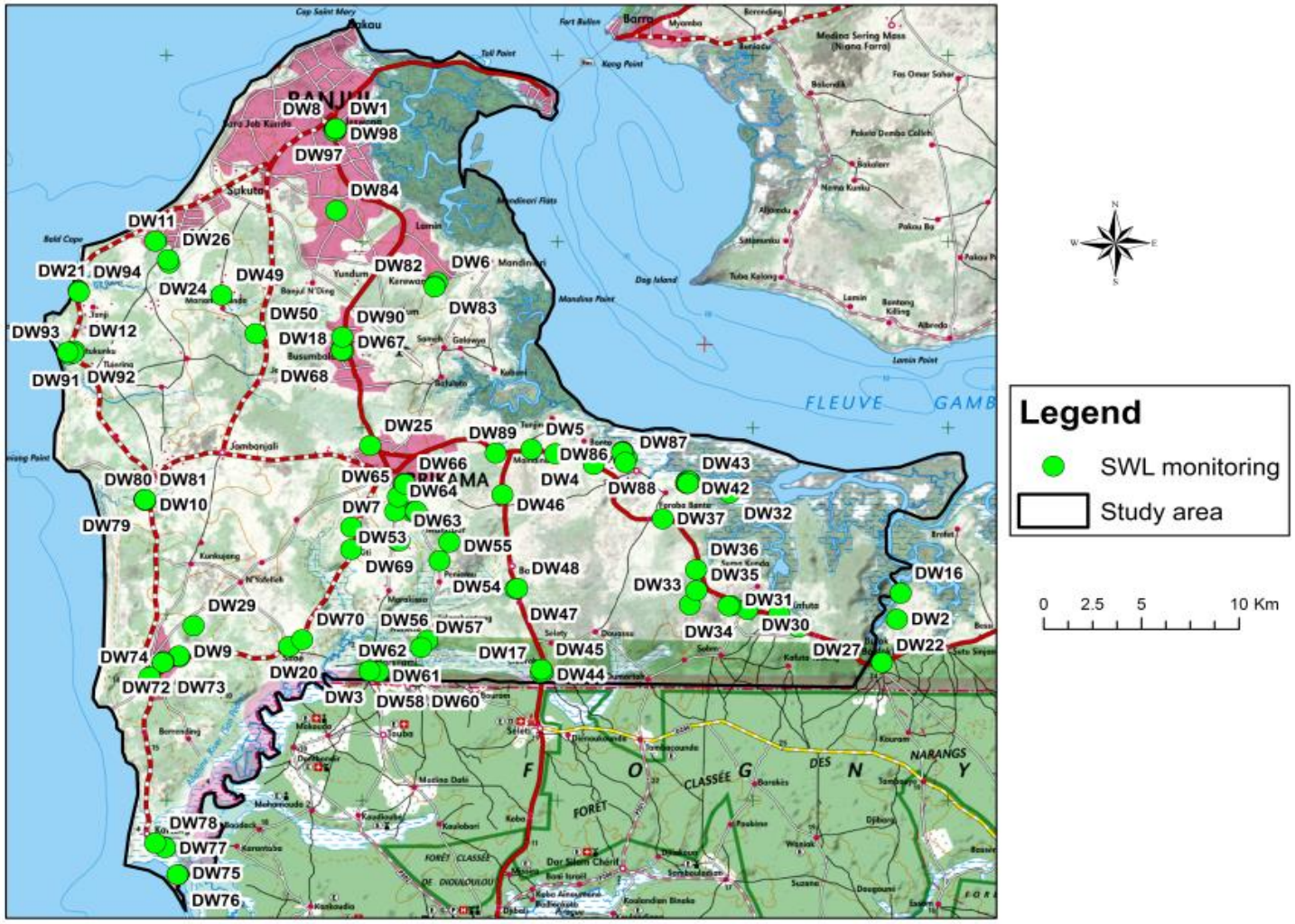

FIGURE 34: LOCATION OF STATIC WATER LEVEL (SWL) MEASUREMENT POINTS

3.4 Hydrochemistry

3.4.1 Laboratory Analysis

The hydrochemical data were obtained from chemical analyses performed for 52 groundwater and 6 surface water samples were collected throughout the study area. This analysis was carried out in the Hydrochemistry Laboratory of the Department of Geology, Faculty of Science and Technology, Cheikh Anta Diop University, Dakar, Senegal using standard methods. The analyses were carried out using the ionic chromatography method through AQUION-DIONEX equipment. The exchange processes were realized through AS14 A – AERS 500 columns for anions, and CS12 A – CERS 500 for cations. A WTW MULTI 3430 SET G multiparameter was used to determine pH, temperature and electrical conductivity at the laboratory. The samples were analyzed for their physicochemical quality to identify the contamination problems and propose suitable solutions. Although, the measured field parameters were used in this study to compare their variation in the two seasons. A hydrochemical analysis was carried out on the samples from the second campaign for four major cations (Ca^{2+}, Mg^{2+}, Na^{+}, and K^{+}) and four anions (Cl^{-}, HCO^{3-}, $SO4^{2-}$, and NO^{3-}) and a tracer ion Br (Appendices 1).

3.5 Methods of Estimating Groundwater Recharge

3.5.1 Methods of Estimating Recharge in the Unsaturated Zone

Estimation of groundwater recharge is extremely important for proper management of groundwater systems.

Groundwater recharge estimation is indispensable for the assessment of groundwater potential and for sustainable groundwater development, utilization (Dandekar et al., 2018) and management of groundwater systems (Lee et al. 2008). The net infiltration to the groundwater table moves through unsaturated or vadose zones. Water below the surface can be divided into three zones: (I) the unsaturated zone, or vadose zone, (II) the capillary fringe, and (III) saturated zone. The vadose zone and capillary fringe together form the zone of aeration, which is not fully saturated with water. The unsaturated zone is the part between the land surface and the top of the phreatic zone. Groundwater in this zone is exposed to atmospheric pressure. The unsaturated zone has three important functions: (1) protecting the phreatic (saturated) zone from surface contamination; (2) determining the rate, mode and location of

aquifer recharge; and (3) governing processes such as soil moisture retention, shallow interflow, throughflow, and the formation of some types of springs and wetlands (Breedt & Huisamen, 2014).

The processes within the vadose zone play a significant part in groundwater recharge in semi-arid regions where the water table depth is high (Dandekar et al., 2018). These processes in the vadose zone control the amount of water available for irrigation, rate and timing of aquifer recharge. The capillary fringe is the upper part of the saturated zone or the lower limit of the unsaturated zone which is subjected to upwelling by capillary rise of the water of the saturated zone; having saturation coefficient of 100% at its lower part (Emvoutou et al., 2018). Unsaturated-zone techniques for estimating recharge are applied mostly in semiarid and arid regions, where the unsaturated zone is generally thick (Scanlon et al., 2002).

The three methods stated below are used to estimate recharge in the unsaturated zone:

I. Soil moisture Techniques

Recharge estimation by soil moisture regimes includes the water balance methods, lysimetric methods, and water profiles (Emvoutou, 2018). Penman (1950) was the first to develop the soil water technique for assessing groundwater recharge. Rainfall is the principal means for the replenishment of moisture in the soil water system and recharges to groundwater. Moisture movement in the unsaturated zone is controlled by capillary pressure and hydraulic conductivity.

II. Water Budget Methods

These are methods based on simple water balance accounting for water entering and leaving a watershed. The water balance of a particular watershed usually aims to estimate the infiltrated water based on monthly/annual hydro-meteorological parameters (rainfall, evapotranspiration, runoff, and change in soil water storage) (N. Breedt et al., 2014; EMVOUTOU et al., 2018). The water-budget methods are flexible (Scanlon et al., 2002) and they can be applied over a wide range of spatial and temporal scales (Sophocleous, 2004). Scanlon et al. (2002) proposed the water budget to be calculated as:

$$P + Q_{on} = ET + Q_{out} + \Delta S \qquad (2)$$

Where, P = precipitation (mm/day), Q_{on} and Q_{out} are water flow in and out the site (mm/day), ET = evapotranspiration (mm/day) and ΔS = change in storage (mm/day).

III. Lysimetric Methods

Lysimeters are used for the measurement of filtration of water below the vegetation root zone and water use through evaporative processes. Lysimeters allow direct determination of the amount of water percolating through the soil profile, and the type and amount of solutes contained in it. They are also used in environmental pollution, applied geochemistry, hydrology, soil biology, and biochemistry waste management and water quality management meteorology, agronomy, agricultural management, and so on (Meißner, Prasad, Laing, & Rinklebe, 2010). These methods are based on the principle of infiltrating a known volume of water (V1) through a layer of soil insulated by well-sealed walls to maintain ideal conditions of the environment. At the base of the soil layer, the volume of infiltrated water (V2) is collected and the retention water of bare soil is obtained from the difference (V1-V2).

That of lysimeters consists of infiltrating a known volume of water (V1) through an isolated soil by watertight walls while maintaining as much as possible conditions close to those of the environment. The volume collected at the base thus gives the infiltrated volume (V2) while the difference (V1 - V2) expresses the quantity retained in the case of bare soil.

IV. Water profile methods

These methods are based on the principle of recurrent and concurrent measurements along water content profiles using neutron probes and loads by tensiometers.

V. Physical methods

The physical methods describe the movements of the water during its journey to the saturated zone. It is a mathematical principle that takes into account the physics of transfers with the main parameters the water content (θ) measured using a neutron moisture meter and the effective water pressure (h) obtained with a blood pressure monitor. These two parameters make it possible to calculate the equation of the flow of water in the unsaturated zone.

VI. Tracer techniques

These methods are based on the study of the transfer of a tracer in the unsaturated zone towards the aquifer. Tracer methods seem the most reliable for point recharge measurements in (semi-) arid areas (Sophocleous, 2004). Tracer methods are used to estimate groundwater recharge and determine the recharge sources, the flow speed, travel time, and to identify the preferred flow direction. These methods can be used in hydrogeological and hydrological systems to obtain information about water movement and pollutants

transportation (Xin et al., 2018), identification and analyses of groundwater ages, flow directions, recharge zones, etc. The commonly used tracers are the conservative elements such as chloride or constituent isotopes of the molecule of water (tritium, deuterium, and oxygen 18) (Dieng et al., 2017). These are the natural tracing methods. The artificial tracing methods are ones such as dye and electrolytes.

3.5.2 Methods based on the study of the saturated zone

I. Water Table Fluctuation (WTF) Method

The water level fluctuation method of estimating recharge can be applied to the saturated zone (Lawrence, 2006). The water table fluctuation (WTF) method is based on the principle that rises in water levels in unconfined aquifers are caused by recharge water reaching the water table and going immediately into storage (Healy & Cook, 2002). The method is focused on analyzing the effects of infiltration by the fluctuation of piezometric levels. Hence, it is considered that a steady state of time series rainfall corresponds to a steady-state of time series of water table levels and its flow and that any variation of the rainfall regime causes a change in the regime of the water table and thus its level (Dieng M., Faye S., 2017). The WTF method can also be to determine the magnitude of future changes in aquifer recharge due to land-use change or climate change.

II. Numerical methods

Calibration of hydrogeological or inverse models gives recharge rates estimation from values of piezometric heights, hydraulic conductivity, and other parameters of the aquifer (Scanlon et al., 2002). These methods allow, after calibration of hydrogeological or inverse models, to obtain the recharge from the values of piezometric heights, hydraulic conductivity, and other parameters of the aquifer. They are based on resolving the diffusion equation derived from Darcy's law and the principle of conservation of mass in the saturated zone (Dieng et al., 2017). Hence, the reliability of the estimated recharge values depends inter alia on the accuracy of the hydraulic conductivities. Because hydraulic conductivity ranges over several orders of magnitude, estimation of recharge rates using model calibration may not be very accurate. Hydrogeological models are valuable for aquifer management and the results obtained greatly depend on input data.

3.5.3 Method of Estimating ETo and Recharge by Water Balance Method

Naorem & Devi, (2014) defined evapotranspiration (ET) or consumptive use of water as the total amount of water removed from the soil by evaporation and transpiration. Evaporation is the removal of water in the form of gas from soil, water surfaces, or plant leaf surfaces holding water droplets from rain, irrigation, or dew formation while Transpiration is the loss of water through the stomata leaves of plants into the atmosphere during the process of photosynthesis (Naorem & Devi, 2014).

Many factors affect the rate of ET such as soil type, climate, vegetation, and so on. Climatic factors affecting ET comprise wind speed, humidity, air temperature, solar radiation, etc. Potential Evapotranspiration (ETP) is the maximum of ET for a crop in a given climate which is defined as the evapotranspiration that would happen if there was always an adequate water supply available to a fully vegetated surface (Naorem & Devi, 2014). Many methods of estimating ETP through the Water Budget method exist Lysimeter method, empirical methods, field experimental plots, remote sensing & GIS techniques, etc. The ETP and corresponding recharge estimations were done with three different empirical models for our study area.

Recharge estimation is based on the determination of terms that express the distribution of the rain that falls on the ground, during a given period, according to the equation below:

$$P = R + ETR + I_{eff} + \Delta S \quad (3)$$

Where P is precipitation; R is surface runoff; ETR, the actual evapotranspiration; I_{eff} is effective infiltration; ΔS change in soil water storage. The effective infiltration was therefore given by:

$$I_{eff} = P - (R + ETR + \Delta S) \quad (4)$$

Effective infiltration [Ieff] is the amount of precipitation that truly reaches the water table.

The ETP values used to approximate ETR are calculated by Thornthwaite, Turc, and Penman empirical formulas using meteorological data such as mean temperature, mean relative humidity, sunshine/radiation, wind speed, and precipitation. The Department of Water Resources of the Gambia (DOW) provided daily climate data for Banjul and Yundum for the

period 1984 to 2016. The soil storage capacity (stock) used in this research ranges between 100 mm to 200 mm. In the light of the uncertainty involved, four different stock values (100 mm, 125 mm, 145 mm, and 178 mm) were used to run the software to observe if the water balance parameters are sensitive to variations in the stock.

I. Thornthwaite's Method of Calculating Potential Evapotranspiration

An empirical method of estimating potential evapotranspiration from mean temperature data was developed by Thornthwaite (1948). Thornthwaite & Mather (1955) later improved the method for usage over a wide range of soil and vegetation types. The water balance technique of Thornthwaite is a mere comparative study of rainfall and evapotranspiration, which plays a crucial role in many fields of earth science, especially agriculture and water resource development and management. The parameters essential for the calculation of water balance based on the Thornthwaite-Mather model are mean temperature and precipitation. The model permits estimation of potential evapotranspiration, actual evapotranspiration, effective water (infiltration), and soil moisture storage. These parameters were obtained by using a monthly time step from the Standard Thornthwaite model (Thornthwaite, 1948).

Many researchers (Emvoutou et al., 2018; Dieng et al., 2017) had applied the Thornthwaite method to estimate the potential and actual recharge in their areas. The method first calculates the annual values of the heat index (***I***) (Fischer, 2013):

$$I = \sum_{n=1}^{12} i_n \qquad \textbf{(5)}$$

Where ***n,*** the number of months and (***i***) the monthly indices given by:

$$i = \left(\frac{T}{5}\right)^{1.514}$$

Hence, potential evapotranspiration is calculated from the formula below:

$$ETP = C * \left(10\frac{T}{I}\right)^{a} F(\lambda) \qquad \textbf{(6)}$$

Where, $F(\lambda)$ correction is a factor depending on the latitude and taking into account the number of hours of day **C** = 16, ***T*** **=** mean monthly temperature and ***a*** is a function of (**I**)

$$a = (0.492 + 0.0179I - 77.1 * 10^{-6}I^2 + 67.5 * 10^{-8}I^3)$$

The Thornthwaite conceptual model of the water balance based on three considerations (DASSARGUES, 2006):

The unsaturated zone of the soil is considered a refillable water stock. This hypothesis makes it possible to discharge the complexity of the flows in porous media that is partially saturated, modeling this area by a stock or rechargeable water tank;

The stock modeling the partially saturated medium has a maximum capacity, which is known as the soil water capacity (SWC) with a known value. The hypothesis is vindicated with the fact that the soil cannot hold more water than that of the water at its saturation level;

Finally, infiltration to the water table or run-off can only occur when the soil moisture capacity is satisfied.

The Thornthwaite approach is a model based on the following conditions:

- Precipitation reconstitutes the evapotranspiration reservoir (with a variable-capacity of one month to month);
- The surplus (P-ETP) satisfies the soil water stock reservoir first;

If the soil water stock is satisfied, then the extra surplus infiltrates to the water table.

The Thornthwaite method involves calculating potential evapotranspiration (ETP) and then compares it with the precipitation of the month considered. The conditions for these comparisons are as follows:

- If P ≥ ETP: precipitation is surplus, then ETR = ETP, and the excess [P-ETR] will first recharge the soil water capacity (SWC) before infiltrating to the water table;
- If P ≤ ETP: precipitation is a deficit, so the precipitation is insufficient to satisfy the evapotranspiration, the water in the stock (initial soil moisture (ΔSi)) will fully or partially fill the water deficit [ETR-P].

II. Penman's Method of Calculating Referemce Evapotranspiration

The Penman-Monteith method is the most widely used for the evaluation of reference evapotranspiration ET_o (Allen et al., 1998). The FAO Penman-Monteith method combines aerodynamic and surface resistance into the original Penman-Monteith equation to give a

more accurate estimation of evapotranspiration. This empirical method used meteorological data like radiation/sunshine, humidity, wind speed, and temperature (minimum and maximum) in addition to site-specific conditions. The evapotranspiration can be derived from the equation below (Silva, Alves, Júnior, & Miranda, 2013):

$$\mathbf{ET_o} = \frac{0.408\Delta(R_n - G) + \gamma \frac{900}{T+273} u_2 (e_s - e_a)}{\Delta + \gamma(1 + 0.34u_2)} \quad \textbf{(7)}$$

$\mathbf{ET_o}$ Reference evapotranspiration [mm day^{-1}],

$\mathbf{R_n}$ Net radiation at the crop surface [MJ m^{-2} day-1],

$\mathbf{G}$ Soil heat flux density [MJ m^{-2} day^{-1}],

T mean daily air temperature at 2m height [°C],

$\mathbf{u_2}$ Wind speed at 2m height [m s^{-1}],

$\mathbf{e_s}$ Saturation vapour pressure [kPa],

$\mathbf{e_a}$ Actual vapour pressure [kPa],

$\mathbf{e_s - e_a}$ Saturation vapour pressure deficit [kPa],

Δ Slope vapour pressure curve [kPa °C^{-1}],

γ Psychrometric Constant [kPa °C^{-1}].

The estimation of crop potential evaporation $\mathbf{ET_0}$ incorporates the single or the dual crop coefficients in the following equation.

$$ET_c = K_c * ET_p$$

Where, K_c single crop coefficient, which averages crop transpiration and soil evaporation.

The actual evapotranspiration (under soil water stress condition), $\mathbf{ET_a}$, when the single crop coefficient, $\mathbf{K_c}$, is used estimated from the equation below (Tilahun & John, 2012):

$$ET_a = K_s * ET_c = K_s * K_c * ET_0 \quad \textbf{(8)}$$

The crop coefficients (K_c), can be derived from the following relationship (Allen et al., 2005):

$$K_c = \frac{ET_c}{ET_o} \quad (9)$$

III. Turc Method of Calculating Potential Evapotranspiration

The Turc method (Turc, 1961) was previously developed for southern France and northern Africa. This method is easy to apply when climatic data is limited. Turc, 1961) proposed a method of calculating monthly evapotranspiration (ET) which is based on climate data like mean temperature, solar radiation, and relative humidity values greater than 50% or less than 50% (Tukimat, Harun, & Shahid, 2012). The Turc equation is as follows:

$$ETP = k * \left[{}^{T_{meam}}/_{(T_{mean} + 15)} \right] * (I_g + 50) \quad (10)$$

If RH > 50%

$$ETP = k * \left[{}^{T_{meam}}/_{(T_{mean} + 15)} \right] * (I_g + 50)[1 + (50 - RH)/70] \quad (11)$$

If RH<50%

Where,

T_{Mean} = Mean air temperature (°C) given by: $T_{mean} = \frac{T_{max}+T_{min}}{2}$

I_g= global solar radiation (MJ m^{-2} day^{-1}) during the period considered and it's evaluated from the duration of sunshine hour h

The factor $k = 0.013 * n \cong 0.4$

n = number of days in the period considered

RH= relative humidity of the air in %

The ETR, on the other hand, is based on precipitation (P) and L-factor, according to the formula:

$$ETR = {}^{P}/\sqrt{\left[0.9 + \left({}^{P^2}/_{L^2}\right)\right]} \quad (12)$$

With:

P = Precipitation (mm / yr.) for the period considered

L = Limit towards which evapotranspiration tends

3.6 choice and justification of methods used in this study

Due to large uncertainties involved in the measurement of individual parameters of each method, some researchers (Healy and Cook, 2002, Scanlon *et al*., 2002) suggested that recharge estimation should be done with multiple methods and the results compared (Islam, Singh, & Khan, 2016b). There are numerous methods of recharge estimation available but choosing the most appropriate method is mostly a challenge. Scanlon et al. (2002) stated that the judicious choice of selecting these methods involved Spatio-temporal, range, and reliability of recharge estimates based on various methods. The choice of method for this study is based mainly on the objectives of the study and available data (field and in-situ).

3.7 Potential Recharge Zone Mapping

3.7.1 Methodology

I. Data Acquisition and Processing

To delineate groundwater recharge zones (GWRZ), multiparametric datasets comprising seven criteria known as factors, and they include geology, land use/land cover, soil texture, aquifer transmissivity, drainage density, slope, and groundwater fluctuation together with integrated GIS, RS, and MCE tools have been in this study. These factors influence infiltration in various ways and are interdependent. For this reason, they must be defined, classified, and assigned a weight according to their importance in the recharge process but also their interdependence. The thematic maps of lineament density, drainage density, slope, and soil are prepared via ArcGIS 10.6. The GIS-based Analytic Hierarchy Process (AHP) method has been used by many researchers (P. Singh, Thakur, & Kumar, 2013; Aghazadeh et al., 2017; Al-Manmi, 2010; Saaty, 2008; Agarwal et al., 2016; Shaban et al., 2006; Ashikin et al., 2013; Das et al., 2019; Argaz, 2019; Ahmed et al., 2019; Valverde et al., 2016) to delineate the groundwater productivity zone of a region of interest. The methodology adopted for the mapping and identification of potential aquifer recharge zones is presented in Figure 33.

All data sets used to prepare the thematic layers are derived from various data sources such as remote sensing data, topographical maps, district resource maps, field surveys, and other secondary data. The data sources have been converted and geographically referenced to UTM-WGS 84 projection and coordinate system by applying the ground control points (GCPs) obtained from the GPS field survey.

The geological setting and the soil characteristic were obtained from the Department of Geology published in 1988 and the National Environment Agency of the Gambia, respectively. Furthermore, the aquifer transmissivity layer was prepared using the pumping test data of the borehole reports obtained from the Water Division of NAWEC, Serekunda, and a drilling company. Groundwater fluctuation data were calculated using the groundwater depth level collected during this present study. This fluctuation rate is the seasonal variation of water depth level measured at 118 wells during the pre-monsoon and post-monsoon of 2018. A kriging interpolation was then used to transform discrete data into gridded layers and to demarcate the variation of the aquifer transmissivity and the groundwater fluctuation. The thematic layer of Land-use/cover was obtained from the European Space Agency S2 prototype with a spatial resolution of 20m. For the drainage density layer, the drainage network and watersheds were extracted using an ASTER DEM (20m) and the topographic map of the study area. The spatial characteristics of drainage density are then computed from the drainage network using the 'line density tool' of the spatial analyst module in ArcGIS 10.7 software. The slope map was delineate using the same ASTER DEM data using the Slope module in Terrset software

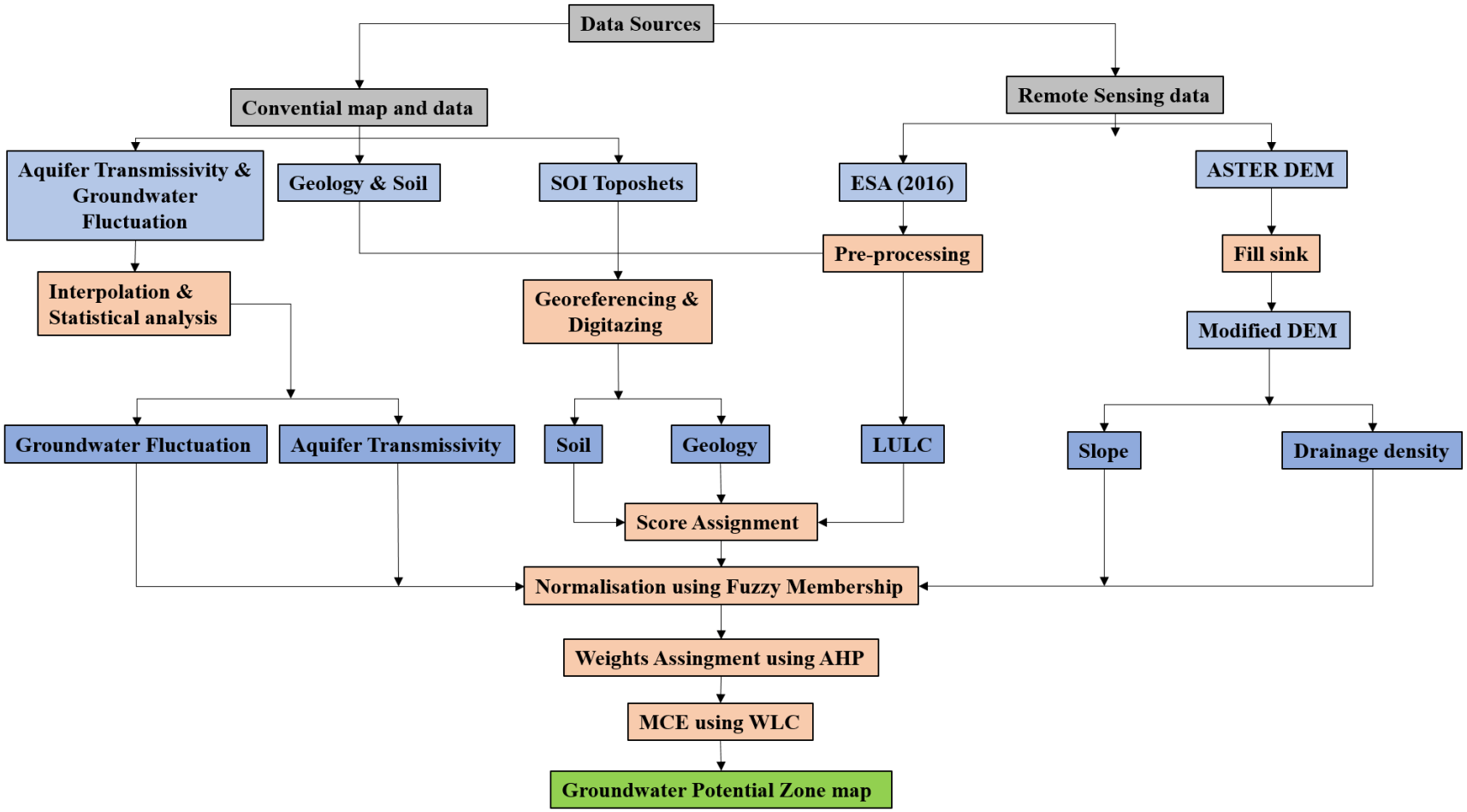

FIGURE 35: FLOW CHART SHOWING GROUNDWATER POTENTIAL RECHARGE MAPPING METHODOLOGY

II. Criterion Weights Assignment

A wide variety of techniques exist for the development of weights. However, breaking the information down into simple pairwise comparisons in which only two criteria need to be considered at a time to greatly facilitate the weighting process, and will likely produce a more robust set of criteria weights. This decision-making process known as the Analytical Hierarchy Process (AHP) developed by Saaty (1980), incorporates the evaluations of all decision-makers into a final decision, without having to elicit their utility functions on subjective and objective criteria, by pairwise comparisons of the alternatives. Moreover, a pairwise comparison method has the added advantages of providing an organized structure for group discussions, where group members can use their experience, values, and knowledge to break down a problem into a hierarchy and then solve it by AHP steps. It also incorporates systematic checks on the consistency of judgments known as consistency ratio (CR) developed by Saaty which indicates the probability that the matrix ratings were randomly generated.

In this present study, weighting assignment to different criteria is based on previous literature and weights suggested by various experts after discussion, subsequently normalized based on Saaty's scale. Geology was taken as the principal factor for the delineation of potential GWRZ. Consideration of geology as a principal factor was based on the infiltration of water which in turn depends on the facies unit, the thickness of formation, grain size, type and degree of cementation, and the extent of the weathering. The other factors such as land use/cover, slope, drainage, aquifer properties (transmissivity and groundwater fluctuation), and soil were the factors incorporated in characteristic expressions of geological units as evidenced by (P. Singh et al., 2013).

The following steps were carried out to apply the AHP procedure and compute the CR [(Saaty, 2008; Agarwal & Garg, 2015)]:

(1) The normalized pairwise comparison matrix A is built as:

$$A = \begin{bmatrix} a_{11'} & a_{12'} & \cdots & a_{n1'} \\ a_{21'} & a_{22'} & \cdots & a_{n2'} \\ \vdots & \vdots & \ddots & \vdots \\ a_{n1'} & a_{n2'} & \cdots & a_{nn'} \end{bmatrix}, a_{ij'} = \frac{a_{ij}}{\sum_1^n a_{ij}} \quad for\ i,j = 1,2,\ldots,n \qquad (13)$$

The values assigned to a_{ij} according to the Saaty scale which is provided on a 9-continuous scale are given in Table 5.

TABLE 5: SAATY'S SCALE OF PREFERENCES IN THE PAIR-WISE COMPARISON PROCESS (SAATY, 1980)

1/9	**1/7**	**1/5**	**1/3**	**1**	**3**	**5**	**7**	**9**
extremely	very strongly	strongly	moderately	equally	Moderately	strongly	very strongly	extremely
	less important					more important		

The eigenvalue and the eigenvector are calculated as:

$$W = \begin{bmatrix} w_1 \\ w_2 \\ \vdots \\ w_n \end{bmatrix} and\ w_i = \frac{\sum_1^n a_{ij'}}{n}\ for\ i = 1,2,\dots,n\ \&\ W' = AW = \begin{bmatrix} w_1{}' \\ w_2{}' \\ \vdots \\ w_3{}' \end{bmatrix}\ \&\ \lambda_{max} = \frac{1}{n}\left(\frac{w_1{}'}{w_1} + \frac{w_2{}'}{w_2} + \cdots + \frac{w_n{}'}{w_n}\right) \quad \textbf{(14)}$$

Where,

W: Eigenvector;

$W_{i:}$ Eigenvalue of criterion*;*

λ_{max}*:* Average eigenvalue of the pairwise comparison matrix.

Consistency index (CI) and consistency ratio (CR) proposed by Saaty to verify the consistency of the comparison matrix are defined as follows:

$$CI = \frac{\lambda_{max} - n}{n-1} \quad \textbf{(15)}$$

$$CR = \frac{CI}{RI} \quad \textbf{(16)}$$

Where n is the number of themes or classes and RI the Ratio Index. This latter represents the consistency index of a randomly generated pairwise comparison matrix. The CR is acceptable if CR ≤ 0.1. Otherwise, the re-evaluation of the comparison matrix is solicited to avoid inconsistency.

III. Delineation of Potential Groundwater Zone

To demarcate the Potential Groundwater Recharge Zone (PGWRZ), the weighted linear combination (WLC) aggregation method as proposed by Malczewski (1999) was used.

This method multiplies each standardized factor map (i.e., each raster cell within each map) by its factor weight and then sums the results. Since the set of factor weights for an evaluation must sum to one, the resulting suitability map will have the same range of values as the standardized factor maps that were used. The WLC was computed using the MCE module of Terrset software, expressed as follow:

$$WLC = \sum_{i=1}^{i=n}(w_i \times x_i) \quad \textbf{(17)}$$

Where WLC refers to weighted index value (raster map of the suitability rate of GWP);

W_i the weight of factors i;

x_i the criterion score of factors i

3.8 Groundwater Modelling

Generally, the groundwater modeling technique has two key components (Middlemis, 2004):

1. Conceptual model
2. Numerical model

3.8.1 Conceptual Model

When designing a groundwater flow model, the first thing to consider is to develop a conceptual model of the flow system. The conceptual model forms an idealized and simplified but accurate representation (Mutasa, 2011) of the situation, including the spatial distribution of the geologic and hydrogeologic conditions, the location of system boundaries and boundary types, values on aquifer parameters, and hydrogeological stresses (Heiden, 2011). According to C. Augusto and G. Peña (2017), the conceptual model describes groundwater movement and occurrence in the study area as well as the physical properties of the aquifer. The setting up of the conceptual model requires specifying the hydrostratigraphic units, preliminary water balance, flow processes, direction and flow rate, hydraulic parameters, physical and hydraulic boundaries (Jackson, 2007; Mutasa, 2011). When an error occurs in constructing the conceptual model, this can lead to the failure of the mathematical model to make precise estimations.

In this study, a conceptual model was built to understand how the aquifer system works. To establish the conceptual model, the SRTM / DEM data was used to create the top layer of the aquifer by interpolation using the SURFER program (Figure 34). The reports and log data allow us to infer the depth of the substratum on each borehole. Based on hydrogeology and hydrochemistry investigations carried out in the course of this study, the conceptual model of the shallow aquifer functioning was defined as follow:

- The unconfined aquifer in the GBA which consists of sand and sandy clay formations with a thickness varying from 10 to 100 m bears the shallow groundwater exploited through traditional dug wells and boreholes drilled in the basin to meet water demand in the study area.
- The groundwater flow pattern is controlled by piezometric mounds, with a general flow direction from these mounds toward the surface water (River Gambia and its tributaries, and the Atlantic Ocean)
- The central zone of GBA is defined as the presidential recharge zone, characterized by freshwater with low EC values that tend to be diluted during infiltration. The mean annual groundwater recharge is estimated at 172 and 97 mm/year respectively in Yundum and Banjul areas.

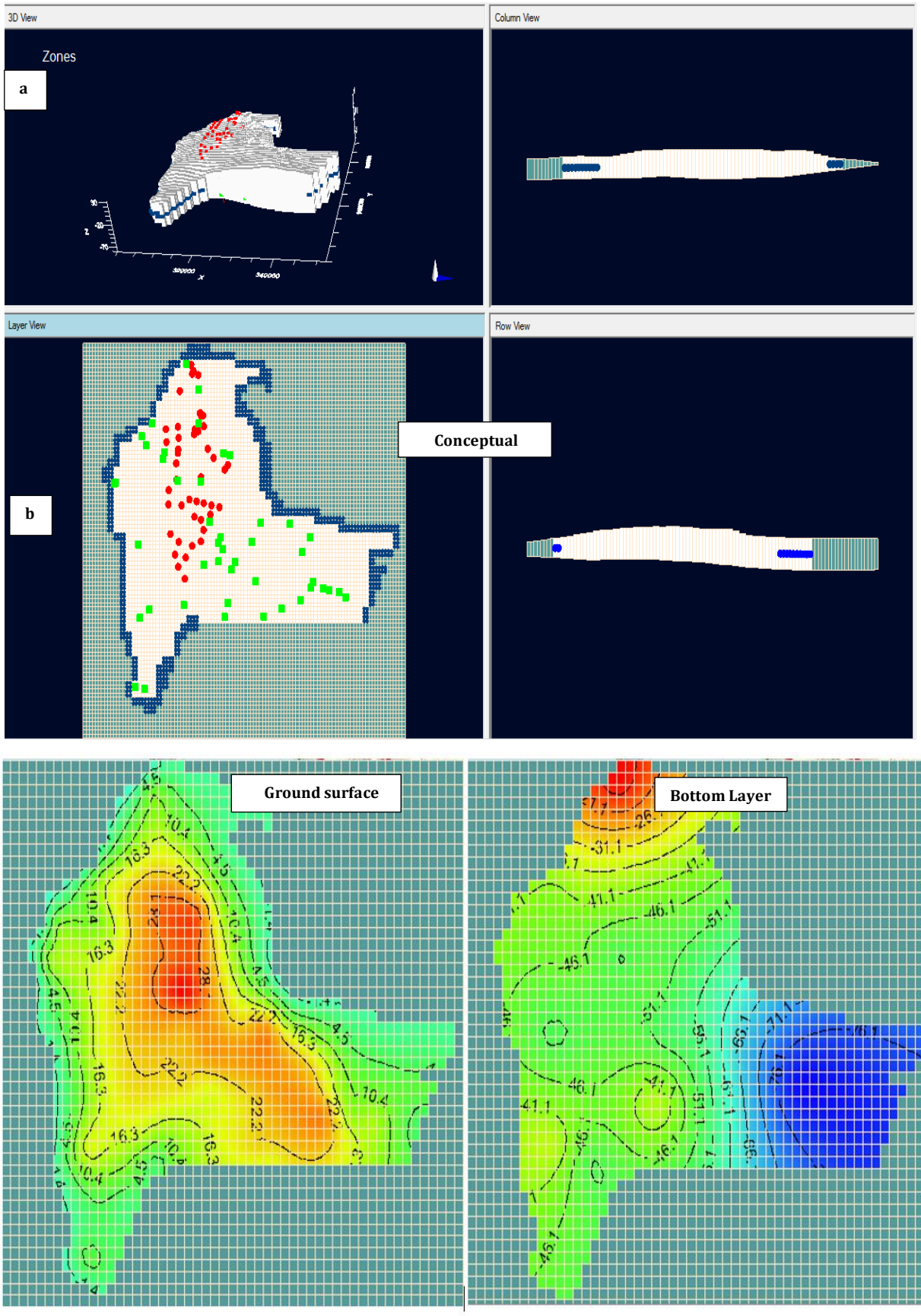

FIGURE 36: (A) CONCEPTUAL MODEL; (B) THE BOTTOM AND TOP SURFACE OF THE SHALLOW AQUIFER

3.8.2 Numerical Model

A mathematical model that gives a good representation of the problem was chosen depending on the conceptual model. Numerical models are mathematical models described by some governing equations, with associated initial and boundary conditions which mathematically express the conceptual model. Numerical models have been broadly utilized for surface water and groundwater interaction, groundwater management, groundwater quality, and quantity stabilization (Lakshmi & Narayanan, 2015; Gautam & Swaroop, 2017). They use approximations (e.g. finite differences, or finite elements) to solve the differential equations describing groundwater flow or solute transport. Models are also used to estimate the future behavior of the aquifer (groundwater). A numerical simulation model of the groundwater flow system was built using Visual MODFLOW Flex mainly focusing on analyzes and conceptualization of the local geological and hydrogeological conditions of the GBA aquifer system. MODFLOW uses the finite difference numerical method to solve the groundwater flow mathematical model (Loudyi, 2014) given below.

The groundwater flow equation relies on the mass balance law and Darcy's law. MODFLOW solves the partial differential equation that describes three-dimensional (3D) groundwater flow in a saturated porous media given below (Kipyegon, 2018 Loudyi, 2014):

$$\frac{\partial}{\partial \times}\left(K_x \frac{\partial h}{\partial x}\right) + \frac{\partial}{\partial y}\left(K_y \frac{\partial h}{\partial y}\right) + \frac{\partial}{\partial y}\left(K_z \frac{\partial h}{\partial z}\right) - W^* = S_s \frac{\partial h}{\partial t} \quad \textbf{(18)}$$

Where K_x, K_y, K_z are the aquifer hydraulic conductivity in the X-, Y- and Z- directions [m/day]; *h* is the potentiometric/piezometric head [m] of the aquifer; S_s is the specific storage of the porous material [m^{-1}]; t is time [day^{-1}]; W^* is the volumetric flux per unit volume and represents the sink and/or source term [$mday^{-1}$]. In steady-state, the term $\frac{\partial h}{\partial t} = 0$, and hence the equation is reduced to the right-hand side equation plus the volumetric flux:

$$\frac{\partial}{\partial \times}\left(K_x \frac{\partial h}{\partial x}\right) + \frac{\partial}{\partial y}\left(K_y \frac{\partial h}{\partial y}\right) + \frac{\partial}{\partial y}\left(K_z \frac{\partial h}{\partial z}\right) + W^* = O \quad \textbf{(19)}$$

Equation (19) can be solved either by using analytical or numerical methods. Dependent on their approaches, assumptions, and capability, both methods may be used to solve the equation (Touré, 2017). MODFLOW has been used by many researchers (Loudyi,

2014; Yihdego et al., 2017; Touré, 2017; Kipyegon, 2018) for modeling groundwater flow dynamics. It is one of the best tools to describe and predict groundwater flow dynamics. The solution of the mathematical model will result in the predictions of the aquifer system behavior in response to various sources and/or sinks.

3.9 Discretization and Boundary Conditions

ArcGIS 10.3 software was used to digitize the study area map and the shapefile of the map was then imported into Visual MODFLOW Flex. Discretization of the grid was optimized to reduce the numerical error of the flow model (Kaviyarasan, Seshadri, & Sasidhar, 2013). The model is conceptualized as a single layer, discretized into 53 rows and 49 columns and the cells are the same regular rectangles. The total cell number is 2597. Model domain and gridding have a mesh of 500×500 m. The average thickness of the aquifer ranges from 10 m to 100 m. The model area is assumed as a closed basin with no flow in or out of the boundaries. The aquifer of the GBA has been considered to be a single layer aquifer having a vertical recharge due to precipitation only. The bottom of the aquifer is assumed to be impermeable clay. Simulation of the groundwater flow was done under the current stress conditions using numerical models of Visual MODFLOW Flex. A steady-state finite-difference model, Visual MODFLOW Flex was developed to model the quantity of groundwater in the GBA basin. It is also used for the description and prediction of groundwater systems. Both Dirichlet and Neumann boundary conditions were used to simulate the hydrological boundaries which represent a specified boundary head and flow rate across a boundary to prescribe an impermeable boundary, respectively.

In this study, the areal extent of the GBA domain (Active cell) is designed based on water bodies surrounding the study area except for the south-East (Figure 35). Therefore, all the boundary conditions were considered as constant head (head=0 mbsl) boundary along the River Gambia on the north and the Atlantic Ocean on the western part of the study area. Along the southern part of the study area, a no-flow (no-flux) condition was assigned to prevent the flow of water in and out of the modeled aquifer. The constant head condition was also used as a boundary condition across the aquifer along the eastern boundary between Bullock and Faraba Bantang (i.e. the Bullock Bolong).

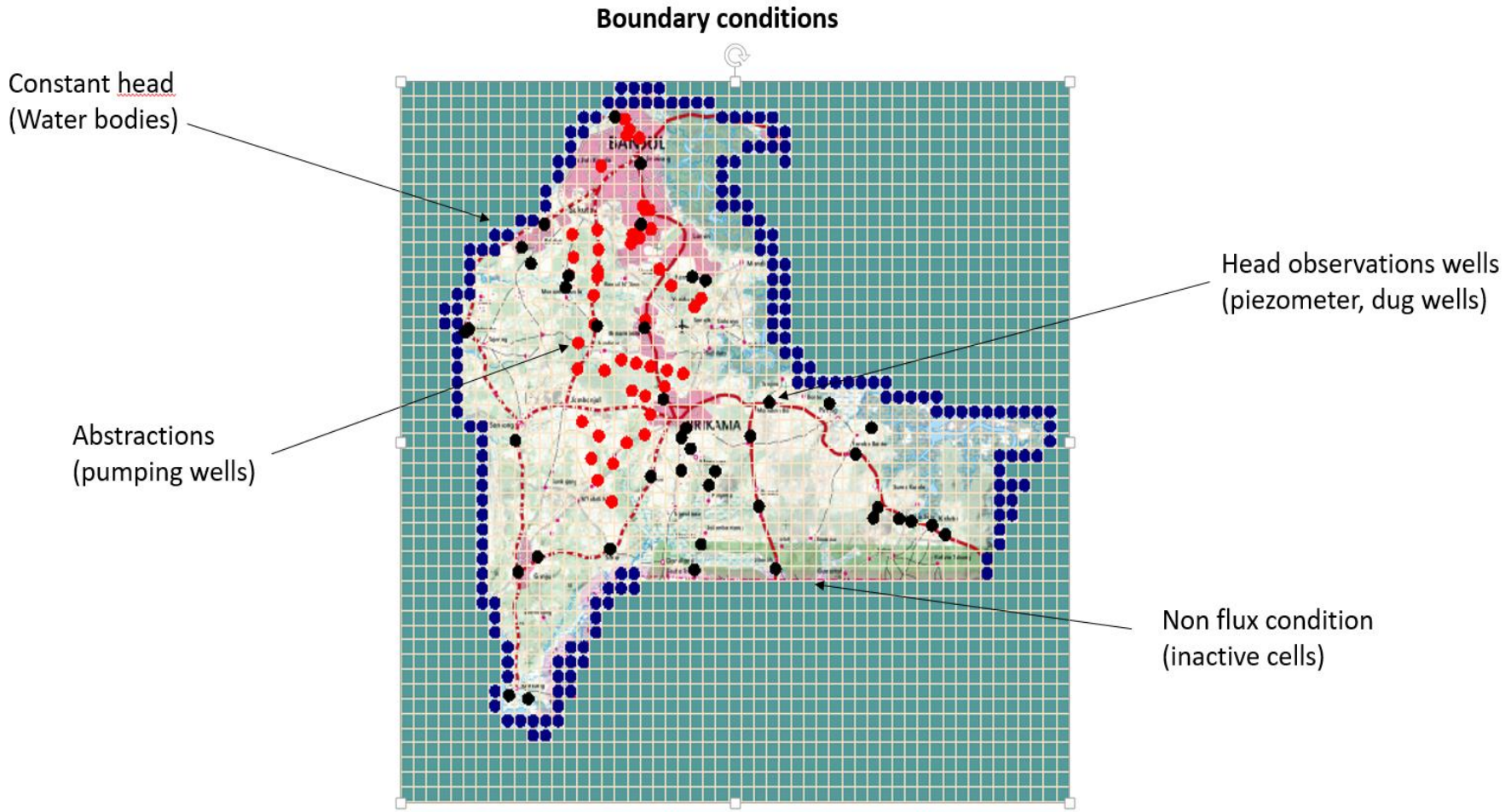

FIGURE 37: MODEL BOUNDARY CONDITIONS WITH LOCATIONS OF BOREHOLES/WELLS

3.10 Calibration

In groundwater modeling study, the actual values of aquifer properties such as hydraulic conductivity, transmissivity, storability, *etc.* are usually not known. Calibration (Parameter Estimation Process) of a model is the procedure of finding model input parameters that produce results of the simulated heads and fluxes that closely match the observed data (field conditions) within an acceptable range (Heiden, 2011; Khadri & Pande, 2016b). The calibration objective is to match the simulated heads with the observed head. Trial and error calibration is used since it allows the modeler to incorporate site knowledge and it helps in gaining a better understanding of the model behavior (Hassen et al., 2014). In this study, two input parameters, the recharge rate from precipitation and the hydraulic conductivity were used to calibrate the model in steady-state flow conditions. These parameters were continuously adjusted until the optimal performance of the parameter was obtained. Simulation of the head was done in steady-state condition only and not in the transient flow state. This is due to no or limited availability of long-term series of observed or field measured data to calibrate the model in the transient flow condition.

3.11 Steady-State Calibration

In a steady-state simulation, an initial guess for the head distribution is needed for the model whilst in the transient flow simulation, a starting head distribution is needed (Khadri & Pande, 2016b). Steady-state calibration is used in regions where data availability such as initial conditions and hydraulic conductivities is insufficient because one of the objectives of steady-state simulation is to estimate the hydraulic conductivity of the area by comparing simulated heads against observed (Touré, 2017). In a steady-state simulation, MODFLOW requires an initial guess for the head distribution while in the transient simulation it desires a starting head distribution (Khadri & Pande, 2016a). The model was calibrated for only the steady-state condition. Calibration in the transient condition could not be done due to the limited availability of long-term observation data.

The steady-state model was calibrated using mean groundwater levels measured in the field for 52 wells and boreholes in 2018 and the water table collected by the DOW from 14 observation wells. This calibration was first done through the trial-and-error method. The strategy of varying the hydraulic conductivity and recharge values results in the best fit between the simulated and observed values.

3.12 Global Climate Models

Global Climate Models (GCMs) (known in other terms as General Circulation Models) are mathematical frameworks that were originally built on fundamental equations of physics (Hayhoe et al., 2017). GCMs are numerical representations of the climate system based on the physical, chemical, and biological properties of its components and their interactions and feedback processes (Rodriguez-camino, 2016). GCMs can simulate many important features of Earth's climate ranging from large-scale patterns of temperature and precipitation, general characteristics of storm tracks and extratropical cyclones, and observed changes in global mean temperature and ocean heat content as a result of human emissions (Hayhoe et al., 2017). Many GCMs have been developed to assess the impact of climate change on water resources. They are also referred to as Earth system models (ESMs) because of their capacity to simulate many features of the climate system (Hayhoe et al., 2017). The hydrological cycle at the regional scale is likely to be impacted by climate change, thereby causing challenges like water management issues, such as groundwater recharge and storage. To quantify and forecast the effects of anthropogenic climate change on groundwater recharge, reliable regional climate scenarios are needed as input data for hydrological modeling (Boe et al., 2007).

Three types of GCMs are available: ocean GCMs, atmospheric GCMs, and a couple of both atmospheric-ocean general circulation models (AOGCMs). The coupled atmosphere-ocean global climate models are mostly used for generating future climate change projections and scenarios under different greenhouse gas emissions (Nazarenko et al., 2015, cited in Mearns, *et al.*, 2003; Vasiliades *et al.*, 2009; Lupo et al., 2013). Because of their coarse resolution (i.e. spatial resolution ranging between 150 to 300 km), GCM is not ideal tools to provide high spatial resolution climate change scenarios needed for impact studies (Vuuren et al., 2011; Rodriguez-camino, 2016), whereas hydrological models often need input meteorological variables at a resolution lower than 10 km (Boe et al., 2007). Thus, there is a need for downscaling coarse-scale resolution of the AOGCM scenarios to high-resolution scenarios at the regional and local scale for impact studies. Evaluating the impacts of climate change for water resources needs climate change projections with very good spatial and temporal resolution (Rodriguez-camino, 2016).

GCMs are downscaled to Regional Climate Models (RCMs) using statistical or dynamical downscaling techniques that provide more reliable climate change scenarios. It is

most recommended to use ensemble GCMs outputs for downscaling scenarios which are most accurate for impact studies because they depict a more realistic climatic condition of the region. Observations and downscaled scenario projections should be well understood in the evaluation of the impacts of climate change.

3.13 Representative Concentration Pathways

The World Climate Research Programme's (WCRP's) Coupled Model Intercomparison Project phase 5 (CMIP 5) (Taylor et al., 2012) provides output from over 50 GCMs. The CMIP5 comprises of simulations of the 21st Century climate with four different Representative Concentration Pathways (RCPs) scenarios with radiative forcing level of 8.5, 6.0, 4.5, and 2.6 W/m^2 to the end of the 21st century and extensions of the climate change projections from 2100 to 2300 (Vuuren et al., 2011; Nazarenko et al., 2015).

In this study, the COordinated Regional climate Downscaling EXperiment (CORDEX) data of Representative Concentration Pathways RCPs (RCP 4.5 and RCP 8.5) were used for climate change impact studies of the present and future climate of the Gambia and evaluate its impact on groundwater resources of the GBA. RCPs are referred to as pathways to emphasize that their primary purpose is to provide time-dependent projections of atmospheric greenhouse gas (GHG) concentrations (Wayne, 2013). For climate change simulation, projected precipitation and temperature data of Coupled Model Intercomparison Project phase 5 (CMIP 5) in the initiative of COordinated Regional climate Downscaling EXperiment (CORDEX) project of the representative concentration pathways (RCPs) were directly used without any further downscaling (regionalization) processing. The raw climate data from the web-geoportal of ANACIM-IRD project (http://retd1.teledetection.fr/climap/. (Accessed in 2019)), which used the Bias-adjusted RCM data of CORDEX were downloaded for this purpose. The projected precipitation and temperature of RCM climate scenarios for the period 2006-2060 were used to generate recharge rates in a water budget model, which were the inputs to a groundwater flow model.

3.14 Climate Change Impacts on Groundwater Resources

I. Scenarios Development

In this study, the scenarios have been developed for the time interval 2018–2050, with the year 2018, the baseline (reference). Hence, the model is calibrated in steady model flow to

simulate the piezometry of pre-monsoon 2018 considering reliable available data. Each month was considered as a stress period so the total stress period number was 390 and total time simulation of 11680 (2050). The predicted heads were computed under different scenarios of changes in pumping and climate change impacts.

Hence, the groundwater dynamic of the CT shallow aquifer to the 2050 horizon is simulated under four scenarios such as:

- **Reference scenario**

  It refers to the steady-state baseline where the groundwater levels are calibrated to simulate the pre-monsoon piezometric. The groundwater head is then computed based on actual withdrawal information and constant boundary conditions from 2019–2050.
- **Abstraction scenarios:** a set of 13 new boreholes are established in the locality with a deficit water supply (lack of boreholes) to meet their water demand.
  - **Abstraction scenario A1:** For each well, a pumping rate of 2500 m^3/day are computed. Other parameters are used as reference scenarios.
  - **Abstraction scenario A2:** The pumping rate of new boreholes is increased to 4000 m^3/day. Other parameters are used as reference
- **Climate change scenarios:** Results from recharge trends are used as input data.
  - **RCP4.5:** Only the climate data from the RCP4.5 scenario was used. The abstraction and other boundary conditions were not changed (same as reference).
  - **RCP8.5:** Only the recharge forecasting from the RCP8.5 scenario was used. The abstraction and other boundary conditions were not changed (same as reference).
- **High abstraction under climate change:** Abstraction and climate change scenarios are merged to simulate the behavior of the groundwater under high abstraction and climate change.
  - **A1-RCP4.5:** A1 (abstractions) and RCP4.5 (boundary conditions) scenarios are used together
  - **A1-RCP8.5:** A1 (abstractions) and RCP8.5 (boundary conditions) scenarios are used together

3.15 Conclusion

This chapter describes the different types of data collected, tools, and methods used in analyzing the data to achieve the objectives of the study. The types of data used are:

I. Primary data were collected in the field for two periods and these include pH, temperature, EC, water level. The analyses were carried out using the ionic chromatography method through AQUION-DIONEX equipment. The exchange processes were realized through AS14 A – AERS 500 columns for anions, and CS12 A – CERS 500 for cations. A WTW MULTI 3430 SET G multiparameter was used to determine pH, temperature, and electrical conductivity at the laboratory.

II. Secondary data such as Landsat images, climate data (CORDEX and station), outputs from regional climate models, and soil maps.

The different models, tools, and software used to analyze the data are: Thornthwaite model for water balance components, R-Software, QGIS, and ESPERE for estimation of evapotranspiration. ArcGIS 10.3 software was used to digitize the study area map and the shapefile of the map was then imported into Visual MODFLOW Flex for simulation of flow and groundwater heads. Also, SRTM/DEM data was used to create the top layer of the aquifer by interpolation using the SURFER program.

CHAPTER 4: HYDRODYNAMIC ASSESSMENT

4.1 Introduction

Water is a fundamental requirement for life. Although 90% of the earth's surface is covered with water, only 2% of this resource is freshwater. Water on earth is found on the surface (surface water), sub-surface (groundwater), and glaciers (Sridharan, 2017). In many parts of the world, groundwater is the main source of freshwater that is used for domestic, industrial, and agricultural purposes. In 2015, it is projected that 663 million people worldwide still do not have access to improved drinking water sources, which are mostly supplied by unprotected wells and surface water. Since water is regarded as the fundamental pillar of life, safeguarding its quality and quantity is very paramount for effective and sustainable water resource management. Groundwater is generally defined as water that is found in the zone of saturation below the ground (Ochungo et al., 2019). It is the only source of water for domestic and irrigation purposes in the Greater Banjul Areas (GBA) like most semi-arid regions of the world. The demand for groundwater has increased due to population growth in the study area. Surface water is not used for domestic and irrigation practices in the study area due to the salinization of the river and its tributaries. Thus, it is indispensable to assess the quality and quantity of groundwater resources of the GBA as the only source of drinking water. The major ions of groundwater have to be analyzed to determine its suitability for domestic and irrigation purposes (Brindha & Elango, 2011). The main objective of this chapter is to determine the hydrodynamic functioning of the hydro-system of the study area. No studies on the hydrodynamics and hydrochemical analysis of groundwater have been carried out in the GBA before. This study will serve as a reference and baseline data for comparing future groundwater quality.

4.2 Water Depth

According to the survey conducted in May and November 2018, the static water level for 118 structures within the continental terminal (CT) aquifer of the GBA was measured. These measurements will help in determining the vulnerability of an aquifer to environmental pollution through infiltration (DIONGUE et al., 2018) of rainwater and irrigation water. The spatial variation of the water depth during the two field campaigns show areas where shallow water levels are encountered. The shallow water levels are found at the center of the study

area with a depth of 15m. The depth of the water relative to the ground varies from 1.74 m to 25.60 m and 1.25 m to 24.10 m in the shallow aquifer water table in May and November 2018 respectively (Figure 36). The highest depths for the two seasons were noted in the center of the study area where the piezometric domes are found having an iso-piezometric line of 20 m. This mound indicates a privileged area for groundwater recharge (Gassama et al., 2020; DIONGUE et al., 2018) and an ideal area for borehole drilling.

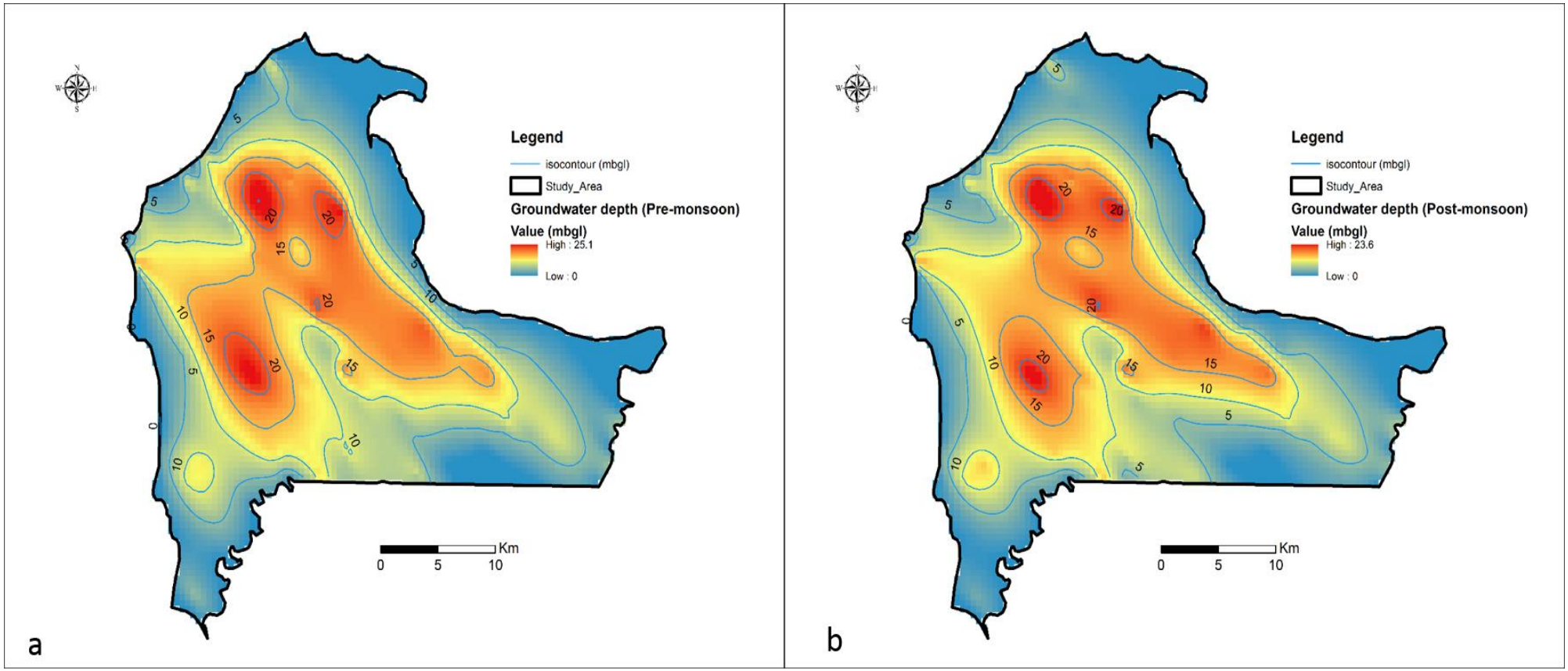

FIGURE 38: WATER DEPTH MAP OF THE SHALLOW AQUIFER OF THE STUDY AREA: (A) PRE-MONSOON (MAY) AND (B) POST-MONSOON (NOVEMBER), 2018 FIELD CAMPAIGNS.

A slight increase in the water table level is observed in almost all the piezometers in post-monsoon that results in a decrease in the depth of the water. On the contrary, areas (piezometers) with a decrease in water table level showed an increase in depth. This could be due to heavy abstraction in the location which can lead to an increase in water table depth even in the rainy season. A very shallow area where the water level is 2 m is encountered around the coastal areas such as the Tanji area in the west and Kartong in the South of the study area.

4.3 Piezometric Level and Groundwater Fluctuation

The groundwater level contour map shows the distribution of piezometric head in the continental shallow aquifer system within the study area. The groundwater depth measured during the pre-monsoon and post-monsoon was used as basic data to calculate the piezometric level. The piezometric maps obtained by kriging interpolation show two piezometric mounds located in the Center (+15m) and South-East (+25m) of GBA which control the groundwater flow (Figures 37a and 37b). The general flow pattern from these mounds occurs in all directions toward the South and water bodies suggesting that groundwater drains into the River Gambia and its tributaries at the North, the Casamance River in the South, and the Atlantic Ocean at the West. The tightening of the piezometric contours in the South-East, as well as the low hydraulic gradient, suggest low hydrodynamic parameters in this area. This is evidenced by the low transmissivity value in this area ranging from 81 to 200m/day. Sparse recharge exists around the river and its tributaries having low hydraulic conductivity and permeability values due to the clayed nature of the soil found in these areas. The regional flow pattern that exists within the groundwater flow system under natural conditions is predominantly horizontal, from the points of recharge in the center towards the River Gambia and the Atlantic Ocean. The groundwater fluctuation maps (Figure 37c) also indicates high water level in the Center and South-East of the study area where the mounds are. Recharge in the study area is expected to happen in the mound.

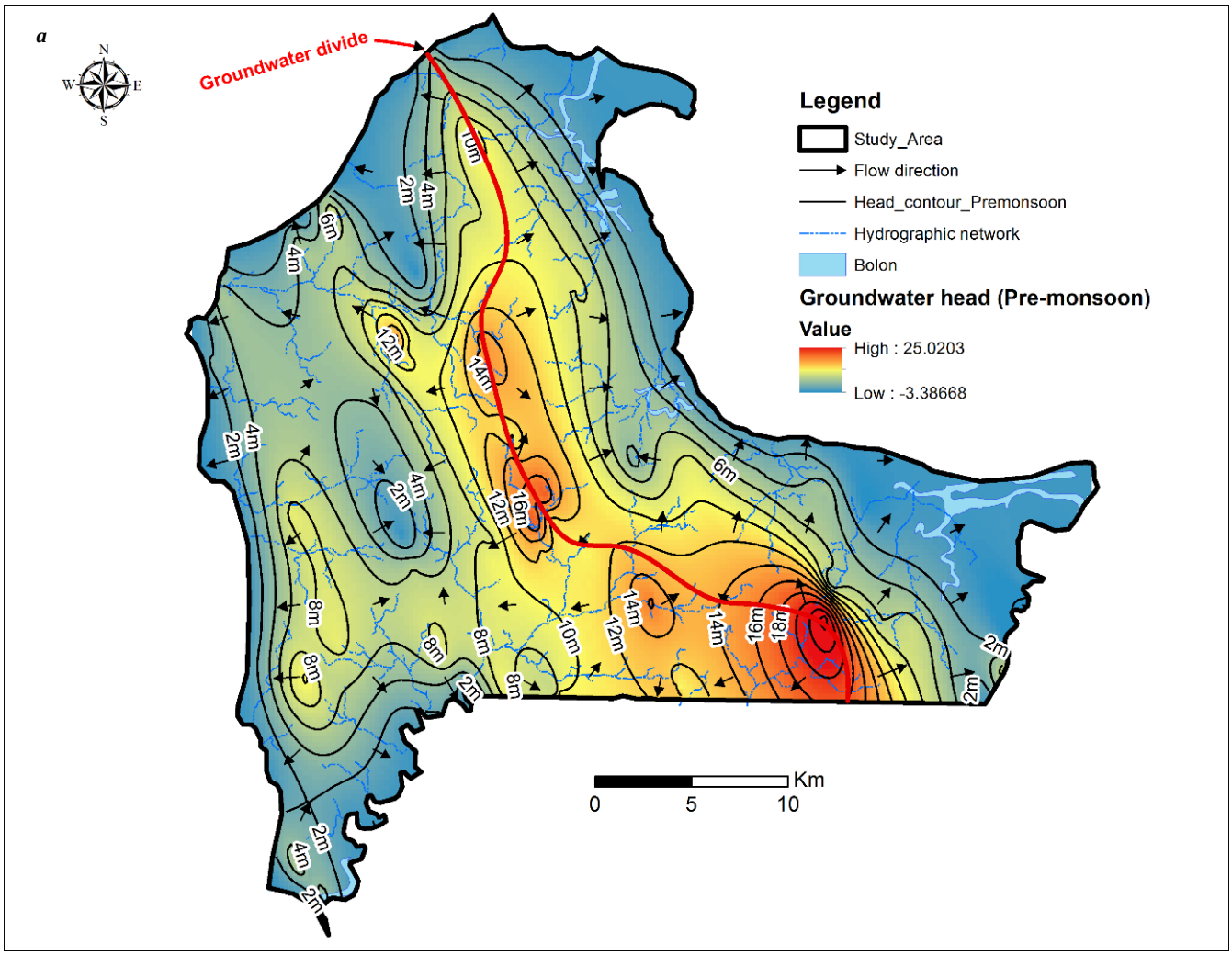

FIGURE 39: PIEZOMETRIC MAP OF THE SHALLOW AQUIFER OF THE STUDY AREA: (A) PRE-MONSOON AND

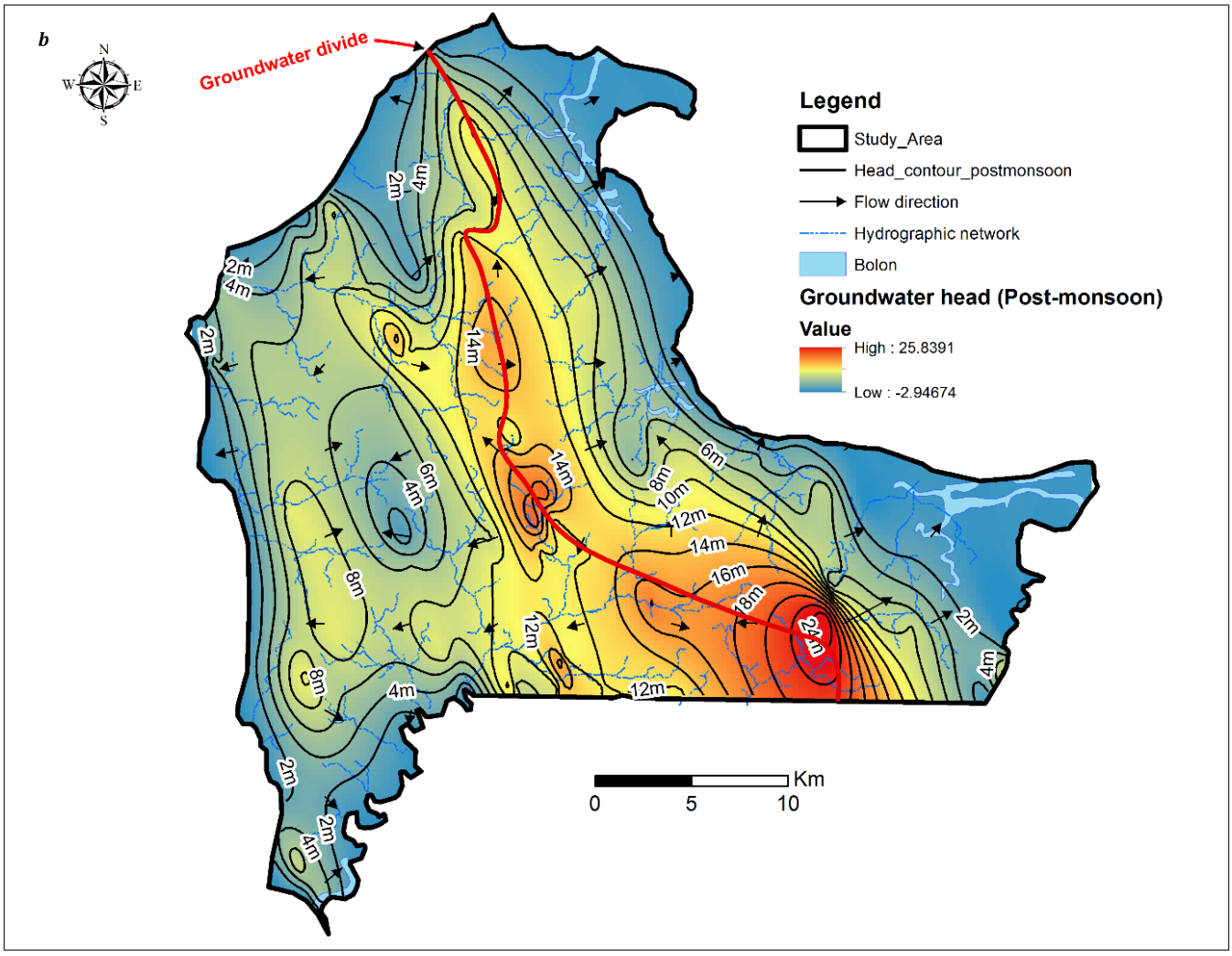

FIGURE 40: PIEZOMETRIC MAP OF THE SHALLOW AQUIFER OF THE STUDY AREA: (B) POST-MONSOON, 2018;

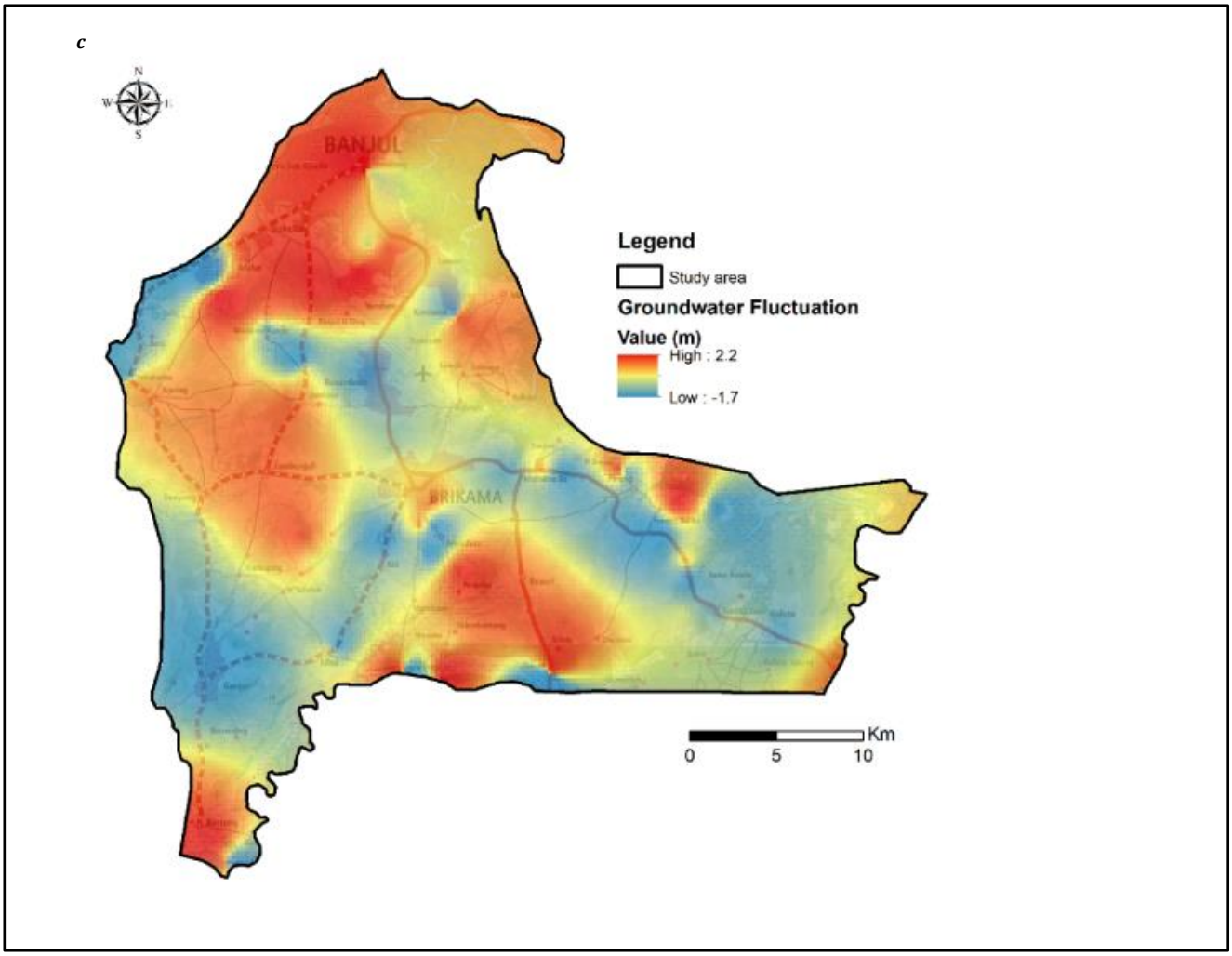

FIGURE 41: PIEZOMETRIC MAP OF THE SHALLOW AQUIFER OF THE STUDY AREA: (C) GROUNDWATER FLUCTUATION MAP

4.4 Groundwater Table Fluctuation

In total, sixteen piezometers are installed in the study area and are monitored by the Department of Water Resources (DOW). These monitoring wells are Casagrande piezometers drilled on sandstone aquifer. Measurement of the water levels are taken with the probe meter. Groundwater level data measurements have been performed both automatically and manually at monthly time step. One piezometer (OB2) at Mariama Kunda was selected in this study because most of the data from the piezometers are unreliable and not recommended for use to estimate recharge. Unfortunately, the selected piezometer is not enough to do spatial interpolation the result through the entire study area. As the water level is critical in estimating recharge with Water Table Fluctuation (WTF) method, then, the hydrograph extrapolated approach was used in this study to estimate groundwater level rise (ΔH).

It is observed that the groundwater level for the piezometer starts rising during the period of the rainy season (Figure 38). This implies that the recharge in the study area is mostly due to the precipitation. However, the highest monthly rainfall occurred in August in the study area, while the highest water level is measured in October and November (Figure 0.2). Thus, there is a time delay (lag) between the initial precipitations and water reaching the groundwater table. This is due to the dryness of the soil and the first rain falls have to saturate the soil before water infiltrates to reach the groundwater table. The frequency and number of rainy days is another reason for the delay in rain water reaching the groundwater table to cause a rise in water level.

Another cause may be due to the frequency of rainy days; before July there are many days without rain, while after this month, the number of rainy days is high (Figure 38). For that reasons above, the water level takes a while before rising at the beginning of the rainy season (generally from May). Furthermore, large-scale groundwater flow may also influence local-scale groundwater dynamic.

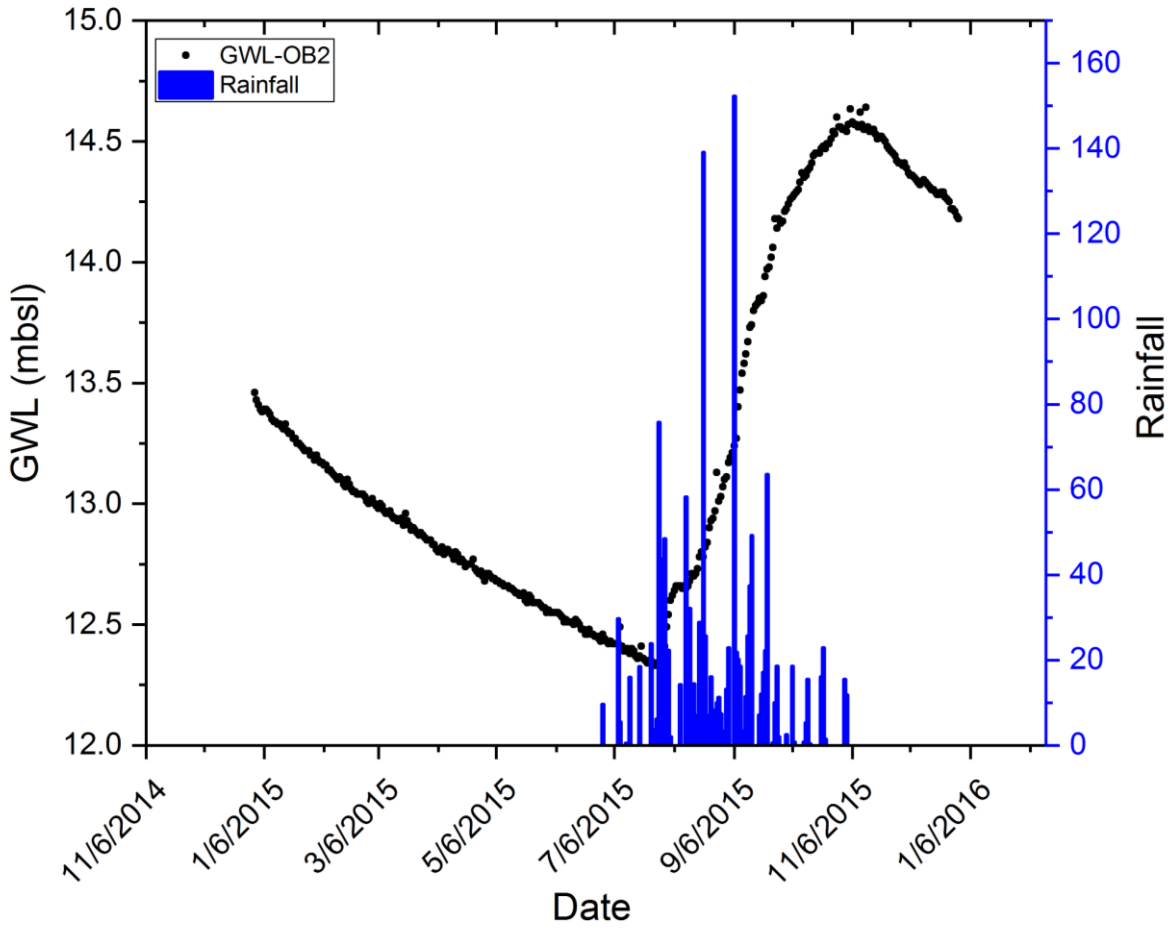

FIGURE 42: SEASONAL FLUCTUATION OF GROUNDWATER WATER LEVEL AT OB2 PIEZOMETER

4.5 Aquifer Thickness

The top of the aquifer defined through a 20m Digital Elevation Model (DEM) highlights a plateau in the center and south-eastern part of GBA which rise from +32 to +20 mbsl. Toward the coastland in the North, West, and East, the topography is at around +4 mbsl. The substratum layer was identified through borehole logs drilled throughout GBA. It consists of clay formations that separate the CT and the intermediate aquifer (Oligo-Miocene). The corresponding layer thickness ranges from 20m in the north up to 100m in the South-Eastern GBA (Figure 39).

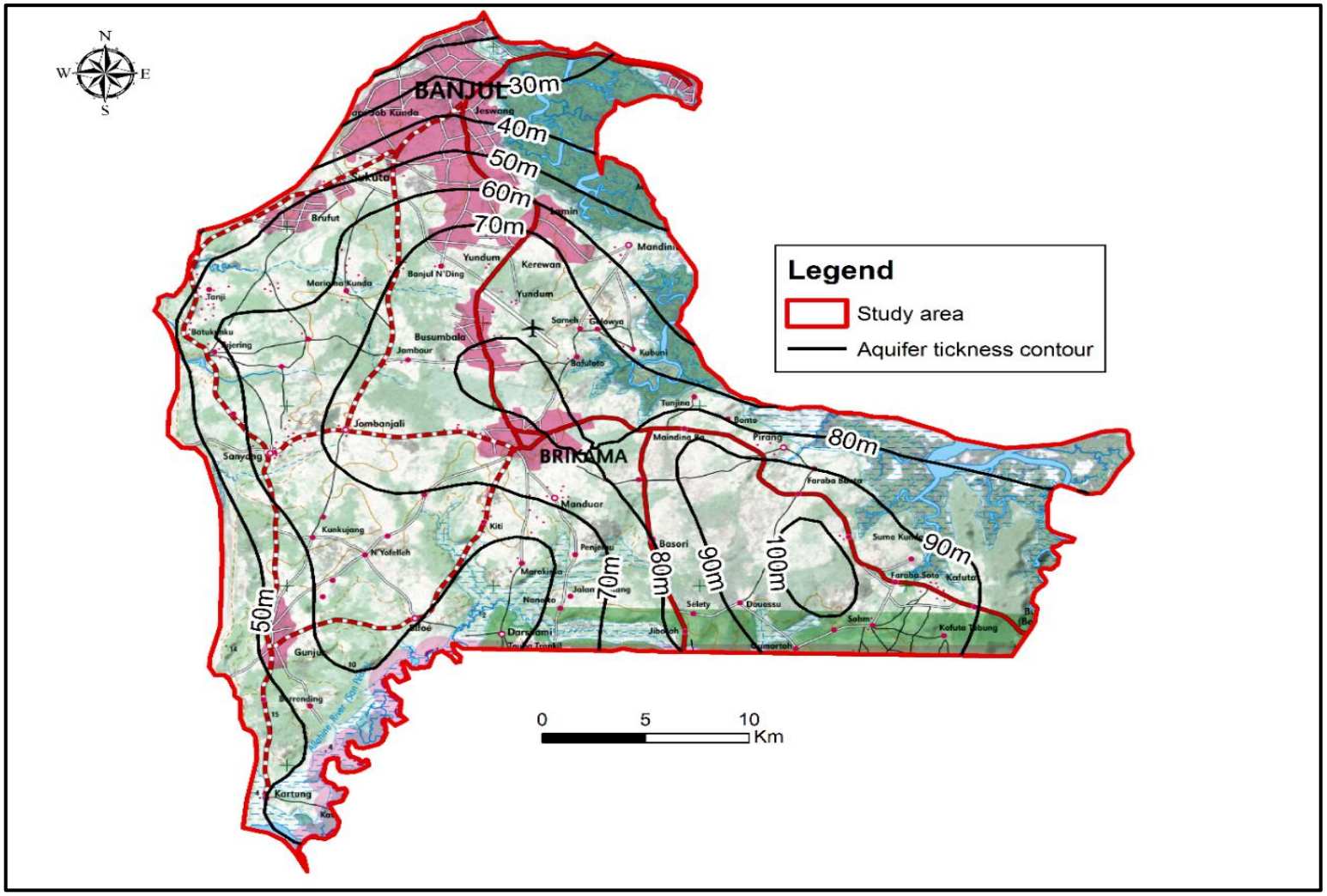

FIGURE 43: AQUIFER THICKNESS OF THE CT OF THE STUDY AREA.

4.6 Hydrodynamic Parameters

Transmissivity and hydraulic conductivity of CT aquifer have been extracted from an available pumping test document from the Department of Water Resources on a set of 48 boreholes distributed in the GBA. Based on these studies, the transmissivity values range from 16.5 to 4207 m/day with an average of 780 m/day. Considering the screen length of the boreholes, the hydraulic conductivity varies between 0.83 and 210 m/day with an average of 36 m/day. This spatial distribution variability is explained by the nature of sediments and their variations from silt, clayey sand to coarse sand.

4. 7 Conclusion

The groundwater hydrodynamics of the continental shallow aquifer of the GBA was assessed for samples collected from 118 wells and boreholes during the field campaign of pre-monsoon and post-monsoon of 2018. The data collected in the field and from borehole logs were used to analyze the aquifer hydrodynamic properties of the GBA such as transmissivity and hydraulic conductivity, water depths, aquifer thickness, and piezometric levels. The transmissivity values range from 16.5 to 4207 m/day with an average of 780 m/day whilst the hydraulic conductivity varies between 0.83 and 210 m/day with an average value of 36 m/day.

The aquifer thickness ranges from 20m in the North up to 100 m in the South-Eastern GBA. The water depth varies from 1.74 m to 25.60 m and 1.25 m to 24.10 m in the shallow aquifer water table in May and November 2018 respectively. The highest depths for the two seasons were noted in the piezometric domes at the center of the study area. This dome indicates an advantageous area for groundwater recharge (Gassama et al., 2020; DIONGUE et al., 2018) and an ideal area for borehole drilling.

CHAPTER 5: GROUNDWATER RECHARGE ESTIMATION TECHNIQUES

5.1 Introduction

Groundwater recharge is defined as the fraction of rainwater falling into a watershed that will ultimately reach the water table in the unsaturation zone of an aquifer forming an addition to the groundwater reservoir. Groundwater recharge can occur either naturally or by anthropogenic recharge. Anthropogenic recharge is recharge occurring due to human activities like irrigation and disposal of waste. Natural groundwater recharge is the rate at which vertical movement of water reaches the water table without any physical interference. Natural recharge is classified as diffuse or localized. Diffuse recharge is an extensive movement of rainwater from the surface to the water table through the unsaturated zone. Localized recharge on the other hand refers to the occasional infiltrations of water from surface water bodies at the level of temporary depressions in the absence of well-defined drainage systems to the aquifer system. Groundwater recharge can be categorized into four modes:

- The flow of infiltrated water downward via the unsaturated zone to the water table;
- Lateral and/or vertical inter-aquifer flow;
- Recharge caused by nearby surface water systems as a result of groundwater abstraction; and
- Artificial recharge from borehole injection or man-made infiltration ponds.

Groundwater recharge is an integral parameter in the water balance of a groundwater system, the rate of which can be used for sustainable water resource vulnerability and quantity assessment and management of groundwater systems. In arid and semi-arid regions, the recharge component of the hydrologic cycle is considered the most important element after rainfall events (Mutoti, 2015). The spatial and temporal variability of recharge is important in these regions, where reference evapotranspiration (ETo) exceeds precipitation (P) over long term, where as high intensity rainfall events exceed ETo, which permits infiltration of rainwater into the water table (Carrera-Hernández et al., 2012). Direct calculation of recharge is not possible, thus, it should be cautiously and accurately estimated. Estimation of aquifer recharge is one of the components of water cycle most difficult to measure in the evaluation of groundwater resources (C. P. Kumar, 2003); (Melo, et al., 2015). However, owing to its difficulty of direct measurement, numerous methods have been developed to estimate

recharge. The recharge rate of an aquifer approximates the actual recharge using different techniques that include:

physical methods (using either direct techniques based on the use of lysimeters or the water table fluctuation, or indirect techniques based on the estimate of soil physical parameters);

Geochemical (Tracer) methods (using chemical-chloride and isotope techniques–tritium, for example);

Inverse methods (using numerical models to solve the groundwater flow equation for recharge instead of groundwater heads);

However, these recharge estimation techniques have been described and their associated limitations addressed by various authors (Scanlon *et al*., 2002, De Vries 2002; etc.) in their work. Many studies have alluded that estimated recharge over an area can be derived using field data with methods stated above.

Recharge is one of the components of the hydrologic cycle most difficult to estimate. Regardless of the method chosen, recharge estimates are subject to uncertainties that can be identified by means of comparison with other methods. In this study, groundwater recharge estimates based on the water balance method in the unsaturated zone based on Thornthwaite and Mather (1955), Penman-Monteith (1995), and Turc methods is evaluated. The approach is assessed by comparing the results of one method with those of another method. It also employed the numerical model (MODFLOW) to estimate groundwater recharge for the study area. The techniques were adopted to investigate whether our aquifer system is water surplus or deficit under natural environmental conditions as well as to find out which method best estimates recharge in our area. The focus will be mainly on recharge processes occurring in the unconfined aquifers (that is flow of infiltrated water downward through the unsaturated zone to the water table) which are more vulnerable to contamination.

5.2 Application of the Thornthwaite Method to Calculate Infiltration

The application of Thornthwaite's method to calculate infiltration requires the use of the following climatic parameters: mean temperature and precipitation. The Thornthwaite infiltration calculation is also dependent on runoff and the maximum value of the soil water capacity (SWC) or water stock. The latter depends on the quantity of water that a soil can hold, vegetation cover, nature, and texture of the soil. Hence, the calculation of infiltration was done by applying different stock values for different soil types. The SWC values used for calculating recharge (effective infiltration) in the study area were 100, 125, 145, and 178

mm. The effective rain is the difference between the total precipitation and the runoff. The runoff value considered is on average 20% of precipitation. The period considered for the calculation was from 1984 to 2016 for both Banjul and Yundum stations. The choice of the period relates to the availability and reliability of data at the station level. Tables 6 and 7 present the monthly average values of effective rain, temperature, ETP, ETR, and infiltration for the different "water stock" values in the period 1984 to 2016 for both stations. The average annual infiltration during the rainy months from July to October is between 144 and 212 mm/year for Banjul, and 214 and 433 mm/year for Yundum with the different water stock values (Table 8).

TABLE 6: RESULTS OF CALCULATION OF THE BALANCE ACCORDING TO THORNTHWAITE METHOD FOR THE PERIOD 1984-2016 AT BANJUL STATION

Month	Eff. Rain	ETP	ETR	Infiltration			
				Stock 100	Stock 125	Stock 145	Stock 178
Jan	0	69	37	0	0	0	0
Feb	0	75	39	0	0	0	0
Mar	0	79	41	0	0	0	0
Apr	1	76	39	0	0	0	0
May	18	79	48	0	0	0	0
Jun	81	89	74	3	1	1	0
Jul	190	92	90	50	38	32	22
Aug	230	**91**	**91**	113	104	95	81
Sep	114	**93**	**93**	44	45	43	39
Oct	30	102	93	2	2	2	2
Nov	1	94	66	0	0	0	0
Dec	1	80	44	0	0	0	0
Average	**664**	**1018**	**756**	**212**	**191**	**171**	**144**

TABLE 7: RESULTS OF CALCULATION OF THE BALANCE ACCORDING TO THORNTHWAITE METHOD FOR THE PERIOD 1984-2016 AT YUNDUM STATION

Month	Eff. Rain	ETP	ETR	Infiltration			
				Stock 100	Stock 125	Stock 145	Stock 178
Jan	0	67	2	0	0	0	0
Feb	0	78	2	0	0	0	0
Mar	0	85	0	0	0	0	0
Apr	0	82	0	0	0	0	0
May	1	84	2	0	0	0	0
Jun	43	95	41	0	0	0	0
Jul	169	93	87	21	14	38	5
Aug	273	**89**	**89**	148	132	219	97
Sep	208	**90**	**90**	118	116	170	110
Oct	47	95	95	2	2	6	2
Nov	1	86	69	0	0	0	0
Dec	0	71	8	0	0	0	0
Average	**744**	**1014**	**486**	**289**	**265**	**433**	**214**

TABLE 8: RESULTS OF THE ANNUAL AVERAGE OF THE THORNTHWAITE CALCULATION FOR THE PERIOD 1984-2016 AT BANJUL AND YUNDUM STATIONS

Annual Average 1984 - 2016							
				Infiltration			
Month	**Eff. Rain**	**ETP**	**ETR**	**Stock = 100**	**Stock = 125**	**Stock = 145**	**Stock = 178**
Banjul	664	1018	756	212	191	171	144
Yundum	744	1014	486	289	265	433	214

The investigation of monthly averages of effective rain, ETP, ETR, soil "water stock" and infiltration calculated over the entire study area for the period 1984 - 2016 for Thornthwaite method in Banjul and Yundum (Figures 40 and 41), provides a conceptual model of infiltration into the continental terminal shallow aquifer system. Infiltration in the study area takes place during the rainy season (July – October). From November to May, when there is no rainfall in our area, the ETP is greater than rainfall (P < ETP). Thus, the "water stock" satisfies the ETR and it continues to decrease until May. At the onset of the rains around June/July, rainfall continues to reinforce the ETR and the surplus refills the “water stock” does not get to saturation level. At the peak of the rainy season from August to September, when the ETR is equal to ETP, rainfall continues to fill the “water stock” until it reaches its maximum, at which point the excess water infiltrates to the groundwater table. According to the Thornthwaite method, infiltration in the area reaches its average maximum values of 104 mm/month and 132 mm/month for August in Banjul and Yundum respectively. As rainfall decreases, infiltration decreases as well. In October when rainfall starts to decrease, ETP is higher than rainfall and rainwater only serves the ETR, which also takes up part of the declining "water stock". Infiltration also decreases to zero during the dry season.

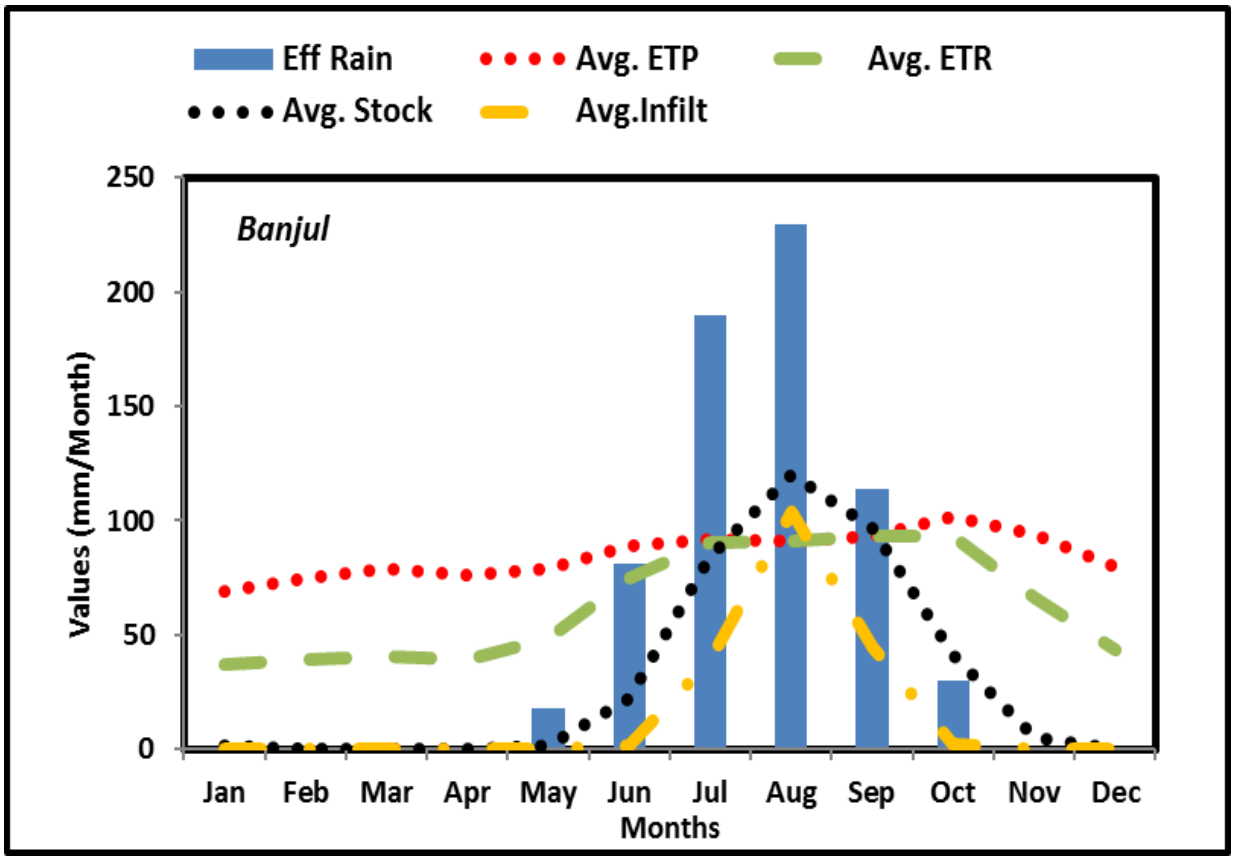

FIGURE 44: RELATIONSHIP BETWEEN EFF. RAINFALL, AND MONTHLY AVERAGE VALUES OF INFILTRATION, ETP, ETR, AND STOCK OF 125 MM FOR BANJUL STATION (1984-2016) CALCULATED WITH THE THORNTHWAITE

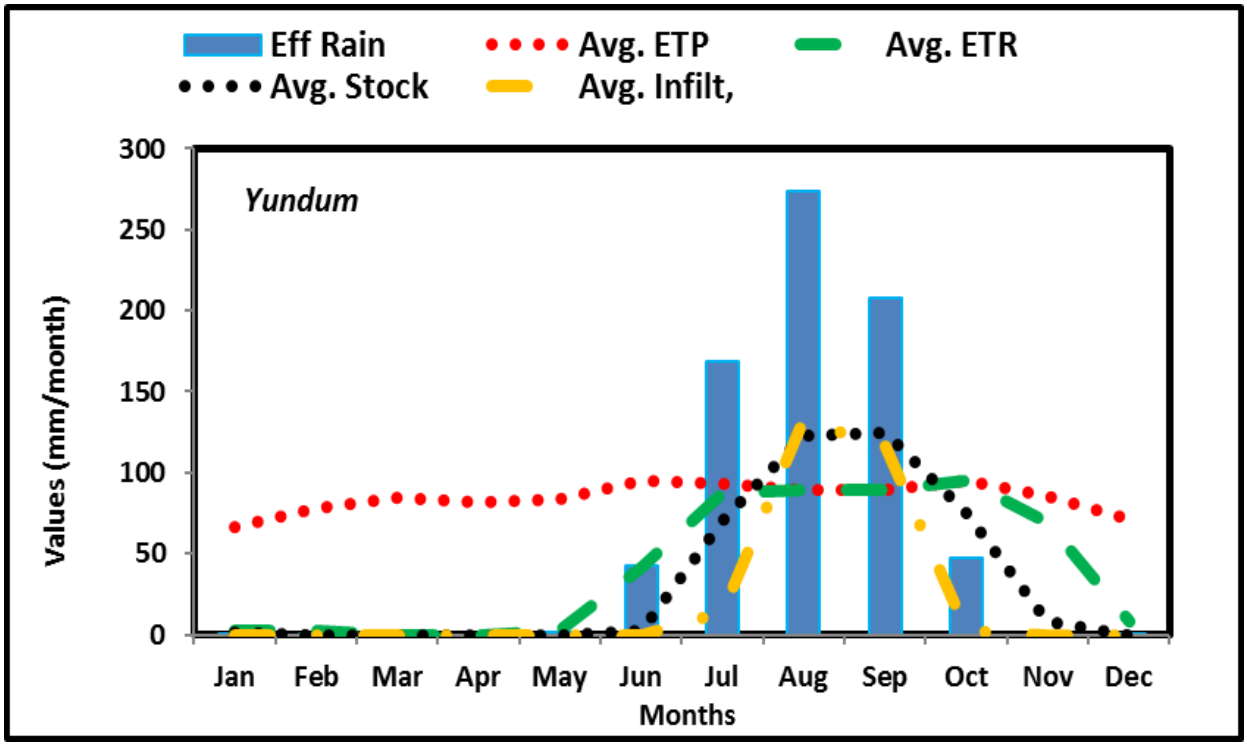

FIGURE 45: RELATIONSHIP BETWEEN EFF. RAINFALL, AND MONTHLY AVERAGE VALUES OF INFILTRATION, ETP, ETR, AND STOCK OF 125 MM FOR YUNDUM STATION (1984-2016) CALCULATED WITH THE THORNTHWAITE

5.3 Application Penman Method to Infiltration Calculation

The same climatic periods were considered for the estimation of ETP, ETR, and Infiltration by the Penman method. The monthly average ETP increase during the dry season reaching its maximum in March of about 222 mm and 249 mm respectively in Banjul and Yundum then decrease from May onwards reaching a minimum of about 134 mm in Banjul and 133 mm Yundum in September (Figures 42 and 43). During the rainy season between June and September, when insolation and wind speed are low while temperatures and relative humidity are high the ETP values become low. The differences in ETP values between Banjul and Yundum are also observed in the annual averages of 2131 mm/yr. and 2287 mm/yr. respectively (Tables 9).

TABLE 9: RESULT OF CALCULATION OF THE BALANCE ACCORDING TO THE PENMAN METHOD FOR THE PERIOD 1984-2016 AT BANJUL STATION

Month	Eff. Rain	ETP	ETR	Infiltration			
				Stock 100	Stock 125	Stock 145	Stock 178
Jan	0	215	4	0	0	0	0
Feb	0	205	0	0	0	0	0
Mar	0	222	0	0	0	0	0
Apr	1	193	1	0	0	0	0
May	18	182	18	0	0	0	0
Jun	81	163	77	0	0	0	0
Jul	190	156	136	15	10	8	5
Aug	230	142	136	62	53	45	34
Sep	114	134	110	26	23	20	14
Oct	30	150	78	0	0	0	0
Nov	1	166	21	0	0	0	0
Dec	1	204	1	0	0	0	0
Average	664	**2131**	**582**	**103**	**86**	**73**	**53**

TABLE 10: RESULT OF CALCULATION OF THE BALANCE ACCORDING TO THE PENMAN METHOD FOR THE PERIOD 1984-2016 AT YUNDUM STATION

Month	Eff. Rain	ETP	ETR	Infiltration			
				Stock 100	Stock 125	Stock 145	Stock 178
Jan	0	228	4	0	0	0	0
Feb	0	228	0	0	0	0	0
Mar	0	253	0	0	0	0	0
Apr	0	217	0	0	0	0	0
May	1	207	1	0	0	0	0
Jun	43	183	43	0	0	0	0
Jul	169	160	133	7	3	2	1
Aug	273	143	143	78	67	58	45
Sep	208	139	139	66	61	56	48
Oct	47	153	126	0	0	0	0
Nov	1	174	26	0	0	0	0
Dec	0	201	0	0	0	0	0
Average	**744**	**2287**	**616**	**151**	**131**	**116**	**94**

TABLE 11: RESULTS OF THE ANNUAL AVERAGE OF THE PENMAN CALCULATION FOR THE PERIOD 1984-2016 AT BANJUL AND YUNDUM STATIONS

Annual Average 1984 -2016							
Month	Eff. Rain	ETP	ETR	Infiltration			
				Stock = 100	Stock = 125	Stock = 145	Stock = 178
Banjul	664	2131	582	103	86	73	53
Yundum	744	2287	616	151	131	116	94

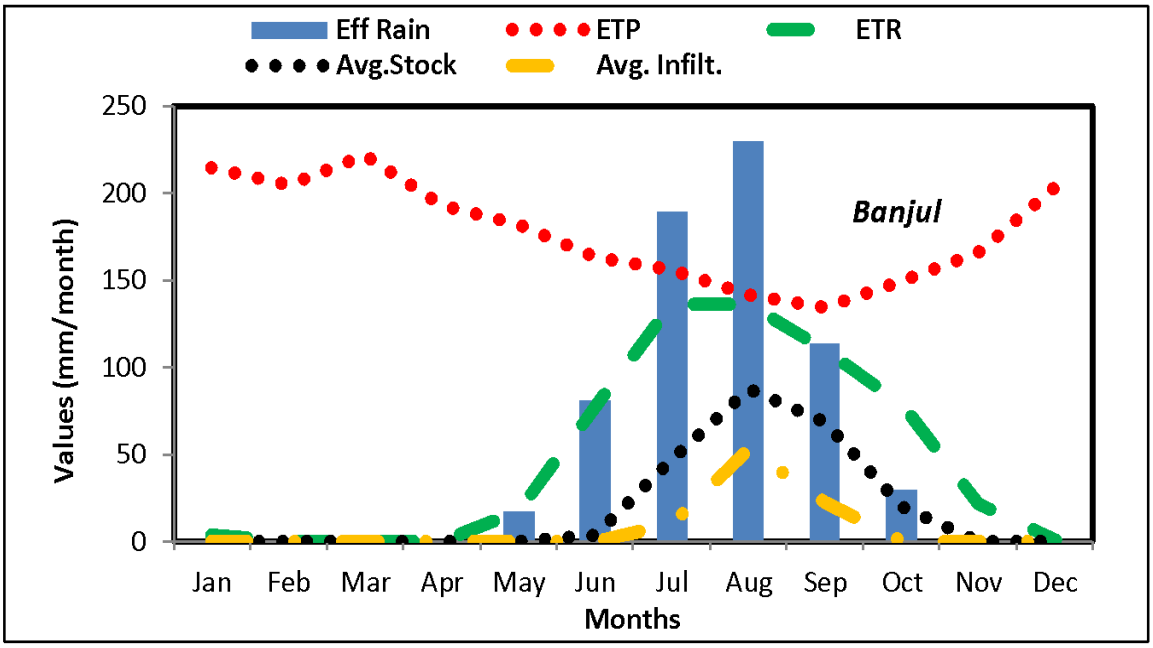

FIGURE 46: RELATIONSHIP BETWEEN EFF. RAINFALL, AND MONTHLY AVERAGE VALUES OF INFILTRATION, ETP, ETR, AND STOCK OF 125 MM FOR BANJUL STATION (1984-2016) CALCULATED WITH THE PENMAN

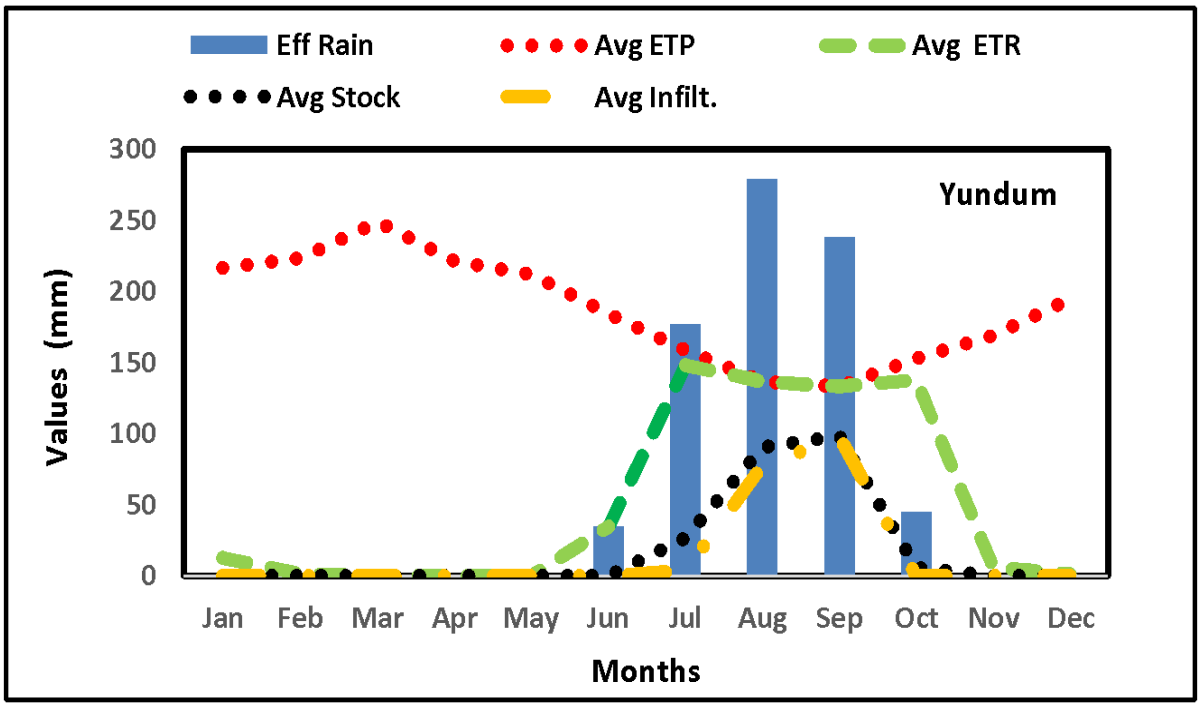

FIGURE 47: RELATIONSHIP BETWEEN EFF. RAINFALL, AND MONTHLY AVERAGE VALUES OF INFILTRATION, ETP, ETR, AND STOCK OF 125 MM FOR YUNDUM STATION (1984-2016) CALCULATED WITH THE PENMAN

5.4 Application of Turc Method to Potential Evapotranspiration Calculation

The method of calculation of ETP and ETR with the Turc takes into account fewer parameters compared to the Penman and Thornthwaite methods. The method of calculating ETP and ETR is directly dependent on rain recorded during the period under consideration. Tables 12 and 13 showed the results of the calculations.

TABLE 12: RESULTS OF CALCULATION OF THE BALANCE ACCORDING TO TURC METHOD FOR THE PERIOD 1984-2016 AT BANJUL STATION

Month	Eff. Rain	ETP	ETR	I
Jan	0	100	0	0
Feb	0	123	0	0
Mar	0	111	0	0
Apr	1	133	1	0
May	18	126	19	0
Jun	81	116	85	12
Jul	190	108	198	88
Aug	230	103	239	128
Sep	114	109	119	36
Oct	30	114	32	1
Nov	1	108	1	0
Dec	1	96	1	0
Sum	**664**	**1347**	**695**	**265**

TABLE 13: RESULTS OF CALCULATION OF THE BALANCE ACCORDING TO TURC METHOD FOR THE PERIOD 1984-2016 AT YUNDUM STATION

Month	Eff. Rain	ETP	ETR	I
Jan	0	99	0	0
Feb	0	124	0	0
Mar	0	113	0	0
Apr	0	135	0	0
May	1	127	1	0
Jun	43	117	45	2
Jul	169	108	177	70
Aug	273	102	284	171
Sep	208	108	217	100
Oct	47	114	50	1
Nov	1	108	1	0
Dec	0	93	0	0
Sum	**744**	**1348**	**777**	**344**

TABLE 14: RESULTS OF THE ANNUAL AVERAGE OF THE TURC CALCULATION FOR THE PERIOD 1984-2016 AT BANJUL AND YUNDUM STATIONS

Annual Average 1984-2016				
Month	**Eff. Rain**	**ETP**	**ETR**	**Infiltration**
Banjul	664	1347	695	265
Yundum	744	1348	777	344

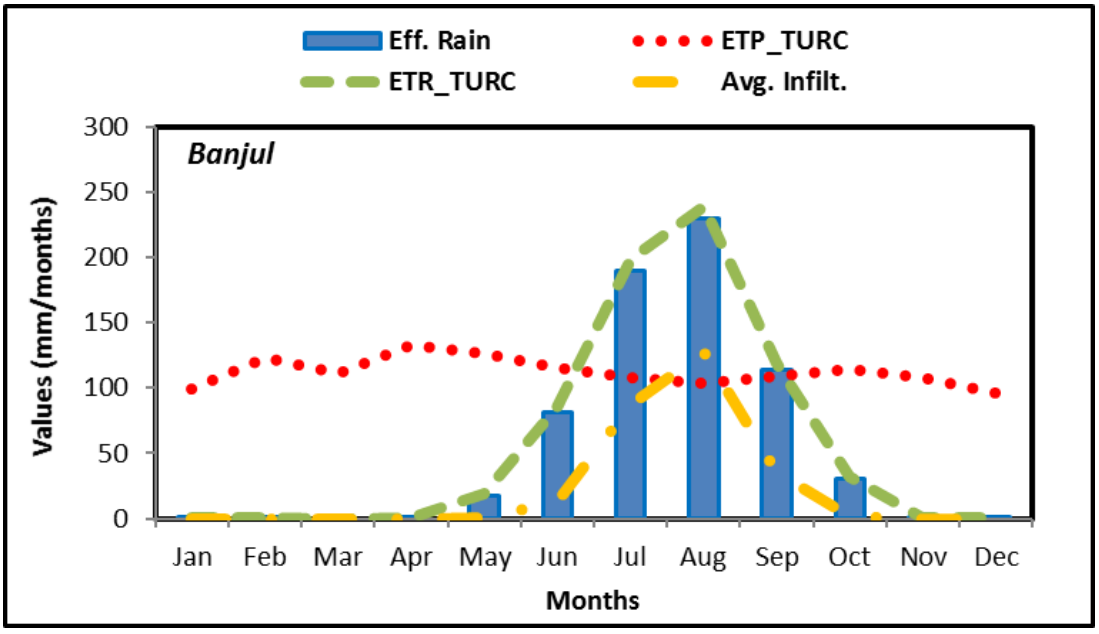

FIGURE 48: RELATIONSHIP BETWEEN EFF. RAINFALL, AND MONTHLY AVERAGE VALUES OF INFILTRATION, ETP, ETR, AND STOCK OF 125 MM FOR BANJUL STATION (1984-2016) CALCULATED WITH THE TURC

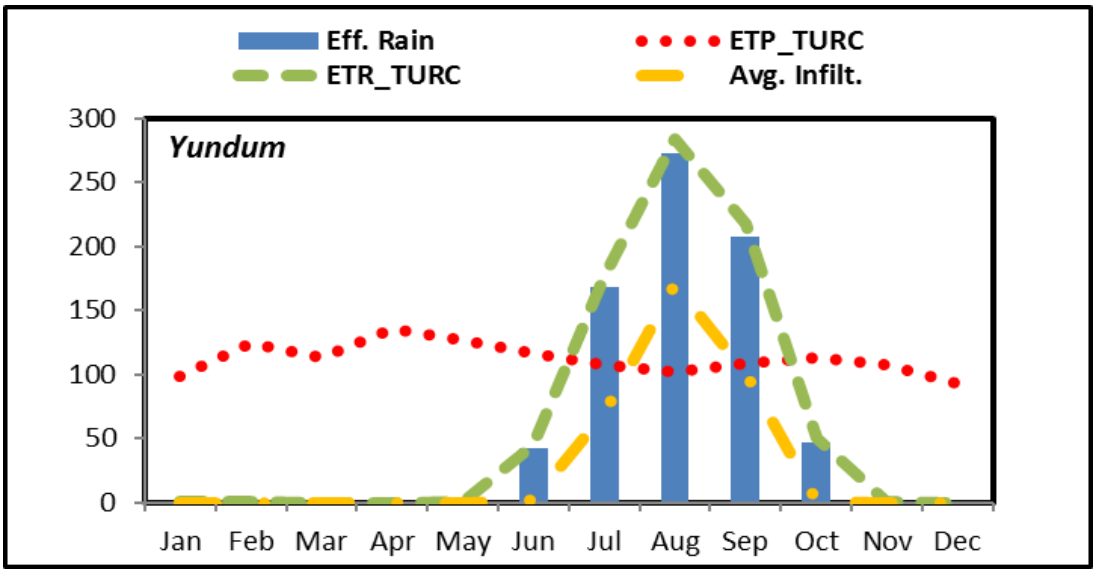

FIGURE 49: RELATIONSHIP BETWEEN EFF. RAINFALL, AND MONTHLY AVERAGE VALUES OF INFILTRATION, ETP, ETR, AND STOCK OF 125 MM FOR YUNDUM STATION (1984-2016) CALCULATED WITH THE TURC

5.5 Comparison and Critical Analysis of the Results Obtained

Table 15 illustrates the report of a comparative study made between the results of Thornthwaite, Penman, and Turc methods based on the different SWC values. Report 1 shows the comparison between the values of Penman and Thornthwaite and Report 2 between Thornthwaite and Turc. In Report 1, the average ETP and ETR values according to Thornthwaite are 0.5 and 1.3 times respectively lower than Penmen. The average infiltration values for stocks of 100, 125, 145, and 178 are 0.3, 2.1, 2.3, and 2.7 times higher than that of Penman for the same stock values. The higher rate of infiltration in the latter two methods as compared to the Penman is mainly due to the high potential evapotranspiration with the Penman. The peaks in Penman's ETP values (Figure 46) observed in March could be due to an increase in water levels by plants during this period. These values, although not identical, are of the same order of magnitude; the ETP is a function of the ETR (Emvoutou et al., 2018). Report 2, on the other hand, shows the average ETP and ETR by the Turc method are respectively 1.3 and 0.9 times for Banjul and 1.3 and 1.6 times for Yundum higher than that of Thornthwaite methods. Also, the results obtained from all three methods show that maximum recharge occurs in August and September, the time when the area experience high rainfall. This study distinguished the differences between the parameters considered for the ETP calculations with the three methods. However, the empirical formulas used has limitations (Emvoutou et al., 2018). Nonetheless, the Turc method seems to be the most appropriate water balance model for estimating ETP and infiltration in the study area. The Penman model applied in the study area overestimates the possibility of using soil water stock to calculate ETP while the Thornthwaite method underestimates the ETP.

TABLE 15: COMPARISON OF RESULTS OBTAINED BY THE THORNTHWAITE, PENMAN, AND TURC METHODS FOR THE PERIOD 1984-2016 AT BANJUL AND YUNDUM STATIONS

Station	Method				Infiltration			
		Eff. Rain	ETP	ETR	Stock 100	Stock 125	Stock 145	Stock 178
Banjul	Penman	664	2131	582	103	86	73	53
	Thornthwaite	664	1018	756	212	191	171	144
	Turc	664	1347	695				
	Report 1	1.0	≈0.5	≈1.3	≈0.3	≈2.1	≈2.3	≈2.7
	Report 2	1.0	≈0.6	≈1.2	-	-	-	-
		1.0	≈1.3	≈0.9	-	-	-	-
Yundum	Penman	744	2287	616	151	131	116	94
	Thornthwaite	744	1014	486	289	265	433	214
	Turc	744	1348	777				
	Report 1	1.0	≈0.4	≈0.8	≈1.9	≈2.0	≈3.7	≈2.3
	Report 2	1.0	≈0.6	≈1.3	-	-	-	-
		1.0	≈1.3	≈1.6	-	-	-	-

Comparing the three different ETP calculation methods applied in the study area offered different results. The annual maximum, minimum, and average ETP values (Table 16) from the Penman method are 3179 mm, 1843 mm, and 2131mm in Banjul, and 2696 mm, 2138 mm and 2287 mm in Yundum while these values are 2 to 3 times higher than the values provided by Thornthwaite and Turc methods. Likewise, the Turc method gave results of 1.2 to 1.4 times higher than those values calculated by the Thornthwaite method.

Dieng et al., (2017) in their study estimated recharge using the water balance methods (Penman and Thornthwaite) in the Saloum region of Senegal which has almost the same climatic conditions as the Gambia, and their results showed. Their estimated maximum, minimum and average ETP of 2400 mm, 2022 mm and 2198 mm respectively in Kaolack and 2114 mm, 1688 mm and 1863 mm in Nioro by Penman's method (ETPp) while they are 1.5 to 2 times lower with Thornthwaite's formula (ETPth). Their results confirms the results of this study of the Thornthwaite's result of ETP estimation being 1.5 to 2 times lower than the Penman's.

TABLE 16: STATISTICAL ANALYSIS OF ANNUAL AVERAGES OF POTENTIAL EVAPOTRANSPIRATION FROM THORNTHWAITE (ETPTH), PENMAN (ETPP), AND (ETPTURC) FOR BANJUL AND YUNDUM.

Statistics	Banjul					Yundum Station				
	ETPp	ETPth	ETPturc	Report 1	Report 2	ETPp	ETPth	ETPturc	Report 1	Report 2
Max	3179	1043	1426	3	2	2696	1027	1416	3	2
Min	1843	986	1186	2	2	2138	988	1226	2	2
Avg.	2131	1018	1347	2	2	2287	1014	1348	2	2
STD	265	15	52			103	9	47		

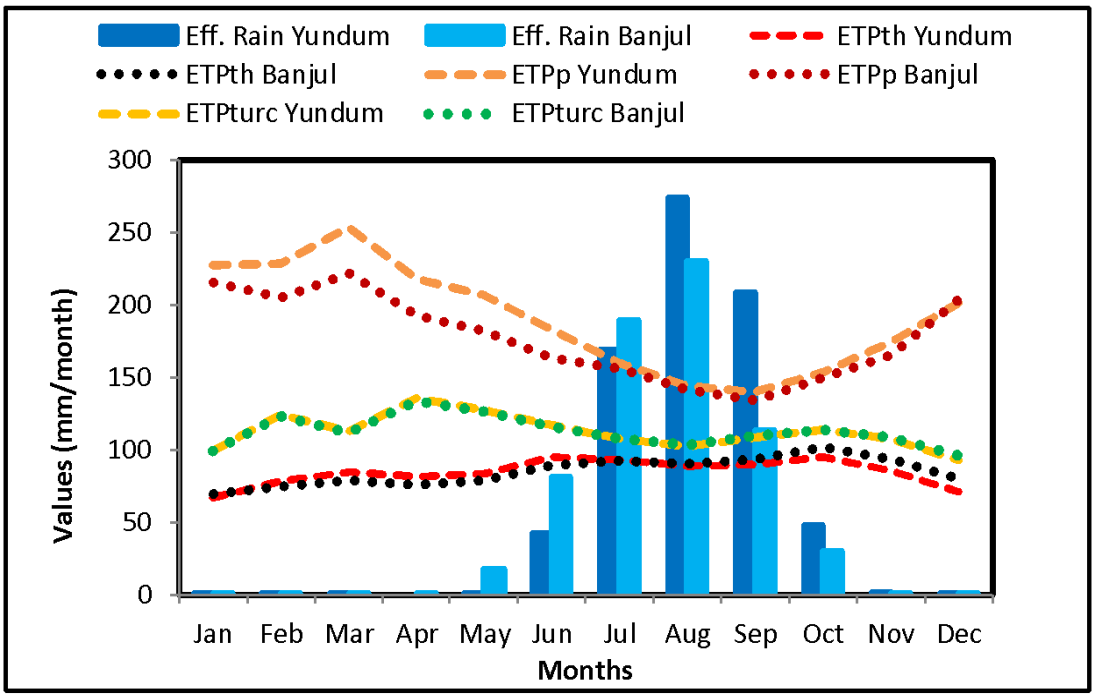

FIGURE 50: MONTHLY EVOLUTION OF MEAN POTENTIAL EVAPOTRANSPIRATION USING ETPP. ETPTH AND ETPTURC METHODS COMPARED TO EFFECTIVE RAIN (EFF. RAIN) FROM 1984-2016 AT BANJUL AND YUNDUM STATIONS.

5.6 Potential Recharge Zone Mapping

5.6.1 Introduction

Groundwater is the largest available freshwater resource in the world, especially in semi-arid areas characterized by climate variability and change which has a significant impact on water availability. In the GBA, the shallow groundwater system constitutes the only source of potable water for the present and future generation. This resource has become an important issue with respect to appropriate water resource planning and management in the face of climate change impact on the replenishment (recharge) of the aquifer. Therefore it is crucial to

identify and delineate the potential recharge zones of the GBA for proper planning and management of the groundwater resources.

The three recharge estimation methods above only provide point values and their spatial distribution in the study area have some uncertainties that can alter the overall assessment of the potential recharge in the Continental shallow aquifer. The uncertainties are greater in the direct calculated values due to input data in the model and the time step used in the Thornthwaite, Penman, and Turc budget (Dieng M., Faye S., 2017). Geographical Information System (GIS) and Remote Sensing (RS) have a pivot role to understand the partition of groundwater. This study aims to use GIS, RS, and Multi-Criteria Evaluation (MCE) techniques to identify and delineate the potential recharge zones of the GBA basin.

5.6.2 Geology

The CT formations of the study area consisted of brown ferruginous quartz sandstone and sand-bearing ferruginous rock with ferruginous kaolinitic quartz greywacke. The lowlands and river floodplains are made of the Quaternary formations (Holocene and Pleistocene). The Pleistocene formation is composed of earth-yellow clayey fine-grained sandy clay distributed on terraces of the River Gambia and its tributaries and the red sub-sandy, sandy mild clay and gravelly mild clay formation distributed throughout the study area. The Holocene formation comprised of medium-fine quartz sand, locally ilmenite-bearing quartz sand; and grey symmict sand, silt, clay, and salt, containing cockle shells which are distributed on the marine fluvial deposits are found on the estuary of the River Gambia and its tributaries.

The spatial distribution of the geological facies and their suitable score to groundwater recharge by fuzzy membership is presented in Figure 47. The ferruginous quartz sandstone formation has been given higher preference because of its high porosity and availability of water content. In contrast, clayey silts formations have lower suitability scores.

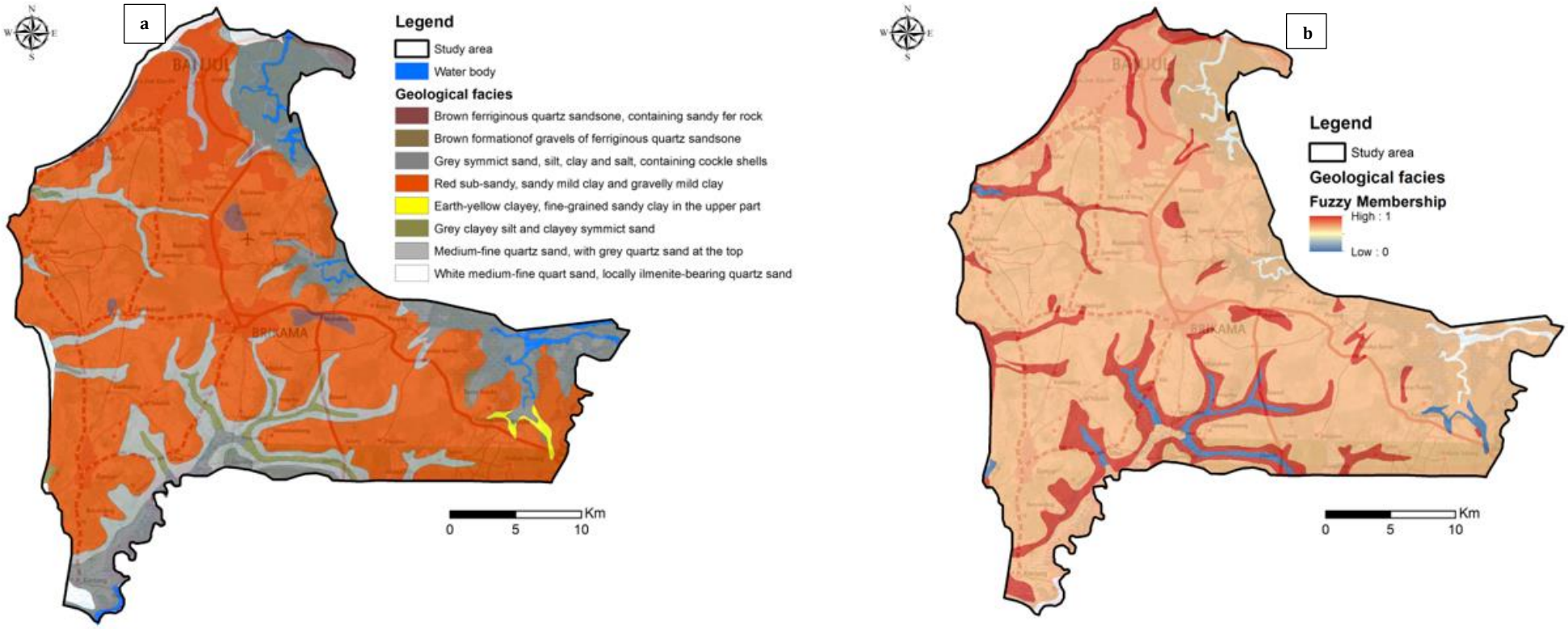

FIGURE 51: GEOLOGY: (A) THEMATIC LAYER; (B) FUZZY NORMALIZATION

5.6.3 Land Use/Land Cover

The Climate Change Initiative (CCI) S2 prototype land-use/cover of the European Space Agency (ESA, 2016) with its high resolution of 20m was used in this study. To translate the LULC map into an infiltration capacity map, it classified into 7 classes (Figure 59a), tree cover (40.8%), shrubs and grassland (11.0%), cropland (30.5%), wetlands (1.7%), open water (3.2), bare area (0.3) and urban area (12.4). More than 80% of the total area is covered by vegetation (trees, shrubs and grassland, and crops). It is known that LULC affects the surface runoff, evapotranspiration, and groundwater recharge of a region. The water body, cropland, and wetlands are excellent groundwater recharge hotspots, while built-up area and tree cover or forest are considered to be less significant because of high runoff and evapotranspiration respectively. Therefore ranking the different land-use types from the most infiltrating to the least infiltrating was done assigning the highest weightage to a water body, wetland, and cropland, and lowest to the urban area and Tree cover as shown in Figure 48b.

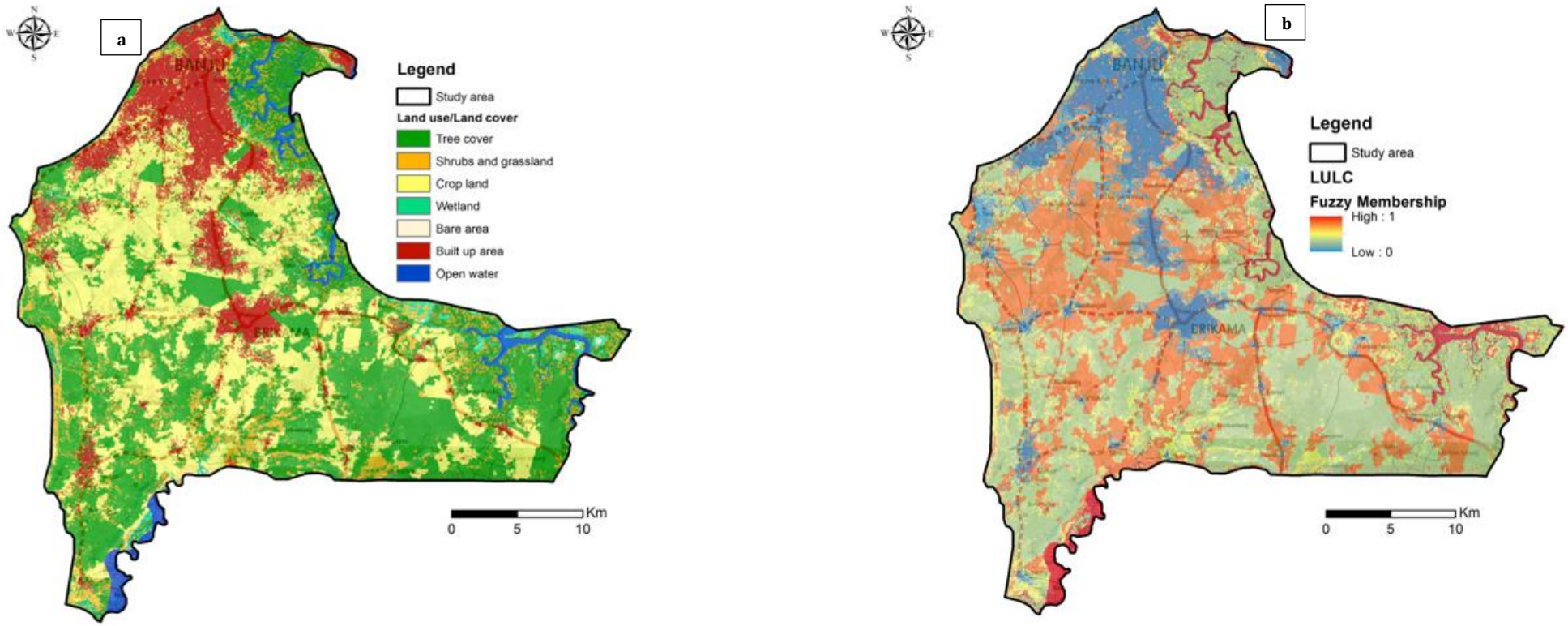

FIGURE 52: LULC: (A) THEMATIC LAYER; (B) FUZZY NORMALIZATION

5.6.4 Slope of the Land

The slope of the study area was generated from the ASTER DEM with values ranging from 0.0 to 22.7 %. However, most areas lie between 0 to 2% (Figure 49a). The areas with high slopes are mainly located in the center towards the east of the zone. Zones with high slope (elevated lands) favor runoff at the expense of infiltration, while the low slope (Lowlands) favors infiltration and thus facilitate recharge. Therefore, steep slopes correspond to the least infiltrating areas and shallow slopes to the most infiltrating areas. On this basis, a decreasing membership function shape was used to fuzzy the slope, in order to give the highest score to the lowest slope and the elevated lands lowest score as shown in Figure 60b.

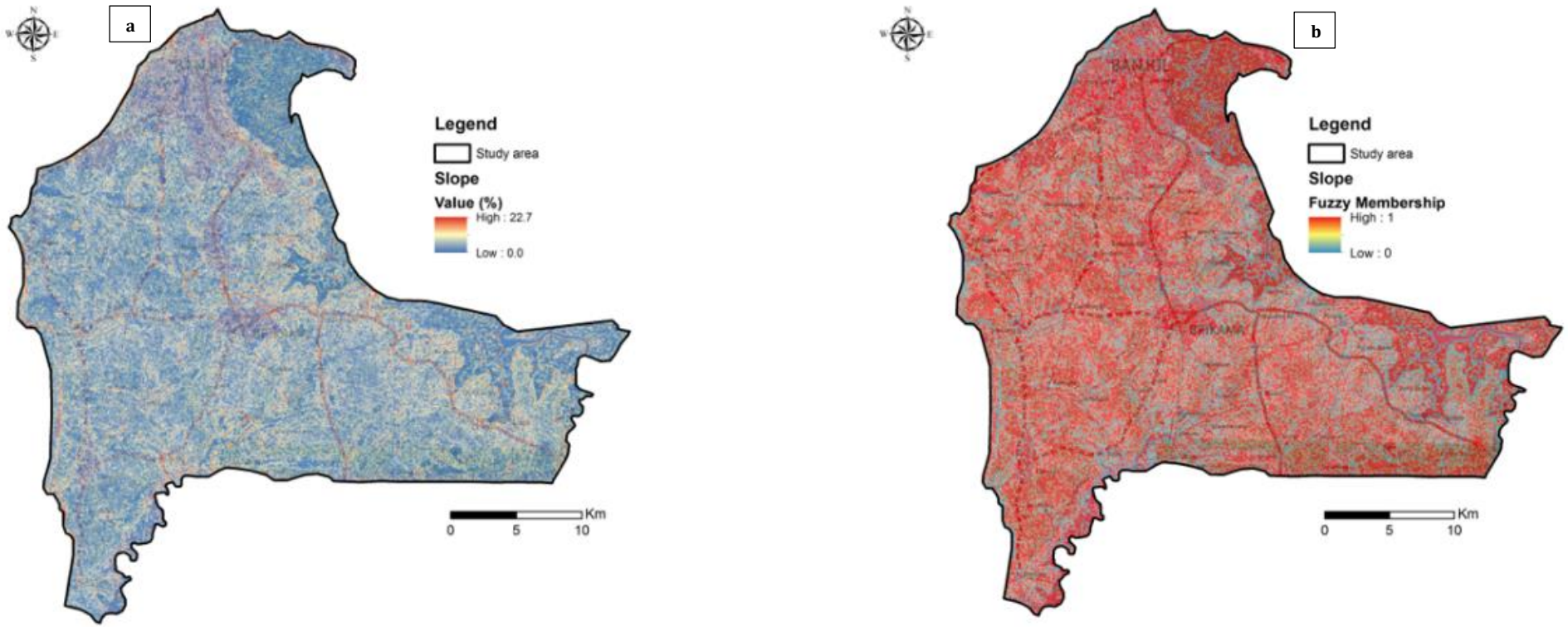

FIGURE 53: SLOPE: (A) THEMATIC LAYER; (B) FUZZY NORMALIZATION

5.6.5 Drainage

The drainage network is obtained from the digital terrain model. The resulting map was used to calculate the drainage density, which corresponds to the total length of the drainage network per unit area (km/km^2). It is an expression to indicate the closeness of spacing of stream and regarded as an inverse function of permeability and thus indirectly indicates the suitability of groundwater recharge in an area. The drainage density layer of the study area is prepared using line density tools in ArcGIS software and was fuzzy using the decreasing membership function shape because high drainage density is expected to generate more runoff and thus less infiltration.

In the study area, drainage density values ranged from low (0.0) and high (1.0) km/km2. Drainage density depends, among other things, on topographical characteristics, with the highest values observed in depressions with low permeability clayey substrates and the lowest values in sandy environments with high permeability (Figure 50).

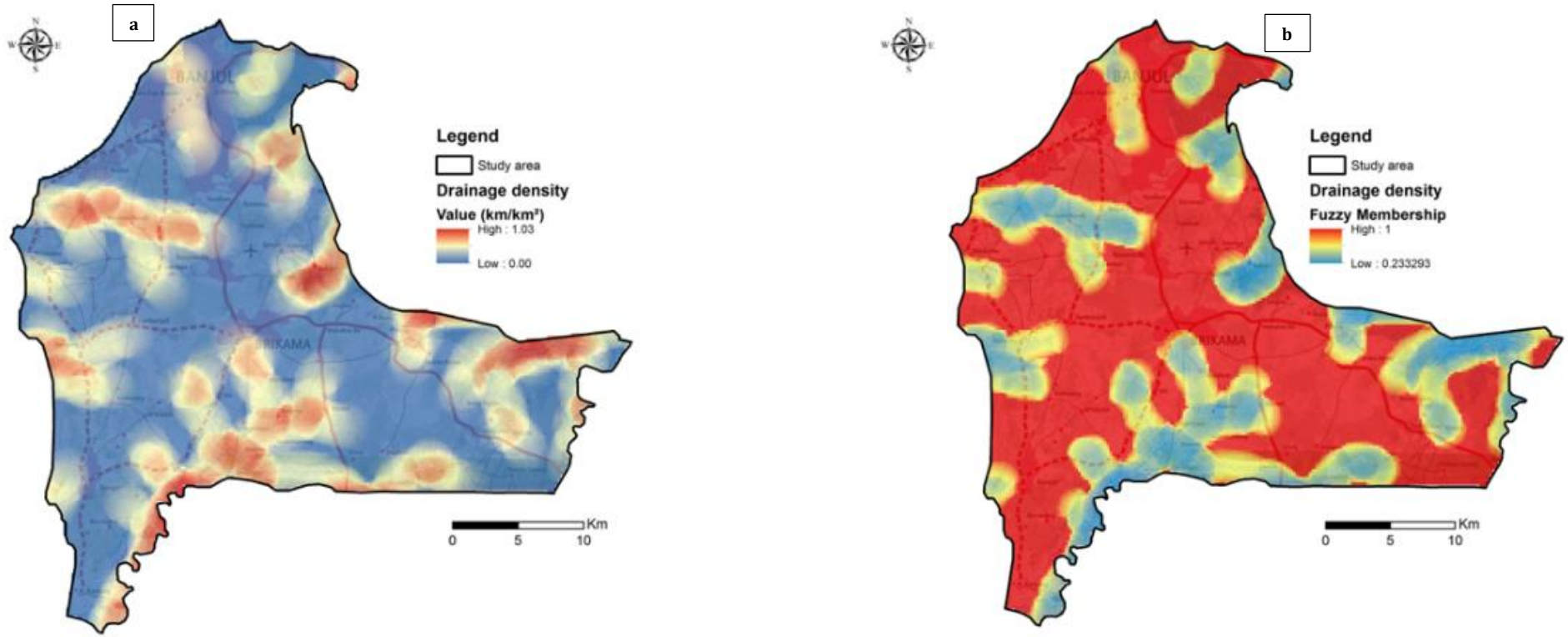

FIGURE 54: DRAINAGE DENSITY: (A) THEMATIC LAYER; (B) FUZZY NORMALIZATION

5.6.6 Groundwater Fluctuation

The water table depth measured during pre-monsoon and post-monsoon of 2018 has been used to calculate the seasonal groundwater fluctuation which is an important indicator for groundwater recharge. The water depth of 118 water points was used to prepare the layer by interpolation (kriging method) (Figure 51a). The higher fluctuation values (2m) are observed in the northern part at Banjul and in the West and South at Sanyang and Basori localities. In the central and south-western as well as south-eastern part of the study area, the fluctuation rate is low and reaches negative values (-1.7m). These areas are considered to be the discharge site of the study area due to high evapotranspiration and/or high abstraction rate. On this basis, a linear fuzzy membership function shape was applied for layer weightage as shown in Figure 51b.

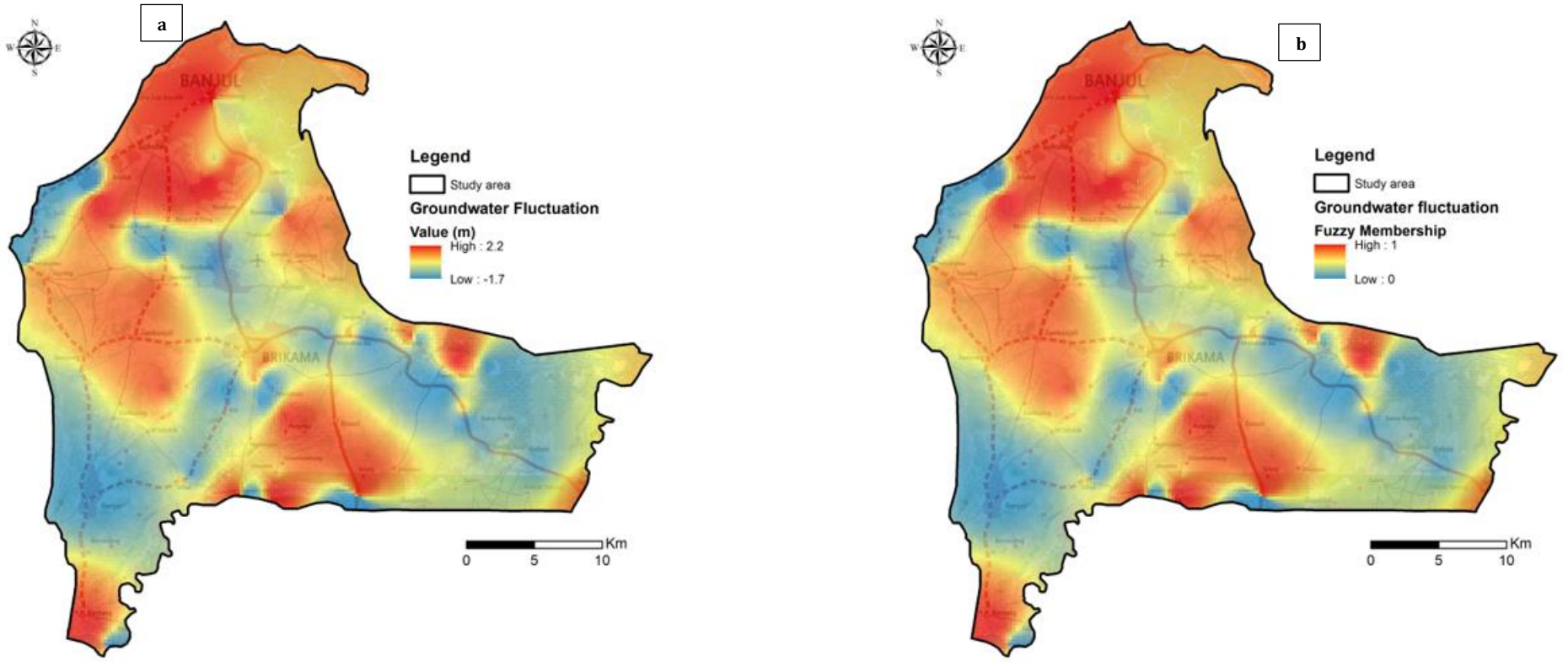

FIGURE 55: GROUNDWATER FLUCTUATION: (A) THEMATIC LAYER; (B) FUZZY NORMALIZATION

5.6.7 Transmissivity

The aquifer transmissivity is defined as the groundwater discharge through the unit width of the aquifer for the fully saturated depth under a unit hydraulic gradient. Its layer was prepared from pumping test data applying a kriging interpolation. The values vary from 16.4 to 4178.8 m^2/day in the study area. The central and south-eastern parts of the study area have high transmissivity values whereas the northern part falls under the lowest transmissivity zone. As the suitability of groundwater recharge is correlated to the transmissivity value, a linear fuzzy membership function shape was applied for layer weightage as shown in Figure 52b.

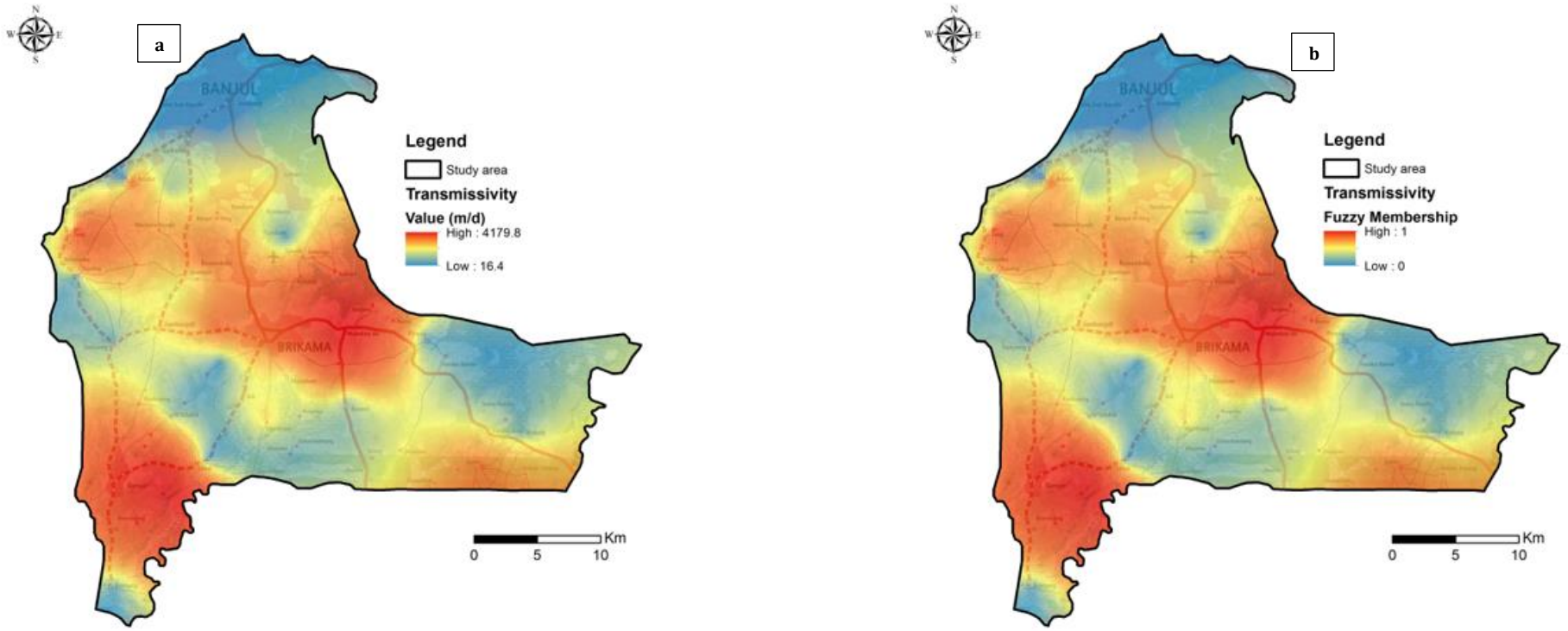

FIGURE 56: AQUIFER TRANSMISSIVITY: (A) THEMATIC LAYER; (B) FUZZY NORMALIZATION

5.6.8 Soil

The map of soil texture was translated into an infiltration capacity map by classifying it into 5 classes according to CPCS (1976) based on the relative percentage of Coarse sand represented by coastal dune portions in the North-East and South-West, Ferritic sand distributed throughout the study area (70%), loam and loamy sand in the river floodplains, and mudflats throughout the estuarine portions of the study area (Figure 53a). Thus the five soil classes are defined and rated from the most infiltrating to the least infiltrating according to their increasing clay content. Coarse sand has a high infiltration rate, while mudflats (clayey soil) have lower infiltration rates, hence it was given the lowest weights. Then the linear fuzzy shape is applied to normalize the weightage as shown in Figure 53b.

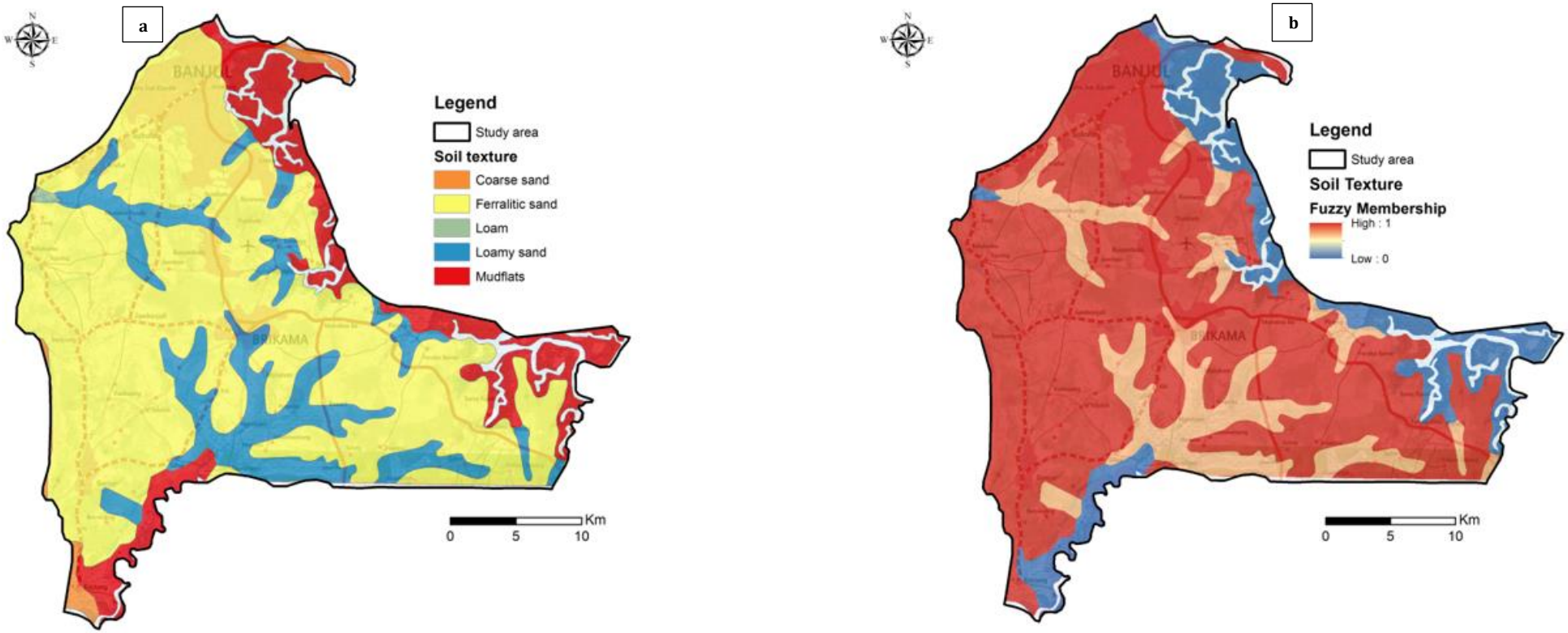

FIGURE 57: SOIL: (A) THEMATIC LAYER; (B) FUZZY NORMALIZATION

5.6.9 Delineation of Groundwater Recharge Zone

The GWRZ of the study area was obtained by WLC of Geology, LULC, slope, groundwater fluctuation, soil texture, drainage density, and aquifer transmissivity using the Multiple Criteria Evaluation (MCE) module of Terrset software. Analytical hierarchy processes (AHP) have been used to calculate suitable weights of the 7 criterions using a pairwise comparison matrix illustrated in Table 17. The consistency ratio of the matrix is 0.09, therefore the matrix was not randomly generated and is acceptable.

TABLE 17: PAIRWISE COMPARISON MATRIX FOR CRITERION WEIGHTAGE BY AHP

Criterion	GG	LULC	Slope	GWF	DD	AT	Soil	Weightage
Geology	1	3	3	5	5	7	7	**0.372**
LULC	1/3	1	4	4	5	5	7	**0.24**
Slope	1/3	1/3	1	3	4	5	7	**0.169**
Groundwater Fluctuation	1/5	1/3	1/3	1	1	3	5	**0.084**
Drainage Density	1/5	1/5	1/4	1	1	3	3	**0.051**
Aquifer Transmissivity	1/7	1/5	1/5	1/3	3	1	3	**0.059**
Soil	1/7	1/7	1/7	1/5	1/3	1/3	1	**0.025**

The GWRZ map (Figure 54) shows that the least suitable zone is located in the estuarine portion of the study area, while the suitable recharge falls in some parts of the center, the North-West and South-East regions due to the distribution of quartz sandstone and fine quartz sand, cropland, high fluctuation and transmissivity values with high infiltration capacity. This indicates that geology, land use/land cover, aquifer transmissivity, groundwater fluctuation, and soil texture play a vital role in groundwater recharge. Moreover, drainage density and slope are less favorable to the infiltration capacity of the groundwater system as evidenced by their occurrence in low suitable zones. Only 0.5% of the total study area falls under poor suitable zone (index < 0-2.5), 10 % falls under moderate suitable zone (index= 0.2.5-0.50), 49.5% falls under good suitable zone (index= 0.50-0.75) and 40% under very good (index= 0.75-1). Therefore, the study area has great potential for infiltration. Finally, the cumulative effect of multi-influenced factors weighted by WLC through GIS modeling revealed the mapping of the GWRZ in the Great Banjul Area. It thus clearly indicates that the results are consistent with the results based upon the seven factors, which influence the groundwater recharge.

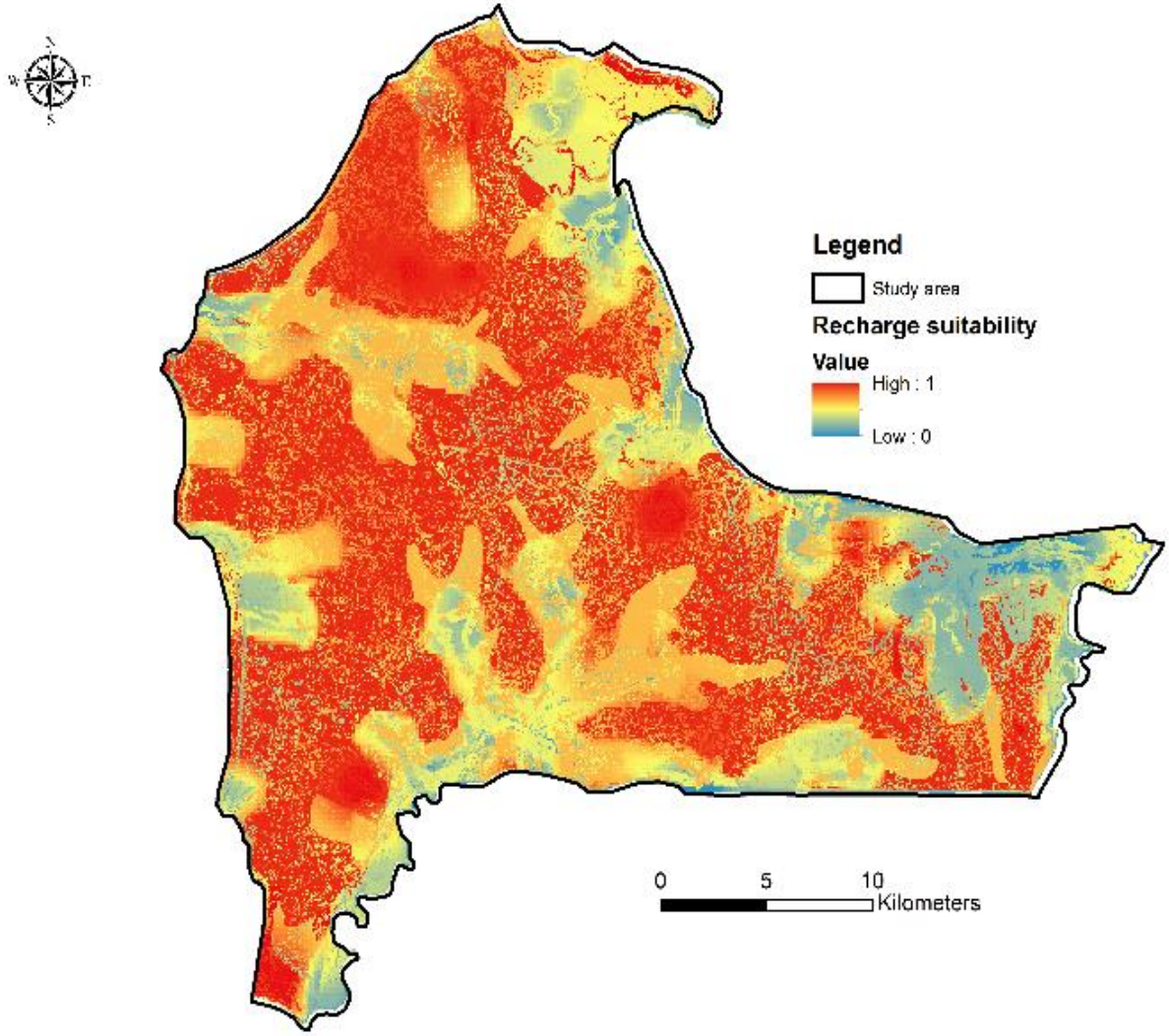

FIGURE 58: GROUNDWATER POTENTIAL RECHARGE ZONE MAP

5.6.10 Conclusion

Recharge is a vital element in the hydrological balance of a watershed. Knowing the evapotranspiration, which consequently leads to the estimation of recharge is very significant to water resource management. It is almost impossible to estimate an accurate value for evapotranspiration and/or recharge due to a lack of required data for most models. However, researchers developed numerous evapotranspiration estimation models, which are subjected to some errors. For this research, the water balance model of Penman, Thornthwaite, and Turc was used to estimate potential evapotranspiration and recharge. The choice of methods chosen for this research is purely based on the availability of data. The most popular and widely used model by researchers is the Penman, which required many input parameters for evapotranspiration estimation.

The results obtained from the three recharge estimation methods showed that the Thornthwaite model underestimates the possibility of the use of the soil water storage by evapotranspiration while the Penman overestimates evapotranspiration. The Turc method, on the other hand, gives the best estimate of recharge for our study than the two methods mentioned above.

The Thornthwaite, Penman, and Turc recharge estimation methods above only provide point values with uncertainties in their spatial distribution. To map the spatial distribution of the recharge at the Greater Banjul Area basin, remote sensing and GIS and MCDM techniques tools are used to identify and delineate the groundwater potential zones (GWPZ). It was found that the combination of the 7 factors is helpful to understand the behavior of groundwater in the study area. The delineated map was classified into four zones, viz., ‘poor’, ‘moderate’, ‘good', ‘very good’. Results indicate that about 10.5 % of the total study area falls under ‘poor’ and ‘moderate’ zones which indicates the least groundwater recharge occurrence. These areas are found in the estuarine portion of the study area and are a result of geological formation and soil texture composed of more clayey facies and high drainage density. 40% of the total area falls under the ‘very good’ zone which is a good indication for future artificial recharge planning and potential drilling of boreholes. This method can be widely applied as a valuable tool for solving groundwater problems of semi-arid areas with inherent limitations of data scarcity and multi-criteria evaluations.

CHAPTER 6: HYDROCHEMISTRY OF GROUNDWATER

6.1 Introduction

Assessment of the hydrochemical characteristics of groundwater is crucial to better forecast its usages. Groundwater quality is highly affected by the processes happening in groundwater and reactions with aquifer minerals. Knowledge of the geochemical evolution of groundwater in arid and semi-arid regions could lead to sustainable development and effective management of these water resources (Ndoye et al., 2018). Hydrochemical analyses of groundwater also help to understand the nature of groundwater, its spatial and temporal variation, and as well to determine the groundwater types in the study area. It is used by many researchers to assess the groundwater resources of an area (Blanchette et al., 2010). To have a comprehensive understanding of the nature of groundwater, a hydrogeochemical study of groundwater of an area has to be carried out. The chemical parameters of groundwater play a crucial role in classifying and assessing water quality (Sadashivaiah et al., 2008). Seher Dirican, 2015 stated that the purpose of using the physicochemical parameter is to test the quality of water before it is used for domestic, agriculture, or industrial purposes.

Gambia, like most semi-arid countries, faces some challenges in providing safe drinking water to its population. The shallow continental groundwater which is the major source of water supply for domestic and irrigation purposes in urban as well as rural parts of the Greater Banjul Area (GBA) is overexploited due to increase in water demand. In addition, issues such as urbanization, industrialization, unscientific land-use, lack of awareness of people and saline intrusion deteriorate the quality of groundwater in the GBA. Agriculture is a one of the main economic activities in the GBA. As surface water is saline and not fit for irrigation, groundwater is the only source of water for agricultural purposes. Hence, the assessment of groundwater quality is required for proper planning and regulation of water resources.

The objective of this work is to identify the chemical processes that control the hydrochemistry of groundwater of the whole GBA and to assess the quality of groundwater to determine its suitability for drinking and agricultural purposes. Diversity of groundwater quality in the GBA is a function of physical and chemical parameters that are greatly influenced by geological formations and anthropogenic activities.

Physicochemical parameters (water depth, pH, T°C, EC) were measured from 52 sampling points of the continental shallow aquifer (borehole and wells) and 6 surface water

during the 2018 pre-monsoon (May) and post-monsoon (November). Also, water samples were collected in November to analyze major ions and minor elements. The aim was to evaluate: (1) the groundwater quality based on different indices for drinking and irrigation uses, and (2) hydro-geochemical facies and processes driving groundwater mineralization. The Piper plots of major ions concentration of dissolved anion (SO_4, Cl, Br, and NO_3), and alkalinity (HCO_3) and cations (Na, Mg, Ca, and Ka) were used to identify the water types of groundwater in the GBA. Similarly, a statistical description of these ions is given in Table 13.

Multivariate analysis methods, such as Principal Component Analysis (PCA) Factor Analysis (FA), and Hierarchical Classification Analysis (HCA), are mostly used to identify major groundwateclusters and factors that affect the groundwater chemistry in aquifers (Dieng et al., 2017). Nonetheless, multivariate analyses are generally based on linear principles (Dieng et al., 2017, cited in Mudry, 1991; Gamble and Babbar-Sebens, 2012) and cannot overcome difficulties arising from biases due to complexity and non-linearity in datasets and from the inherent correlations between variables.

In this study, the multivariate statistical analysis was also applied on 11 water parameters using PCA, HCA and correlation matrix, to evaluate factors influencing the groundwater chemistry. With this method, the relationships between different groundwater parameters were determined using Pearson's correlation coefficient.

6.2 Statistical Analysis of Hydrochemical Data

Descriptive statistics is a statistical analysis method that makes it possible to study: (i) the parameters of data dispersion such as standard deviation, variance, asymmetry, coefficient of variation; (ii) the central tendency or position parameters, namely the mean, median, sum and (iii) the range parameters which are the minimum, maximum, and range (Titulaire et al., 2018). These descriptive statistical parameters thus made it possible to characterize the series of data used in this study.

The basic statistics for the physicochemical and hydrochemical variables are therefore classified according to a minimum, maximum, mean, standard deviation, variance, and sum. The values of the dataset analyzed statistically were presented in (Table 18). The statistical analysis of the major ions shows maximum values of chloride, bicarbonate, sodium, sulfate, nitrate, potassium, calcium, magnesium and Bromide are 308.18; 335.50; 191.03; 110.44; 544.72; 20.37; 40.66; 97.14 and 0.62 mg/l respectively. Descriptive statistics of the major groundwater parameters in the study area show that concentrations of major ions have mean

values within the acceptable range of the WHO standards. The order of dominance of the anions in the groundwater of the study area is HCO3 > NO3 > Cl > SO4 and the cations Na > Ca > Mg > K. Therefore HCO3, NO3, Cl, Na, and SO4 and are the dominant ions present in groundwater of the study area.

TABLE 18: DESCRIPTIVE STATISTICS OF HYDROCHEMICAL PARAMETERS

	Parameter	Type	N total	WHO (2000)	Mean	Standard Deviation	Sum	Minimum	Median	Maximum
Physico-chemical	pH	GW	52		5.95	0.96	309.17	4.04	5.85	7.80
	EC	GW	52		251.31	317.53	13068.00	30.00	130.50	1610.00
ANIONS	HCO3	GW	52	300	49.33	67.54	2565.05	12.20	24.40	335.50
	Cl	GW	52	200	30.70	57.62	1596.53	3.16	7.71	308.18
	Br	GW	52	-	0.59	0.05	1.17	0.55	0.59	0.62
	NO3	GW	52	50	41.39	90.08	2152.14	0.27	8.78	544.72
	SO4	GW	52	250	6.67	16.09	347.05	0.06	2.20	110.44
CATIONS	Na	GW	52	200	22.75	36.31	1182.98	2.01	8.48	191.03
	K	GW	52	100	3.21	3.35	166.92	0.73	1.93	20.37
	Mg	GW	52	<200	4.43	6.20	230.56	0.78	2.20	40.66
	Ca	GW	52	<200	19.12	23.23	994.34	1.58	8.61	97.14

The Box-plot of major ions content reveals freshwater for irrigation and drinking waters, with mean and median values below the WHO standard (Figure 55). However, Nitrate (NO_3) content (mean value: 41.4 mg/L) is much closed to the WHO guidelines of 50.0 mg/L but in some samples Nitrate contents are high according to their maximum values. The occurrence of high nitrate content is observed in some of the urbanized areas in The Gambia (Banjul, Brikama, Busumbala, and Sifoe), where it reaches 544 mg/L. Thus, nitrate occurrence in GBA is mainly due to anthropogenic pollution of infiltration of nitrate ferterlizers in irrigated areas and waste water (or liquid waste) infiltration into groundwater.

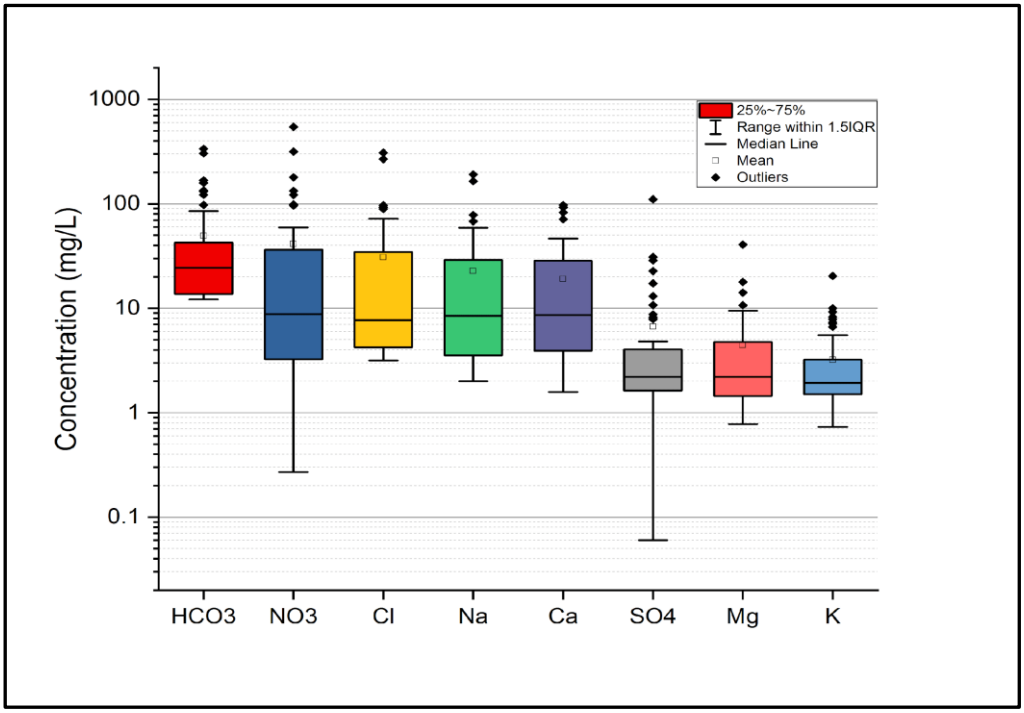

FIGURE 59: BOX PLOT OF THE GROUNDWATER CONCENTRATION OF MAJOR IONS IN THE GBA SHALLOW AQUIFER

6.3 Physicochemical Characterization

Twelve physicochemical groundwater quality parameters have been examined. These include pH, EC, T, four major cations magnesium (Mg), potassium (K), sodium (Na), and calcium (Ca), and five major anions: chloride (Cl), nitrate (NO_3), bromide (Br), bicarbonate (HCO_3) and sulfate (SO_4). Temperature, pH, electrical conductivity, have been measured in-situ for each sample.

Physicochemical characteristics of groundwater from pre-monsoon and post-monsoon campaigns are evaluated according to a descriptive statistical analysis (Table 19). The temperature values range between 24.5 and 33.0°C reflecting the shallow character of the CT groundwater in GBA where heat exchanges are easily achieved through ambient temperature. The pH values vary from 3.9 to 8.6 with average and median values of 5.7 and 5.5 reflecting the acidic character of the shallow aquifer waters. The lowest acidic values (pH 3.9–5) are found in wells located near the bolongs (i.e. the mangrove area). This could be as a result of the oxidation of pyrite, which is characteristic of mangrove degradation groundwater conditions (Dieng et al., 2017, cited in Ford et al., 1992).

The Electrical Conductivity (EC) goes from 24 to 1985 µS/cm with high variance and standard deviation values suggesting variables sources, geochemical, and dilution processes

depending on zones. According to World Health Organisation WHO (2008), this broad range of EC values differentiates two types of groundwater in the system:

1. Fresh water with EC values lower than 1000 µS/cm. This group includes water sampled from boreholes/wells in the western, central and eastern parts of the study area;
2. Saline and/or contaminated waters with EC values higher than 1000 µS/cm. These samples are from wells located in the coastal areas, near the Gambia River, tributaries and from a few wells in the central part of the study area.

The lowest EC values (250 µs/cm) observed in some areas in the Centre of GBA (Figure 56), indicates the preferential recharge zones as evidenced by the groundwater mound in this zone. Mean and median EC values of pre-monsoon (225 and 104 µs/cm) compare to post-monsoon (247 and 125µs/cm) suggest that acquisition of mineralization is achieved by dissolving salts in the unsaturated zone and mobilization ions through geochemical reactions during infiltration.

TABLE 19: DESCRIPTIVE STATISTIC OF THE PHYSICOCHEMICAL PARAMETERS

Parameter	**pH**		**Electric Conductivity**		**Temperature**	
Units	-		µs/cm		°C	
Sampling date	Pre-monsoon	Post-monsoon	Pre-monsoon	Post-monsoon	Pre-monsoon	Post-monsoon
N total	52	52	52	52	52	52
Mean	5.9	5.6	225.0	247.6	28.6	29.9
Stan Dev	0.8	0.9	336.7	310.8	1.6	1.4
Variance	0.7	0.8	113390.7	96587.1	2.7	1.8
Minimum	5.1	3.9	24.8	30.0	24.5	26.7
Median	5.7	5.3	104.8	125.0	28.7	29.7
Maximum	8.6	7.8	1985.0	1530.0	32.2	33.0

6.3.1. Spatial Distribution of Electrical Conductivity

Electrical conductivity (EC in µS/cm) expresses the degree of mineralization and salinization of water (Andr & Christine, 2013). The physicochemical parameters of groundwater in the shallow aquifer show a high variation in electrical conductivity from 24.8 to 1958 µS/cm during pre-monsoon and from 30 to 1530 µS/cm during post-monsoon of 2018 (Table 19). The mean and median EC values of pre-monsoon (225 and 104 µs/cm) compare to post-monsoon (247 and 125µs/cm) suggest that acquisition of mineralization is achieved by dissolving salts in the unsaturated zone and mobilization ions through geochemical reactions

during infiltration. The EC value in post-monsoon is higher than that of pre-monsoon may be due to infiltration of sulfate acid from rainfall.

The conductivity values greater than the WHO accepted EC value (1000 µS/cm) for drinking water is found in two dug wells (DW22, and DW24), located in the center of the study area (Figure 56a, 56b). DW22 is a dug well situated very close to the Tanji River. The high EC value of this particular well could be due to water contamination of the brackish/saline water of the river. Similarly, DW24 is located in Brikama Newtown in the center of the study area has a high EC value greater than the WHO standard drinking water. It has an EC of 1164 µS/cm during pre-monsoon and 1420 µS/cm in post-monsoon of 2018. This is could be seen in Figures 56c and 56d where the EC contour lines are stronger and closer together, which is an indication of high EC values. Higher values of EC can be due to the dissolution of minerals and the influence of anthropogenic contamination, causing increases in ionic concentration and/or marine water intrusion into coastal aquifers. All other sampled boreholes and dug wells have low EC values between 40 and 670 µS/cm which are below the acceptable WHO standard for drinking water. This is a clear indication of freshwater in the study area. The low conductivity values (EC < 100 µS/cm) in the dome area indicate a groundwater recharge zone. Mean and median EC values of pre-monsoon (225 and 104 µs/cm) compare to post-monsoon (247 and 125µs/cm) suggest that acquisition of mineralization is achieved by dissolving salts in the unsaturated zone and mobilization ions through geochemical reactions during infiltration.

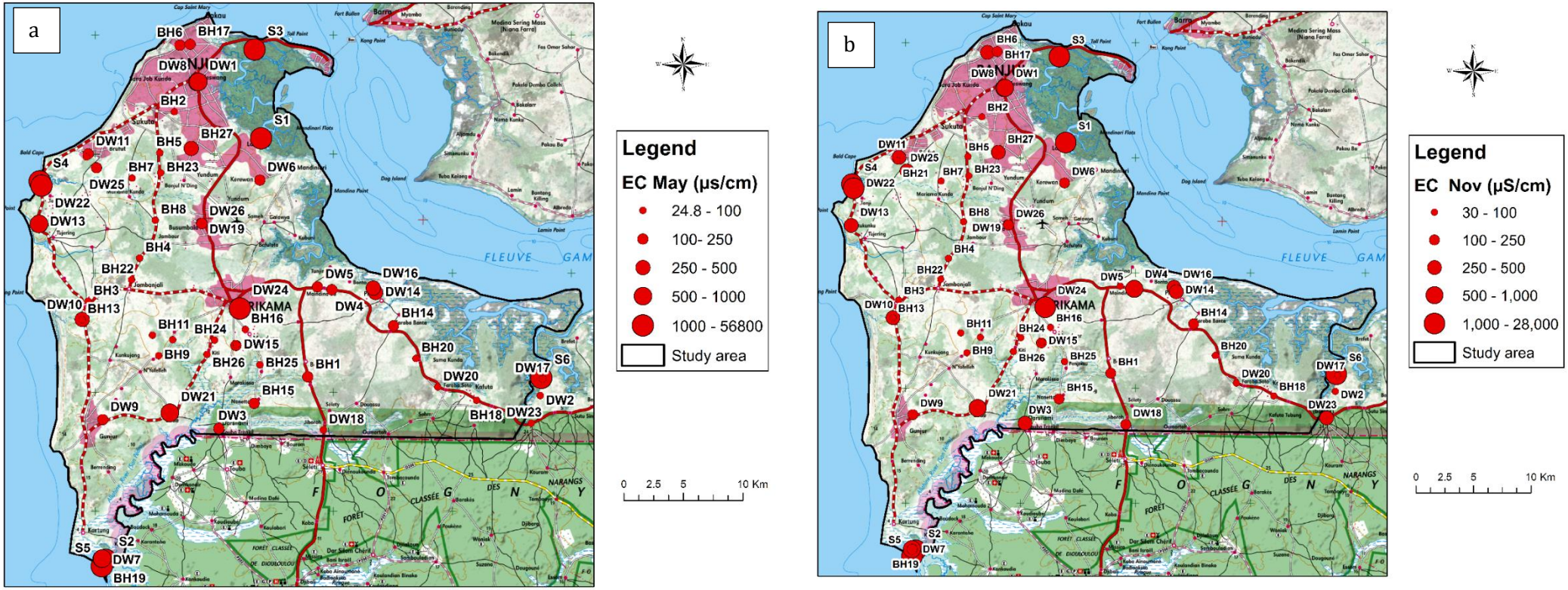

FIGURE 60: SPATIAL DISTRIBUTION OF EC (µS/CM) MEASURED IN THE FIELD: (A) PRE-MONSOON, (B) POST-MONSOON 2018;

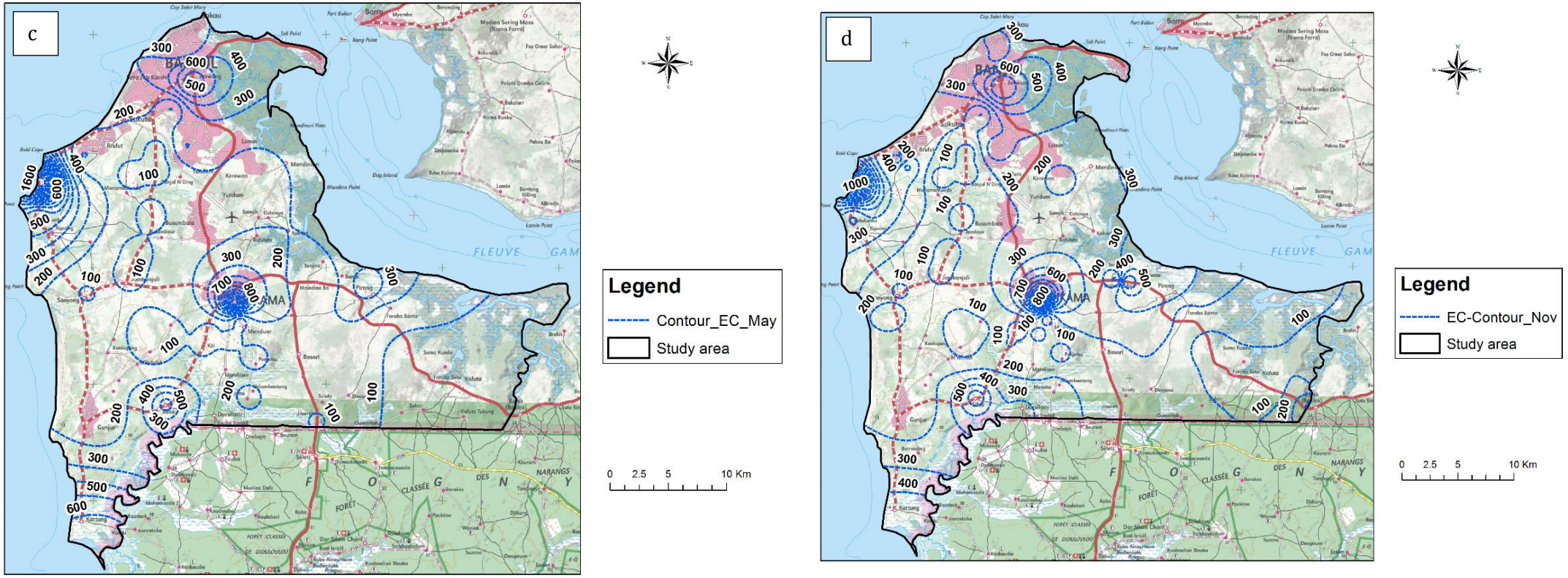

FIGURE 61: SPATIAL DISTRIBUTION OF EC (µS/CM) MEASURED IN THE FIELD: EC CONTOUR: (C) PRE-MONSOON AND (D) POST-MONSOON 2018

6.3.2. Spatial Distribution of pH

The pH of water is to determine how acidic or alkaline the water is on a scale of 0 to 14 (Mensah Mawuli, 2011). Water having a pH below 7 indicates acidity and it contains more hydrogen (H+) ions than hydroxide (OH-) ions. Those with measurements above 7 show that the water is alkaline (basic). The pH values measured in the study area range from 5.1 to 8.6 in pre-monsoon of 2018 with an average of 5.6 (Figure 57). In the post-monsoon of the same year, the pH values range from 3.9 to 7.8 having an average of 5.9. This range of pH values reflects the acidic to the slightly basic character of the CT waters.

The pH measured was categorized into three classes. The first group is pH values >6.5 and this class is considered very acidic. The second class is ranged from 6.5 - 7.5 and this class is referred to as slightly acidic to neutral. The third class is >7.5 and it is regarded as basic. The acidic pH values may be related to the presence of sulfate soils in the area. The leaching of sulfate soils by infiltration can lead to a decrease in pH value. Most of the groundwater in the study area is acidic. Some boreholes and dug-wells (BH3, BH4, BH19, BH21, DW4, DW7, DW10, DW13, and DW21) close to the sea are basic which could be due to intrusion of seawater. Some of the boreholes and dug-wells pH values that were found to be very acidic in pre-monsoon become moderately acidic and basic in post-monsoon. This could be due to the interaction of infiltrated rainwater with carbonate-rich rocks will usually change the pH acidic to neutral or basic.

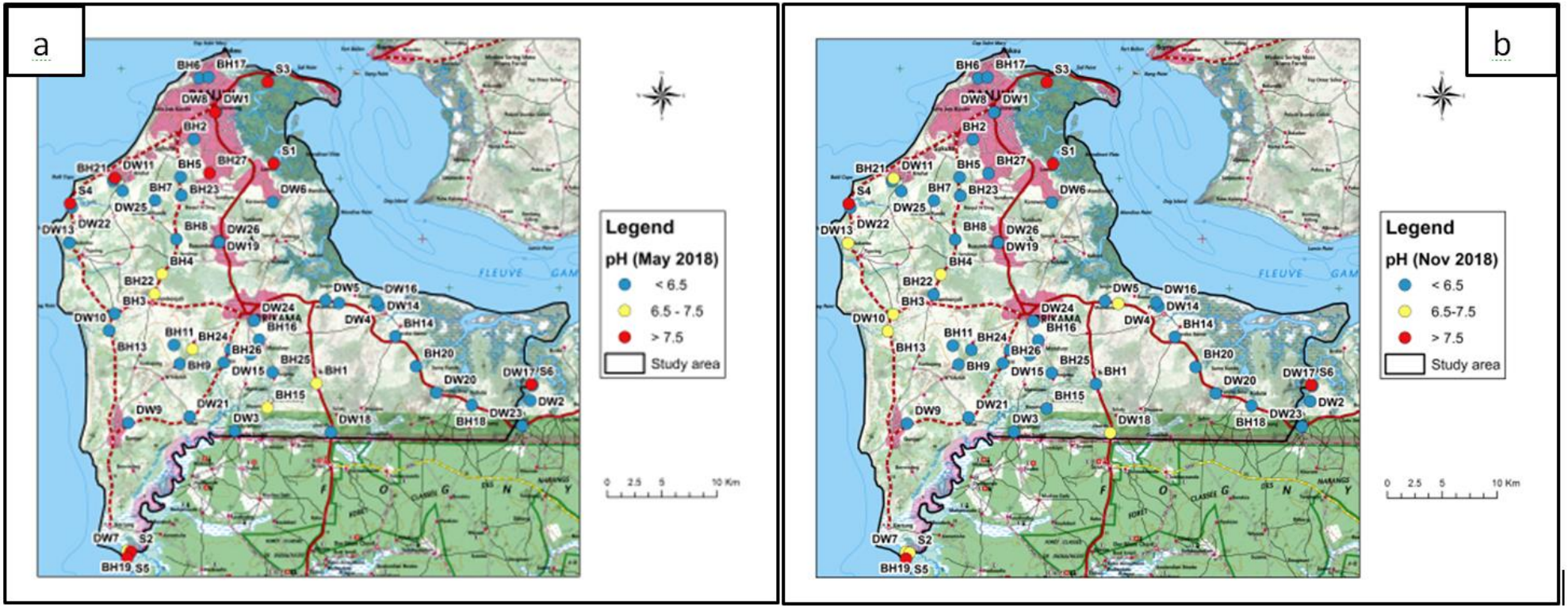

FIGURE 62: DISTRIBUTION OF PH MEASURED IN THE FIELD: (A) PRE-MONSOON AND (B) POST-MONSOON, 2018

6.3.3 Temperature

Groundwater temperatures range from 24.5 to 32.2 ^{o}C with an average of 25.6 ^{o}C in May 2018 (Table 19). Similarly, the temperature values range from 26.7 to 33 ^{o}C with an average value of 26.8 in November 2018. These temperature values are close to the ambient temperature which reflects the shallow character of the CT groundwater where heat exchanges are easily achieved through ambient temperature (Faye et al., 2010). These temperature values also highlight the open nature of the aquifer, and therefore its vulnerability to pollution from the surface.

6.4 Piper Diagram

The major cations and anions concentrations are plotted in the Piper trilinear diagram to be able to understand the geochemical nature of groundwater. The Piper diagram (Piper, 1944) is an important tool to infer hydrochemical facies, understand and identify the water composition in different classes. The analysis of the Piper diagram identified the presence of three (3) main hydrochemical facies based on the major ion chemistry of groundwater is spatially distributed in the GBA (Figure 58): i) bicarbonate (m-HCO_3, Ca-HCO_3, and Na-HCO_3) facies, ii) chloride (Na-Cl and m-Cl) facies, iii) and mixed (m-m and Na-m) facies. The first group located mostly in the centre and eastern parts of the the study area is featured fresh groundwater of Ca-HCO_3 derived from calcite dissolution reactions and the Na-HCO_3 type and less mineralized indicates freshening processes by recently infiltrating rainwaters. The second group, Na-Cl, and m-Cl rich waters derived from saline water intrusion at the vicinity of the Gambia River and its tributaries accompanied by ion exchange reactions and pollution dominate this group.

The majority of the samples about 39.7% are plotted in the m-HCO_3 field, 25.9 % of the samples shows Na-Cl type, Ca-HO_3 represents 15.5%, m-Cl is represented by 5.2%, 3.4% by the Na-m of the water type and 1.7% represents Ca-HCO3 and Na-HCO3 types in the study area. The piper diagram revealed that most of the groundwater of the GBA is characterized by bicarbonate water type which is dominant in all geological and hydrogeological settings. The concentrations of the groundwater constituents are affected by the hydrogeological conditions and geological setting of the basin (Blanchette et al., 2010b). Overall, the bicarbonate water types are dominant (56.9%) and are found throughout the study area except the coastal areas. The chloride water types are the second dominant (31.1%)

which are located in aquifers near the coastline which indicates mixing with seawater. The third water type of the GBA is mixed facies (12%).

- The mixed bicarbonate (m-HCO3), observed at water points BH3, BH4, BH5, BH7, BH8, BH9, BH10, BH11, BH13, BH15, BH16, BH18, BH20, BH22, BH23, BH24, BH25, BH27, DW2, DW5, DW10, DW15 and DW25 located on the west and south and few are located in the eastern part of the study area. These waters are characterized by low conductivity (EC: 24-100 μS/cm) and a pH of less than 6.5.
- Calcium bicarbonate (Ca-HCO3), at water points B12, BH14, BH19, DW4, DW7, DW9, DW11, DW18, and DW20, are sparsely distributed in the region. Dissolution of carbonate minerals (dolomite, calcite) generates a Ca-HCO3 groundwater type. This water type represents the freshwater in these aquifers.
- Sodium chloride (Na-Cl), is the second dominant water type aside from m-HCO3. This water type is found in BH17, DW3, DW6, DW8, DW14, DW21, DW22, DW23, and DW24. These aquifers are located along the Gambia River which is evidence of a mixing process with the saline waters of the river. Sodium mixed (Na-m) is observed in BH21 and BH26 only. This water type is less dominant in the study area
- Calcium Sulphate (Ca-SO4), only found at Pirang (DW16). It is the least occurring water type (1.7%). This well is not far from the mangrove area with acid Sulphate soil resulting from the influence of sulphate soils or the dissolution of gypsum. Ca-SO_4 rich waters can be derived from saline water intrusion at locations close to the Gambia River together with ion exchange reactions and pollution.

The occurrence of bicarbonate facies in areas considered as the preference recharge zone (low EC values, piezometric mound), indicate predominantly that m-HCO_3, Na-HCO_3, and Ca-HCO_3 result from the dissolution of calcite minerals during infiltration. Moreover, the m-HCO_3 is the most representative water type in the study area suggesting the occurrence of cationic ion exchange processes. Also, sulphate water type occurs also during the first step of groundwater recharge.

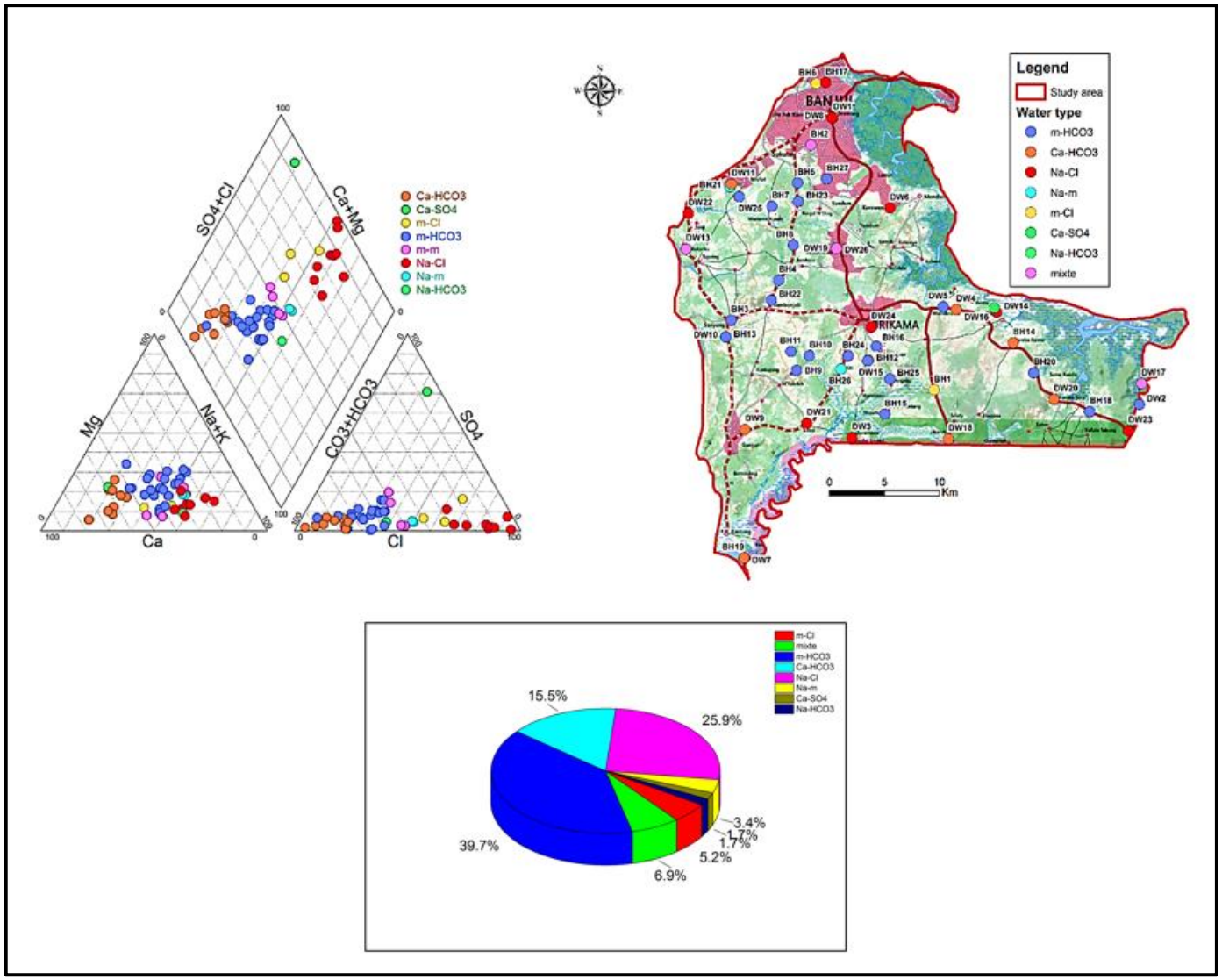

FIGURE 63: PIPER TRILINEAR DIAGRAM SHOWING HYDROCHEMICAL REGIME OF GROUNDWATER AND DISTRIBUTION OF GROUNDWATER TYPES IN THE STUDY AREA. M=MIXED, CL-CHLORIDE, MG=MAGNESIUM, CA-CALCIUM, NA-SODIUM. K=POTASSIUM, SO4-SULPHATE, CO3-CARBONATE, AND HCO3-BICARBONATE

6.5 Geochemistry of Groundwater

Water reacts with minerals in rocks as it infiltrates through the ground and these rock-water interactions give water its characteristic chemistry (Earle, 2013). The major ion chemistry of groundwater is a very useful tool for detecting solute sources as well as describing groundwater evolution as a result of rock-water interaction leading to the dissolution of carbonate minerals, silicate weathering, and ion exchange processes (Kumar et al., 2009). Groundwater appropriateness for domestic, industrial, or agricultural use can be determined through its chemical characteristics (Mallick et al., 2018). The evolution of groundwater chemicals is the result of the geochemical processes happening within the aquifer (Blanchette et al., 2010a). Groundwater geochemistry is the science that explores the processes controlling the chemical composition of groundwater.

Hydrochemical facies characteristics of groundwater evaluation help to provide an initial idea about the multifaceted hydrochemical processes in the subsurface/unsaturated zone and hence gives enough information on the chemical quality of water. Results from the chemical analyses were used to identify the geochemical processes and mechanisms in the groundwater aquifer system of the GBA.

The bivariate diagram (Figure 59) shows the relationship between ions/Cl ratios and Cl which are crucial in the assessment of the source and mineralization in the GBA groundwater. In Figure 59a (Na/Cl *vs.* Cl), the low Na/Cl molar ratio of up to 2.5 in the groundwater is an indication of freshwater. The presence of Na/Cl molar ratio suggests water-rock interaction which is due to Na being derived mainly from weathering and/or cation exchange. The discrepancies of the other cations/Cl ratios vs. Cl concentrations (Figures 59b, c, and d) are similar to the Na/Cl *vs.* Cl trend which supports the model discussed above where the chemistry of the low salinity groundwater is controlled by water-rock (Faye et al., 2010).

Similarly, the bivariate diagram of HCO3/Cl *vs* Cl is presented to separate the mixing mechanisms of freshwater and saline water from chemical reactions (Chen et al., 2008). The indicating. The HCO3/Cl *vs* Cl (Figure 44g) shows that the HCO3/Cl molar ratio < 1.00 indicates freshwater of the GBA aquifer system in general except for aquifers near the coastline and saline reaches of the River Gambia and tributaries. Saline intrusion into the aquifer system can be determined using SO4. Marine water generally has very high concentrations of SO4 than in groundwater. The relationship between SO4/Cl and Cl (Figure

59e) shows saltwater intrusion has affected the aquifers near the coast but the majority of the groundwater is freshwater.

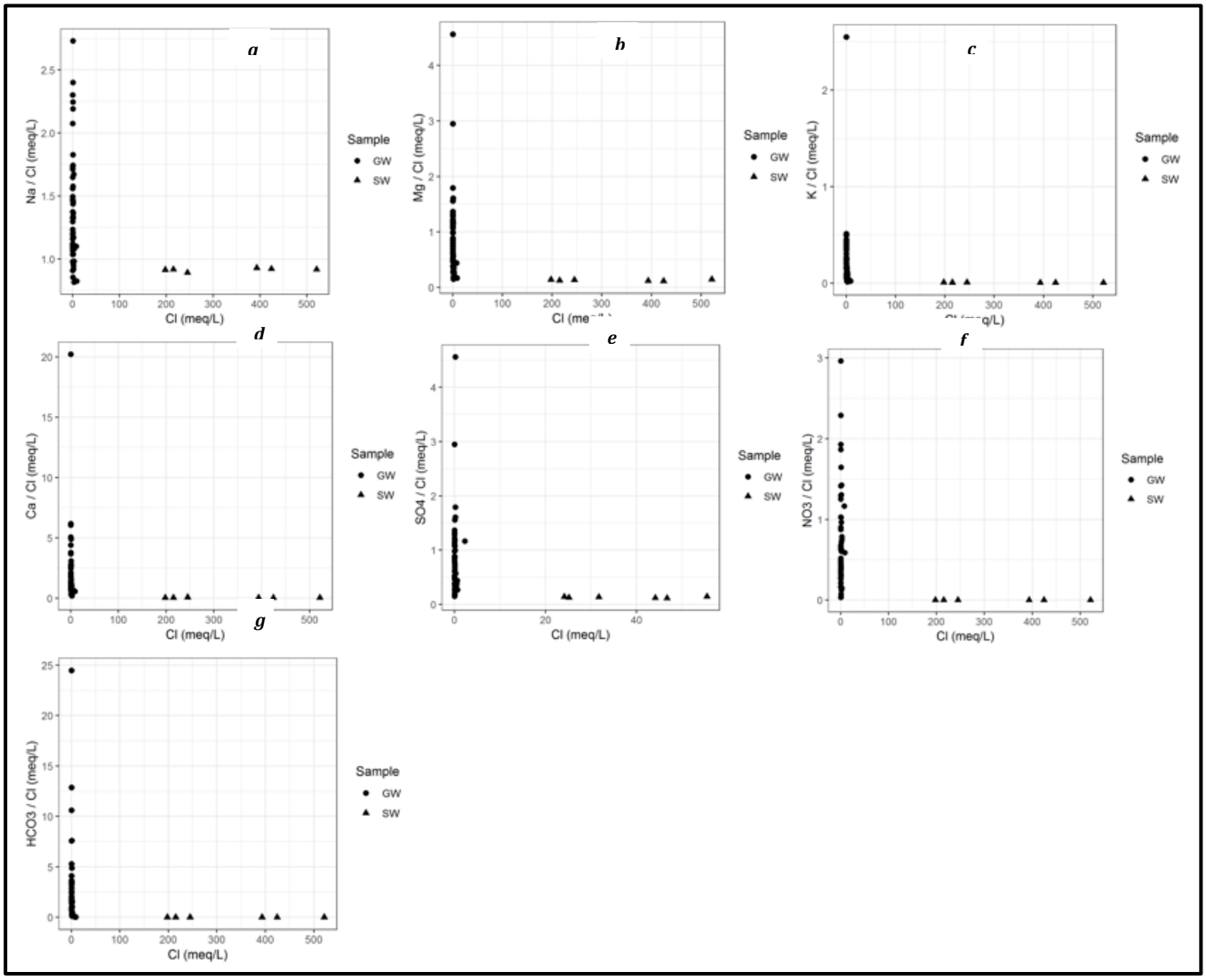

FIGURE 64: GEOCHEMICAL PROCESSES OF GROUNDWATER IN THE STUDY AREA. MAJOR IONS/CHLORIDE RATIOS VS. CHLORIDE: (A) NA/CL VS. CL, (B) MG/CL VS. CL, (C) K/CL VS. CL, (D) CA/CL VS. CL, (E) SO4/CL VS. CL, (F) NO3/CL VS. CL AND (G) HCO3/CL VS. CL (CIRCLES: FRESH GROUNDWATER; TRIANGLES: SURFACE WATER)

Ion exchange is one of the significant processes in semi-arid regions, contributing to the chemistry of groundwater (P. J. S. Kumar & James, 2016). The bivariate plot of Ca+Mg-HCO3-SO4 versus Na+K-Cl (Figure 60b) is used to verify the evidence for cation exchange process in groundwater chemistry. Na+K-Cl represents the amount of Na+K gained or lost relative to that provided by chloride salt dissolution, while Ca+Mg-HCO3-SO4 represents the amount of Ca and Mg gained or lost relative to that provided by gypsum, calcite, and dolomite dissolution (Luo, Gao, & Zhang, 2018; Road, 2014). If ion exchange occurs in the groundwater, the slope of the trend line must be **-1** (Mora, Mahlknecht, Rosales-lagarde, &

Hernández-antonio, 2017). Figure 60b has a negative slope which indicates that there is a relationship between Ca, Mg, and Na through the reverse ion exchange process.

The scattered plot of (Ca + Mg) versus (HCO3 + SO4) shows that most of the points are on or above the mixing line, towards the Ca+Mg field indicating the abundance of these ions (Figure 60d). It revealed that the prevailing reverse ion exchange process is the dissolution of carbonate minerals (calcite and dolomite) and some salt rocks such as anhydrite and/or gypsum, rather than silicates. The excess of Ca and Mg originates from clay minerals, with an exchange of sodium ions from groundwater (Luo et al., 2018).

The weathering of silicate minerals is one of the crucial processes responsible for generating sodium (Na) and potassium (K) in groundwater. This wreathing process can lead to the production of various materials including clay. The bivariate plots of HCO3 versus Na + K (Figure 60c) were used to study the major impact of silicate weathering on groundwater chemistry. All the groundwater samples fell on the HCO3 axis or below the equiline (i.e. under the 1:1 line) of the HCO3 versus Na + K bivariate plot. This suggested that silicate weathering was not the dominant process responsible for major ions in the shallow groundwater of the GBA.

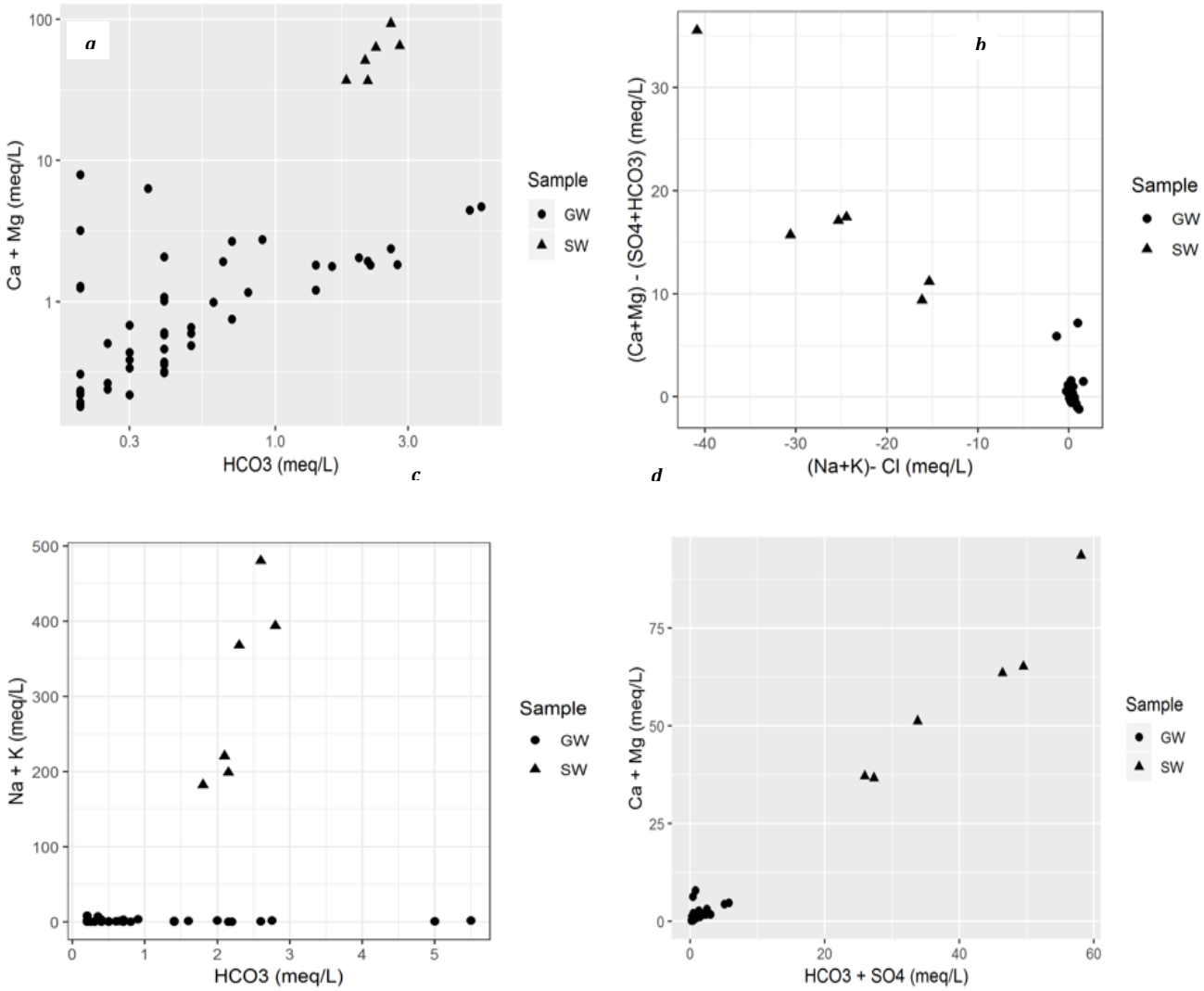

FIGURE 65: BIVARIATE PLOTS SHOWING THE RELATIONSHIP BETWEEN: (A) CA + MG VERSUS HCO3 + SO4. (B) (CA + MG) – (SO4 + HCO3) VERSUS NA + K - CL; (C) NA + K VERSUS HCO3; AND (D) CA + MG VERSUS HCO3 + SO4

6.6 Multivariate Statiscal Analysis

Multivariate statistical techniques such as principal component analysis (PCA), Hierarchy cluster analysis (HCA) and factor analysis (FA) are effective methods of manipulating, interpreting and representing data concerning groundwater pollutants and geochemistry (Jena & Deepak, 2018). Principal component analysis (PCA) is a multivariate statistical analyses technique that provides a reliable alternative method for understanding and interpreting the complex system of water quality with the ability of analyzing large dataset and segregating complex relationships among many variables (Umar Kura et al., 2013; Tay et al., 2017). The aim of utilizing the multivariate statistical analysis is to assess the groundwater quality by identifying the spatial correlations between clusters of elements (lithological

characteristics, enrichment phenomena, anthropogenic pollution, etc.) in a complex system and reduce a multidimensional dataset to more basic components. It also aims to analysis and evaluate several factors and processes influencing the hydrochemistry of groundwater and by how much each factor contributes to the variations in groundwater chemistry of the GBA.

This statistical method has been applied by many researchers to evaluate water quality. For instance, Umar Kura et al., used multivariate statistical analysis to assessing the groundwater quality and evaluating various factors and processes influencing the hydrochemistry and quantitative contributions of each factor to the variations in groundwater chemistry of Kapas Island. Ako et al., 2014, also used the multivariate statistical technique of principal component (PC) and factor analysis (FA) for the identification of factors responsible for nitrate contamination of groundwater in the Banana Plain and Mount Cameroon area. Tay et al., 2017 applied multivariate statistical analysis to assess the hydrogeochemistry of groundwater in order to facilitate the unveiling of hidden structures in the datasets and assist in delineating the factors responsible for groundwater pollution for proper development and management of groundwater within the Lower Pra Basin, Ghana. In India, Mohapatra et al., 2011 used the PCA and HCA on the physicochemical properties of groundwater to identify dominant processes affecting groundwater quality in the coastal unconfined aquifer of Puri city.

The multivariate statistical techniques such as principal component analysis (PCA), Hierarchy cluster analysis (HCA) and correlation matrix were used on the standardized dataset of 11 groundwater quality parameters measured for 52 groundwater samples collected from 27 boreholes and 25 dug wells during the post-monsoon of 2018 to identify distinct groundwater groups, the geochemical processes controlling the groundwater and sources of pollution of groundwater in the GBA shallow aquifer.

6.6.1 Principal Component Analysis

PCA is the most widely used technique (Tay et al., 2017; Umar Kura et al., 2013; Sânchez-martos et al., 2001) among the different multivariate statistical analysis. The aim of PCA is construction of new variables called principal components out of a set of existing original variables (Mohapatra et al., 2011; Abou et al. 2017; Tay et al., 2017). It is a technique which recognizes patterns in a multivariate dataset (Ako et al., 2014) and then grouped them based on their similarities and differences (Umar Kura et al., 2013) and as well to note any correlations that exist between the physicochemical variables of the waters. PCA was applied

to the hydrochemical parameters (T, pH, EC, Ca, Mg, Na, K, HCO3, Cl, SO4 and NO3), expressed in mg/L, except pH and EC in µS/cm (Table 8), using the Origin Pro 2019 v9. 6. The Kaiser's criterion, otherwise known as the eigenvalue-one criterion is one of the most commonly used criteria for solving the number-of-components problem in PCA (Umar Kura et al., 2013; Sânchez-martos et al., 2001). The percentages of eigenvalues are computed which quantify the contribution of each factor to the total variance. Factors having eigenvalues greater than one are considered the most important for final analysis. This allowed the reduction of the 11 variables to three significant principal components (3 PCs) that accounts for 84.31% (Table 20) of the total variance in the hydrochemistry. These three PCs influence the water chemistry and pollution of groundwater within the shallow aquifer of the GBA. The number of eigenvalues can be estimated from a scree plot demonstrated in Figure 46a. As shown in this figure, the eigenvalues sharply decrease within the first three components and then slowly stabilize for the remaining ones. The first component, PC1, which normally accounts for the most significant process, explains 53.42% of the total variance with an eigenvalue of 5.88 (Table 20a). There is significant positive loadings (>0.70) between PC1 and the physiochemical parameters (EC, Ca, Mg, Na, and HCO3) in Table 8b. The PC2 has 2.30 eigenvalue, explained 20.92% of tatal variance and moderate positive loading of 0.57 with pH and 0.60 HCO3. This indicates acidic and fresh water type. The third PC has 1.09 eigenvalue, explains 9.98% of the total variability and consists of positive loading (0.56) of T and strong positive loading (0.74) of SO4. The PC3 positive loading with SO4 could originate from degradation of organic substances from topsoil and runoff water, leached sulfates from agricultural areas due to fertilizer application, sewage and other human activities (Sânchez-martos et al., 2001).

The results revealed that the first component (PC1) factor is most highly correlated with Cl, NO3, Na, Mg and Ca with EC concentration having the strongest influence. The presence of Ca, Mg and Na may be due to cation exchange and mineral precipitation processes, while Cl, Na and NO3 might be because of sea water intrusion and infiltration of irrigation of agricultural fertilizers. During rainy season, when the aquifer is recharge, groundwater becomes rich in Ca, Mg and HO3 due to dissolution of calcium, magnesium and carbonate present in the aquifer. During this period, flushing and reverse ion exchange Na at the exchanger surface is replaced by Ca. This causes groundwater to be rich in sodium and calcium bicarbonate type water converts to sodium bicarbonate type water. With more flushing, sodium bicarbonate type water converts to calcium bicarbonate type water.

The second component (PC2) factor is most highly correlated with HCO3, pH and K with HCO3 concentration having the strongest influence. The third component (PC3) factor is most highly correlated with SO4 and T, SO4 having the strongest influence. It is also observed from the results of the factor analysis using principal component analysis (PCA) that EC, HCO3 and SO4 are the three most important variables affecting the quality of the wells/boreholes waters within the GBA. Therefore, the treatment units to be design must be capable of addressing the effects of high Sulphate observed with the borehole water.

TABLE 20: (A) EIGENVALUE, VARIABILITY AND CUMULATIVE % OF EACH OF THE EXTRACTED COMPONENTS; (B) CORRELATION OF PHYSICOCHEMICAL VARIABLES IN EACH PCS

a

Components	Eigenvalue	Percentage of Variance (%)	Cumulative (%)
PC1	**5.87572**	**53.42**	**53.42**
PC2	**2.30137**	**20.92**	**74.34**
PC3	**1.09734**	**9.98**	**84.31**
PC4	0.75959	6.91	91.22
PC5	0.50611	4.60	95.82
PC6	0.21424	1.95	97.77
PC7	0.15547	1.41	99.18
PC8	0.05224	0.47	99.66
PC9	0.03368	0.31	99.96
PC10	0.00323	0.03	99.99
PC11	0.00102	0.01	100.00

b

	Coefficients of PC1	Coefficients of PC2	Coefficients of PC3
T			0.55726
CE	0.40911		
pH		0.57271	
HCO3		0.59671	
Cl	0.37646		
NO3	0.37004		
SO4			0.74404
Na	0.39215		
K		0.34239	
Mg	0.37722		
Ca	0.37339		

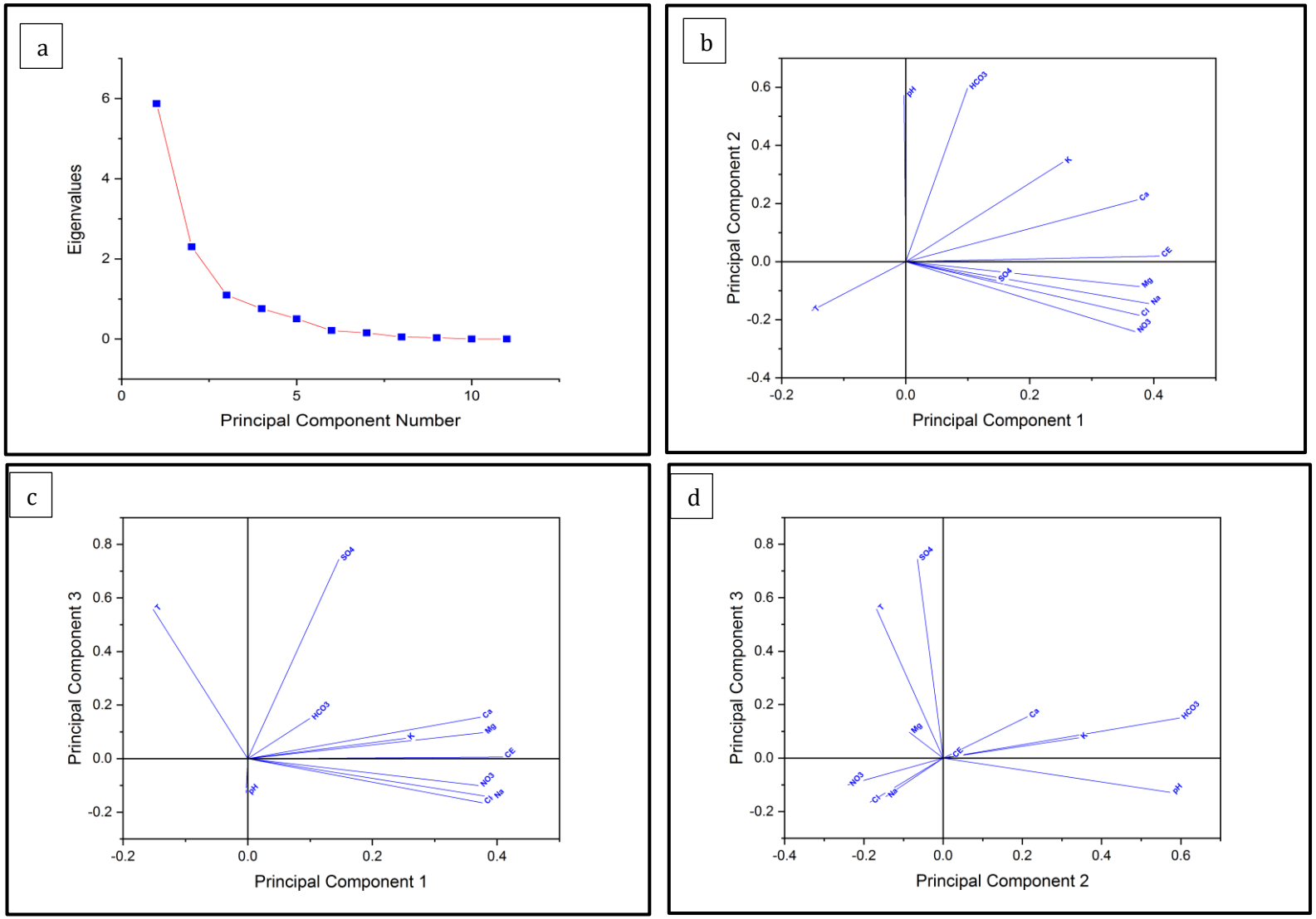

FIGURE 66: (A) CATTEL SCREE PLOT OF PRINCIPAL COMPONENTS WITH EIGENVALUE >1; (B) PLOT OF PC1 AND PC2 LOADING SCORES FOR THE DATASET OF WATER SAMPLES; (C) PLOT OF PC1 AND PC3 LOADING SCORES FOR THE DATASET OF WATER SAMPLES; (D) PLOT OF PC2 AND PC3 LOADING SCORES FOR THE DATASET OF WATER SAMPLES;

The loadings plot (Figure 61b) of the first two PCs (PC1 and PC2) shows the distribution of all the physicochemical parameters in the first (upper right) and fourth (lower right) quadrants. The lines joining the variables and passing through the origin in the plot of the factor loadings are indicative of the contribution of the variables to the samples. Proximity of lines for two variables signifies the strength of their reciprocal association (Ravikumar & Somashekar, 2017 cited in Qu and Kelderman 2001). Grouping of parameters (Mg, Na, SO4, Cl and NO3) in the loadings plot suggests their significant mutual positive correlation. From Figure 61b, it is apparent that samples distributed in lower quadrants are more concentrated with anions (SO4, Cl and NO3) including two cation (Na and Mg) and Temperature, while, those in the upper quadrants with HCO3, K, Ca, EC and pH.

Lastly, it was concluded that PCA analysis yielded three principal components of which, PC1 and PC2 accounting for 53.42 and 20.92 % of total variance, respectively, are mainly responsible for controlling geochemistry of groundwater. This is because 74.34 % of physicochemical parameters assessed in the GBA and they have strong loading (>0.57) fall under these two components. The loadings plot (Figure 61c) of PC1 and PC3 shows the distribution of all the physicochemical parameters in the first (upper right) and fourth (lower right) quadrants except for temperature. The grouping of parameters (NO3, Na, and Cl) and (Ca, K, Mg) in the loadings plot suggests their significant mutual positive correlation. The loading of NO3 in this factor indicates pollution of groundwater from domestic waste water infiltrating from on-site sanitary systems and infiltration of nitrate fertilizer from irrigation. The loading of Na and Cl might be associated with infiltration or interaction of saline water with freshwater groundwater.

In contrast, PC2 and PC3 (Figure 46d) displayed strong positive and negative loading by three parameter each with grouping of (Na, Cl), (Ca, EC) and (Ka, HCO3). During the pre-monsoon (dry season) when sea water intrusion occurs, ion exchange takes place because of hydraulic conditions/gradient.

TABLE 21: TOTAL VARIANCE EXPLAINED BY EACH PC AND THE LOADING MATRIX OF PCS

Extracted Eigenvectors			
	Coefficients of PC1	Coefficients of PC2	Coefficients of PC3
T	-0.15167	-0.16846	**0.55726**
CE	**0.40911**	0.01897	0.00615
pH	-0.00274	**0.57271**	-0.12772
HCO3	0.09949	**0.59671**	0.14975
Cl	0.37646	-0.18477	-0.16496
NO3	0.37004	-0.24094	-0.10007
SO4	0.14610	-0.06508	**0.74404**
Na	0.39215	-0.14461	-0.14401
K	0.25343	0.34239	0.07595
Mg	0.37722	-0.08583	0.09722
Ca	0.37339	0.21274	0.15462
Eigenvalue	5.87572	2.30137	1.09734
%Variance	53.42	20.92	9.98
%Cumulative	53.42	74.34	84.31

6.6.1 Correlation Analysis of Chemical Parameters

Correlation analysis (CA) (Pearson's correlation coefficient) is used to investigate the relationships between the physicochemical, which can identify the source of solutes, and the process that generated the determined water compositions (Chung et al., 2019). The linear correlations between variables are measured by correlation coefficients ranging between −1 and 1. The high coefficients between two variables expresses the importance of the relationship between them (Abou Zakhem, Al-Charideh, & Kattaa, 2017). A positive coefficient expresses similarity and harmony between the correlated variables, and a negative coefficient demonstrates that the variables are developing in opposite directions (Abou Zakhem et al., 2017 cited in Hamzaoui-Azaza et al. 2009).

To have a better understanding of the different relations between the 11 hydrochemical parameters of the groundwater samples, a Pearson correlation matrix (Table 10 and Figure 62) was generated to determine the relationships between the different variables in order to explain factor loadings during PCA and assist in the identification of pollution sources not accessible at first glance (Tay et al., 2017). The correlation coefficient of the raw data its eigenvalue, and eigenvectors are computed.

According to Tay et al., (2017), high correlation coefficient value (i.e. -1 or 1) predicts a good relation between two variables (Ako et al., 2014) and correlation coefficient value around zero (0) predicts no relationship between the two variables at a significant level of P (0.05). Parameters showing r (0.9 - 0.7) are considered to be strongly correlated whereas r

between 0.4 and 0.7 shows moderate correlation and parameters showing r (0.4) shows low to no correlation. The correlation matrix shows a very strong positive correlation between EC and Mg; EC and Ca, EC and Cl; EC and NO3; EC and Na; EC and K; pH and HCO3; Cl and NO3; Cl and Na; Cl and Mg; Cl and Ca; NO3 and Na; NO3 and Mg; NO3 and Ca; Na and Mg; K and Ca; Mg and Ca. This means that paired parameters have a strong to moderate influence between them. In addition, the sources of dissolved salts in groundwater was analysed. The pH has a good positive correlation with HCO3 (r = 0.71), indicating an alkaline environment, in which the dissolved CO2 played a dominant role. This leads to mineral dissolution. A strong positive correlation of EC with Cl (r = 0.91), NO3 (r = 0.87), Na (r = 0.95), K (r = 0.61), Mg (r = 0.88), Ca (r = 0.92) is observed. This means that the aquifer chemistry is mainly controlled by Cl, NO3, Na, K and Mg and Ca. The variation in the values of correlation coefficient is caused by the disparity in solubility and dissolution of mineral, ion exchange, leaching of secondary salts, evaporation, anthropogenic activities and marine sources, following the topographic features and water flow-path conditions (Subba Rao, 2014). A high positive correlation coefficient of Mg with Na (0.88) and Ca with Na (0.76) reflects the weathering and dissolution of plagioclase feldspars and ferromagnesium minerals. A strong positive correlation also exist between Na and Cl (r = 0.97), indicating the same origin of these elements likely related to the halite dissolution (Nagaraju, Thejaswi, & Sreedhar, 2016) also indicating the influences of evaporation and marine influence. Very strong correlation exists between Cl and NO3 (r^2 = 0.91), Cl and Mg (0.82) and strong positive correlation between Cl and Ca (0.73). This is a result of anthropogenic and marine origin. Also a strong positive correlation exists between calcium and magnesium (r^2 = 0.78), calcium and Potassium (r^2 = 0.70),

TABLE 22: PEARSON'S CORRELATION MATRIX OF THE 11 PHYSICOCHEMICAL PARAMETERS

Parameters	T	EC	pH	HCO3	Cl	NO3	SO4	Na	K	Mg	Ca
T	1										
EC	-0.32325	1									
pH	-0.21873	0.02217	1								
HCO3	-0.15374	0.27884	**0.71119**	1							
Cl	-0.29376	**0.91194**	-0.19739	-0.06421	1						
NO3	-0.24566	**0.87414**	-0.26597	-0.13659	**0.91009**	1					
SO4	0.02899	0.32515	-0.17255	0.03152	0.18289	0.24058	1				
Na	-0.31886	**0.9492**	-0.1486	0.02025	**0.97287**	**0.9494**	0.2087	1			
K	-0.33404	**0.61005**	0.26737	**0.56653**	0.3838	0.34023	0.20417	0.43135	1		
Mg	-0.22055	**0.88396**	-0.07806	0.16141	**0.82033**	**0.88741**	0.39369	**0.87511**	0.3948	1	
Ca	-0.27423	**0.91978**	0.24512	**0.55525**	**0.72851**	**0.67265**	0.37534	**0.76438**	**0.70034**	**0.77637**	1

Correlation coefficients >0.5 are marked in bold font
Correlation is significant at the 0.05 level (2-tailed test of significance is used)

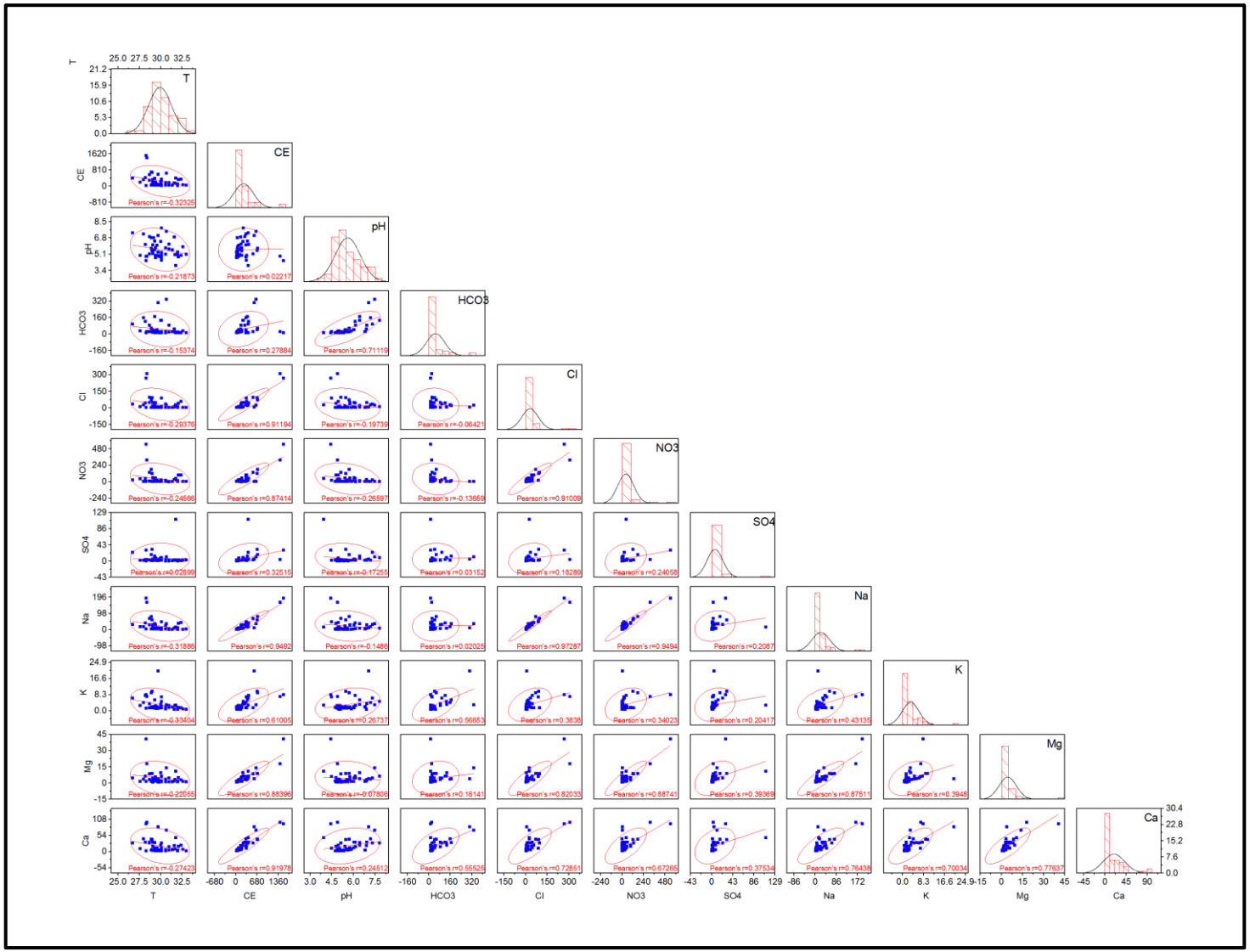

FIGURE 67: CORRELATION MATRIX OF THE 11 PHYSICOCHEMICAL PARAMETERS MEASURED DURING POST-MONSOON OF 2018.

6.6.2 Hierarchy Cluster Analysis

Hierarchy Cluster Analysis (HCA) is useful to group water quality parameters into clusters so that parameters within a cluster are similar to each other but different from those in other clusters. The cluster analysis was used in the study to group the 52 samples into statistically distinct hydrochemical groups that may be substantial in the geologic context. The samples were clustered based on their similarity to each other through comparisons of multiple parameters from different samples. Classifications of samples according to their parameters are known as Q-mode classifications (Belkhiri et al., 2010). The Q-mode HCA was used in this study to classify the samples into distinct hydrochemical groups. A classification scheme using Euclidean distance (straight line distance between two points in *c*-dimensional space defined by *c* variables) for similarity measurement, together with Ward's linkage method (Ward, 1963), produces the most distinctive groups where each member within the group is more similar to its fellow members than to any member outside the group (Belkhiri et al., 2010, cited in Güler et al., 2002). All 11 hydrochemical parameters were used in this analysis. The cluster analysis in this study suggested three groundwater groups (Figure 63, 64 and Table 2). EC seems to be a major distinguishing factor, which increases with concentrations increasing in all major-ions following the order: Cluster 1, 2 and 3. The relationship between different variables can also be seen in the dendogram. This shows a high correlation between major ions (Ca, Mg, Na, NO3, Cl and EC) which indicated saline water intrusion, anthropogenic contamination and water-rock interaction.

The first Cluster (C1) (forming the left-hand group) consists of the western zone cases (boreholes 1-13, boreholes 16-18, boreholes 20-26, and wells 2, 5, 6, 9, 15, 17, 19, 20 and 26). C1 is sulphate and temperature dominated. This could be due to

Cluster 2 (forming the middle group) comprised of wells 1, 3, 4, 7, 8, 10, 11, 13, 14, 16, 18, 21, 23, 25 and boreholes 14, 15, 19, and 27. C2 is bicarbonate dominated. However, sodium, chloride and calsium are also present. This type of water is fresh, having a mean EC value 16.6 µS/cm. The bicarbonate groundwater type is fit for drinking and irrigation purposes. This type of water is fresh, having a mean EC value 16.6 µS/cm. The bicarbonate groundwater type is fit for drinking and irrigation purposes.

This cluster is bicarbonate dominated groundwater type with Na-Cl present in some wells, one well of Ca-SO4 water type and one mixed type, having an EC value of 416.0 µS/cm. The Ca-SO4 groundwater type could be derived from the weathering of gypsum. The

source of Na-Cl groundwater type could be as a result of the weathering of halite. However, sodium, chloride and calsium are also present.

Furthermore, cluster 3 (forming the right-hand group) consists of dug wells 22 and 24 (DW22 and DW24) which depicted the salinity group otherwise referred to as the Na-Cl water type with mean EC of 1475 µS/cm, a maximum of 1530 µS/cm and minimum of 1420 µS/cm. DW22 is located close to the river and it could be concluded that there is sea water intrusion. The third cluster (C3) has the highest EC value, low pH, high content of chloride (287.9 mg/L), and Nitrate (430.6 mg/L), exceeding the WHO acceptable standard for drinking water. This cluster has a high nitrate content for both wells of 544.72 mg/L and 316.55 mg/L respectively with mean value of 430.64 mg/L which could be due to infiltration of fertilizer in irrigated areas, sewage water (septic tanks) and manure storage. Similarly, cluster 3 (C3) has high nitrate content (Table 11) which is above the WHO acceptable standard for drinking water. The groundwater of this cluster is more acidic than C1 and C2. Inaddition, cluster 1 (C1) is acidic and all other parameters and within the WHO acceptable standard for drinking water.

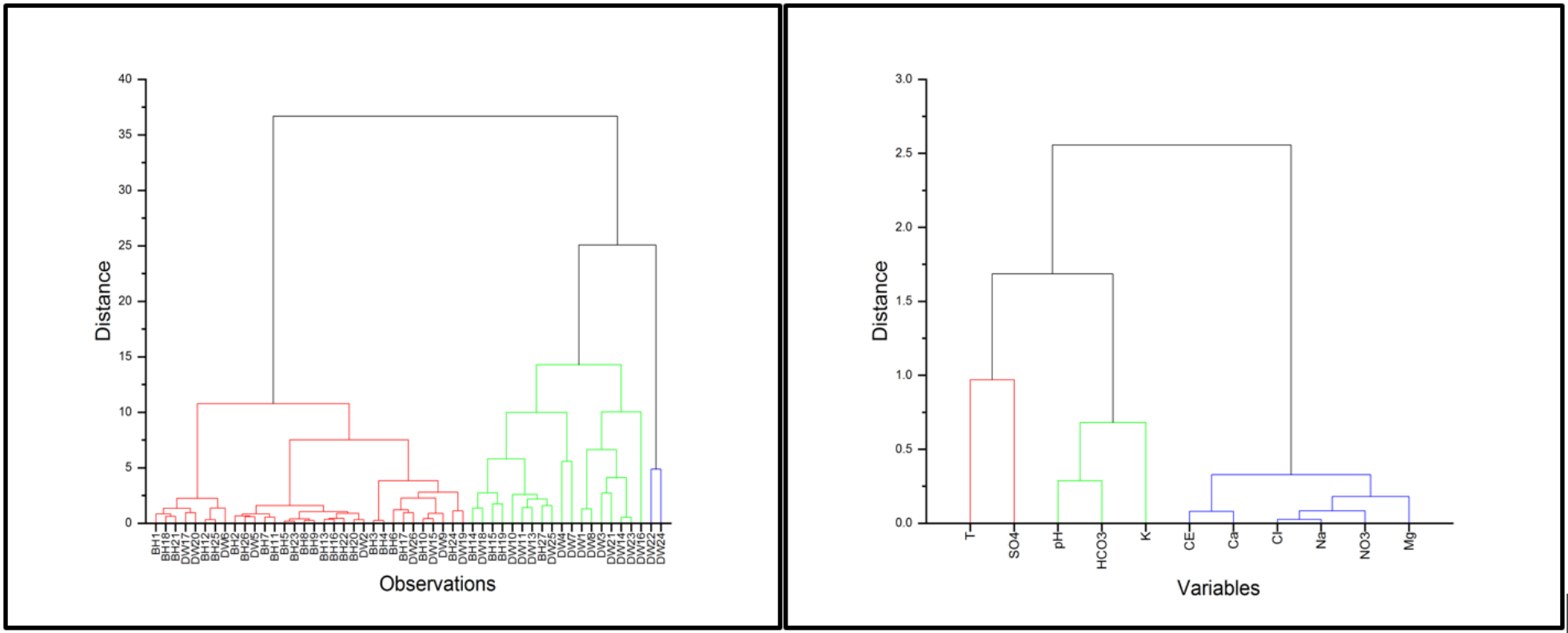

FIGURE 68: DENDROGRAM FOR CLUSTERING OF 52 GROUNDWATER SAMPLING SITES USING THE EUCLIDEAN DISTANCE METRIC (WARD'S METHOD)

TABLE 23: MEAN PARAMETER VALUES OF THE THREE CLUSTER WATER GROUPS (DETERMINED FROM HCA).

Cluster	Count	T	EC	pH	HCO3	Cl	NO3	SO4	Na	K	Mg	Ca
C1	n=32	30.1	84.9	5.4	21.2	9.6	13.9	2.0	7.7	1.7	1.9	6.2
C2	n=18	29.8	400.5	6.1	103.0	39.7	47.0	13.9	32.3	5.4	6.2	33.7
C3	n=2	28.4	1475.0	4.7	16.8	287.9	430.6	16.2	178.0	7.8	29.3	94.8

pH (standard units), EC (µS/cm) and mean (mg/l).

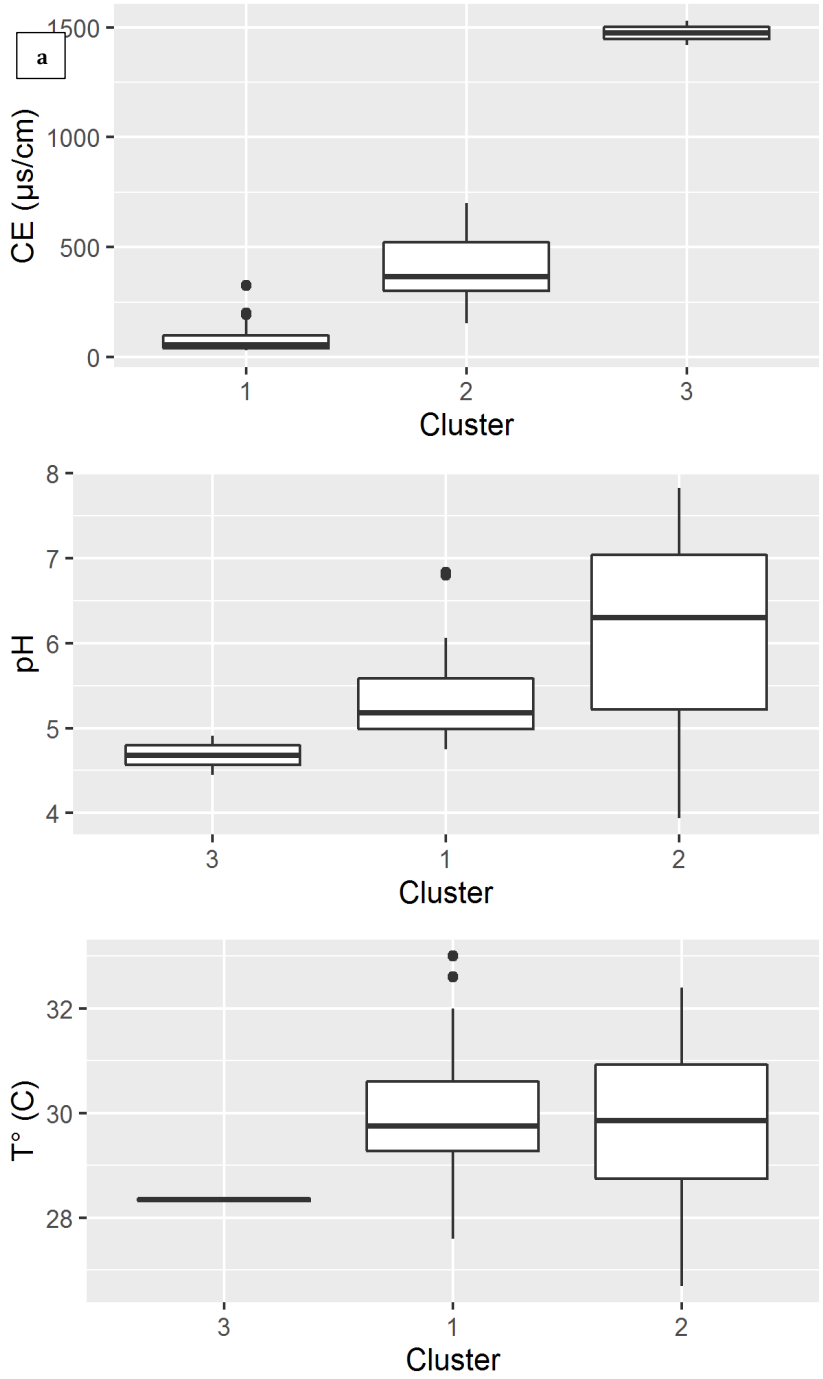

FIGURE 69: (A) MEAN VALUE OF THE PHYSICOCHEMICAL PARAMETERS WITH THE 3 CLUSTERS.

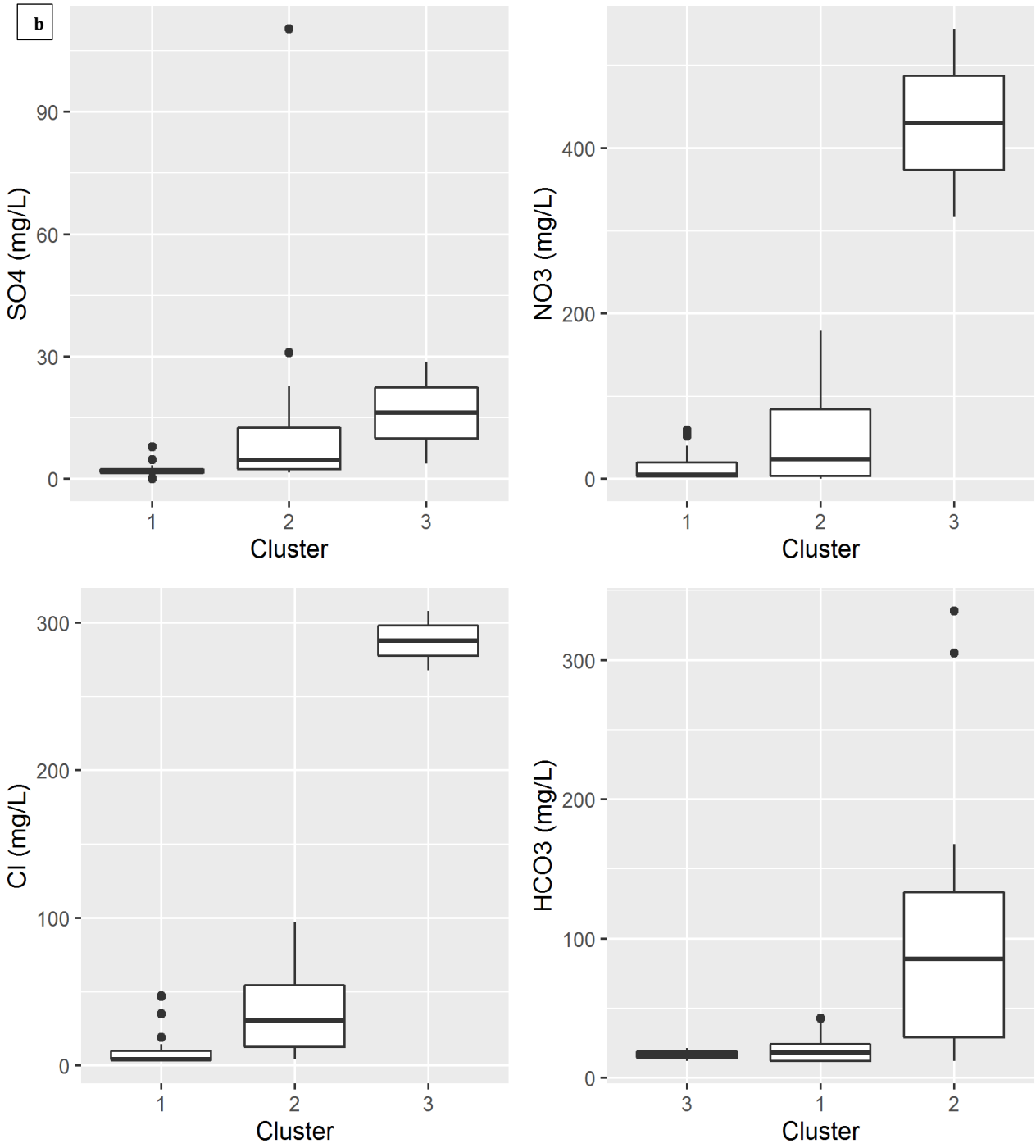

FIGURE 70: (B) MEAN VALUE OF THE PHYSICOCHEMICAL PARAMETERS WITH THE 3 CLUSTERS.

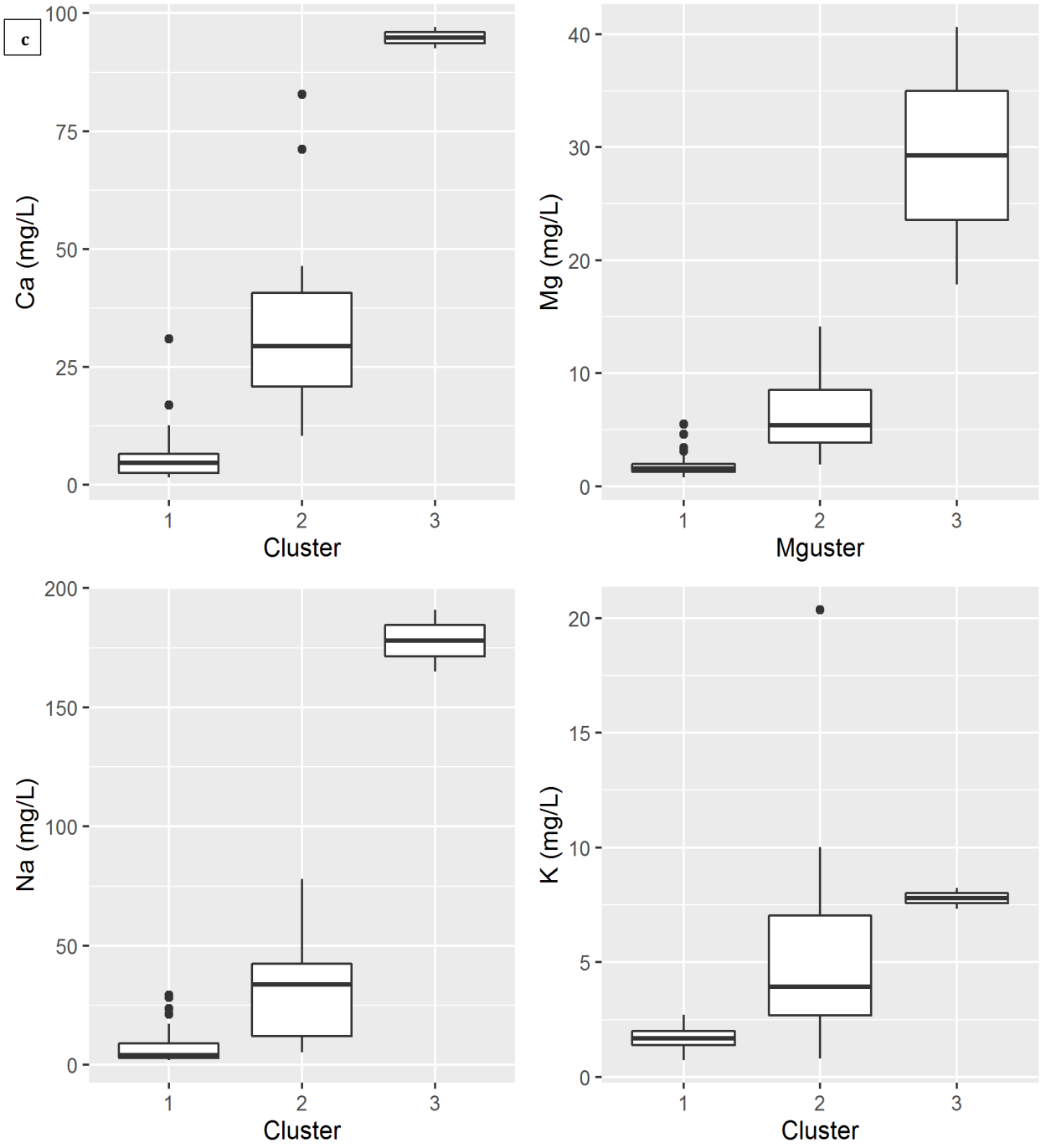

FIGURE 71: (C) MEAN VALUE OF THE PHYSICOCHEMICAL PARAMETERS WITH THE 3 CLUSTERS.

6.7 Saturation Indices (Si)

The saturation index was evaluated using the geochemical code PHREEQC (Mora et al., 2017). Saturation index (SI) is defined as the logarithm of the ratio of ion activity product (IAP) to the mineral equilibrium constant at a given temperature and expressed as (Road, 2014):

$$SI = \log\left({}^{IAP}/_{K_{sp}}\right)SI = \log\left({}^{IAP}/_{K_{sp}}\right) \quad \textbf{(20)}$$

Where IAP is the ion activity product and Ksp is the solubility product of the mineral. The saturation index (SI) describes the deviation of water from equilibrium with respect to dissolved minerals quantitatively.

The reactivity of minerals in groundwater is easily identified with the help of SI. Oversaturation of minerals in groundwater occurs when SI value is greater than zero, and therefore precipitation of these minerals will occur while undersaturation of minerals in groundwater causes dissolution when SI is less than zero (Mallick et al., 2018; Road, 2014). Most of the SI of calcite and dolomite are less than zero except for one sample for calcite and 3 samples for dolomite (Figure 65a, 65b). Water acts as a solvent for calcite and dolomite when it interacts with carbonate minerals. The dissolution of calcite has a fairly faster reaction and acquires Ca^{2+} ion much faster than in dolomite. Ca^{2+} ions react with dolomite in a solution to produce Mg^{2+} and increase Ca^{2+}, $CO_3^{2+,}$ and HCO_3^- concentration (Mallick et al., 2018). The negative values of SI for these minerals indicate under-saturation and therefore indicating the dissolution of these minerals in groundwater. Likewise, groundwater is undersaturated with halite and gypsum because the SI values for these minerals are all negative (Figure 50c and 50d), and the dissolution of the above minerals is the predominant factor for groundwater quality in the GBA.

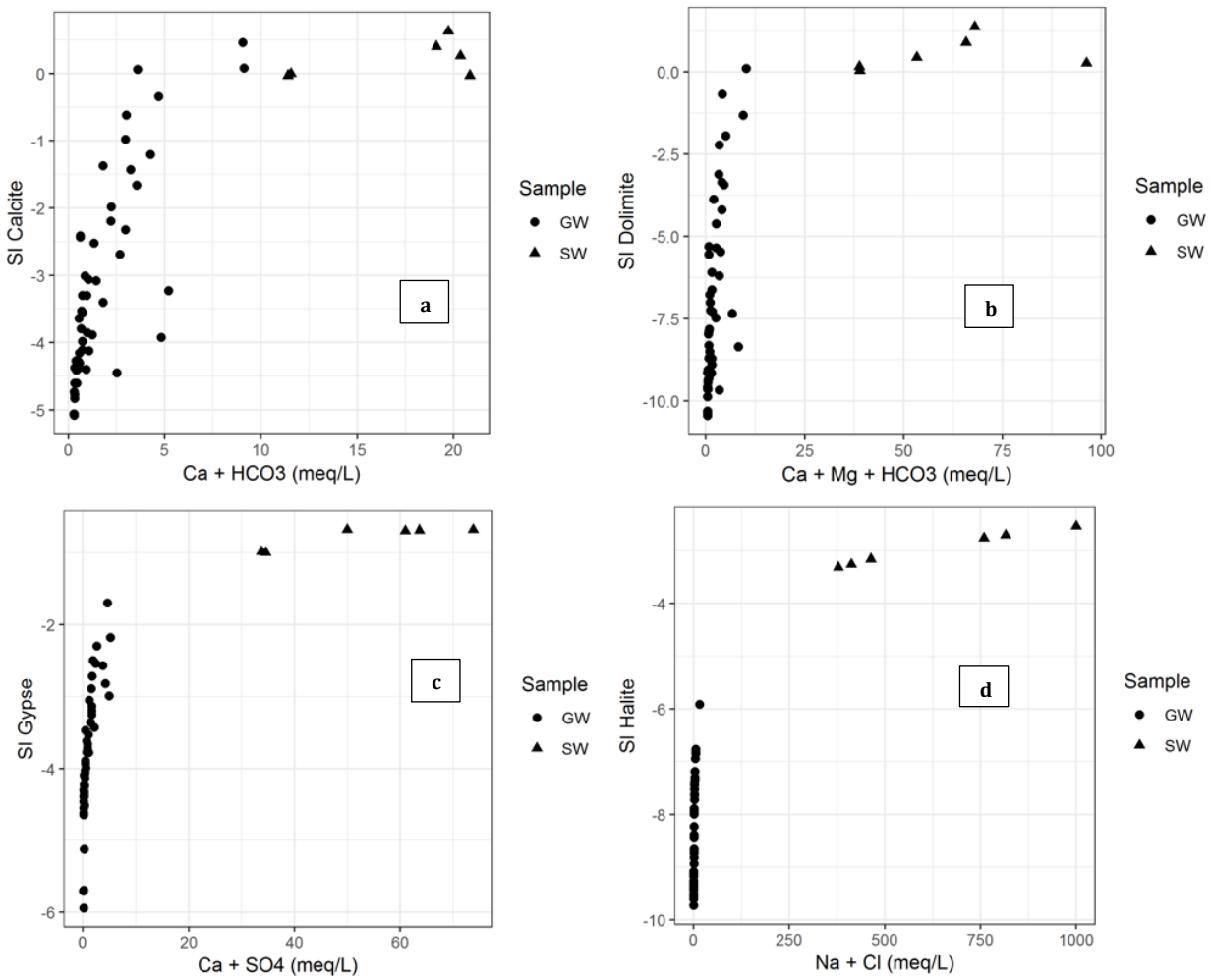

FIGURE 72: SATURATION INDICES (SI): (A) CALCITE VS. CA + CO3; (B) DOLOMITE VS. CA + MG + HCO3; (C) GYPSUM VS. CA + SO4; (D) HALITE VS. NA + CL

6.8 Conclusion

The shallow sand (continental terminal) aquifer signifies an important groundwater resource in the GBA, where it is the main source of drinking water and agricultural irrigation for the population. Thus, the evaluation of processes responsible for the mineralization and degradation of water quality and of the groundwater quality changes of the shallow sand aquifer is of great importance. A groundwater quality assessment of the shallow continental aquifer was conducted for 52 samples collected from wells and boreholes. The analysis of hydrogeochemical data using conventional and statistical methods allows the assessment of the groundwater quality in the GBA. Statistical analyses of the geochemical data demonstrate the spatial variability of the chemical characteristics of the groundwater. The results from the water analysis were used to identify the processes and mechanisms affecting groundwater chemistry in the GBA. The physicochemical parameters show a large variation in EC from 24.8 to 1958 µS/cm with an average of 225.0 µS/cm, in May and from 30 to 1530 µS/cm with

an average of 222 μS/cm in November of 2018. Thus showing low to high mineralization of the groundwater that reflects different sources, geochemical and dilution process. The pH values vary from 3.9 to 8.6 with average and median values of 5.7 and 5.5 reflecting the acidic character of the CT waters. The average temperature values of 29°C reveals the shallow characters of the aquifer where heat exchanges are easily achieved through ambient temperature. This.

The analysis of the Piper diagram resulted to the identification of main groundwater types which is characterized by bicarbonate (m-HCO_3, Ca-HCO_3, and Na-HCO_3) water type 56.9% in the center and eastern part of the GBA corresponding to a mound at +19m indicates the preferential recharge zones as suggested with the piezometric map. This group featured fresh groundwater of Ca-HCO_3 derived from calcite dissolution reactions and the Na-HCO_3 type and less mineralized indicates freshening processes by recently infiltrating rainwaters. The chloride (Na-Cl and m-Cl) rich waters derived from saline water intrusion at the vicinity of the Gambia River and its tributaries accompanied by ion exchange reactions and pollution dominate this group. However, 23% of samples have NO_3 content above the WHO guideline (50mg/L) with a maximum of 545 mg/L located in the urbanised areas. The high nitrate concentration in this context suggests organic pollution through one-site sanitation, domestic wastewater and agricultural irrigation. It is therefore recommended that proper construction of dug and hand-pumped wells as well as a safe distance between septic tanks and wells are are considered. It's also necessary to sensitize the general public on groundwater and pollution issues.

Binary plots of major ions and saturation index calculation of minerals shows that the main geochemical processes are calcite and dolomite dissolution followed by reverse base-exchange. Regarding surface water, all samples are saline to brine water with average EC raging from 48ms/cm (May) to 37ms/cm (November) attesting dilution process with rainfall events (July-October). In addition to this process, it involves the dissolution of evaporates (Halite and Gypsum) as well as the basic exchanges as evidenced by binary plots of major ions and saturation index calculation.

Similarly, the water quality dataset of variables from post-monsoon sampling was analysed using two different multivariate statistical techniques such as PCA and HCA to investigate the relationships between the physicochemical, which can identify the source of solutes, and the process that generated the determined water compositions to understand dominant processes affecting the water quality parameters. The results like the piper diagram, showed bicarbonate water type as the dominant for most of the well expect for few

wells/boreholes located in the coastal areas due to sea water intrusion and anthropogenic pollution of some inland wells with the injection of nitrate from septic tank, agriculture irrigation, etc.).

Three grouping of variables (clusters) were classified from the dendrogram of post-monsoon dataset using the HCA method. The variables and processes suggested by PCA factor groups are identical and confirmed by the variables in the HCA clusters. Hence the present study validated the usefulness of the PCA and HCA techniques for interpretation of geochemical processes in the fresh water of the shallow continental aquifer of the study area.

In general, the processes responsible for determining groundwater type of the GBA are dissolution of minerals and ion exchange, weathering with anthropogenic pollution, and sea water intrusion. The outcome of the results reveals that most of the shallow continental groundwater system of the GBA is fresh and is suitable for drinking and irrigation purposes in the GBA the water of the, except for some well that have high content of nitrate beyong the WHO acceptable standard for drinking water.

CHAPTER 7: GROUNDWATER MODELLING AND CLIMATE CHANGE IMPACTS ON GROUNDWATER RESOURCES

7.1 Groundwater Modelling

This chapter addresses the potential effects of climate change on the water resources in the continental terminal aquifer of the GBA. It models the flow paths of the groundwater flow system of the GBA, It also examines the sensitivity of the GBA recharge to long-term changes in temperature, Potential evapotranspiration, and precipitation.

7.1.1 Introduction

Groundwater modeling makes use of computer-generated models of the crucial features of a natural hydrogeological system that uses the laws of science and mathematics (Middlemis, 2004) in the prediction of the flow of water (Mutasa, 2011). Groundwater flow models are conceptual estimates that give descriptions of physical systems using mathematical equations but do not represent the exact descriptions of physical systems or processes (Michigan Department of Environmental, 2014). They are used to calculate the rate and direction of movement of groundwater through aquifers and confining units in the subsurface, and the exchange of groundwater between aquifers (Khadri & Pande, 2016b) and sources and sinks, where groundwater is added or removed from the aquifer (Michigan Department of Environmental, 2014). The U.S. Geological Survey's MODFLOW (McDonald, 2005), a three-dimensional finite-difference numerical model, which is used to make predictions about the behavior of the groundwater flow system for water supply (Toure et al., 2016b) and evaluate the potential impact of groundwater pumping on the aquifer.

In this study, a numerical groundwater flow model (Visual MODFLOW Flex) developed by Waterloo Hydrogeologic was used to quantify the groundwater resources and simulate the groundwater flow of the GBA. Visual MODFLOW Flex is a graphical user interface for MODFLOW groundwater simulations. Visual MODFLOW Flex is a software that is meant for predicting the outcome of future groundwater behavior, forecast the aquifer conditions, and to represent the natural groundwater flow, hydraulic heads, recharge, and groundwater flow rates within and across the boundaries of the system and concentrations of a

substance dissolved in groundwater (Gautam & Swaroop, 2017). Below is a simplified flow chart of the groundwater modeling methods (Figure 66).

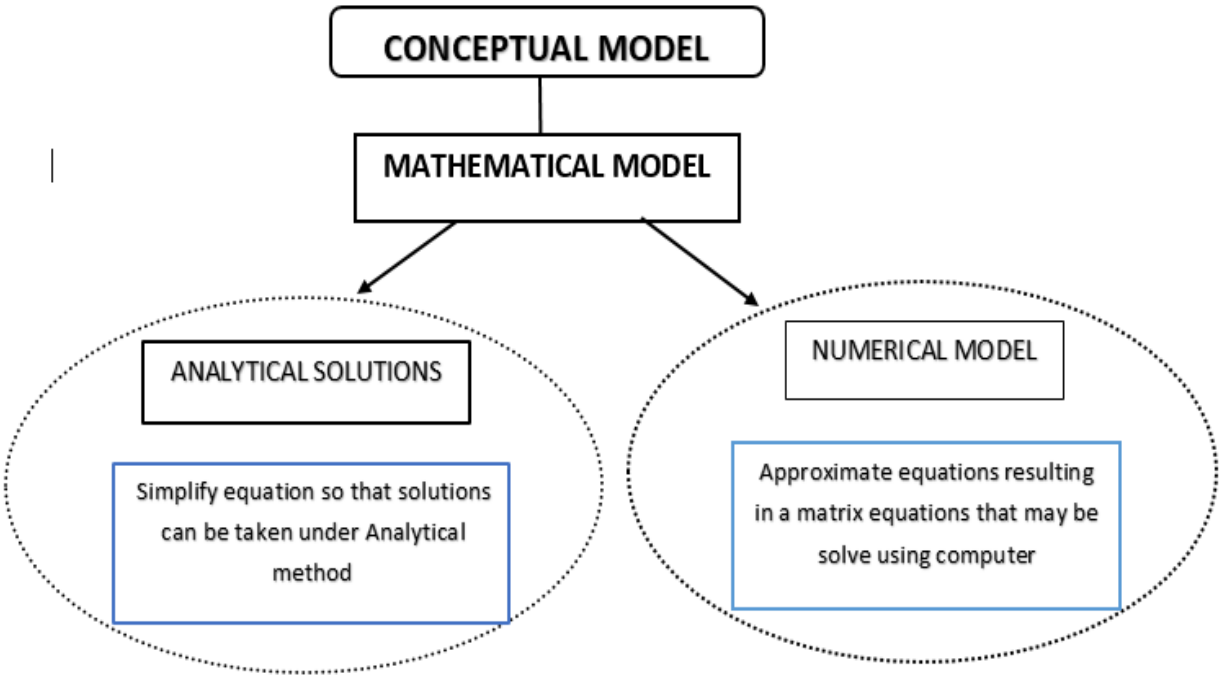

FIGURE 73: FLOW CHART SHOWING THAT MATHEMATICAL MODELS ARE BASED ON THE CONCEPTUAL UNDERSTANDING OF THE AQUIFER SYSTEM AS EXPRESSED BY MATHEMATICAL EQUATIONS (MODIFIED FROM MERCER AND FAUST, 1981)

7.1.2 Results

This section presents the results obtained from the simulation of the model in the steady-state condition. The model gives out the calibration results showing the difference between the observed and calculated hydraulic head, recharge distribution, and the water budget of the study area.

7.1.2.1 Calibration Results

Throughout the model calibration, the hydraulic conductivities of the modeled aquifer and recharge were adjusted. The hydraulic conductivity values were changed to match the field condition at acceptable values. The results of the calibration process yielded hydraulic conductivity values that vary between 8.10^{-4} /day for coarse sand to 1.10^{-6} /day which is for sandy clay (Figure 67A). High hydraulic conductivity values are noticed to be found in the central part (mound) of the study area. Similarly, the recharge calibration under steady-state conditions yielded results as shown in Figure 67B. The result shows that recharge is expected

to occur around the central and northern part (mound) of the study area where the hydraulic conductivity is high and hence the soil in this area of the model domain has high permeability. Sparse recharge exists around the river and its tributaries. The hydraulic conductivity is low due to the clayed nature of the soil found in these areas.

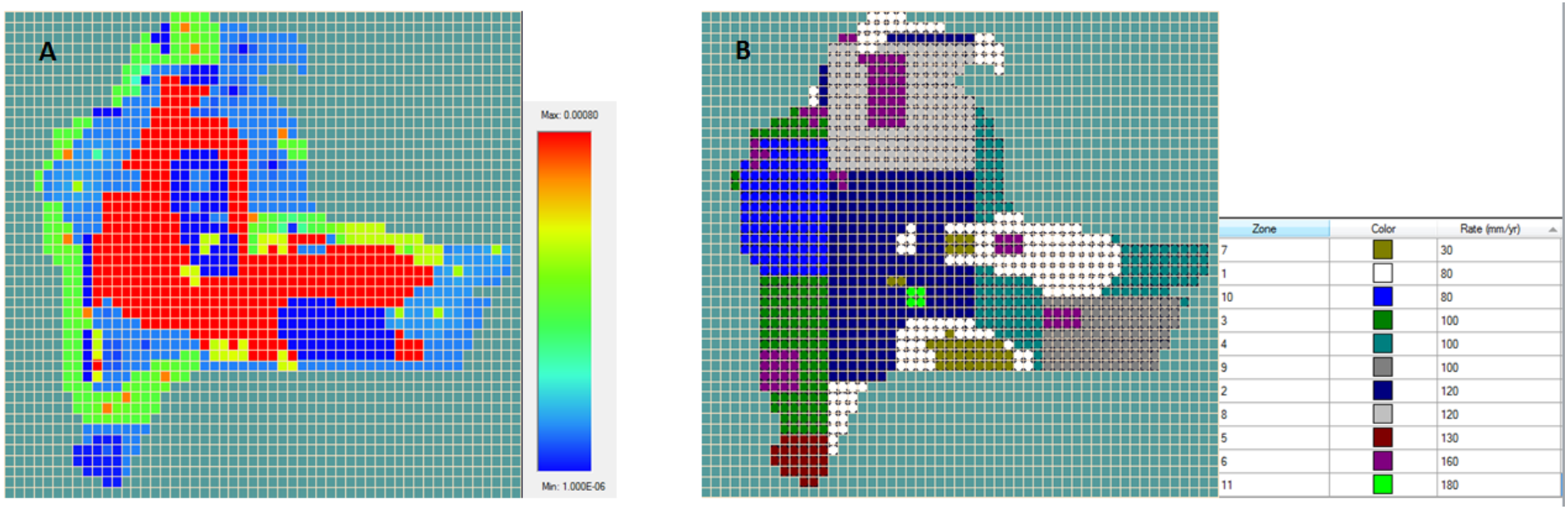

FIGURE 74: MODEL CALIBRATION IN STEADY-STATE FLOW (A) HYDRAULIC CONDUCTIVITY DISTRIBUTION; (B) RECHARGE ESTIMATION

The scatter plot of the observed head versus simulated head for selected observation boreholes and dug wells were shown in Figure 68. The Calibrated results showed a good agreement between observed and the simulated groundwater levels in almost all of the boreholes/wells giving the correlation coefficient of 0.99 (R^2 = 0.99) (Table 24). The standard error of the simulated heads is 0.14m. The Root Mean Square (RMS) error was used to measure the accuracy of the model calibration. The RMS error of the final model is 1.24 m.

TABLE 24: SUMMARY OF STEADY-STATE CALIBRATION STATISTICS

SI. No	Parameter	Values
1	Number of Observation wells/boreholes	54
2	Maximum residual at the observation well no DW13	-2.8 (m)
3	The standard error of the estimate	0.19 (m)
4	Minimum residual at observation well no.DW39	0.0048
5	Root Mean Square	0.91 (m)
6	Residual Mean	-0.19 (m)
7	Normalized RMS	3.29 (%)
8	Absolute Residual Mean	0.71 (m)
9	Correlation coefficient	0.99

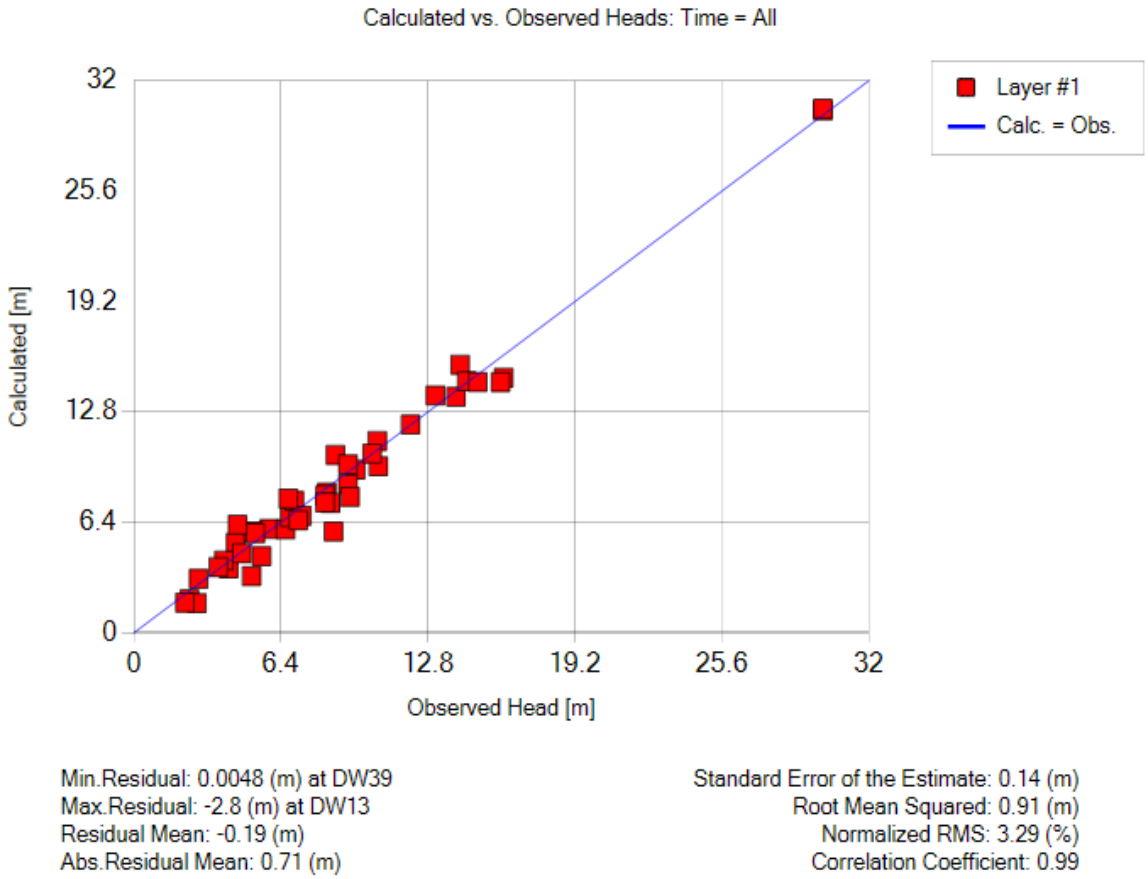

FIGURE 75: COMPARISON BETWEEN OBSERVED AND MODEL SIMULATED HYDRAULIC HEADS (MBSL) IN THE STEADY-STATE CONDITION IN THE GBA BASIN

7.1.2.2 Calibrated Hydraulic Head

` The map presented in Figure 69 shows the distributions of hydraulic heads (potentiometric map). The hydraulic head values obtained after the calibration under steady-state varies between 0 and 32 meters. Hydraulic head values are noticed to be higher in the central part and Eastern part of the study area where the mound is found. The mound is an area of high recharge zones where the hydraulic conductivity is high and hence the soil in this area of the model domain has high permeability.

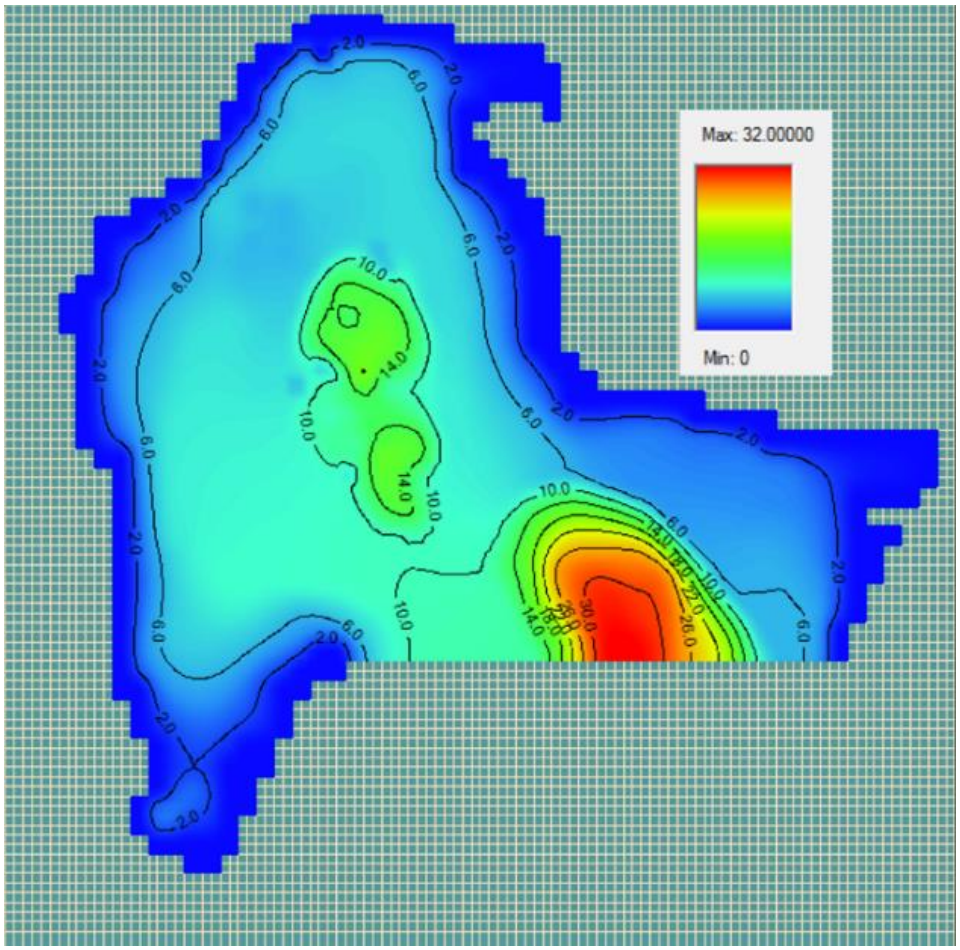

FIGURE 76: HYDRAULIC HEAD DISTRIBUTION UNDER STEADY-STATE SIMULATION

7.1.2.3 Water Budget

A water budget is a quantitative measurement of the balance between water inflow and outflow of a watershed during a specific period. One of the best ways to assess model simulation quality is by analyzing the water budget (Toure et al., 2016a). The calibrated groundwater model produced an estimated mean annual water budget for the model domain summarized in Table 18. The difference between the total inflow (source) and total outflow (discharge) should equal zero (i.e. change in storage should be zero) for steady-state simulation. Since the model boundary condition is a no-flow boundary, the only source of water entering the aquifer is recharge due to infiltration of rainfall into the modeled area. The areal recharge accounts for 100% of the water entering the aquifer while inflow through constant head boundaries is zero. On the other hand, discharge from the GBA aquifer is leakage through constant head boundaries to the River Gambia and the Atlantic Ocean

accounting for about 73% (calculated from Table 25). The other discharge from the aquifer system is withdrawal by wells which accounts for about 23%.

TABLE 25: MEAN ANNUAL WATER BUDGET FOR GROUNDWATER IN GBA BASIN

Flow	Inflow (m3/day)	Outflow (m3/day)
Storage	0	0
Constant Head	0.0	213127.0
Pumping	0.0	79965.4
Recharge	293090.0	0.0
Total	293090.0	293092.3

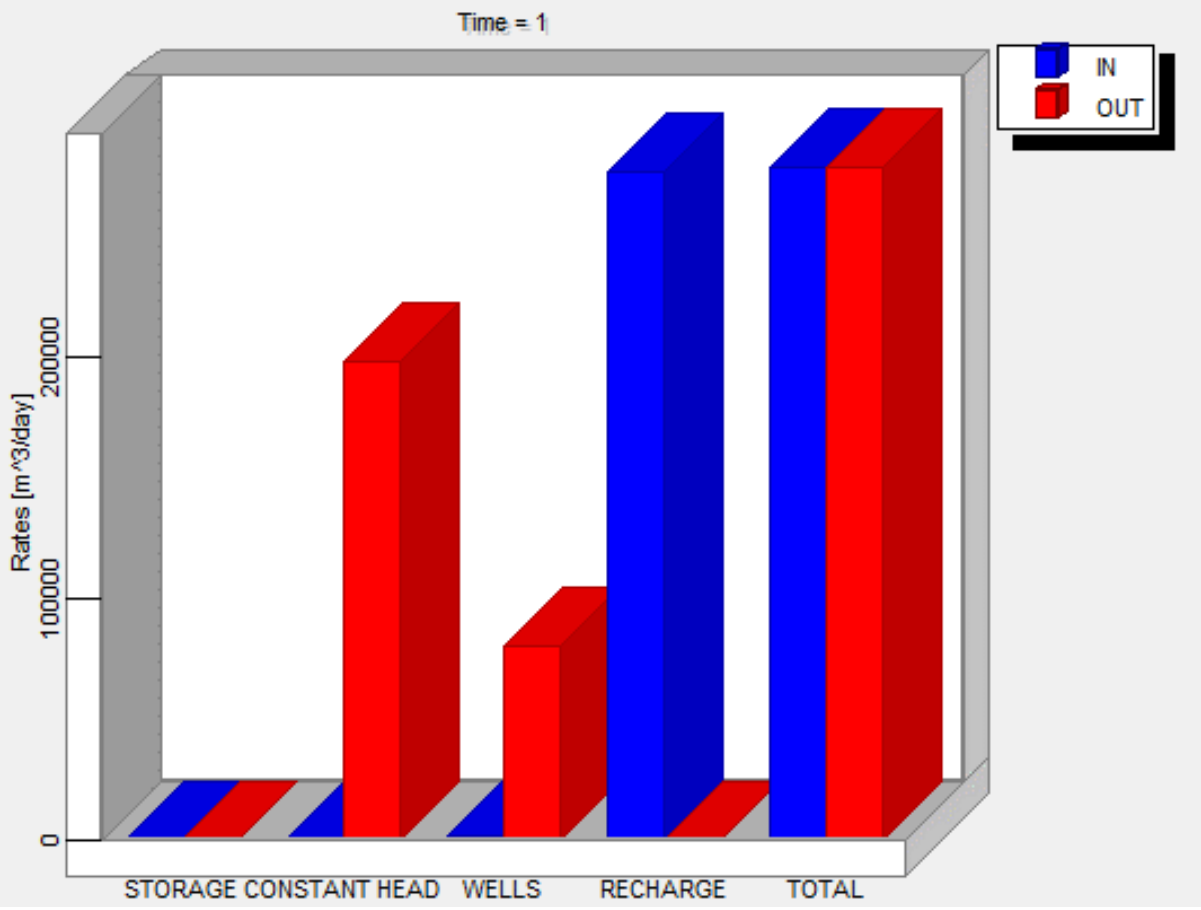

FIGURE 77: MASS BALANCE DURING STEADY-STATE CALIBRATION

The single representation of the continental shallow aquifer receives recharge directly from precipitation. The only discharge from the groundwater flow system is the withdrawal of water by production boreholes/wells (Figure 70). The regional flow pattern that exists within

the groundwater flow system under natural conditions is predominantly horizontal, from the points of recharge in the center towards the River Gambia and the Atlantic Ocean.

7.1.3 Conclusion

The water balance of the GBA was simulated with MODFLOW. Results revealed that the hydraulic conductivity values generated during the calibration process vary between 8.10^{-4} /day for coarse sand to 1.10^{-6} /day for sandy clay. The central and eastern parts of the study area have high hydraulic conductivity values and hence recharge is expected to occur in these areas. On the other hand, low hydraulic conductivity and sparse recharge are found in areas around the river and its tributaries. Similarly, the hydraulic head values obtained vary between 0 and 32 meters. Hydraulic head values are also noticed to be higher in the central part and eastern part of the study area where the mounds of the basin are found. The mound is an area of high recharge zones where the hydraulic conductivity and hydraulic heads are high and the soil in these areas has high permeability.

Furthermore, the simulated water budget suggested that all the recharge into the basin is due to infiltration of rainwater. Discharge is mainly due to linkage of water through the constant head boundaries to the Atlantic Ocean, river, and its tributaries, and also by abstraction from dug wells and boreholes. In conclusion, the simulated groundwater heads match the measured historical groundwater heads. Thus the model can be used to predict the future evolution of groundwater flow, recharge, and water balance of the study area in the face of climate change impacts.

7.2 Climate Change Impacts On Groundwater Resources Of The GBA

7.2.1 Introduction

The Gambia is among the least developing countries that are most vulnerable to climate change and variability. Being a low-lying country, climate change poses major development challenges on productive sectors such as agriculture, forestry, wildlife, and tourism would be adversely affected by rises in sea level (Camara, 2013). Groundwater is an essential water resource in the Gambia, particularly in the Greater Banjul Area (GBA), where groundwater is the only source of water for domestic, agricultural, and industrial purposes.

The study area is located downstream of the River Gambia where the river and its tributaries are constantly saline because of the permanent tidal influence of seawater. Hence using surface water for domestic, agricultural irrigation and industrial purposes in the GBA is almost impossible unless a desalinization technology is applied to the water. The economic growth of the GBA depends among other things on the availability, quality, and accessibility of freshwater.

The quality of groundwater in coastal aquifers is deteriorating due to marine water intrusion caused by sea level rise and in other parts of GBA due to pollution from infiltration of agricultural chemicals. Recharge in the shallow aquifer of the study area is mainly from infiltration of rainwater through the unsaturated zone. Climate change and variability will likely have variable long-term effects on groundwater recharge rates and mechanisms through reduced rainfall. However, the effects of climate change on recharge may not necessarily be negative in all aquifers during all periods (Jakeman et al., 2016). In the face of climate change and other factors affecting the quantity and quality of groundwater, urgent actions need to be taken to assess its availability and quality to make sustainable management and planning of the resources.

Climate change impacts have been felt in the Gambia in the mid-20th century. Long-term rainfall recorded from Banjul station for the last half of the 20th century (i.e. 1950 to 2000) indicates a decrease in annual rainfall amounts of about 30%. This has been evident in the reduction in rainfall amounts recorded in the month of August and also the length of the rainy season, particularly during the period 1968 to 1985, and in 2002 (P. A. O. Jarju, 2009). This erratic rainfall pattern has led to lowering of groundwater level due to less amount of infiltrated rainwater to the water table and also marine water intrusion into coastal aquifers.

7.2.2 Groundwater Recharge Estimation with Thornthwaite Model

The Thornthwaite monthly time-step water balance model was used to simulate the temporal variation of Groundwater Recharge (GWR) during the last three decades (1984-2016) are inferred through the stations of Banjul and Yundum, located respectively in the northern and central part of the GBA. The results (Figure 71) show the temporal variation of precipitation, groundwater recharge, and actual evaporation from Banjul and Yundum stations generated by the Thornthwaite mass balance model. It can be observed that GWR depends mostly on precipitation since actual evapotranspiration values are more or less the same in

both stations. It occurs mostly during the peak of the rainy season (August) where precipitation exceeds the actual evapotranspiration and the moisture storage.

Although, regional variation of GWR occurs in which the highest recharge value is observed in Yundum, the central part of the GBA, and the lowest value is observed in Banjul, the northern part of the study area. Thus, recharge values increase from the North to the South as a precipitation pattern. The mean annual value of the recharge is estimated at 172 mm in Yundum and 97 mm in Banjul during the period 1984-2016 (Table 26).

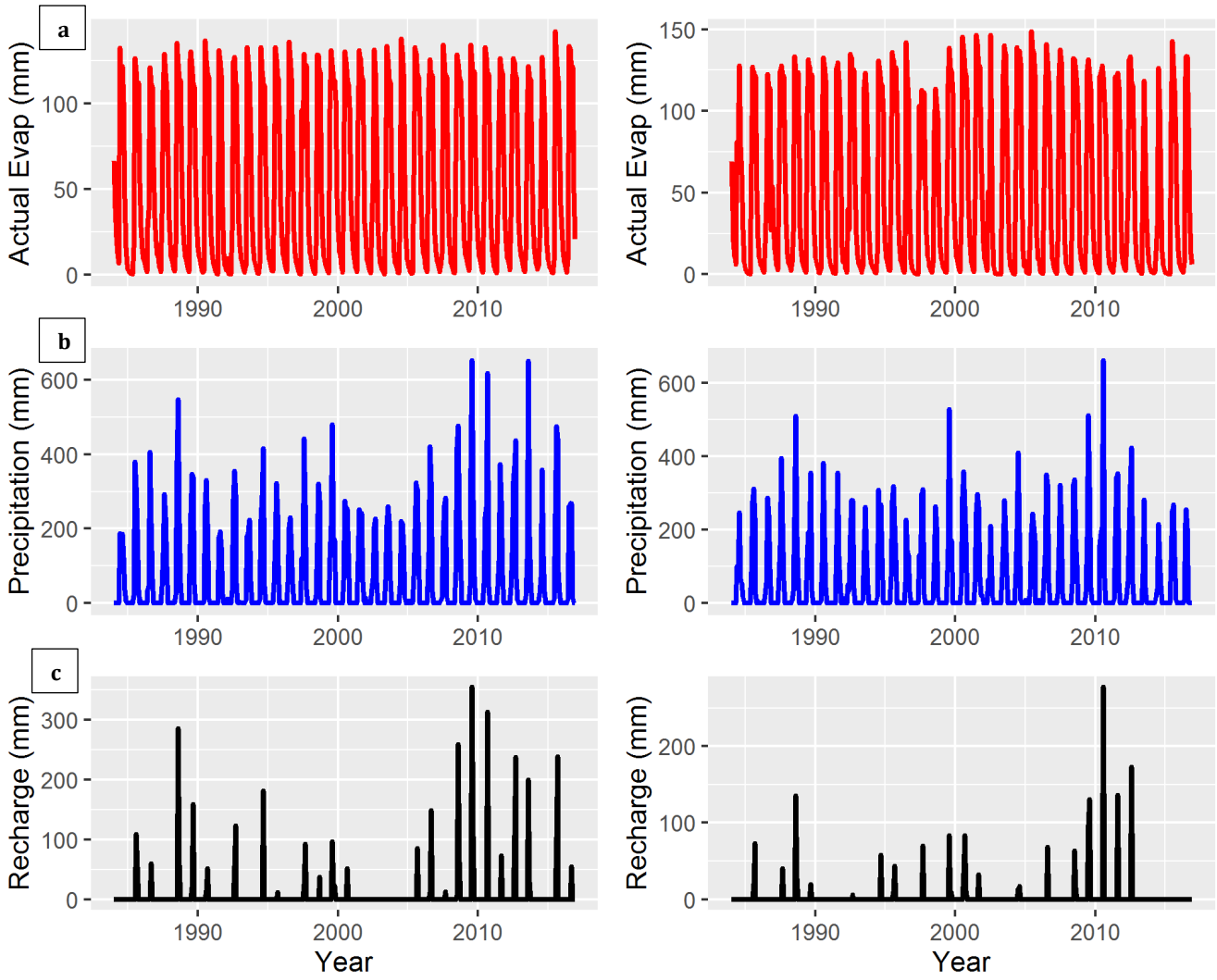

FIGURE 78 : (A) TEMPORAL VARIATION OF ACTUAL EVAPORATION; (B) PRECIPITATION; AND (C) GROUNDWATER RECHARGE, FROM BANJUL AND YUNDUM STATION GENERATED BY THE THORNTHWAITE MODEL FROM 1984-2016

TABLE 26: MEAN ANNUAL VALUE (MM) OF OUTPUT PARAMETERS FROM THORNTHWAITE MODEL, PET: POTENTIAL EVAPOTRANSPIRATION (MM); P: PRECIPITATION; AET: ACTUAL EVAPOTRANSPIRATION (MM); RO: RUNOFF; R: RECHARGE FROM 1984-2016

Stations	PET	P	AET	RO	R
Yundum	1343	930	628	186	172
Banjul	1356	830	616	166	97

7.2.3 Projected Groundwater Recharge

The Thornthwaite monthly time-step water balance model was used to simulate the future groundwater recharge trend of the GBA. The time series raw climate data from the online CLIMAP portal of the ANACIM-IRD project. A bias correction time series raw climate data from the online CLIMAP portal of the ANACIM-IRD project was used in this study to the simulated climate data to correct the climate input data provided by General Circulation Model (AOGCMs) or Regional Climate Models (RCMs) of CORDEX. To estimate the recharge trend over the 2006-2020 horizon, projected precipitation and temperature data of RCP4.5 and RCP8.5 scenarios were used as inputs into the model.

The results of Figure 72 show recharge forecasting of RCP4.5 and RCP8.5 scenarios from the Thornthwaite model. In RCP4.5, the annual recharge trend decreases by 5% (-5%) during the period 2006-2020 and by 8% (-8%) during the period 2030-2060 while it increases between these two periods (2006-2020 and 2030-2060) by 5.5% (+5.5%).

Generally, groundwater recharge for the two scenarios is decreasing and this is more significant in RCP8.5 than in RCP4.5. The decreasing trend over time with RCP8.5 has a growth rate estimated at -14%. These growth rate values will be implemented on the calibrated model to assess the impact of climate change on groundwater head over the 2050 horizon.

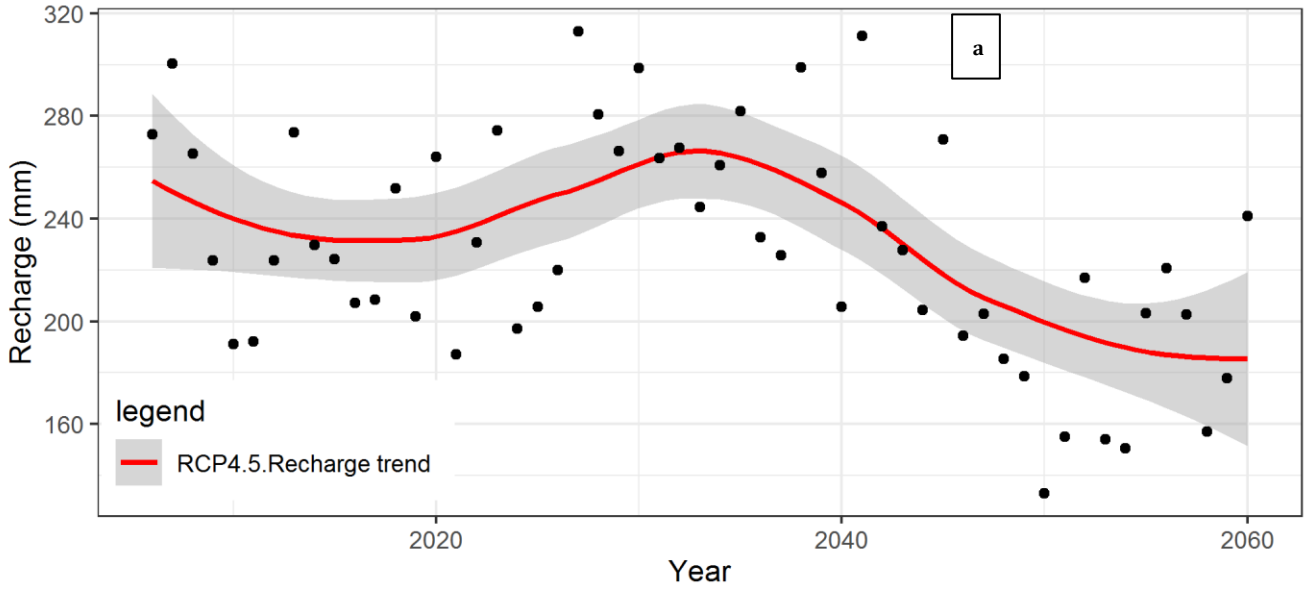

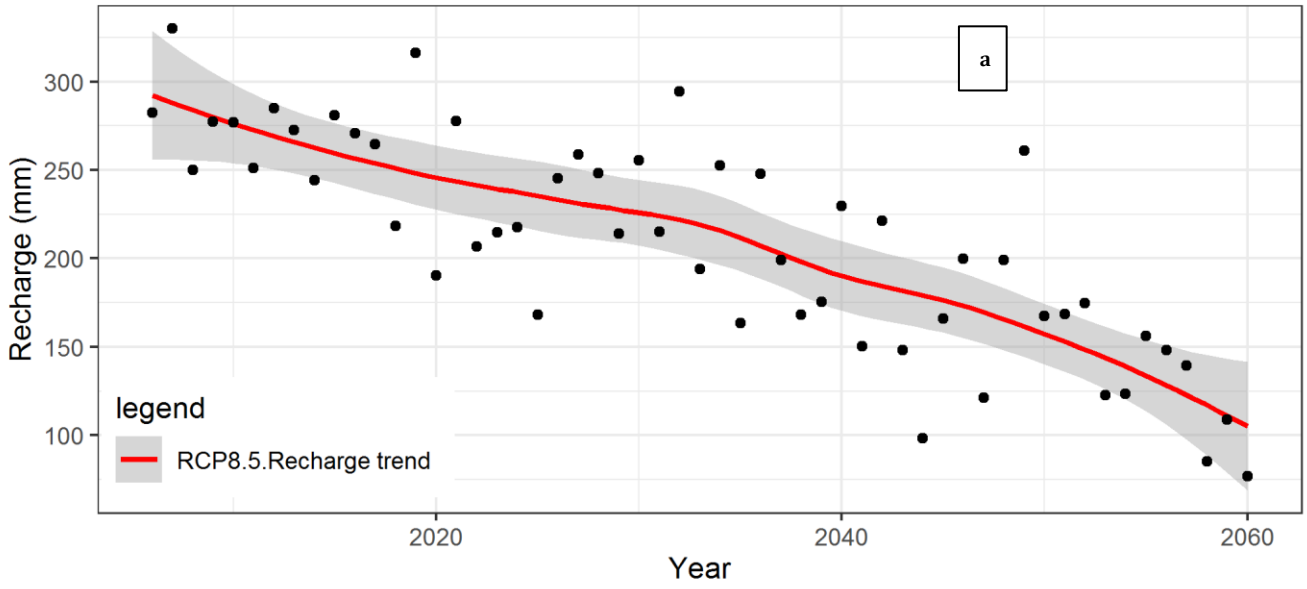

FIGURE 79: MEAN ANNUAL RECHARGE TREND THROUGH RCP4.5 AND RCP8.5 SCENARIOS DURING 2006-2050

TABLE 27: MEAN ANNUAL VALUE (MM) OF OUTPUT PARAMETERS FROM THORNTHWAITE MODEL. PET: POTENTIAL EVAPOTRANSPIRATION (MM); P: PRECIPITATION; AET: ACTUAL EVAPOTRANSPIRATION (MM); RO: RUNOFF; R: RECHARGE FROM

Scenarios	PET	P	Moisture	AET	Surplus (Recharge)	Run Off total
Rcp4.5	1381	1218	1198	818	341	402
Rcp8.5	1399	1194	1187	822	314	374

Thus this can be explained by the fact that the mean annual precipitation for RCP8.5 (Figure 73b, Table 27) is lower than that of RCP4.5 (Figure 73a, Table 27). Likewise, recharge decreases in both scenarios but in RCP4.5, it stabilizes during the mid-century because of the mitigation measure put in place to reduce emissions. Unlike RCP8.5, a long-

term emissions scenario of GHGs (that is business as usual scenario), without any mitigation measures, the trend for recharge continues to decline to the end of the 21st century. It could be therefore concluded that there is a good correlation between recharge and precipitation (Figure 73).

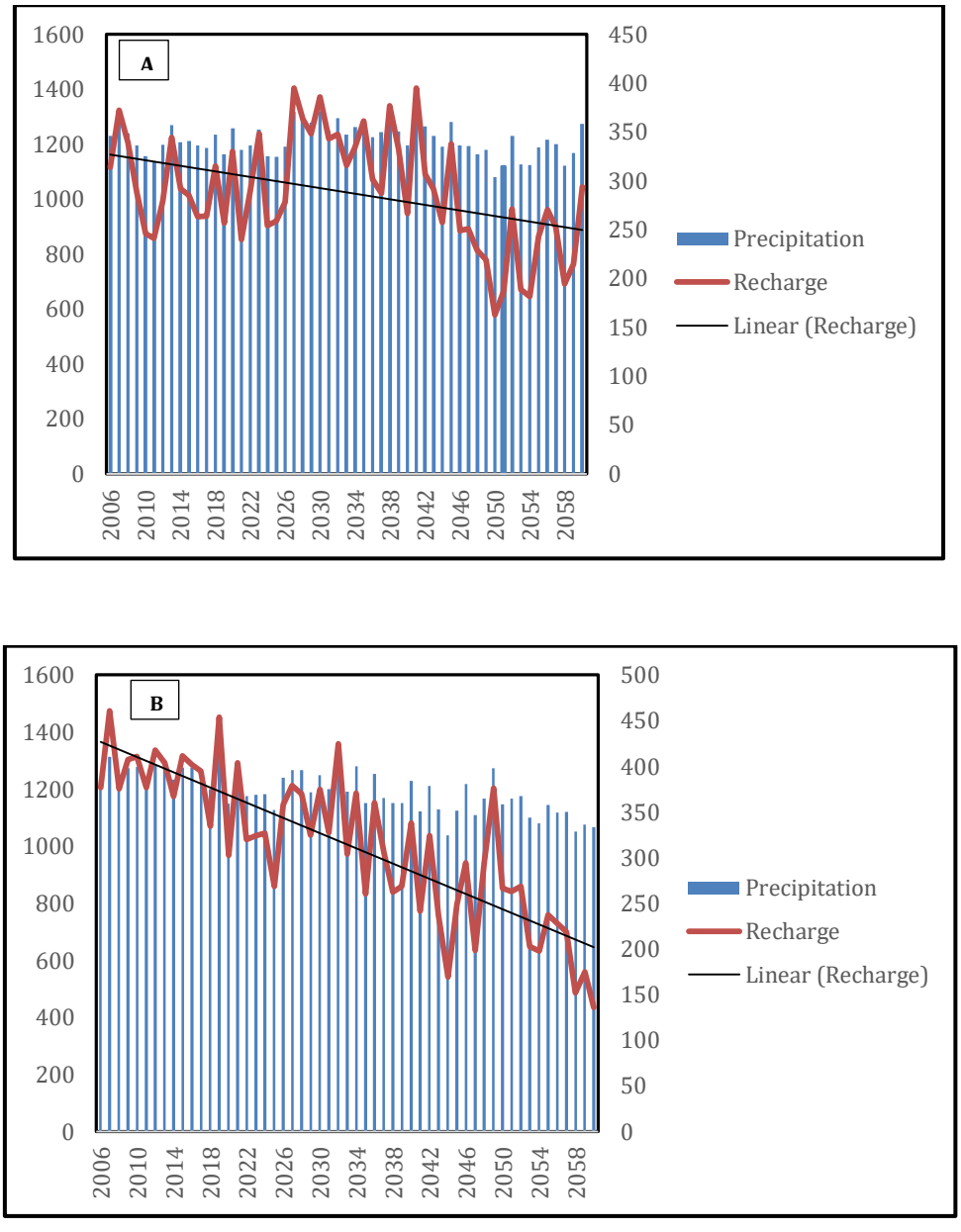

FIGURE 80 : RELATIONSHIP BETWEEN PRECIPITATION AND RECHARGE: (A) RCP4.5; (B) RCP8.5

7.2.4 Groundwater Dynamics under High Abstraction and Climate Change

The most important objective of this modeling study is to simulate the groundwater dynamics of the GBA for present and future under different stress. Thus, recharge values for both RCP4.5 and RCP8.5 scenarios estimation with Thornthwaite model were used as input

data into the MODFLOW to simulate the groundwater dynamics of the GBA under high abstraction and climate change. The evolution of groundwater heads for the future was predicted under different stresses such as climate change and pumping conditions for four observation wells (Obs.1-4). Four scenarios were developed for this purpose as stated in chapter 3.

7.2.5 Results and Interpretations

7.2.5.1 Abstraction Scenario

Under this scenario, two different situations of pumping rates (A1 and A2) have been modeled compared to the Reference (the controlled scenario where the boundary conditions do not change over time). For this purpose, 13 new wells were established into the aquifer to meet the population's water demand with a pumping rate of 2500 m^3/day (A1) and 4000 m^3/day (A2). The impact of the pumping rate on hydraulic heads is assessed through 4 head observation wells (Obs 1-4) located in the vicinity of the pumping catchment.

The results of simulation over the 2050 horizon show a decrease of hydraulic heads in the piezometric mounds concerning the increased pumping rate. This decrease is more noticeable in A2 than A1 in all the 4 head observation wells (Figure 74). At Obs1, Obs2 and Obs3, the recession is quite linear for both A1 and A2 scenarios showing that the steady-state regime (drawdown stabilization) is not reached during the entire simulation. At Obs4, the steady-state regime is almost achieved at the end of the simulation (2050 horizon) especially for the A1 scenario (Figure 75d). This period indicates the hydraulic head stabilization which is 7mbsl in Obs4 in case of transient pumping and boundaries condition under the A1 scenario.

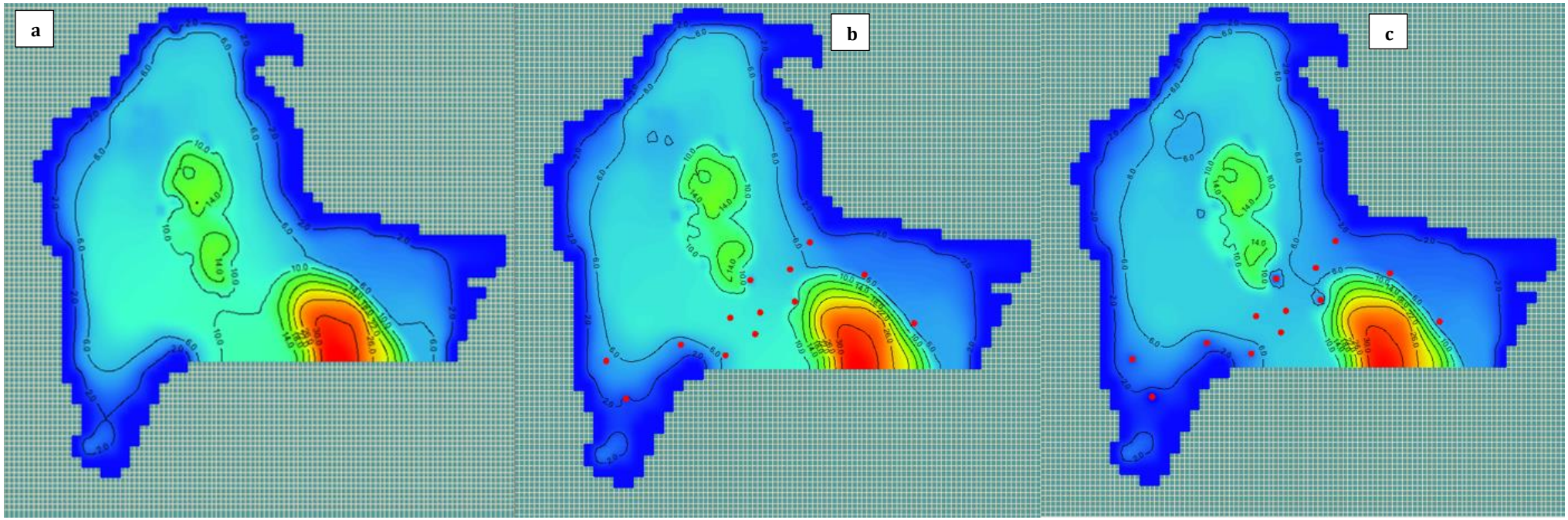

FIGURE 81: SIMULATED HEAD OF 2019-2050 HORIZON BASED ON (A) REFERENCE; (B) AL; AND (C) A2 SCENARIOS

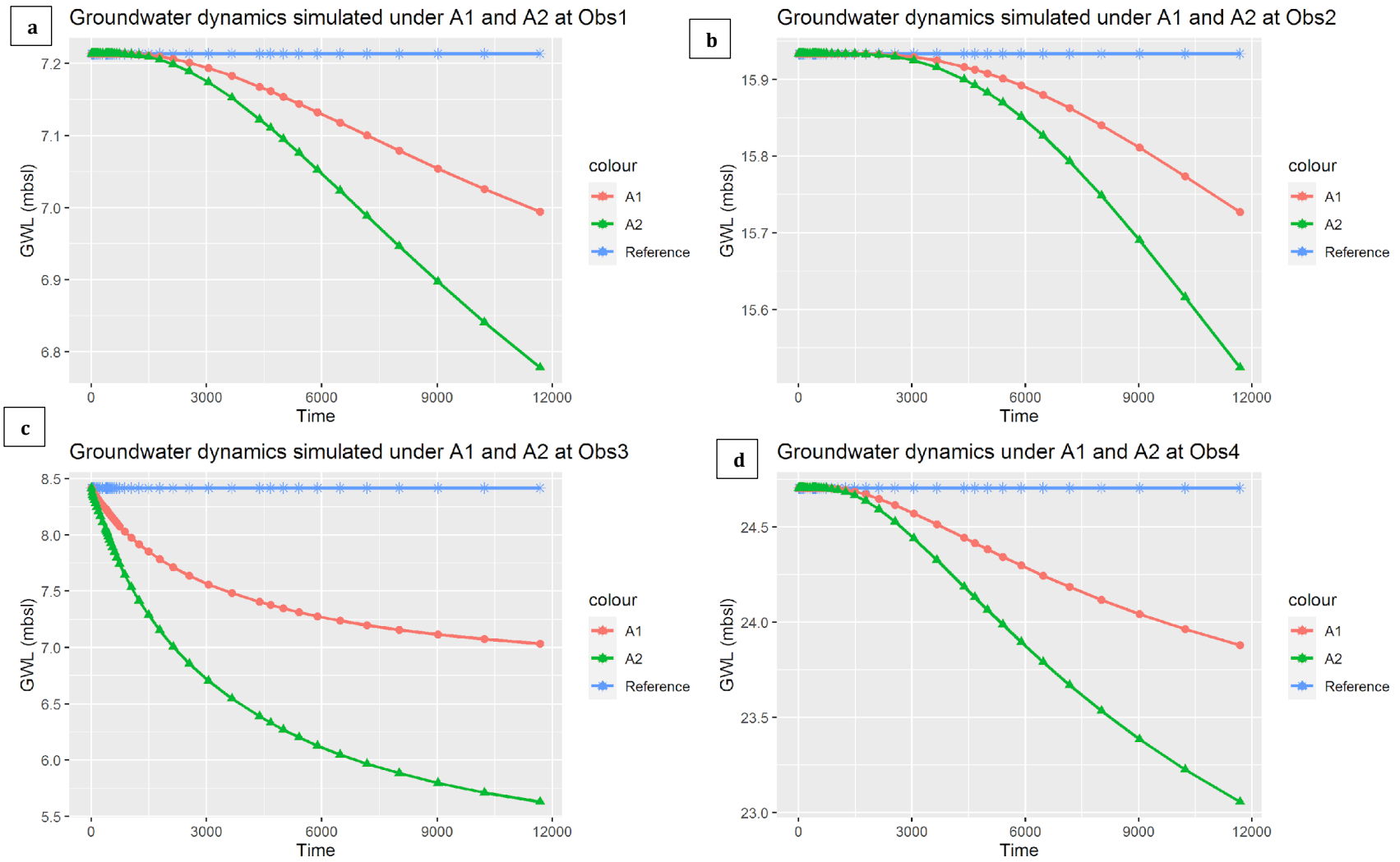

FIGURE 82: HEAD TIME SERIES BASED ON REFERENCE, A1, AND A2 SCENARIOS DURING 2019-2050

7.2.5.2 Climate Change Scenario

Under this scenario, two RCPs (RCP4.5 and RCP8.5) were used to simulate the impact of climate change on groundwater resources of the GBA. The recharge calculated with the Thornthwaite model for RCP4.5 and RCP8.5 scenarios were used as input into MODFLOW to simulate the groundwater dynamics under climate change impacts. In each simulation, only one RCP is used as input and the other parameters (abstraction and boundary conditions) were kept constant as in the case of the reference scenario. The scenario data mentioned above was used in the groundwater modeling to predict the future behavior of groundwater of the GBA aquifer systems. Monthly groundwater recharge of RCP4.5 and RCP8.5 scenarios calculated with the Thornthwaite model was used as input MODFLOW to quantify future groundwater heads/levels in the GBA basin from 2019 to 2050.

The simulation results of the groundwater dynamics of the study area revealed a decrease in groundwater level (GWL) over time (Figure 76). The piezometer drops were approximately 1.75 mbsl at Obs1, obs2 is 2.25 mbsl, obs3 by 1.20 mbsl, and obs4 mbsl by 1.79 mbsl, for the RCP8.5 scenario (Figure 77). Furthermore, it is noticed that there is a continuous decline in groundwater head in the RCP8.5 scenario, and in the case of the RCP4.5 scenario, a rise in the head is realized and then dropped over time. This could be explained by the fact that RCP4.5 is a medium-term scenario in which emission stabilizes in the mid-21st century while RCP8.5 is a long term scenario in which emissions continue until the end of the 21st century. It can also be supported by the fact that recharge into the aquifer system had decreased in the mid-century due to a decrease in rainfall amount in this period. However, there is continuous depletion in groundwater level for both RCPs over the simulation period but this is more significant in the RCP8.5 scenario than in the RCP4.5 scenario for all the piezometers simulated.

Similarly, Figure 77 shows the simulated groundwater head of the GBA over the 2019-2050 time slice for both RCPs against the reference. It could be noticed that there is a decrease in groundwater head which is more critical in RCP8.5.

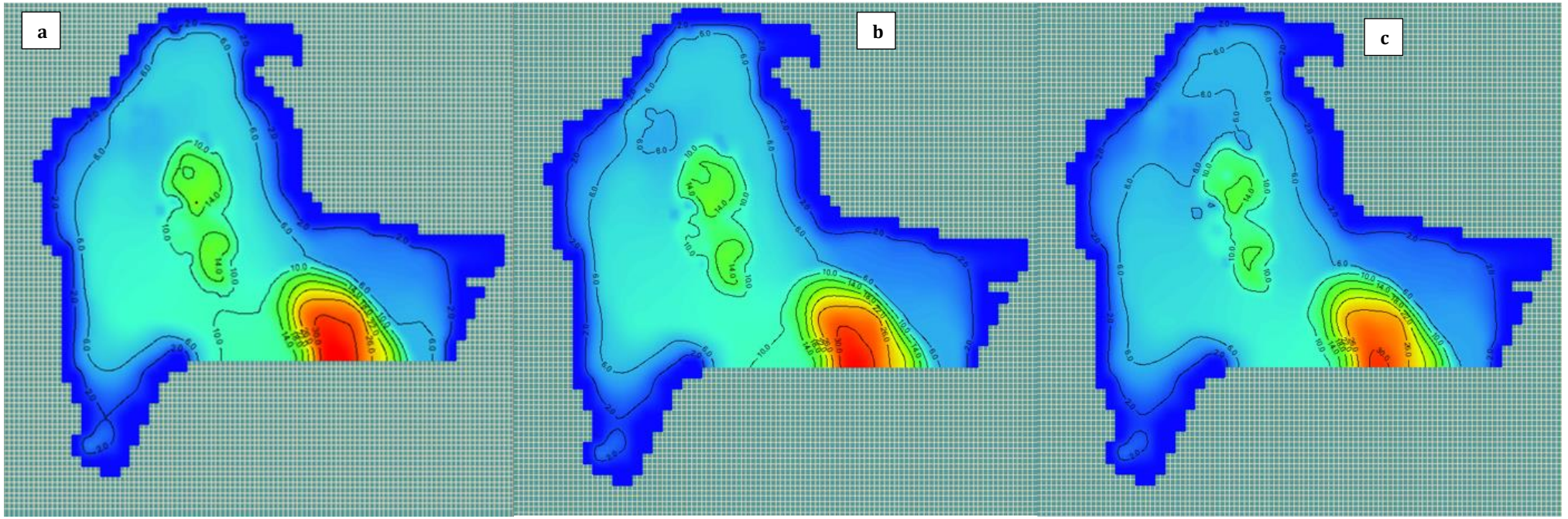

FIGURE 83: SIMULATED HEAD FOR 2050 HORIZON BASED ON: (A) REFERENCE; (B) RCP4.5; AND (C) RCP8.5 SCENARIOS

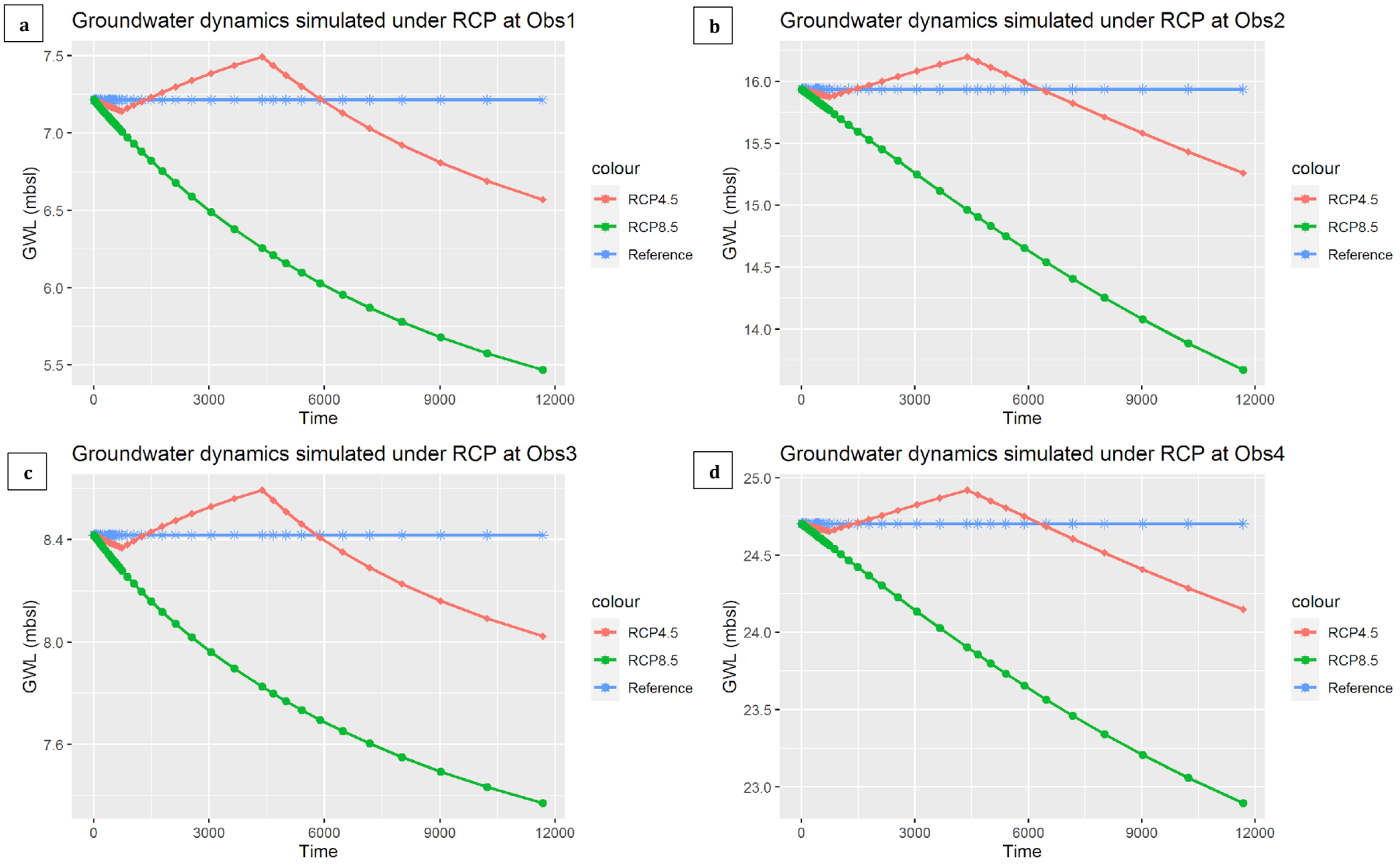

FIGURE 84: TIME SERIES HEAD BASED ON REFERENCE, RCP4.5 AND RCP8.5 SCENARIOS DURING 2019-2050

7.2.5.2 High Abstraction under Climate Change

In this scenario, both climate change (RCP8.5 and RCP4.5) scenarios and high abstractions (A1 and A2) are simulated to see the groundwater dynamics for the future (2019-2050) with respect to the reference period. It has been noticed that groundwater head reductions have intensified due to an increase in water extraction in the GBA basin. The increase in water demand is mainly due to an increase in population in the study area and the demand for domestic and irrigation in coastal areas where the surface water is saline. This situation is exacerbated by climate change through a decline in rainfall and recharge.

In Future 78, GWL has declined in both the A1-RCP8.5 scenario and A1-RCP4.5 scenario compared to the reference period but the decrease is more important in the A1-RCP8.5 scenario.

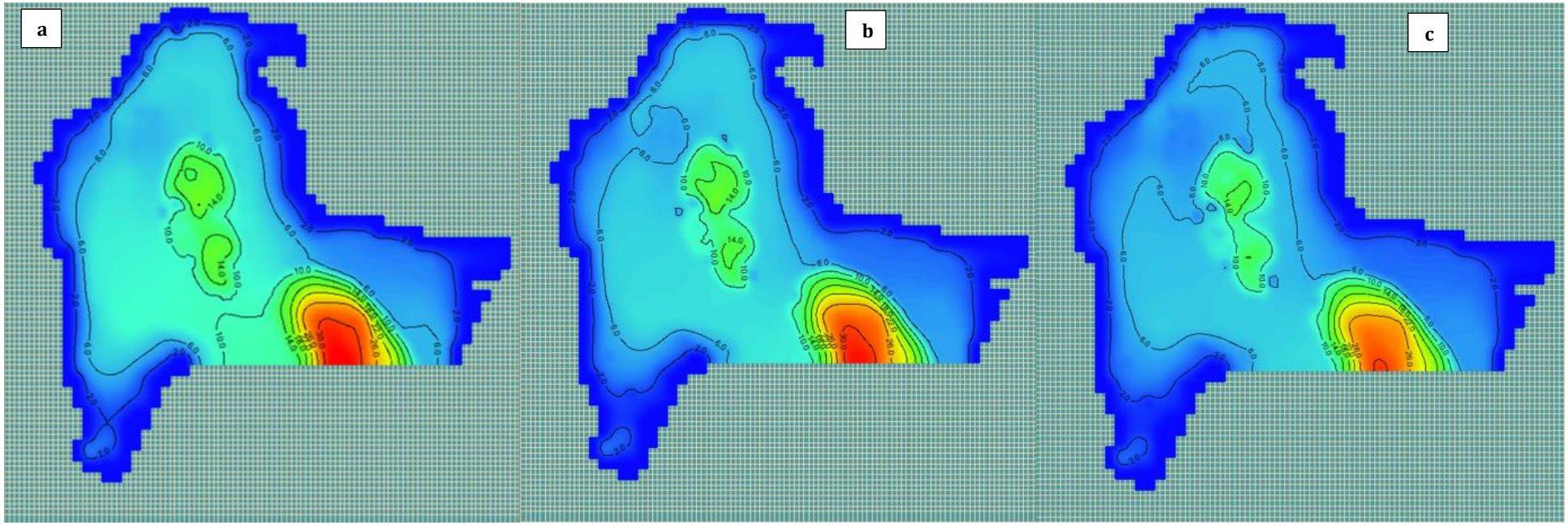

FIGURE 85: SIMULATED HEAD OF 2050 HORIZON BASED ON (A) REFERENCE; (B) A1-RCP4.5; AND (C) A1-RCP8.5 SCENARIOS

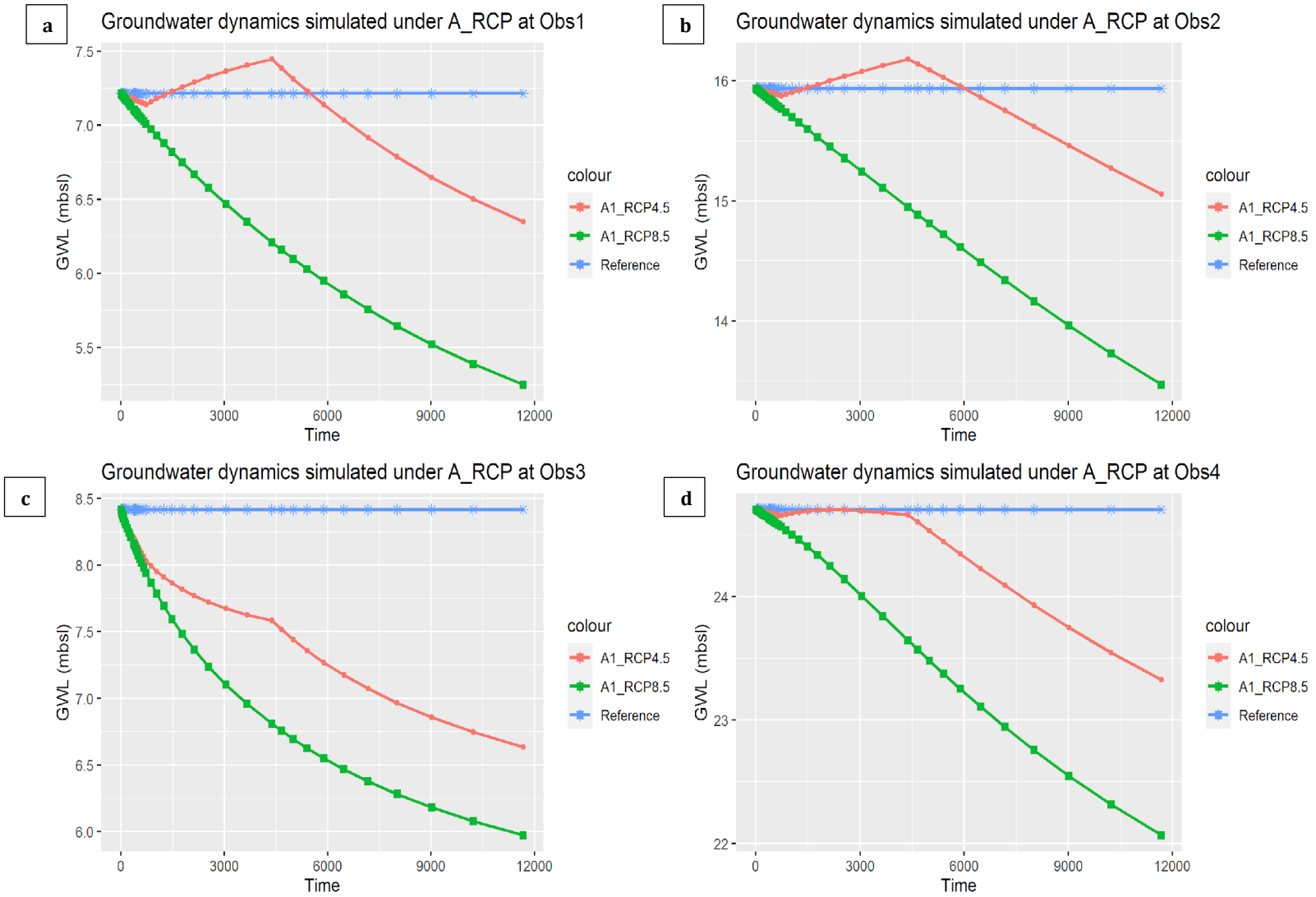

FIGURE 86: TIME SERIES HEAD BASED ON REFERENCE, A1-RCP4.5 AND A1-RCP8.5 SCENARIOS DURING 2019-2050 TIME SLICE

7.2.3.2 Comparison of the Different Scenarios

The assessment impacts Climate Change scenarios generated from 29 Regional Climatic Models (RCMs) under two emission scenarios, RCP4.5, and RCP8.5) in the shallow aquifer system of the GBA affected by intensive groundwater use over the 2019-2050 horizon. The simulation was carried out for a reference scenario which refers to the steady-state baseline where the groundwater levels are calibrated to simulate the pre-monsoon piezometric.

A comparison of the different scenarios under different stress conditions. Four boreholes mentioned above are used to simulate the impacts of high abstraction and climate change on groundwater head. In Figure 80, it can be seen that all the four boreholes reflected a decline in groundwater heads but this decline is more significant in Obs4 and Obs3 for all scenarios. In Figure 80A, the decline in groundwater head is more prominent under high abstraction together with climate change (RCP8.5 a high emission scenario). Under high abstraction (A1), there is a steep decline and RCP 8.5 scenario as well. The high abstraction plus the climate change scenarios (A1+RCP8.5) has a very critical impact on the groundwater head in Obs4. Similarly, Figure 80C reflects the same behavior as that of Figure 80A in which high abstraction under climate change scenarios (RCP8.5) affects the groundwater head (i.e. sharp decline in groundwater head). In Figure 80B, high abstraction (A1) is more prominent that climate change impacts on groundwater heads. Although, high abstraction under climate change will cause a significant decline in groundwater head.

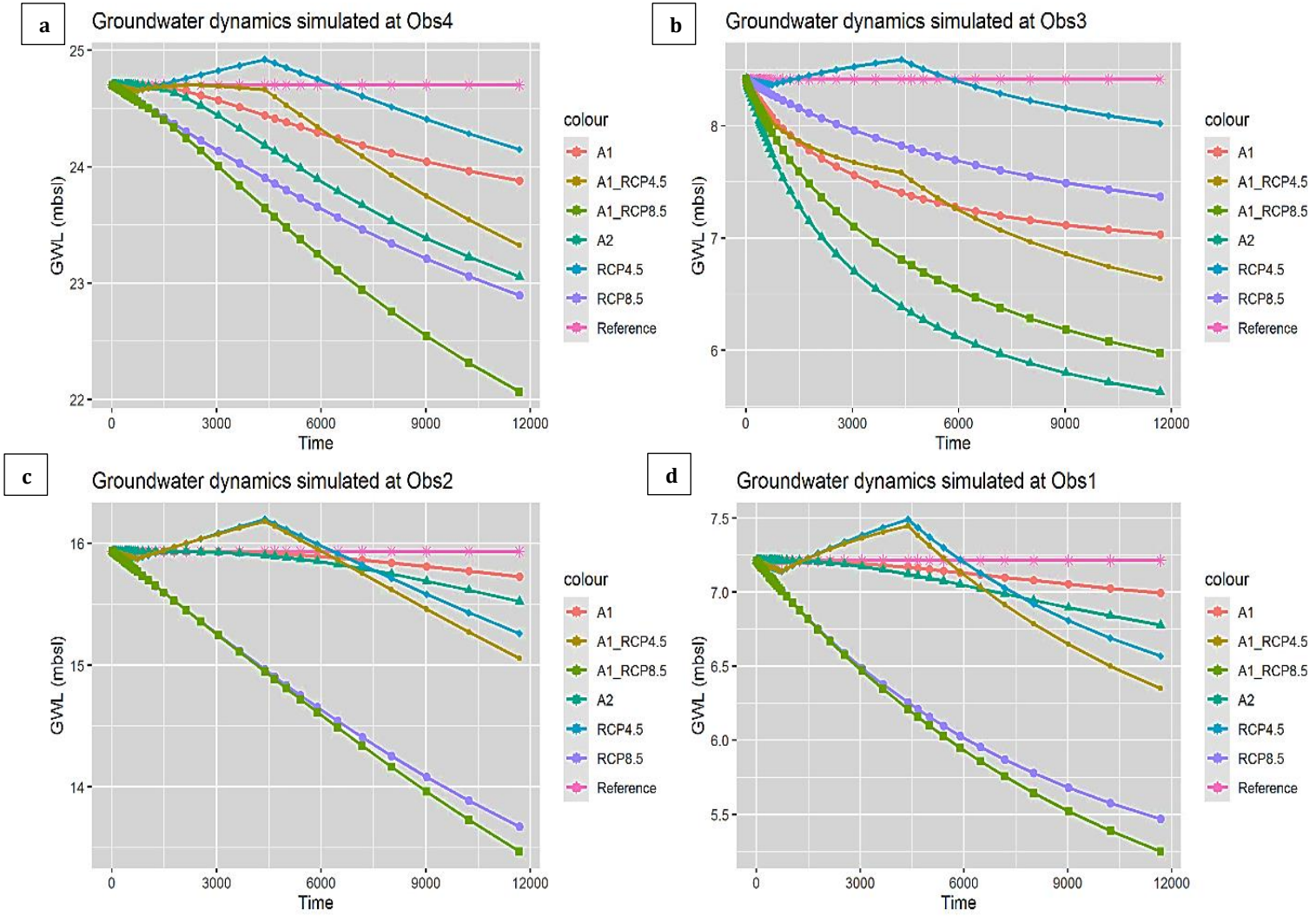

FIGURE 87: COMPARISON OF CLIMATE CHANGE SCENARIOS (RCP4.5 AND RCP8.5) AND HIGH ABSTRACTION (A1=2500 M3/DAY) ON THE GROUNDWATER DYNAMICS OF THE FOUR OBSERVATION BOREHOLES (OBS1-OBS4) IN THE SHALLOW AQUIFER OF THE GBA.

7.2.4 Conclusion

The finite-difference model (MODFLOW) was applied to evaluate the impact of climate change on groundwater resources for the Greater Banjul Areas basin. The overall results show that the groundwater level is decreasing mainly due to high water abstraction and climate change effect. Before simulating the groundwater dynamics of the GBA basin, groundwater recharge was estimated using the Thornthwaite model for two climate change scenarios (RCP 4.5 and RCP8.5). The results revealed that there is a continuous decrease in both RCP4.5 and RCP8.5 scenarios to the end of 2050. This decrease in recharge rate is more prominent in RCP8.5. Similarly, the groundwater dynamics simulation results show a depletion of groundwater levels at the basin in 2050. Because of high extraction caused by increasing water demand for domestic, agricultural, and industrial development, coupled with climate change effects, groundwater level diminishes over time and consequently leading to a decline in groundwater storage.

This study, therefore concludes that groundwater resources are affected by climate change and unsustainable abstraction. Thus, sustainable use and management strategies should be in place for the security and availability of water supply for the future. The decision-makers should be informed of these results, although the study has been performed with some model uncertainties as well as observation data. Overall, the model gave a good simulation of the real climate conditions of the study area.

CHAPTER 8: GENERAL CONCLUSION AND PERSPECTIVES

8.1 Introduction

The GBA continental shallow groundwater is the most important water resource for its socio-economic development (domestic, agriculture, and industrial) as surface water is contaminated by seawater intrusion. The quantity of groundwater resources available currently is sufficient to meet the present demand. However, it is crucial to realize that this quantity and quality of groundwater is deteriorating over time due to over-extraction (rapid population growth), high urbanization rate, contamination from seawater intrusion, climate variability and change, and anthropogenic pollution.

The Intergovernmental Panel on Climate Change (IPCC), 2007 predicted that the future climate is expected to be drier and hence this will affect the recharge rate of some aquifers. In turn, the decrease in recharge rate coupled with high abstraction will lead to the depletion of groundwater resources. In this regard, a sustainable management strategy for groundwater resource use should be in place for the future availability of these resources. For this reason, this study is designed to develop a groundwater model and scenario analyses in the study area to contribute to the sustainable management of groundwater resources of the GBA. Two numerical methods (Penman and Turc) and the Thornthwaite model were used in this study to estimate the groundwater recharge which was used as input in MODFLOW to evaluate the groundwater dynamics of the study area.

8.2 Recharge Estimation

The recharge rate was estimated using three numerical methods:

8.2 .1 Thornthwaite Method

The Thornthwaite's method was used to calculate infiltration which uses climate parameters (mean temperature and rainfall) and also depends on runoff (20% of rainfall) and the maximum value of the soil water capacity (SWC) or water stock. The SWC values used for calculating recharge in the study area were 100, 125, 145, and 178 mm. The period considered for the calculation was 1984 - 2016 for both Banjul and Yundum stations. The result presents the monthly means of effective rain, temperature, ETP, ETR, and infiltration

for the different "water stock" values mentioned above. The annual mean infiltration during the rainy months from July to October ranges between 190 and 215 mm/year for Banjul, and between 215 and 434 mm/year for Yundum with the different water stock values. With a stock of 125, the infiltration values calculated were 191 mm and 265 mm respectively for Banjul and Yundum stations.

8.2 .2 Penman method

Like the Thornthwaite method, the Penman method had the same climatic periods that were considered for the estimation of ETP, ETR, and Infiltration. The monthly mean ETP increased during the pre-monsoon reaching its maximum in March of about 222 mm and 249 mm for Banjul and Yundum respectively. The mean annual infiltration estimated with this method ranges between 80 and 105 mm for Banjul and between 90 and 150 mm for Yundum for the different stock values. The infiltration calculated with this method is 86 mm and 131 mm for Banjul and Yundum respectively for a stock value of 125. This method gives recharge values that are close to reality.

8.2 .3 Turc Method

Similarly, the Turc method was calculated for the same period as the two methods mentioned above to calculate the same parameters. The mean annual infiltration calculated with this method is 265 mm for Banjul station and 344 mm for Yundum station. The Turc gives a better approximation of recharge for the study area than the Penman and the Thornthwaite.

8.2 .4 Groundwater Potential Recharge Zone

The Groundwater Potential Recharge Zone (GWPZ) map of the GBA was delineated using GIS and MCDM techniques. It was found that the combination of the 7 factors is helpful to understand the behavior of groundwater in the study area. The delineated map was classified into four zones, viz., ‘poor’, ‘moderate’, ‘good', ‘very good’. The areas of the estuary in the study area fall under moderate to poor in terms of recharge potential which is as a result of geological formation and soil texture composition, composed of more clayey facies and high drainage density.

40% of the total area falls under the ‘very good’ zone which is a good indication for future artificial recharge planning and potential drilling of boreholes. This method can be widely applied as a valuable tool for solving groundwater problems of semi-arid areas with inherent limitations of data scarcity and multi-criteria evaluations.

8.3 Geochemistry

In this study, physicochemical parameters (water depth, pH, T°C, EC) were measured from 58 sampling points of the shallow aquifer (borehole and wells) and 6 surface water during 2018 pre-monsoon (May) and post-monsoon (November). In addition, water samples were collected in November to analyze major ions and minor elements such as Br. The specific objectives are to evaluate: (1) the groundwater quality based on different indices for drinking and irrigation uses, and (2) hydro-geochemical facies and processes driving groundwater mineralization.

The hydrochemistry characterization of major ions in groundwater of the study area has been done with the help of the Piper diagram, bivariate diagrams, saturation indices, and statistical analysis together with the physicochemical parameters reveals the different water types and origin of mineralization of groundwater. The analysis of the Piper diagram identified eight major water-types based on the major ion chemistry of groundwater: i) bicarbonate (m-HCO_3, Ca-HCO_3, and Na-HCO_3) facies, ii) chloride (Na-Cl and m-Cl) facies, iii) and iv) mixed (m-m and Na-m) facies. The order of dominance of the anions in groundwater samples is HOC3- > NO3 > Cl-> SO4 ->Br, and the cations >Na+> Ca2+ >Mg2+ >K+. Mean and median values show that most groundwater samples do not exceed the WHO standard.

8.4 Recharge Projection with Thornthwaite Model

To simulate long term groundwater recharge under the future climate, the Thornthwaite model was used. The GCM climate data of RCP4.5 and RCP8.5 for precipitation and temperature of CORDEX was used in the model to estimate the long-term recharge rate for the GBA aquifer system. The results show a decreasing trend in recharge for both RCPs but this is more prominent in RCP8.5. Regardless of the uncertainty of the model due to the hydrogeological data package into the model, the results produced are realistic.

8.5 Climate Change Impact on Groundwater

In this study, the impacts of climate change on groundwater resources have been evaluated using RCP4.5 and RCP8.5 scenarios of CORDEX data from the GCM downscaled at 0.50° resolution. The time-series climate data (precipitation and temperature) were deemed to be appropriate for direct use because they were already bias corrected. The data was used to estimate recharge with the Thornthwaite model as mentioned above which was then used as input in the MODFLOW model to evaluate the impact of climate change on groundwater dynamics of the GBA basin under current and future climate. The results indicate that groundwater head is decreasing over time for both scenarios considered in this study, especially in the RCP8.5, where the decline is expected to continue to the end of the 21st century as compared to the medium-term scenarios RCP4.5 which will rise again in the mid-century due to mitigations measures considered to reduce emissions. The decline in the water head can be highlighted with evidence that increased abstraction due to population growth and socio-economic development together with climate change are determining factors. Consequently, the decrease in recharge rate leads to depletion of groundwater storage.

Some uncertainties exist in the modeling such as a computational error in the model, input data (historical climate data, future climate projections), and boundary. Nevertheless, the results produced by the model are authentic and hence the model can be applied in water management programs in the study area.

8.6 General Conclusion

Based on the results obtained in this study, a general conclusion is drawn to infer that the quality and quantity of groundwater resources are negatively affected mainly by anthropogenic pollution, sea water intrusion, climate change and high abstraction due to increasing population growth and socio-economic development. Presently, the groundwater resources of the GBA cover the water demand but to satisfy the future demand for freshwater is at threat considering the projected decline in recharge rates and groundwater head. The quality of groundwater is expected to deteriorate due to pollution of the resources from infiltration of agricultural chemicals, indiscriminate dumping of household and municipal waste, septic tanks and intrusion of saline water due to high abstraction and sea level rise. Therefore, it is of utmost urgency to adapt an integrated groundwater resource management

and groundwater regulation framework and have a regulation/law inorder to prevent the quality deteoration and rapid depletion of this vital resource.

8.7 Perspectives

Groundwater is the only source of fresh water in the GBA. Surface water is saline and not fit for domestic, agricultural, and industrial uses. Therefore, the sustainable use and management of the resources for the future should be the main focus of the Government and the population in general. The results of this study contribute to groundwater management of the study area and can be replicated in other regions of the country. However, they should be considered with some discretion as the quality and quantity of primary and secondary data used were limited as well as the spatial and temporal hydrological and hydrogeological data. Therefore, the authorities responsible for the management and protection of the basin should improve on their data collection methods and tools and have a strong database that has to be regularly updated to facilitate future studies and research in the region.

During the field campaign, some of the piezometers were not functioning correctly and the reading they gave was constant for several consecutive months which gives a constant water level and a big jump between months. These piezometers should be repaired to facilitate accurate data readings. Also the number of Piezometers are limited and spatially distributed in the study area. Some of the NAWEC production boreholes that have been closed due to quality issues can be fit out and used as piezometers for monitoring groundwater levels. This will be far less costly than installing new piezometers. There are a lot of discrepancies and gaps in the available hydrogeological data, especially groundwater level data. Thus regular data collection should be done, treated, and stored appropriately. Long-term pumping test data is not available for estimation of specific yield which is very important in groundwater modeling. The availability of geophysics data for most of the piezometers in the study area is limited due to data loss. Proper handling and storage mechanisms should be in place for the safekeeping of the data. Furthermore, Climate change adaptation policies and sustainable management strategies for the basin should include having legislation in place to regulate the indiscriminate drilling of boreholes and dumping of solid and liquid waste and regulate the abstraction of groundwater in an unsustainable manner.

The methods of groundwater recharge estimation employed in this study were based on available data financial resources. There are other methods of groundwater recharge estimation that can yield better results such as the chloride mass balance and isotope methods.

Future research could explore these methods based on available data and resources. Furthermore, since the actual boundary of the basin is unknown, determination of potential lateral groundwater flow to the basin is required for establishing the water budget.

Climate change adaptation policies and sustainable management strategies for the basin should include having legislation in place to regulate the indiscriminate drilling of boreholes and dumping of solid and liquid waste and regulate the abstraction of groundwater in an unsustainable manner.

REFERENCES

Agarwal, R., & Garg, P. K. (2016). Remote Sensing and GIS Based Groundwater Potential & Recharge Zones Mapping Using Multi-Criteria Decision Making Technique. *Water Resources Management*, *30*(1), 243–260. https://doi.org/10.1007/s11269-015-1159-8

Aghazadeh, N., Chitsazan, M., & Golestan, Y. (2017). Hydrochemistry and quality assessment of groundwater in the Ardabil area, Iran. *Applied Water Science*, *7*(7), 3599–3616. https://doi.org/10.1007/s13201-016-0498-9

Ahmed, T. H., & Al-manmi, D. A. M. (2019). *Delineation of Groundwater productivity Zones with the integration of GIS and Remote Sensing methods, Bazian Basin, Sulaymaniyah, Kurdistan*. *2*(2).

Al-Manmi, T. H. A. D. A. M. (2010). *Groundwater Recharge Zone Mapping Using GIS-Based Multi-criteria Analysis : A Case Study in Central Tunisia (Maknassy Basin)*. (March). https://doi.org/10.1007/s11269-009-9479-1

Allen, R. G., Asce, M., Pereira, L. S., Asce, M., Smith, M., Raes, D., … Asce, M. (2005). *FAO-56 Dual Crop Coefficient Method for Estimating Evaporation from Soil and Application Extensions*. (February), 2–13.

Allen, R. G., Pereira, L. S., Raes, D., Smith, M., & W, a B. (1998). Crop evapotranspiration - Guidelines for computing crop water requirements - FAO Irrigation and drainage paper 56. *Irrigation and Drainage*, (January 1998), 1–15. https://doi.org/10.1016/j.eja.2010.12.001

André, B., & Christine, G. G. (2013). *UCAD/FST/Département Géologie/Master Hydrogéologie/2013 Page I*.

Argaz, A. et al. (2019). Application of Remote Sensing Techniques and GIS-Multicriteria Decision Analysis for Groundwater Potential Mapping in Souss Watershed, Morocco. *J. Mater. Environ. Sci*, *10*(5), 411–421.

Ashikin, N., Yusof, M., & Hasliah, S. (2013). Analytical Hierarchy Process in Multiple Decisions Making for Higher Education in Malaysia. *Procedia - Social and Behavioral Sciences*, *81*, 389–394. https://doi.org/10.1016/j.sbspro.2013.06.448

Atlas, S. (1979). *Examples of large-scale soil maps*. (849), 129–176.

Blanchette, D., Lefebvre, R., Nastev, M., & Cloutier, V. (2010a). Groundwater quality, geochemical processes, and groundwater evolution in the Chateauguay River watershed, Quebec, Canada. *Canadian Water Resources Journal*, *35*(4), 503–526. https://doi.org/10.4296/cwrj3504503

Blanchette, D., Lefebvre, R., Nastev, M., & Cloutier, V. (2010b). Groundwater quality, geochemical processes, and groundwater evolution in the Chateauguay River watershed, Quebec, Canada. *Canadian Water Resources Journal*, *35*(4), 503–526. https://doi.org/10.4296/cwrj3504503

Breedt, N., & Huisamen, A. (2014). *Vadose Zone Hydrology : CONCEPTS AND TECHNIQUES*.

Brindha, K., & Elango, L. (2011). *Hydrochemical characteristics of groundwater for domestic and irrigation purposes in Madhuranthakam, Tamil Nadu, India*. *15*(2), 101–107.

Camara, I. F. (2013). *Mainstreaming climate change resilience into development planning in Kenya*. (April 2013), 12. Retrieved from http://pubs.iied.org/10044IIED.html

Chen, X., Chen, Y. D., Xia, J., & Zhang, H. (2008). *Hydrological Sciences for Managing Water Resources in the Asian Developing World*. (October 2015).

China National Complete Plant Import and Export (Group). (n.d.). *Geology and Mineral Resources of the Gambia*.

Courtney, B. D. M. (2016). *NAMA design document for rural electrification with renewable energy in The Gambia*.

Dandekar, A. T., Singh, D. K., Sarangi, A., & Singh, A. K. (2018). *Modeling vadose zone processes for assessing groundwater recharge in semi-arid regions*. *114*(3).

Das, B., & Pal, S. C. (2019). Combination of GIS and fuzzy-AHP for delineating groundwater recharge potential zones in the critical Goghat-II block of West Bengal, India. *HydroResearch*, *2*, 21–30. https://doi.org/10.1016/j.hydres.2019.10.001

Diène, Moustapha Kane; Cheikh Hamidou; Sarr, D. (2015). *Overview of the aquifer system in the Senegalese and Mau- Ruritanian sedimentary basin Abstract : 1*(January), 86–91.

Dieng M., Faye S., D. A. (2017). *Etude de la relation Eaux de Surface-Eaux Souterraines dans l ' estuaire inverse du Saloum (Sénégal) : Apport des outils géochimiques , isotopiques , de la télédétection , des*.

DIONGUE, D. M. L. (2018). *Mémoire de Master de Géosciences*. UNIVERSITE CHEIKH ANTA DIOP DE DAKAR.

Diouf, O. C. (2012). *Apport des outils cartographiques et géochimiques à la validation des paramètres d' entrée du modèle hydrogéologique de la nappe des sables quaternaires de Dakar : implication sur les inondations en zone péri-urbaine*. 236.

Earle, S. (2013). *3 Groundwater geochemistry*. 2–3. Retrieved from https://web.viu.ca/earle/geol304/304g.pdf

Emvoutou, H. C. (2018). *Thèse de Doctorat en Cotutelle Spécialité : Hydrogéologie Présentée par : Soutenue le 11 Août 2018 Composition du Jury : " Le travail éloigne de nous trois grands maux : l'ennui, le vice et le besoin ". François-Marie Arouet dit Voltaire (1694-1778).*

EMVOUTOU Huguette Christiane; FAYE Serigne; KETCHEMEN-TANDIA Béatrice. (2018). *Thèse de Doctorat Spécialité : Hydrogéologie Présentée par : Huguette Christiane EMVOUTOU Composition du Jury : " Le travail éloigne de nous trois grands maux : l'ennui, le vice et le besoin ". François-Marie Arouet dit Voltaire (1694-1778) et par*.

Faye, S., Ba, M. I., Diaw, M., & Ndoye, S. (2010). *The groundwater geochemistry of the Saloum delta aquifer : Importance of silicate weathering, recharge and mixing processes*. *4* (December), 815–830.

Fischer, S. (2013). *Exploring a water balance method on recharge estimations in the Kilombero Valley, Tanzania*.

The Gambia, G. (2012a). *Republic of The Gambia National Report 2012*.

The Gambia, G. (2012b). *The Gambia's Second National Communication under the United Nations Framework Convention on Climate Change*.

Gambia Government. (2020). Land Resources. *Dictionary of Geotourism*, pp. 330–330. https://doi.org/10.1007/978-981-13-2538-0_1325

Gassama Jallow, A., M. L Diongue, D., C. Emvoutou, H., Mama, D., & Faye, S. (2020). Groundwater Recharge Zone Mapping Using GIS-based Analytical Hierarchy Process and Multi-Criteria Evaluation: Case Study of Greater Banjul Area. *American Journal of Water Resources*, *8*(4), 182–190. https://doi.org/10.12691/ajwr-8-4-4

Gautam, S. K., & Swaroop, V. K. (2017). *A Study on Groundwater and Solute Transport Modeling Using Visual Modflow*. *6*(6), 2015–2017.

GBoS. (2013). The Gambia 2013 Population and Housing Census Preliminary Results. In *The Gambia Bureau of Statistics*. Retrieved from www.gbos.gov.gm

Gorin, G. E., Ndiaye, M., Malick, P., Gorin, G., & Villeneuve, M. (2016). A new interpretation of the deep-part of Senegal-Mauritania Basin in the Diourbel-Thies area by integrating seismic, magnetic, gravimetric and borehole data : Implication for petro ... Journal of African Earth Sciences A new interpretation of the deep-. *Journal of African Earth Sciences*, *121*(June), 330–341. https://doi.org/10.1016/j.jafrearsci.2016.06.002

GoTG. (2014). *ESTABLISHMENT OF NEW GROUNDWATER MONITORING NETWORK AND INITIAL RESULTS ON GROUNDWATER OCCURRENCE*. (December), 1–29.

Government, G. (1995). *Investigation of Regional Geology and Mineral Resources of the Gambia*.

Government, T. G. (1992). *Sub-Saharan Africa Hydrological Assessment of West African Countries*.

Graham, J. (2015). *Climate Impact on Groundwater Flow Processes in the Cedar Creek Watershed and Cedarburg Bog*. (August).

Hayhoe, K., Edmonds, J., Kopp, R. E., LeGrande, A. N., Sanderson, B. M., Wehner, M. F., & Wuebbles, J. (2017). Climate Models, Scenarios, and Projections. *Climate Science Special Report: Fourth National Climate Assessment*, *I*, 133–160. https://doi.org/10.7930/J0WH2N54.U.S.

Healy, R. W., & Cook, P. G. (2002). *Using groundwater levels to estimate recharge*. https://doi.org/10.1007/s10040-001-0178-0

Heiden, F. V. A. N. D. E. R. (2011). *Groundwater Modelling of the Vårgårda Aquifer*. CHALMERS UNIVERSITY OF TECHNOLOGY, Göteborg, Sweden.

Hidayat, R., & Prasasti, I. (2018). *Assessment of the Standardized Precipitation Index (SPI) in Tegal City, Central Java, Indonesia Assessment of the Standardized Precipitation Index (SPI) in Tegal City, Central Java, Indonesia*. https://doi.org/0.1088/1755-1315/129/1/012019

IAEA. (2017). *Integrated and Sustainable Management of Shared Aquifer Systems and Basins of the Sahel Region BASIN*.

Islam, S., Singh, R. K., & Khan, R. A. (2016a). *Methods of Estimating Groundwater Recharge Methods of Estimating Groundwater Recharge*. (May).

Islam, S., Singh, R. K., & Khan, R. A. (2016b). *Methods of Estimating Groundwater Recharge Methods of Estimating Groundwater Recharge*. (May).

J. Boe; L. Terray; F. Habetsb; E. Martinc. (2007). Statistical and dynamical downscaling of the Seine basin climate for hydro-meteorological studies. *International Journal of Climatology*, *2029*(March 2008), 2011–2029. https://doi.org/10.1002/joc.1602

J R Dunsmore, A Blair Rains, G D N Lowe, D J Moffatt, I. P. A. and J. B. W. (1976). *22 The agricultural development of The Gambia : an agricultural, environmental, and socioeconomic analysis Volume 1* (Vol. 1).

Jackson, J. M. (2007). *Hydrogeology and groundwater flow model, the central catchment of Bribie island, southeast queensland*.

Jaiteh Malanding, S. (2010a). *Climate Change and Development in the Gambia Challenges to Ecosystem Goods and Services*. 57. https://doi.org/10.13140/2.1.1731.1040

Jaiteh Malanding, S. (2010b). *Climate Change and Development in the Gambia Challenges to Ecosystem Goods and Services*. 57.

Jakeman, A. J., Barreteau, O., & Rinaudo, R. J. H. J. (2016). *Integrated Groundwater Management*.

Jarju, P. A. O. (2009). *Why is Water Resources a Key Sector for Adaptation to Climate Change?*

Jarju, P. O. (2009). *National Report on Adaptation of Water Resources in the Gambia By*.

Jones, A., Breuning-Madsen, H., Brossard, M., Dampha, A., D., J., Dewitte, O., Gallali, T., Hallett, S., Jones, R., Kilasara, M., L. R., P., Micheli, E., Montanarella, L., Spaargaren, O., Thiombiano, L., V., & Ranst, E., Yemefack, M. , Zougmoré R., (eds.), 2013. (2013). *SOIL ATLAS OF AFRICA*. https://doi.org/10.2788/52319

Kane, C. H. (2015). *Overview of the aquifer system in the Senegalese and Mau- ritanian sedimentary basin Abstract : 1*(January), 86–91.

Kaviyarasan, R., Seshadri, H., & Sasidhar, P. (2013). *ASSESSMENT OF GROUNDWATER FLOW MODEL FOR AN UNCONFINED COASTAL AQUIFER*. *2*(1), 12–18.

Kevin Hiscock, Y. T. (2006). Potential Impacts of Climate Change on Groundwater Resources: From the High Plains of the U.S. To the Flatlands of the U.K. *National Hydrology Seminar 2006*, 19–26.

Khadri, S. F. R., & Pande, C. (2016a). Groundwater flow modeling for calibrating steady-state using MODFLOW software: a case study of Mahesh River basin, India. *Modeling Earth Systems and Environment*, *2*(1). https://doi.org/10.1007/s40808-015-0049-7

Khadri, S. F. R., & Pande, C. (2016b). Groundwater flow modeling for calibrating steady-state using MODFLOW software: a case study of Mahesh River basin, India. *Modeling Earth Systems and Environment*, *2*(1), 39. https://doi.org/10.1007/s40808-015-0049-7

Kipyegon, S. (2018). *MODELLING GROUNDWATER RESOURCES OF TRANSBOUNDARY OKWA BASIN*.

Kumar, C. P. (2003). ESTIMATION OF GROUNDWATER RECHARGE USING SOIL MOISTURE BALANCE APPROACH. *ISH Journal of Hydraulic Engineering*, *247667*.

Kumar, P. J. S., & James, E. J. (2016). Identification of hydrogeochemical processes in the Coimbatore district, Tamil Nadu, India. *Hydrological Sciences Journal*, *61*(4), 719–731. https://doi.org/10.1080/02626667.2015.1022551

Lakshmi, C., & Narayanan, R. M. (2015). *Study on Groundwater Modeling of Aquifers Using Visual Modflow*. 23–26.

Lawrence, N. N. (2006). *GROUNDWATER RECHARGE ESTIMATION AND WATER RESOURCES*. The Delft University of Technology.

Lee, CH., Yeh, HF. & Chen, JF. Estimation of groundwater recharge using the soil moisture budget method and the base-flow model. *Environ Geol* **54,** 1787–1797 (2008). https://doi.org/10.1007/s00254-007-0956-7

Loudyi, D. (2014). *MODFLOW : An Insight into Thirty Years Development of a Standard Numerical Code for Groundwater Simulations How does access to this work benefit you ? Let us know !*

Luo, W., Gao, X., & Zhang, X. (2018). *Geochemical processes controlling the groundwater chemistry and fluoride contamination in the Yuncheng Basin, China — an area with complex hydrogeochemical conditions*. 1–25.

Mallick, J., Singh, C. K., Almesfer, M. K., & Kumar, A. (2018). *Hydro-Geochemical Assessment of Groundwater Quality in Aseer Region, Saudi Arabia*. 1–14. https://doi.org/10.3390/w10121847

Mauritanian, S. (2017). *Integrated and Sustainable Management of Shared Aquifer Systems and Basins of the Sahel Region*.

Mckee, T. B., Doesken, N. J., & Kleist, J. (1993). The relationship of drought frequency and duration to time scales. *AMS 8th Conference on Applied Climatology*, (January), 179–184. https://doi.org/citeulike-article-id:10490403

Meißner, R., Prasad, M. N. V, Laing, G. Du, & Rinklebe, J. (2010). *Lysimeter application for*

measuring the water and solute fluxes with high precision. (December 2015).

Mensah Mawuli, K. (2011). *Assessment of drinking water quality in Ehi community in the Ketu- South District of the Volta region of Ghana*. 71.

Michigan Department of Environmental. (2014). *GROUNDWATER MODELING*. (4), 1–45.

Middlemis, H. (2004). *The Winston Churchill Memorial Trust of Australia Report by Hugh Middlemiss 2004 Churchill Fellow BENCHMARKING BEST PRACTICE FOR*. *61*(8).

Mora, A., Mahlknecht, J., Rosales-lagarde, L., & Hernández-antonio, A. (2017). *Assessment of major ions and trace elements in groundwater supplied to the Monterrey metropolitan area, Nuevo León, Mexico*. https://doi.org/10.1007/s10661-017-6096-y

Mutasa, C. (2011). *Impacts of climate change on groundwater resources : a case study of the Sardon catchment, Spain Impacts of climate change on groundwater resources : a case study of the Sardon catchment, Spain*.

Naorem, N., & Devi, T. K. (2014). *Estimation of Potential Evapotranspiration using Empirical Models for Imphal*. (7).

Nazarenko, L., G. A. Schmidt, R. L. Miller, N. Tausnev, M. Kelley, R. Ruedy, G. L. R., I. Aleinov, M. Bauer, S. Bauer, R. Bleck, V. Canuto, Y. Cheng, T. L. Clune, A. D. D. G., G. Faluvegi, J. E. Hansen, R. J. Healy, N. Y. Kiang, D. Koch, A. A. Lacis, A. N. L., J. Lerner, K. K. Lo, S. Menon, V. Oinas, J. Perlwitz, M. J. Puma, D. Rind, A. R., M. Sato, D. T. Shindell, S. Sun, K. Tsigaridis, N. Unger, A. Voulgarakis, M.-S. Y., & Zhang, and J. (2015). Future climate change under RCP emission scenarios with GISS ModelE2. *Journal of Advances in Modeling Earth Systems*, *7*, 244–268. https://doi.org/10.1002/2014MS000403.Received

Ndiaye, M., Ngom, P. M., Gorin, G., Villeneuve, M., Sartori, M., & Medou, J. (2016). A new interpretation of the deep-part of Senegal-Mauritania Basin in the Diourbel-Thies area by integrating seismic, magnetic, gravimetric, and borehole data: Implication for petroleum exploration. *Journal of African Earth Sciences*, *121*(June), 330–341. https://doi.org/10.1016/j.jafrearsci.2016.06.002

Ochungo, E. A., Ouma, G. O., Obiero, J. P. O., & Odero, N. A. (2019). *An Assessment of Groundwater Grab Syndrome in Langata Sub County, Nairobi City-Kenya*. 651–673. https://doi.org/10.4236/jwarp.2019.115038

Penny Urquhart. (2016). *National Climate Policy of The Gambia*. Retrieved from http://www.moeccww.gov.gm/sites/default/files/National Climate Change Policy.pdf

Pramudya, Y., Onishi, T., Hidayat, R., & Prasasti, I. (2017). *Evaluation of wet indices using standard precipitation index : A case study of Terengganu states Evaluation of wet indices using standard precipitation index : A case study of Terengganu states*. 1–7. https://doi.org/10.1088/1742-6596/890/1/012159

RITZ, M., Y. B. (1988). *Geologic sections across onshore Senegal -Mauritania basin derived from geoelectric studies*.

Road, B. (2014). *Hydrogeochemical Investigation and Groundwater Quality Assessment of Pratapgarh District, Uttar Pradesh*. *83*(March), 329–343.

Rodriguez-camino, E. (2016). *International Journal of Water Downscaled climate change projections over Spain : application to water resources*. (June 2013). https://doi.org/10.1080/07900627.2012.721700

Saaty, T. L. (2008). Decision making with the analytic hierarchy process. *Int. J. Services Sciences, 1*, pp.83–98. https://doi.org/10.1016/0305-0483 (87)90016-8

Sadashivaiah, C., Ramakrishnaiah, C. R., & Ranganna, G. (2008). *Hydrochemical Analysis and*

Evaluation of Groundwater Quality in Tumkur Taluk, Karnataka State, India. *5*(3), 158–164.

Scanlon, B. R., Healy, R. W., & Cook, P. G. (2002). *Choosing appropriate techniques for quantifying groundwater recharge*. https://doi.org/10.1007/s10040-0010176-2

Shaban, A., Khawlie, M., & Abdallah, C. (2006). Use of remote sensing and GIS to determine recharge potential zones: The case of Occidental Lebanon. *Hydrogeology Journal*, *14*(4), 433–443. https://doi.org/10.1007/s10040-005-0437-6

Silva, B. M., Alves, M. D. C., Júnior, A. D. S., & Miranda, W. L. (2013). *FAO Penman-Monteith equation for reference evapotranspiration from missing data*. 39–48.

Singh, P., Thakur, J. K., & Kumar, S. (2013). Délimitation des zones de prospection d'eaux souterraines en zone de socle à l'aide d'outils. *Hydrological Sciences Journal*, *58*(1), 213–223. https://doi.org/10.1080/02626667.2012.745644

Singh, R. D., & Kumar, C. P. (2010). Impact of Climate Change on Groundwater Resources. *2nd National Ground Water Congress*, *247667*(October), 332–350. https://doi.org/10.4018/978-1-4666-8814-8.ch010

Sophocleous, M. (2004). *GROUNDWATER RECHARGE, in Groundwater, [Eds. Luis Silveira, Stefan Wohnlich, and Eduardo J. Usunoff], in Encyclopedia of Life Support Systems (EOLSS), Developed under the Auspices of the UNESCO, Eolss Publishers, Oxford,UK, [http://www.eolss.net]*.

Sridharan, M. (2017). Groundwater quality assessment for domestic and agriculture purposes in the Puducherry region. *Applied Water Science*. https://doi.org/10.1007/s13201-017-0556-y

The Gambia, G. (2000). *ENVIRONMENTAL IMPACT ASSESSMENT STUDY* (Vol. 1).

The Gambia, G. (2014). The Fifth National Report to the Convention on Biological Diversity. The Republic of The Gambia. In the Department *of Parks and Wildlife Management*. Retrieved from http://meccnar.gm/sites/default/files/NR5 updated MAY 2014.pdf

The Gambia, Government. (2015). *THE STATE OF GAMBIA'S BIODIVERSITY FOR FOOD AND AGRICULTURE*.

Titulaire, P., Titulaire, P., & Titulaire, P. (2018). *Thèse de Doctorat Spécialité : Hydrogéologie Présentée par : Huguette Christiane EMVOUTOU Composition du Jury : " Le travail éloigne de nous trois grands maux : l' ennui, le vice et le besoin ". François-Marie Arouet dit Voltaire (1694-1778) et par*.

Touré, A. (2017). *IMPACTS OF CLIMATE CHANGE AND POPULATION GROWTH ON GROUNDWATER RESOURCES: CASE OF THE KLELA BASIN IN MALI, WEST AFRICA*. University of Abomey-Calavi, Benin.

Toure, A., Diekkrüger, B., & Mariko, A. (2016a). Impact of climate change on groundwater resources in the Klela basin, Southern Mali. *Hydrology*, *3*(2). https://doi.org/10.3390/hydrology3020017

Toure, A., Diekkrüger, B., & Mariko, A. (2016b). Impact of Climate Change on Groundwater Resources in the Klela Basin, Southern Mali. *Hydrology*, *3*(2), 17. https://doi.org/10.3390/hydrology3020017

Tukimat, N. N. A., Harun, S., & Shahid, S. (2012). Comparison of different methods in estimating potential evapotranspiration at the Muda Irrigation Scheme of Malaysia. *Journal of Agriculture and Rural Development in the Tropics and Subtropics (JARTS)*, *113*(1), 77–85.

UNEP. (2008). *Fresh Water under threat Africa: Vulnerability Assessment of Freshwater Resources to Environmental Change*. 1–340.

USDA. (1967). *ARENOSOLS (AR)*.

Valverde, J. P. B., Blank, C., Roidt, M., Schneider, L., & Stefan, C. (2016). Application of a GIS multi-criteria decision analysis for the identification of intrinsic suitable sites in Costa Rica for the application of Managed Aquifer Recharge (MAR) through spreading methods. *Water (Switzerland)*, *8*(9). https://doi.org/10.3390/w8090391

Villeneuve, M., Fournier, F., Cirilli, S., Spina, A., Ndiaye, M., Zamba, J. … Ngom, P. M. (2015). Structure of the Paleozoic basement in the Senegalo-Mauritanien basin (West Africa). *Bulletin de La Societe Geologique de France*, *186*(2–3), 193–203. https://doi.org/10.2113/gssgfbull.186.2-3.193

Vuuren, D. P. Van, Edmonds, J., Kainuma, M., Riahi, K., Nakicenovic, N., Smith, S. J., & Rose, S. K. (2011). *The representative concentration pathways : an overview*. 5–31. https://doi.org/10.1007/s10584-011-0148-z

Wayne, G. P. (2013). The Beginner's Guide to Representative Concentration Pathways By. *Journal of Chemical Physics*, *24*, 1–24. https://doi.org/10.1063/1.478923

Whyte, W. J., & and T. S. Russell. (1988). *GEOLOGY AND · MINERAL RESOURCES OF THE GAMBIA By :*

Whyte, W. J., & Geologist, C. (1988). *GEOLOGY AND · MINERAL RESOURCES OF THE GAMBIA By :*

Xin Cong, Zhenghe Xu, T. W. (2018). *Research on Characteristics of Groundwater Recharge*. https://doi.org/10.3390/w10060799

APPENDICES

APPENDIX 1: CHEMICAL ANALYSES OF GROUNDWATER (MG/L)

BH	pH	EC	TDS	TEMP (°C)	HCO_3^-	Cl^-	Br	NO_3^-	SO_4^{2-}	Na^+	K^+	Mg^{2+}	Ca^{2+}
BH1	6.5	147.0	94.1	31.7	18.3	14.5		32.8	2.3	10.2	2.7	3.1	8.5
BH2	5.2	96.0	61.4	29.4	24.4	9.3		10.9	7.9	7.1	2.6	3.2	6.4
BH3	6.7	57.0	36.5	29.2	24.4	4.3		3.3	1.9	3.1	2.1	1.9	4.2
BH4	7.2	51.0	32.6	28.9	24.4	4.2		1.9	2.5	3.8	2.0	1.3	4.3
BH5	5.1	44.0	28.2	29.7	18.3	4.2		2.4	1.5	3.6	1.6	1.2	2.4
BH6	6.1	325.0	208.0	29.1	39.7	47.3		59.3	4.8	28.2	1.5	4.6	30.9
BH7	5.2	34.0	21.8	29.4	12.2	4.1		3.3	2.8	3.9	1.7	1.6	1.9
BH8	5.1	39.0	25.0	30.1	12.2	3.8		3.4	1.7	2.8	1.8	1.1	1.8
BH9	6.2	32.0	20.5	30.1	12.2	3.7		1.9	1.6	2.6	1.5	1.4	2.2
BH10	5.6	70.0	44.8	29	24.4	4.1		6.5	1.6	3.5	1.6	1.7	6.4
BH11	5.4	40.0	25.6	29.1	15.3	4.2		2.7	1.6	2.9	1.6	0.9	3.3
BH12	5.9	53.0	33.9	31.4	24.4	3.9		2.3	0.8	2.3	1.9	1.1	5.4
BH13	6.1	60.0	38.4	30.1	24.4	4.9		3.1	3.3	5.5	2.3	1.8	3.3
BH14	6.7	158.0	101.1	31	85.4	4.7		0.3	2.0	5.2	2.6	4.7	16.3
BH15	6.7	240.0	153.6	30	134.2	6.1		1.8	8.2	9.1	3.3	9.5	20.8
BH16	5.5	37.0	23.7	30.1	12.2	3.4		5.2	1.6	2.6	1.5	1.5	3.7
BH17	5.7	249.0	159.4	29.4	24.4	46.8		51.4	2.4	29.2	1.5	5.5	12.6
BH18	5.5	31.0	19.8	32	12.2	3.6		4.3	0.1	2.6	1.8	1.2	2.4
BH19	7.3	251.0	160.6	30.1	131.2	10.0		2.8	8.7	7.9	4.8	6.2	28.7
BH20	7.6	40.0	25.6	30.6	15.3	4.5		5.3	0.1	3.2	2.0	1.2	3.3
BH21	5.1	91.0	58.2	32	18.3	11.9		13.7	1.5	10.3	0.7	1.9	4.6
BH22	6.6	58.0	37.1	29.7	24.4	4.4		3.6	1.9	4.3	1.3	1.3	5.3
BH23	5.1	35.0	22.4	29.8	12.2	4.5		3.2	1.7	3.1	1.3	0.8	2.5
BH24	5.0	30.0	19.2	28.3	12.2	3.7		4.0	0.2	3.5	1.4	1.4	1.6
BH25	6.0	45.0	28.8	31	18.3	3.2		2.7	0.2	2.0	1.8	1.3	4.7
BH26	5.1	99.0	63.4	29.6	18.3	11.6		25.4	1.6	10.8	1.1	2.1	5.3
BH27	6.8	385.0	246.4	28	167.8	19.9		13.5	13.1	35.3	5.5	3.9	30.2
DW1	5.8	661.0	423.0	29	42.7	92.8		121.8	31.0	59.1	10.0	8.6	39.4
DW2	5.1	41.0	26.2	29.3	12.2	4.0		7.3	1.5	4.3	0.9	1.7	1.9
DW3	4.5	357.0	228.5	30.6	24.4	89.3		23.0	1.8	47.2	7.2	6.0	10.3
DW4	6.7	563.0	360.3	30.1	305.0	7.2		4.8	4.8	11.3	20.4	3.9	82.8

DW5	5.1	84.0	53.8	30.0	15.3	5.5		28.5	2.1	7.4	2.7	2.3	6.3
DW6	5.7	187.0	119.7	30	24.4	35.1		18.8	2.3	23.6	1.8	3.4	6.4
DW7	7.5	645.0	412.8	30.6	335.5	25.6		3.3	10.7	36.4	3.1	14.1	71.2
DW8	6.0	669.0	428.2	30.7	54.9	71.9	0.6	179.4	17.3	78.0	9.2	8.6	41.1
DW9	6.2	110.0	70.4	28.9	42.7	6.0		14.9	2.9	4.8	2.0	1.5	12.5
DW10	7.8	410.0	262.4	29.6	97.6	34.2		25.2	22.7	32.3	6.6	4.4	28.2
DW11	7.0	332.0	212.5	26.7	158.6	26.5		1.7	1.9	17.9	4.3	3.4	41.9
DW13	6.9	304.0	194.6	28.7	85.4	47.4		10.3	3.5	29.0	3.6	3.1	31.4
DW14	4.9	336.0	215.0	32.1	12.2	43.1		98.6	2.3	38.2	1.7	4.8	17.2
DW15	5.9	114.0	73.0	29.3	30.5	7.3		23.8	2.1	8.6	1.3	2.7	8.7
DW16	4.2	406.0	259.8	31.8	12.2	26.7		47.8	110.4	14.8	2.9	10.7	46.4
DW17	5.7	42.0	26.9	33	12.2	5.0		1.9	2.7	5.0	0.8	1.3	2.4
DW18	7.8	161.0	103.0	31.6	48.8	8.1		32.6	2.4	8.3	0.8	1.9	20.2
DW19	6.2	163.0	104.3	27.6	30.5	11.9		40.2	2.0	17.3	2.7	1.6	9.3
DW20	5.8	60.0	38.4	32.6	30.5	3.4		3.8	1.7	2.5	0.9	1.6	7.2
DW21	5.4	577.0	369.3	28.7	24.4	96.9	0.6	132.9	3.5	67.9	1.6	8.3	28.0
DW22	4.0	1610.0	1030.4	28.3	12.2	267.7		544.7	28.8	191.0	8.2	40.7	92.5
DW23	4.5	367.0	234.9	32.4	12.2	57.0		96.2	1.5	43.3	1.5	3.0	20.9
DW24	5.3	1440.0	921.6	28.4	21.4	308.2		316.6	3.7	165.0	7.3	17.9	97.1
DW25	7.7	432.0	276.5	28.2	122.0	46.4		49.1	4.4	40.0	7.9	6.2	31.0
DW26	6.7	200.0	128.0	29.1	36.6	18.9		54.4	1.7	21.4	2.1	1.8	16.9
S1	7.3	27900.0	17856.0	29.6	128.1	8685.9	99.4	2.2	1523.3	5021.7	83.3	400.9	365.9
S2	7.4	57000.0	36480.0	32	158.6	18483.5	117.4	3.2	2665.5	10991.7	91.1	916.4	365.6
S3	7.7	45000.0	28800.0	28.6	140.3	13938.7	101.7	3.1	2118.9	8403.4	88.8	567.3	337.0
S4	7.9	48000.0	30720.0	29.1	170.8	15041.5	107.7	2.6	2242.4	8996.9	89.6	586.5	339.4
S5	7.5	24000.0	15360.0	32.1	131.2	7622.4	67.7	2.3	1207.9	4538.2	57.1	331.3	188.7
S6	7.6	23800.0	15232.0	28.6	109.8	7003.1	62.1	2.5	1159.8	4153.8	59.2	334.6	192.4

APPENDIX 2: COMPARISON OF MEAN ANNUAL RAINFALL OF RCP4.5 AND RCP8.4 2020-2049 WITH THE OBSERVATION, 2006-2050

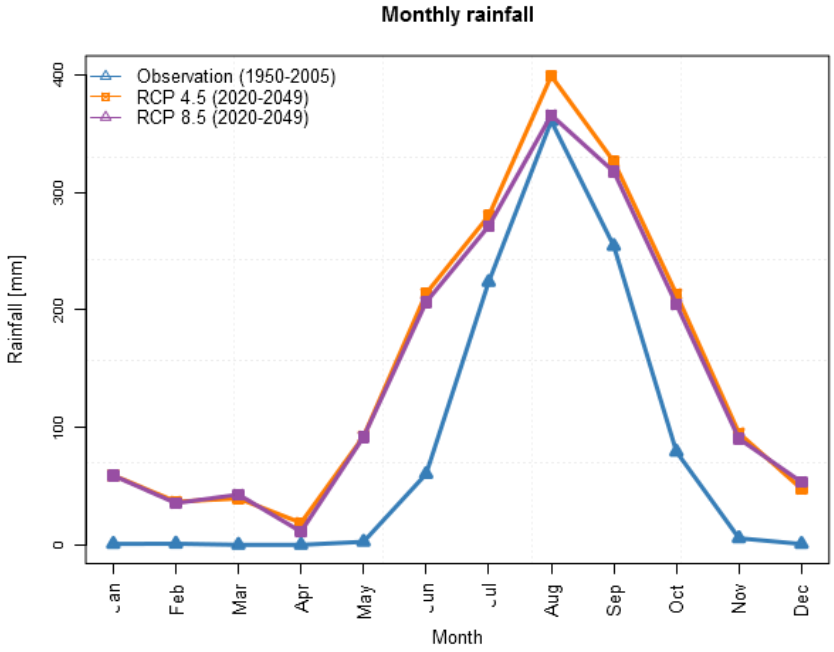

APPENDIX 3: COMPARISON OF MEAN ANNUAL TEMPERATURE OF RCP4.5 AND RCP8.4, 2020-2049 WITH THE OBSERVATION, 2006-2050

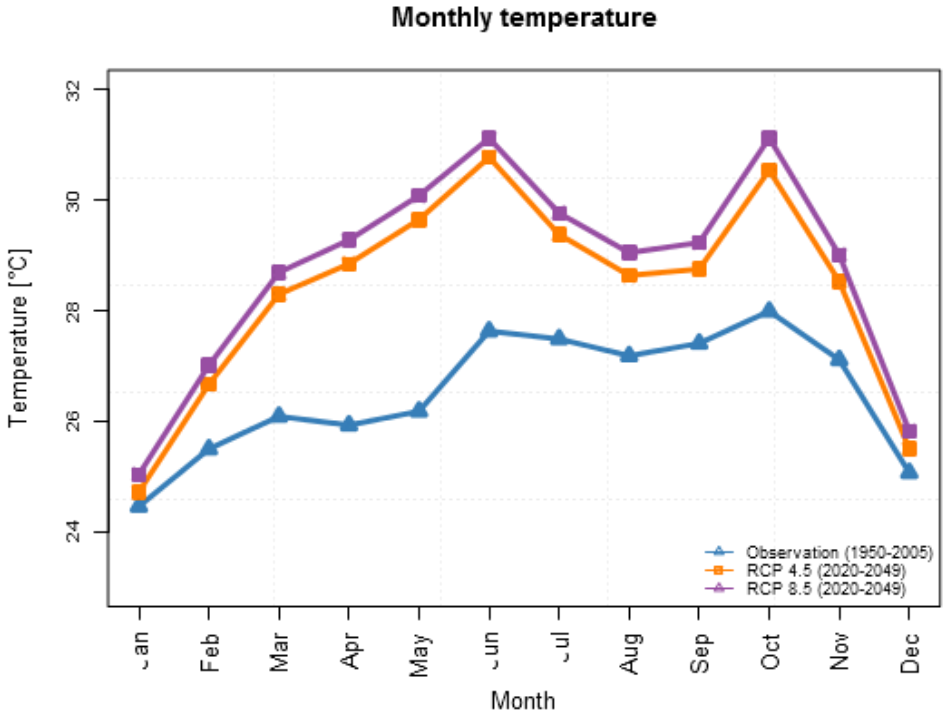

APPENDIX 4: RAINFALL VARIABILITY FROM 2006-2060 WITH RCP4.5 SCENARIO

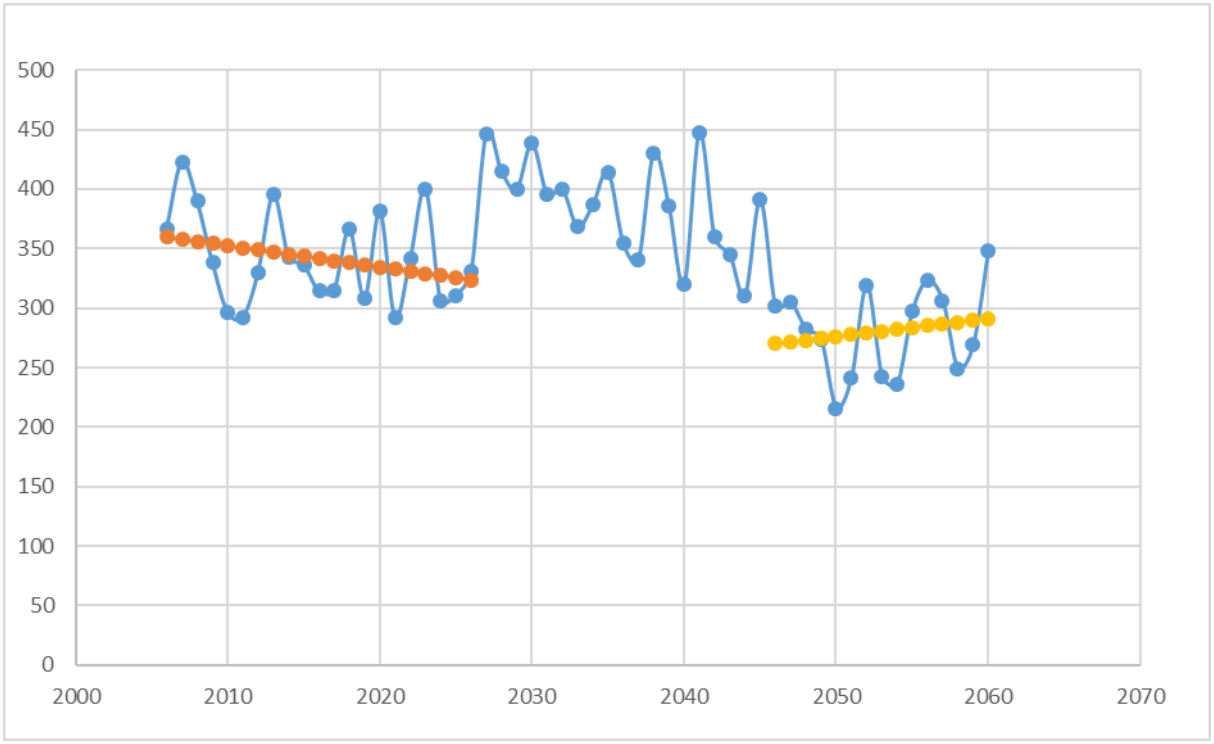

APPENDIX 5: RAINFALL VARIABILITY FROM 2006-2060 WITH RCP8.5 SCENARIO

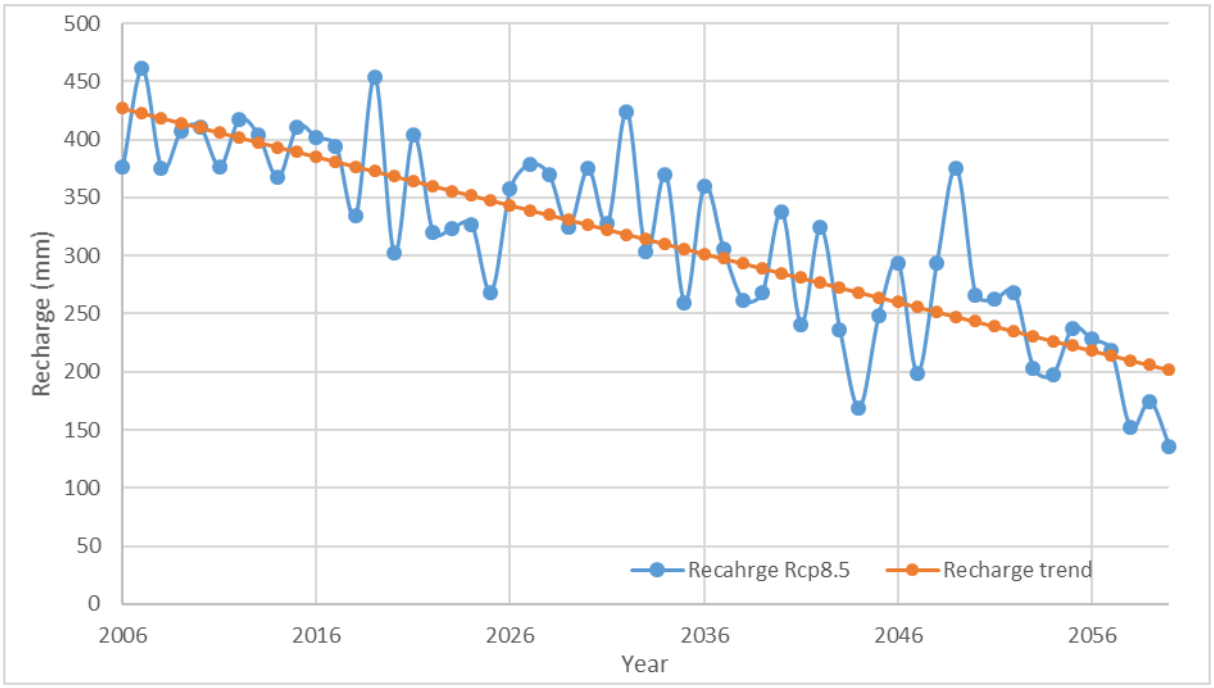

APPENDIX 6: GEOCHEMICAL PROCESSES OF GROUNDWATER IN THE STUDY AREA. MAJOR IONS/BICARBONATE RATIOS VS. BICARBONATE: (A) CA/HCO3 VS. HCO3, (B) MG/ HCO3 VS. HCO3, (C) NA/ HCO3 VS. HCO3, (D) CA + MG VS. HCO3, (E) NA + K VS. HCO3, (CIRCLES: FRESH GROUNDWATER; TRIANGLES: SURFACE WATER)

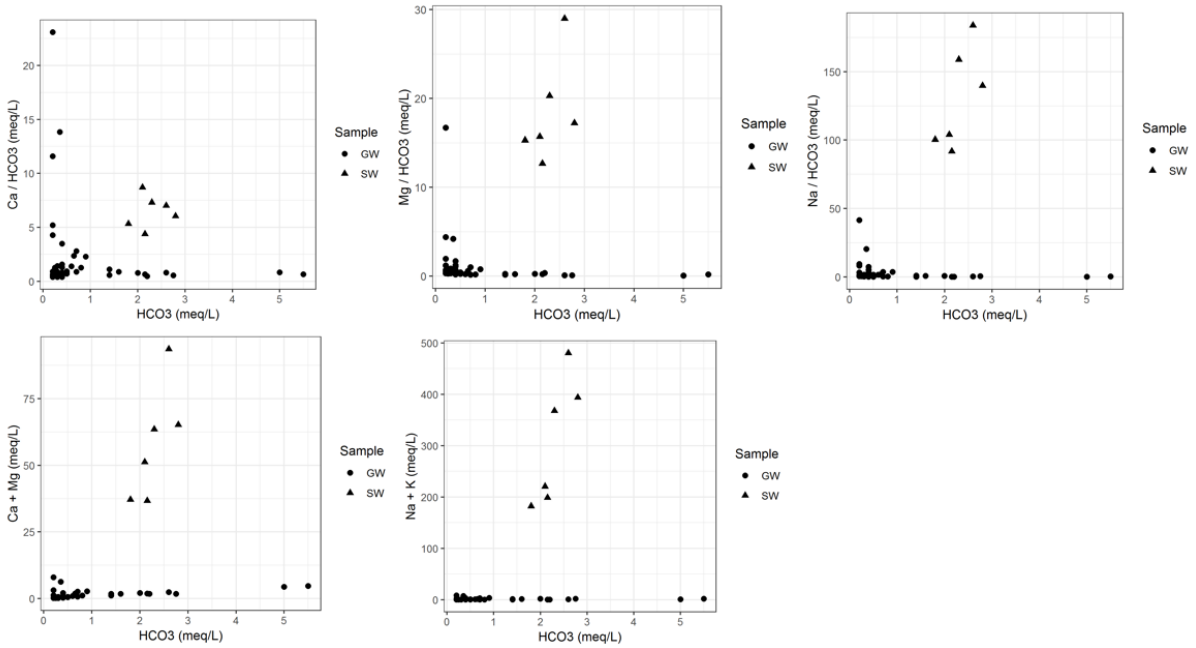

CANDIDATE BIOGRAPHY

Mrs. Adama GASSAMA-JALLOW is a Gambian. She did her primary and secondary education in Bansang. She attended the teachers' training programs known as the Primary Teacher's Certificate and the Higher Teacher's Certificate in 1996-1998 and 2000-2003 respectively at the Gambia College. In 2005-2009, she did her Bachelor's program in Mathematics and Physics at the University of The Gambia. She secured a German Government Scholarship under the West African Science Service Center on Climate Change and Adapted Land Use (WASCAL) Program to pursue her Master's and Doctoral degrees. She did her Master's degree in Climate Change and Energy at the University of Abdou Moumouni Niger in 2013-2015. She is a Ph.D. candidate in the Graduate Research Program (GRP) in Climate Change and Water Resources Program at the University of Abomey-Calavi, Benin. She is also a senior official at the Energy Division of the Ministry of Petroleum and Energy of the Gambia. She is the author of an article on "Groundwater Recharge Zone Mapping Using GIS-Based Analytical Hierarchy Process and Multi-Criteria Evaluation: Case Study of Greater Banjul Area"

ABSTRACT

Groundwater is an important natural water resource, and it serves as an alternative source of water supply for surface water in the Greater Banjul Areas (GBA), which is saline. Thus resources regardless of their importance have been increasingly threatened by pollution due to saline intrusion and infiltration of chemicals from agricultural activities, urbanization, industrial development, seasonal climate variability, and climate change. Subsurface storage and groundwater recharge are affected by climate variability and change through changes in precipitation pattern and intensity. In coastal areas of the GBA, the aquifers are affected by marine water intrusion sea level rise.

The hydrodynamics and hydrochemistry of the GBA basin were assessed for 118 wells and 52 boreholes and wells respectively. The Piper diagram was used to assess the groundwater type of the study area. The analysis of the Piper diagram identified eight major water-types based on the major ion chemistry of groundwater: i) bicarbonate (m-HCO_3, Ca-HCO_3, and Na-HCO_3) facies, ii) chloride (Na-Cl and m-Cl) facies, iii) and iv) mixed (m-m and Na-m) facies. The Thornthwaite model was used to estimate groundwater recharge trends for RCP4.5 and RCP8.5 scenarios. The output of the Thornthwaite model (recharge) was used as input into the three-dimensional finite-difference groundwater flow model MODFLOW was used to simulate groundwater dynamics and the impacts of present and future climate change on groundwater recharge and groundwater levels. Three different scenarios (Abstraction scenario: A1=2000m^3/day; A1=4000m^3/day, Climate change scenario and Abstraction and climate change scenario) are used to evaluate the recharge trend over the 2006-2050 period. The results obtained show a decreasing recharge trend for both the RCP4.5 and RCP8.5 scenarios with the Thornthwaite model. In RCP4.5, the annual recharge trend decreases by 5% (-5%) during the period 2006-2020 and by 8% (-8%) during the period 2030-2060 while it increases between these two periods (2006-2020 and 2030-2060) by 5.5% (+5.5%). Generally, groundwater recharge for the two scenarios is decreasing and this is more significant in RCP8.5 than in RCP4.5. The decreasing trend over time with RCP8.5 has a growth rate estimated at -14%.

***Keywords*:** Greater Banjul Area, Climate Change, Recharge, Hydrochemistry, MODFLOW, RCP

Ph.D	**Adama GASSAMA-JALLOW**	**ASSESSMENT OF THE IMPACT OF CLIMATE CHANGE ON GROUNDWATER RESOURCES OF THE REATER BANJUL AREAS (GBA) IN THE GAMBIA**	**GRP/CCWR/INE/WASCAL – UAC March, 2021**